AUTOMATIC CLASSIFICATION OF CARDIAC ARRHYTHMIAS USING SIGNAL PROCESSING TECHNIQUES

Submitted in partial fulfilment of the
requirements for the award of the degree of

Doctor of Philosophy

By

V. Rama

(Roll No. 715103)

Under the guidance of

Prof C.B. Rama Rao

DEPARTMENT OF ELECTRONICS AND COMMUNICATION ENGINEERING

NATIONAL INSTITUTE OF TECHNOLOGY

WARANGAL, TELANGANA, INDIA — 506004

October-2020

DECLARATION

I hereby declare that the matter embodied in this thesis entitled **"Automatic Classification of Cardiac Arrhythmias Using Signal Processing Techniques"** is based entirely on the result of the investigation and research work carried out by me under the supervision of **Prof C.B.Rama Rao,** Department of Electronics and Communication Engineering, National Institute of Technology, Warangal. I declare that this work is original and has not been submitted in part or full, for any degree or diploma to this or any other university and was not submitted elsewhere for the award of any degree.

I also declare that this written submission represents my ideas, in my own words and where others ideas or words have been included, I have adequately cited and referenced the original sources. I have adhered to all principles of academic honesty and integrity and have not misrepresented or fabricated or falsified any idea/data/fact/source in my submission. I understand that any violation of the above will cause for disciplinary action by the institute and can also evoke penal action from the sources which have thus not been properly cited or from whom proper permission has not been taken when needed.

(Mrs V.Rama)

(Roll No. 715103)

Date: 28.10.2020

Place: Warangal

National Institute of Technology, Warangal

CERTIFICATE

This is to certify that the thesis entitled **"Automatic Classification of Cardiac Arrhythmias Using Signal Processing Techniques"** is being submitted by **Mrs. V.Rama (Roll No. 715103),** is a bonafide work submitted to National Institute of Technology, Warangal in partial fulfilment for the requirement of award of the degree of **Doctor of Philosophy in Electronics and Communication Engineering** of National Institute of Technology, Warangal is a record of bonafide research work carried out by her under my supervision.

To the best of my knowledge, the work incorporated in this thesis has not been submitted elsewhere for the award of any degree.

Prof. C. B. Rama Rao,
(Research Supervisor)
Professor, Dept. of ECE,
National Institute of Technology,
Warangal – 506004, India.

This thesis is dedicated to the following who transformed my life

My Beloved Parents; Late Sri V. Laxminarayana & Sathyamma

Teachers; Prof. C.B.RamaRao, Prof. Raghu Ram and Mrs Roy

-Rama Valupadasu

Acknowledgement

It gives me an immense pleasure to convey my sincere gratitude to my research supervisor **Prof. C. B. Rama Rao**, ECE Dept., NIT Warangal, for his consistent support and guidance throughout my research process. His steady influence throughout my research career has oriented me in a proper direction and supported me with promptness and care. I truly appreciate his logical and thought provoking advices both technically and morally which I will follow for the rest of my life. I take this privilege to thank **Prof N.V.Ramana Rao**, Director, National Institute of Technology, Warangal for sponsoring me to carry out my research in NIT Warangal.

I am grateful to **Prof. L. Anjaneyulu**, Head, Department of Electronics & Communication Engineering and Chairman of Doctoral Scrutiny Committee for his valuable suggestions and encouragement towards the completion of research work. Also, I take this privilege to thank all my DSC members, **Prof T. Kishore Kumar**, Department of ECE and **Prof. D.V.S.S. Siva Sarma**, Department of EEE for their detailed review, constructive suggestions and advices during the progress of my research work.

I thank all the faculty of ECE Dept., for their kind cooperation during the tenure of this research work. My special thanks to Prof KSR Krishna Prasad, Prof Srihari Rao and Prof. Radha Krishnamacharya. My heartfelt appreciation to all my co-scholars Dr. P.Muralidhar, Dr.Bhalke, Shiva Prasad, Vasanth for their support and encouragement. My special thanks to supporting staff of ECE Dept. for their kind cooperation.

I would like to acknowledge my gratitude to medical doctors Dr.R.Srinivas (Cardiologist) Prof.V.Chandrasekhar (Geriatrician), Dr.K.B.Chandrabhanu and Dr.P.Jagadish. I am very much grateful to all my friends and well-wishers especially Prof.B.Rajitha, Dr.K.Padma, Dr.M.Shilaja, Dr.G.Pushpa Chakrapani, Dr.C.Vanitha, Prof.V.Sharmila, Maruthi Venkat Rao, K.V.Sridhar, Dr.Ravi Kumar, Dr.Ashok Reddy and Nikhil for their constant encouragement during my research. Finally, I am very much grateful to all my family members especially my husband Prakash Rao, my children Divya, Agnivesh, Srilu and my siblings Vijaya, Latha and Vv for their kind support and cooperation during my Ph.D work.

- Valupadasu Rama

Abstract

In the modern industrialized countries every year millions of people die due to cardiac disorders. India has highest incidence of heart related diseases in the world. According to world health organization statistics an estimated 17.9 million people died from cardio vascular diseases in 2016, representing 31% of all global deaths. The life expectancy in India was reduced to 68.3 years. If no initiative is taken to check this most predictable and preventable among all chronic diseases, life expectancy may further decrease. Most of the cardiac disorders can be preventable by taking healthy diet, doing physical activity, avoiding alcohol & tobacco.

Manual analysis of cardiac arrhythmias and disorders is very difficult, computer based analysis is important for early detection of cardiac problem which enable the doctor to save the heart patient. For this purpose, various feature schemes have been proposed by various researchers for classification of cardiac arrhythmias and disorders. There is a large variation in number of features, number of cardiac signals and classification accuracy. However, selecting better signal processing technique for feature extraction, selecting optimum set of features, choosing proper neural network classifier to improve the classification accuracy remains an open problem. This aspect is motivation to take up the issue of automatic classification of cardiac arrhythmias. This research work will enable the clinical doctors and cardiologists to diagnose type of cardiac disorder to initiate proper treatment to save the life of heart patients.

In this thesis, four signal processing techniques (time domain, spectral domain, higher order spectral domain and wavelet domain) and three supervised classifiers (Random Forest, Multilayer perceptron and Radial Basis Function) have been proposed for analysis and classification of cardiac signals to improve the performance of a baseline system.

In the first approach, temporal features extraction has been proposed. Using this feature scheme, the average classification accuracy of two types of cardiac signals has been improved from 96.5% (existing morphological feature scheme) to 100% for temporal features (proposed). For classification of NSR, VT and VF (three types) the average classification accuracy has been 84%. For classification of NSR, SVT, VT, VF, AF, SCA and CI (seven types) the average classification accuracy has been 78.09%.

In the second approach, spectral features are proposed. Using only four spectral features for normal and abnormal (two types) average classification accuracy obtained as 96.6%. This has been improved to 100% by using hybridization of temporal and spectral features. Further classified 7 types of cardiac signals normal(NSR) , cardiac arrhythmias(SVT, VT, VF, AF) and cardiac disorders(SCA and CI) .The average classification accuracy has been obtained as 78.09% using this hybridization feature scheme.

In the third approach, to get the advantage of non-linearity and non-gaussianity, hybridization of temporal, spectral and higher order spectra (HOS) based features have been proposed. Using this feature scheme, 4-types of cardiac signals such as Normal Sinus Rhythm (NSR), Ventricular Arrhythmias (VT and VF) and Atrial Arrhythmia (AF) classified and the obtained sensitivity has been improved from 89.2% (existing) to 90% (proposed) and average specificity enhanced from 93.55% (existing) to 96.62% (proposed). Using this proposed feature scheme, average classification accuracy and specificity of 7-types has been obtained as 74.2% and 95.70%.

In the fourth approach, Wavelet (db4)-6 level decomposition technique is used for feature extraction. This multi resolution analysis has been proposed as a non-stationary, non-linear and quasi periodic signal. Wavelet based features are proposed to classify NSR,VT and VF(3 types) obtained sensitivity has been increased from 90.97%(existing) to 97.77%(proposed) , specificity increased from 97.86% to 98.88 % and classification accuracy from 97.02%(existing) to 97.77%(proposed). In this proposed work equal values of sensitivity and accuracy are obtained. Later, the proposed wavelet based feature scheme has been extended to classify 7 types of cardiac signals and obtained classification accuracy as 95.24%, sensitivity as 95.2% and specificity as 99.20%. The specificity is more important than the sensitivity, since no patient should be defibrillated except SCA patient due to an error of analysis which might cause cardiac arrest. The main objective of this research work is to enhance classification accuracy of cardiac signals, to improve specificity to enable doctors for early diagnose the type of cardiac problem to save the life of heart patients.

Further, performance comparison has been done with the existing works. All the four methods developed in this thesis are novel and better compared to traditional features reported earlier. However, the wavelet based feature scheme proposed in the fourth method is superior in terms of

classification accuracy and specificity. With this efficient wavelet based feature scheme a cardiac alert system has been developed for remote monitoring of cardiac patients. This research work may be further extended to identify and classify few more cardiac disorders.

The feasibility of above proposed methods have been tested using benchmarked MIT-BIH database, European ST_T database, Ventricular Tachyarrhythmia data base, SCD holter data base.

Keywords: Cardiac arrhythmias classification, Feature extraction, Feature Selection, MLP, Random Forest and RBF.

Contents

List of Figures

List of Tables

List of Abbreviations

AF	Atrial Fibrillation
ANN	Artificial Neural Networks
BPF	Band Pass Filter
BPM	Beats per minute
BPNN	Back-Propagation Neural Networks
CI	Cardiac Ischemia
CPR	Cardio Pulmonary Resuscitation
db4	Daubechies 4 wavelet
DFT	Discrete Fourier Transform
ECG	Electrocardiogram
EMG	Electromyogram
FFT	Fast Fourier Transform
HOS	Higher Order Spectra
HOSA	Higher Order Spectral Analysis
LPF	Low Pass Filter
MIT-BIH	Massachusetts Institute of Technology-Beth Israel Hospital
mV	Millivolts
MLP	Multi- Layer Perceptron
NSR	Normal Sinus Rhythm
PNN	Probabilistic Neural Network

Pp	Positive Predictivity
PLI	Power Line Interference
QPC	Quadrature Phase Coupling
RBF	Radial Basis Function
S	Sensitivity
SA	Sinoatrial node
SCA	Sudden Cardiac Arrest
Sp	Specificity
SVM	Support Vector Machine
SVT	Supra Ventricular Tachycardia
VF	Ventricular Fibrillation
VT	Ventricular Tachycardia
WEKA	Waikato Environment for Knowledge Analysis
WSS	Wide Sense Stationary
2D	Two Dimensional

Chapter 1

Introduction

The aim of this first chapter of introduction is to present anatomy and electrical functioning of the heart, need of arrhythmias analysis and classification, motivation for the work, objectives of the proposed research work, overview of research work, ECG database details, tools used for analysis & classification and thesis organization

1.1 Anatomy and electrical functioning of the heart

Heart is an important muscular organ which pumps oxygenated rich blood to each and every cell of human body and carries deoxygenated blood back to the lungs for oxygen as shown in Fig 1.1. Heart consists of four chambers which are divided into two atria and two ventricles.

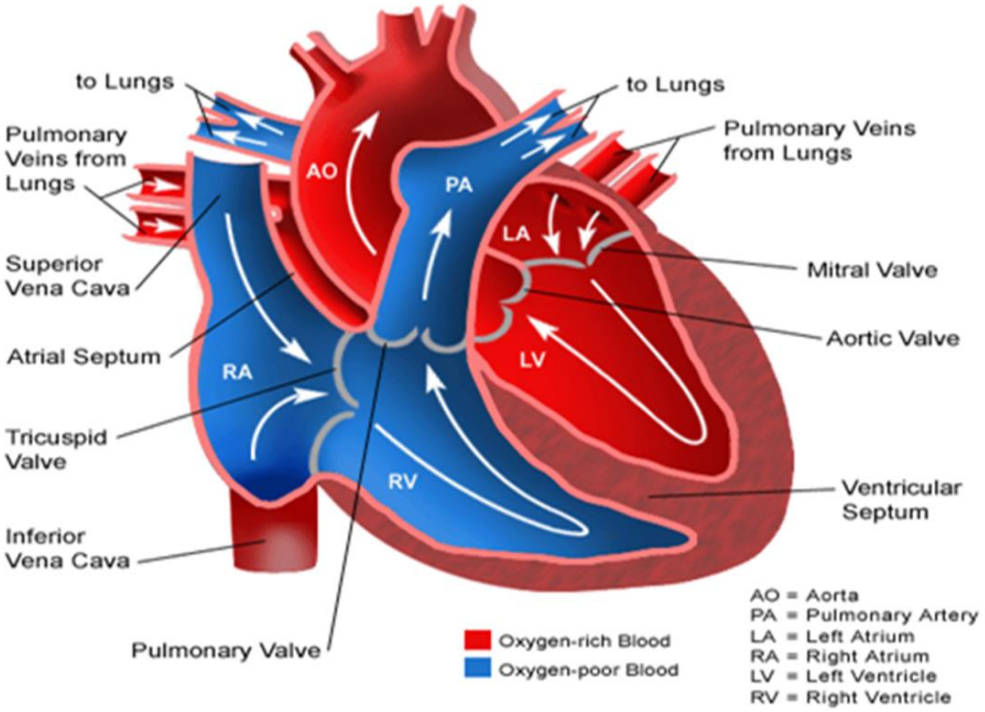

Fig 1.1 Anatomy of the heart [11]

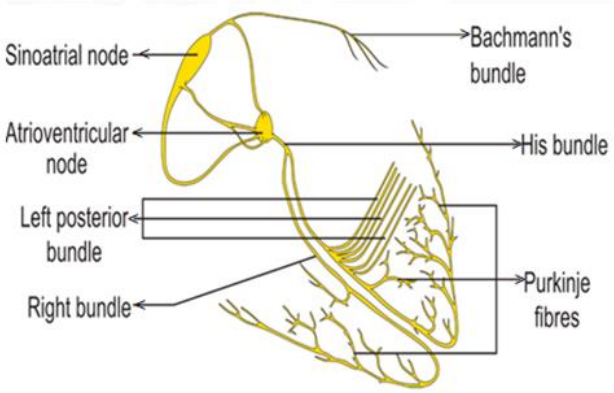

Fig 1.2 Electrical conduction system of the heart [60]

The electrical functioning of heart is shown in Fig.1.2. In the heart, Sinoatrial (SA) node acts as a natural pacemaker of the heart which generates electrical impulses at regular intervals of time under normal conditions that can simulate the atria to contract or depolarise. Due to the depolarisation of atria blood enters from right atrium to the right ventricle through tricuspid valve. During this period, "P" wave is generated on the ECG signal. Later, the electrical impulse travels from SA node to AV node. There will be a pause in the electrical activity in this period which will be referred as the "PR interval" on the ECG. This "pause" allows the atria to contract fully, emptying blood from atria before the ventricles begin to contract. Then electrical signal continue down its conduction path to the ventricles through the "bundle of his". Later, this electrical impulse passes to the right and left bundle branches and to the right and left ventricles, respectively. This causes the ventricles to contract or depolarise and pump oxygen poor blood to the lungs through the pulmonary arteries for re-oxygenation. During this period ventricular depolarization takes place, due to this "QRS complex" is generated on the ECG. Similarly, due to ventricular repolarisation T-wave is generated on the Electrocardiogram (ECG).

Blood circulation in the human body is shown in Fig 1.3. The left atrium receives the oxygenated rich blood from the lungs via the pulmonary veins. Then blood flows to the left ventricle through the mitral valve and finally, it is pumped out this oxygenated blood to all the cells of the human body through the aorta. Willem Einthoven invented the first ECG machine to monitor heart condition and received Nobel Prize for the same in the year 1924 [34].The standard 12-lead ECG recording provides spatial information about the heart's electrical activity in 3 orthogonal directions is shown in Fig 1.4.

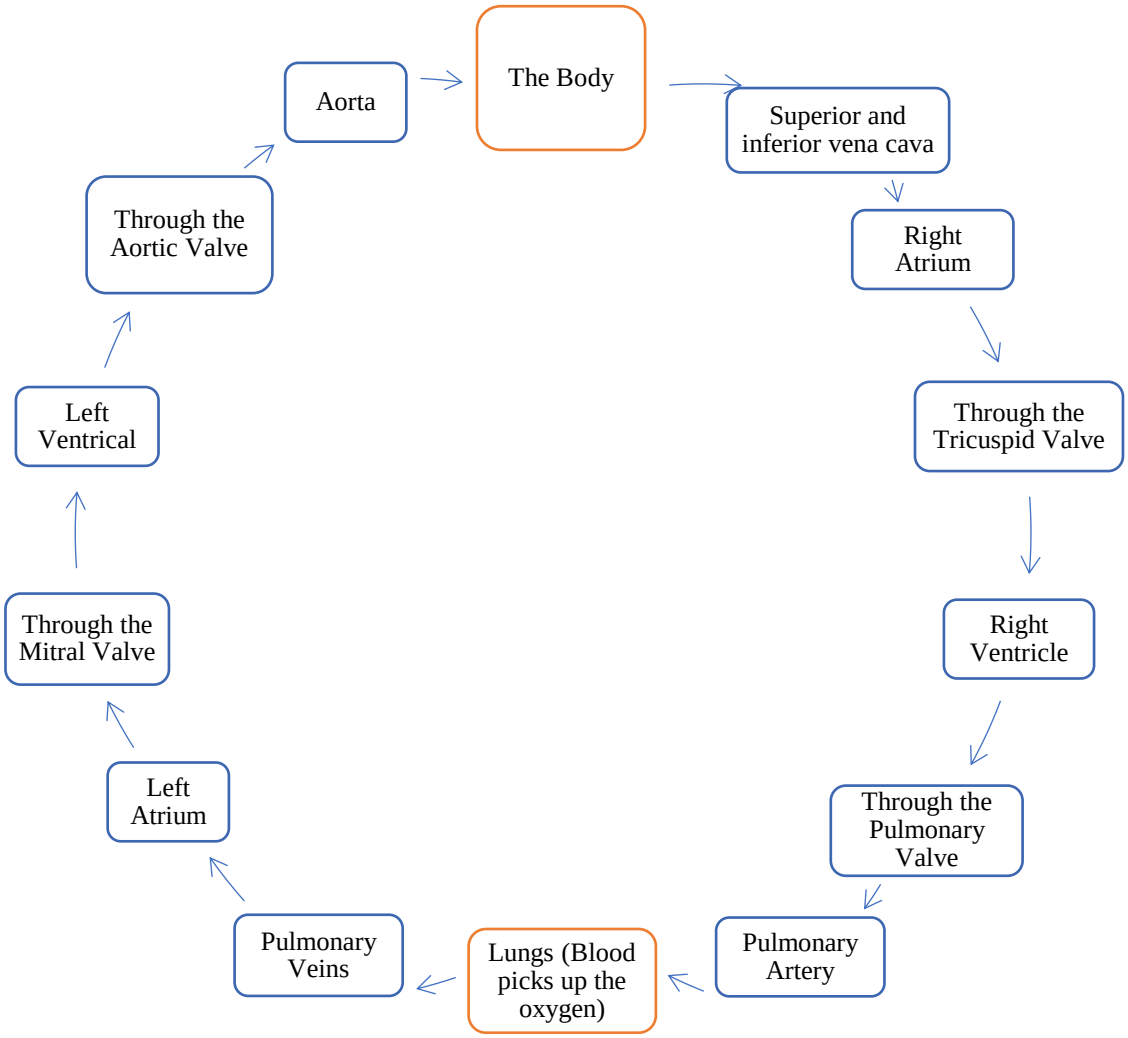

Fig 1.3 Blood circulation in the human body

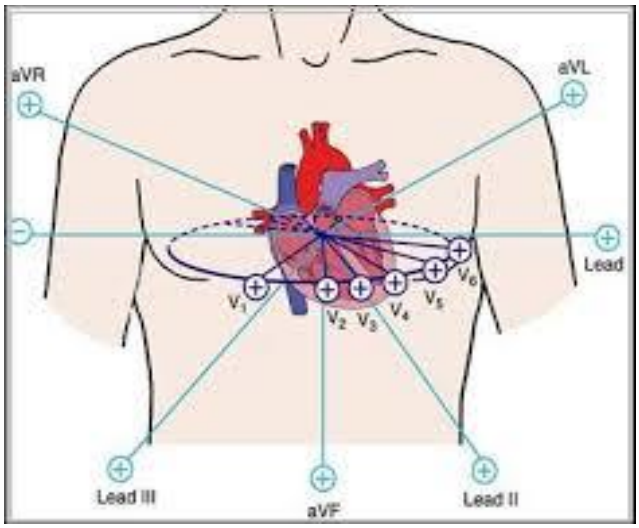

Fig 1.4 Twelve Lead ECG recording [69]

Twelve lead ECG provides 12 different views of the heart's electrical activity. The 12 leads include three bipolar limb leads (I, II and III), three unipolar augmented limb leads and six precordial chest leads. They are aVR, aVL and aVF where aVR means augmented Vector Right, the positive electrode is on the right shoulder; aVL means augmented Vector Left, the positive electrode is on the left shoulder and aVF means augmented Vector Foot, the positive electrode is on the foot and six precordial chest leads are V1, V2, V3, V4, V5 and V6.

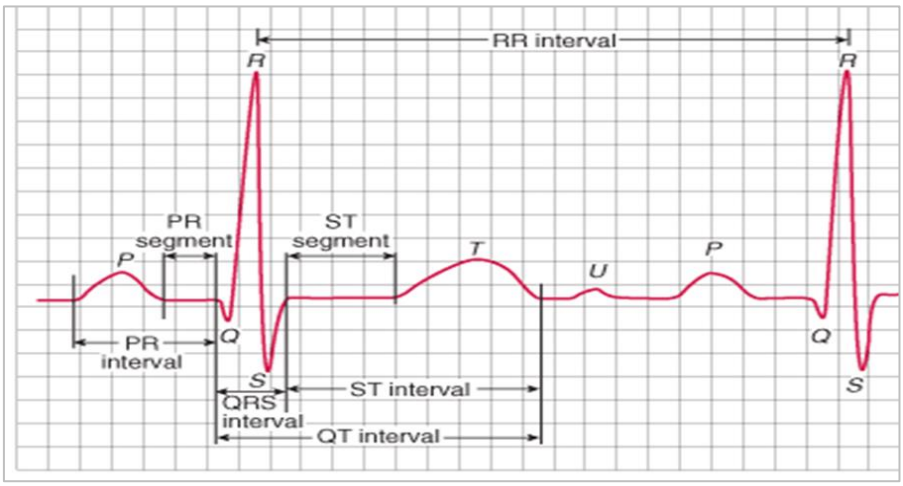

Fig 1.5 Normal ECG Signal [19]

ECG represents electrical activity of the heart [36]. It's not a trace of single action potential but it is an amalgam of various action potentials. Every cardiac cycle of ECG consists of three waves: P, QRS and T waves. The R-R interval plays a significant role in identifying heart beat rate of cardiac signals is shown in Fig 1.5. In ECG strips, horizontal axis represents time in terms of seconds. Each small block equals 0.04s and five small blocks form a large block which equals 0.2 seconds. In ECG strips, vertical axis represents amplitude in terms of mV. Each small block represents 0.1mV. Each five small blocks form a large block which represents 0.5 mV.

Normal ECG features are shown in Table 1.1. The frequency range of normal ECG signal is 0.05–100 Hz and its dynamic amplitude range is 1–10 mV.

Table 1.1 Normal ECG Features

S. No.	Features	Amplitude(mV)	Duration (ms)
1	P-Wave	0.1 - 0.2	60 – 80
2	PR-Segment	-	50 – 120
3	PR-Interval	-	120 – 200
4	QRS-Complex	1 – 10	80 – 120
5	ST-Segment	-	100 – 120
6	T-Wave	0.1 – 0.3	120 – 160
7	ST-Interval	-	320
8	RR-Interval	-	400 – 1200

Irregular electrical activity of the heart represents cardiac arrhythmia (abnormal rhythm). Smoking, physical inactivity, high blood pressure, high blood cholesterol and overweight cause cardiac arrhythmias.

In the proposed work, Normal Sinus rhythm (NSR), 4 types of tachyarrhythmias-Ventricular Tachycardia (VT), Supra Ventricular Tachycardia (SVT), Ventricular Fibrillation (VF) and Atrial Fibrillation (AF) and two cardiac disorders- Sudden Cardiac Arrest (SCA) and Cardiac Ischemia (CI) are considered for arrhythmias classification.

Different types of cardiac signals of 1minute duration are shown below in Fig 1.6 to Fig 1.12. On X-axis of these signals represented as number of samples and on Y- axis, amplitude is represented in mV.

Normal Sinus Rhythm (NSR) is a healthy person's cardiac signal of 1-minute duration is shown in Fig 1.6. Normal person heart beat rate range is 60-100bpm. NSR consists of regular R-R intervals. It is not uncommon to encounter instances of SCA in healthy persons also. Even healthy person may be detected to have a serious heart condition like a hypertrophic cardiomyopathy or dilated cardiomyopathy or an abnormal ECG or echo during routine physician consultation.

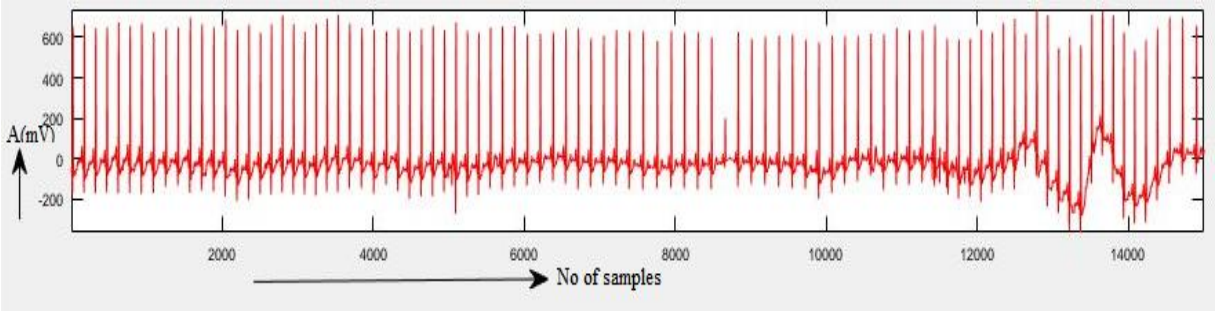

Fig 1.6 NSR

Supraventricular tachycardia (SVT) shown in Fig 1.7 is an abnormal fast heart rhythm due to improper electrical activity in the upper portion of the heart (atria). Most SVTs are unpleasant rather than life-threatening arrhythmias like VT [103]. SVT becomes a problem when it occurs frequently. Its heart beat rate is above 100 bpm.

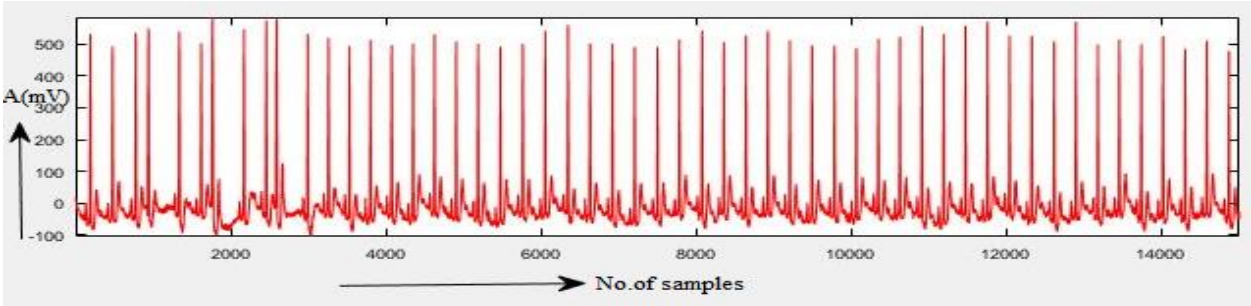

Fig 1.7 SVT

Ventricular tachycardia (VT) shown in Fig 1.8 is an abnormal heart rhythm which causes heart to beat too fast due to wide QRS complex (120ms) [35]. Normally, VT starts in the heart's lower chambers. Most patients who have VT have a heartbeat rate is 170 bpm or more. VT may eventually lead to VF, which is characterized as severe cardiac arrhythmia**.** If the VT terminates within 30 seconds, it is considered a non-sustained VT. If VT lasts more than 30 seconds, it is known as a sustained VT**.**

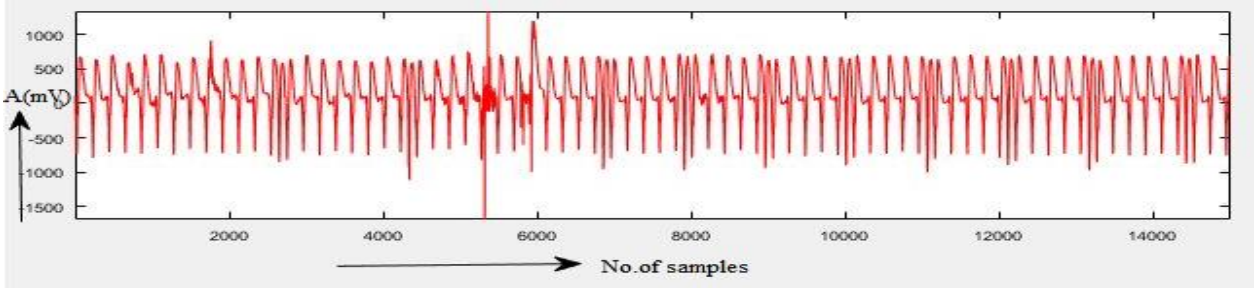

Fig 1.8 VT

Ventricular fibrillation (VF) is life threatening arrhythmia as shown in Fig 1.9. It is existing due to disorganized electrical activity in the ventricles and also heart quivers or fibrillate instead of beating normally. This prohibits the heart from pumping blood. No P- waves are present in VF, only QRS and T waves can be seen. VF can cause sudden cardiac arrest (SCA), which requires immediate medical attention. These patients may die if the rhythm is not restored.

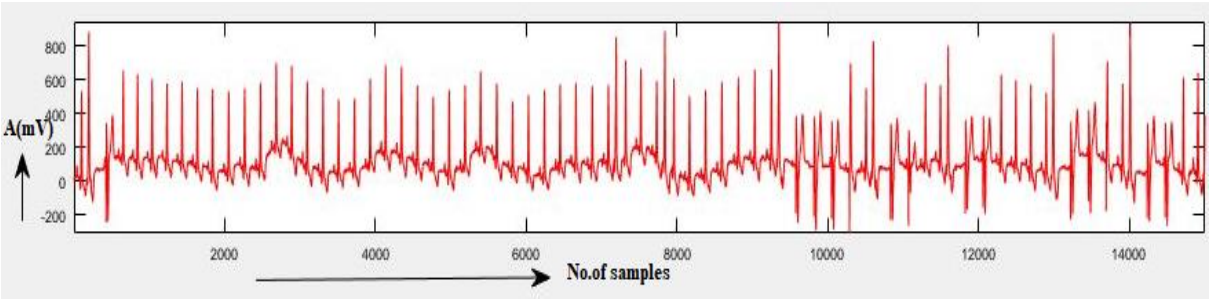

Fig 1.9 VF

Atrial Fibrillation (AF) is an atrial arrhythmia is shown in Fig 1.10, which occurs as action potential triggers at atria instead of at SA node. AF heart beat rate may sometimes exceeds 350bpm. Because of this high heart beat rate, uncoordinated contraction exists which leads to ineffective pumping of blood into the ventricles. In AF, the abnormal heart rhythm affects R-R interval sequence in ECG. Atrial fibrillation (AF) is the most common sustained cardiac arrhythmia. It is associated with a nearly doubled risk of death and an almost 5-fold increase in the risk of stroke.

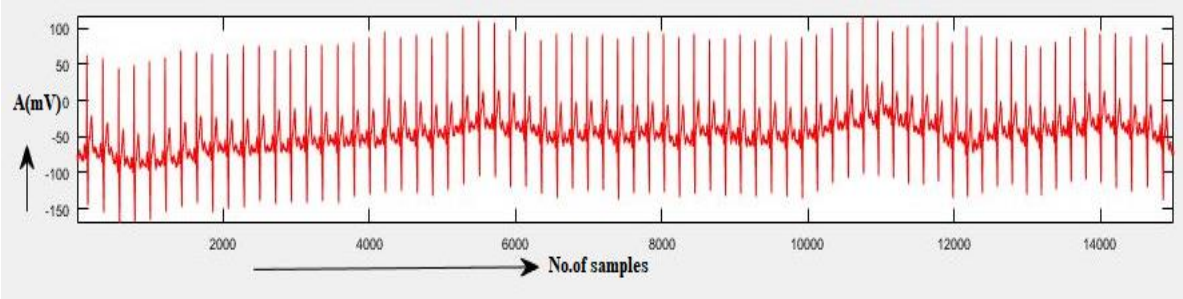

Fig 1.10 AF

Sudden Cardiac Arrest (SCA) is shown in Fig 1.11, occurs when heart suddenly or unexpectedly stops beating due to lack of oxygen supply to the brain cells. If severe ventricular arrhythmias (VT and VF) are not treated in time, lead to sudden cardiac arrest. If SCA patient is not treated, within few minutes, sudden cardiac death may happen. It is a serious health

problem and is responsible for almost half of all sudden cardiac deaths [19]. Its heart beat rate is less than 50bpm [86].

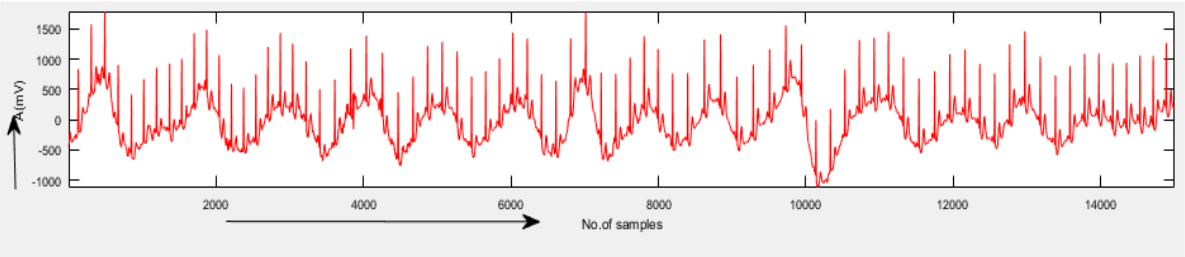

Fig 1.11 SCA

Cardiac Ischemia (CI) is shown in Fig 1.12, it's a heart disease caused by narrowing of the arteries which makes less oxygenated blood to reach the heart muscle. Total occlusion of a coronary artery leads to myocardial infarction or cardiac ischemia and acute myocardial infarction may present as SCA. If timely intervention is not provided as per international guidelines the victim is likely to die. Apart from ischemic causes, other nonischemic causes - cardiomyopathies like hypertrophic cardiomyopathies, genetic causes like LONG QT syndrome, brugada syndrome etc. may lead to serious and life threatening arrhythmias.

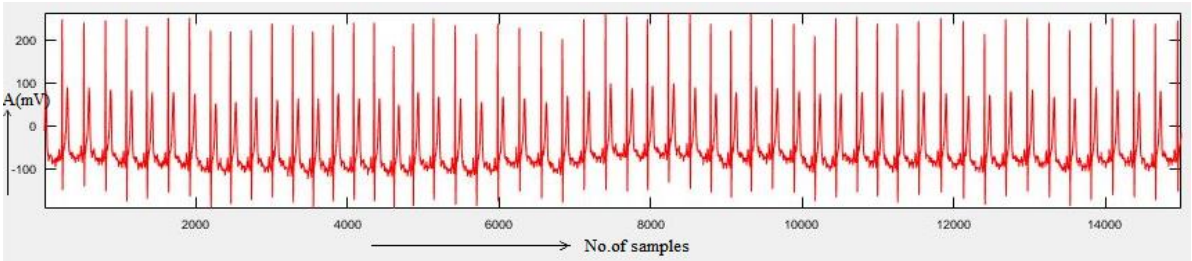

Fig 1.12 CI

Apart from routine ECG, 2D-Echo, 24 hours Holter monitoring, cardiac MRI, electrophysiological studies are useful in risk prediction and management. Apart from antiarrhythmic agents, radio frequency ablation, ICD implantation are management options in such patients.

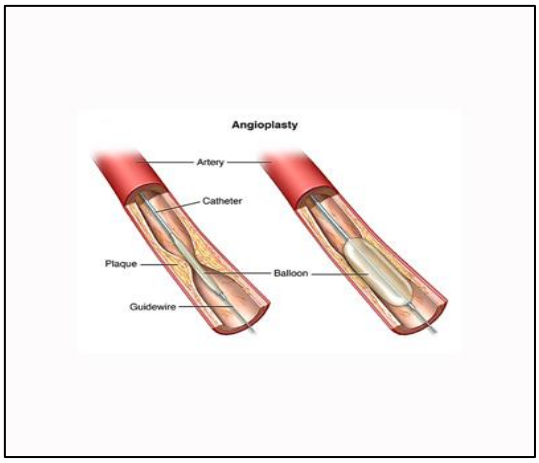

Fig 1.13 Angioplasty (stents) [115]

Fig 1.14 Medication (heparin)

CI patient will be treated with Angioplasty / Medications (heparin /aspirin) is shown in Fig 1.13 and Fig 1.14 and bypass surgery is shown in Fig 1.15. AF patient heart beat rate is more than 300 bpm. This disorder will be treated with medications (Beta blockers, Calcium channel blockers) to bring heart beat rate to normal. For AF treatment when long-term medications were not effective, Ablation catheter (thin, flexible tube) is inserted into the patient's blood vessels and is gently guided to the heart as shown in Fig 1.16. The physician carefully destroys malfunctioning tissue using the catheter to deliver energy by using radiofrequency/laser to scar the problematic areas.

Fig 1.15 Bypass Surgery [117]

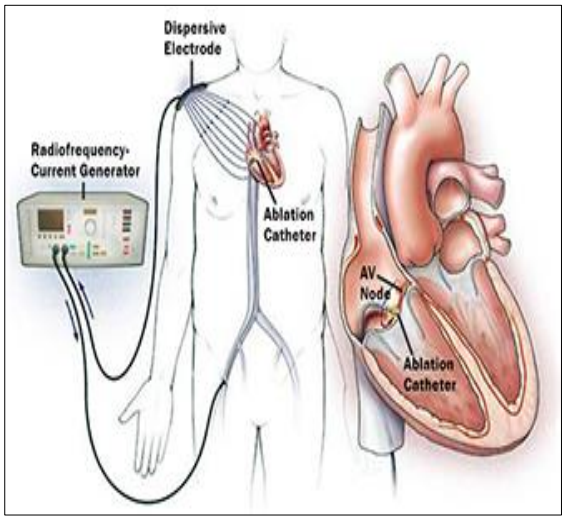

Fig 1.16 Ablation Catheter [114]

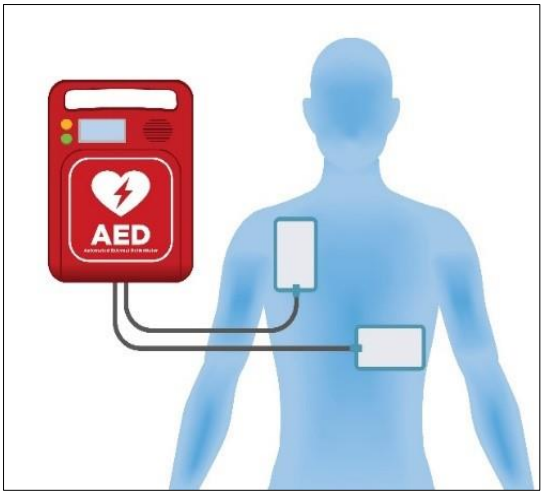

Fig1.17 Automated external defibrillator [93]

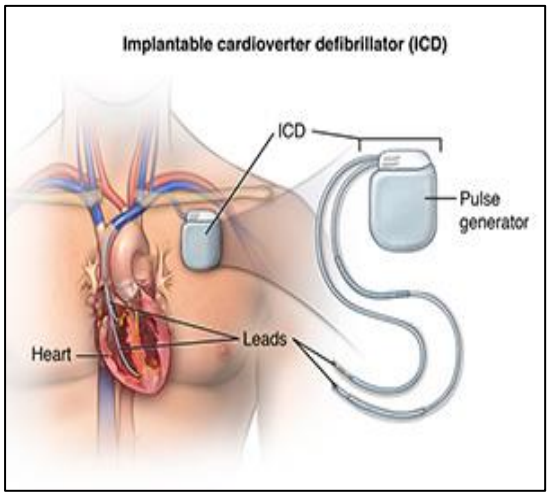

Fig 1.18 Implantable CD [116]

SCA patient will be treated with automated external defibrillators as shown in Fig 1.17, or treated with Implantable Cardioverter Defibrillator (ICD) [93] as shown in Fig 1.18 depending on the emergency. Most of new ICDs can act as both a pacemaker and a defibrillator. A pacemaker may be used if the heart's natural pacemaker of the heart (the SA node) is not working properly causing bradycardia (heart beat rate is less than 60bpm). Ventricular fibrillation and ventricular tachycardia are known as shockable rhythms. The shock can potentially stop arrhythmia by using automated external defibrillator (AED) [17] as shown in Fig 1.18.

1.2 Need of arrhythmias analysis and classification

As the most common cause of sudden cardiac death (SCD) is a ventricular tachycardia (VT) that degenerates into ventricular fibrillation (VF), loss of consciousness and sudden cardiac arrest. Sustained ventricular tachycardia often requires urgent medical treatment, as this condition may sometimes lead to sudden cardiac death. Total occlusion of a coronary artery leads to myocardial infarction or CI, an acute myocardial infarction may present as sudden cardiac arrest. If timely, immediately an intervention is provided as per international guidelines the victim of SCA is likely to survive.

In many instances, the cause of SCA is known, however in certain instances where the cause is difficult to diagnose, other modalities of investigation might be helpful in further management. Apart from ischemic causes, other conditions such as non-ischemic causes-

cardiomyopathies like Hypertrophic cardiomyopathies, genetic causes like LONG QT syndrome, brugada syndrome etc., may lead to serious and life threatening arrhythmias. It is not uncommon to encounter instances of sudden cardiac arrest in an otherwise healthy persons. Also an otherwise healthy person normal sinus rhythm (NSR) may be detected to have a serious heart condition like a hypertrophic cardiomyopathy or dilated cardiomyopathy or an abnormal ECG or echo during routine physician consult. Hence, it is essential from a practical point of view to predict whether such persons are likely to have SCA or not. This helps in early intervention, so that SCA can be prevented and survival rate can be improved.

In this context, translating the knowledge of signal processing and artificial intelligence algorithms to classify 7 types of signals-NSR, 4-tachyarrhythmias and 2-severe cardiac disorders for immediate recognition of serious and life threatening arrhythmias is essential. Prediction of risk of morbid and life threatening situations in subjects with prone conditions is of clinical utility.

1.3 Motivation

The contributions of various researchers have been given in detail in the second chapter. Various signal processing techniques have been proposed by various researchers for identification and classification of cardiac arrhythmias [2]-[5], [19]- [21], [25], [29], [42], [44], [45] and [46]. It is observed that there is a large variation in the feature extraction methods, variation in number of features, variation in different types of cardiac signals and their classification accuracy.

However, there were certain limitations regarding classification accuracy, sensitivity and specificity. In real time applications of automated external defibrillators , the specificity is more important than the sensitivity. Selection of an efficient feature extraction scheme and choosing proper neural network classifier are important for efficient classification of cardiac arrhythmias. Most of the existing works distinguished normal and abnormal signals.

But, there is a necessity to classify abnormal categories also for proper medication and treatment. Early detection of cardiac arrhythmia is of paramount importance for saving the life of a patient as each arrhythmia needs to be treated in a specific manner such as ventricular arrhythmias are treated by using automated external defibrillator or with medications, sudden cardiac arrest is treated by using ICD, atrial arrhythmia is treated with medications or by using

ablation catheter and cardiac ischemia is treated with angioplasty or medications or bypass surgery. Thus, there is a need to classify severe cardiac arrhythmias, cardiac disorders and normal signals which can enable the doctor to give proper attention to save the life of heart patients. This aspect is the motivation for taking up this research work.

1.4 Objectives of the proposed research work

The research work aims at analysis and classification of seven types of cardiac signals (4 types of cardiac arrhythmias, 2- types of disorders and 1- normal sinus rhythm). Objectives of the research work are

- Cardiac arrhythmias analysis and classification in time domain.
- Cardiac arrhythmias analysis in spectral domain and classification using temporal and spectral features
- Cardiac arrhythmias analysis in HOS domain and classification using temporal, spectral and bispectral features.
- Cardiac arrhythmias analysis in wavelet domain and classification using wavelet features
- To develop an experimental setup for cardiac alert system using wavelet feature scheme for remote monitoring of heart patients.

1.5 Overview of the research work

Overview of the research work has been given in a block diagram of automatic arrhythmias classification as shown in Fig 1.19. This shows different signal processing techniques used for feature extraction and different supervised classifiers (RF, MLP & RBF).

ECG data of different cardiac signals has been collected from standard ECG data bases. 66% of ECG data has been used for training purpose and 34% of data is used for testing purpose.

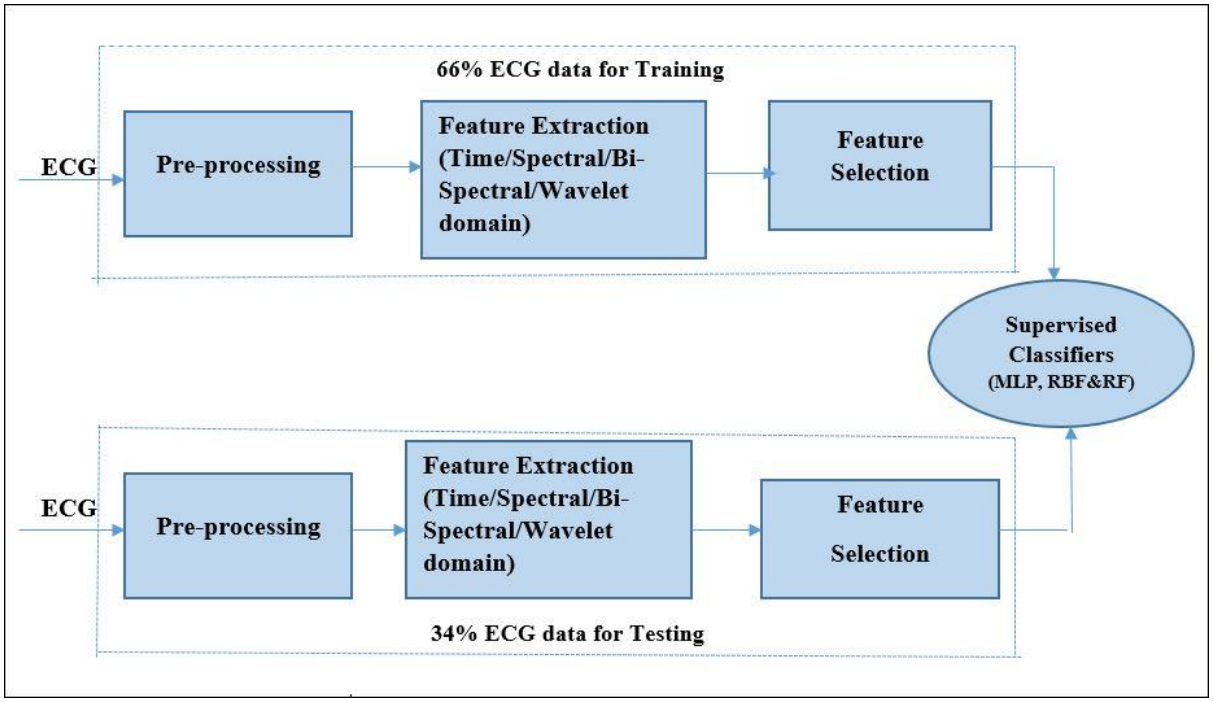

Fig 1.19 Block diagram for Arrhythmias Classification

Artifacts (unwanted noise signals) are present in ECG signals. Presence of these artifacts make the cardiac arrhythmias and disorders diagnosis is very difficult as they corrupt ECG signals. So, it is required to use filters in pre-processing stage to filter artifacts. There are mainly four types of artifacts encountered in ECG signals they are baseline wander, EMG noise and power line interference. Baseline wander is a low-frequency noise of around 0.6 Hz. To remove it, a high-pass filter of cut-off frequency 0.6 Hz can be used. EMG noise is due to muscle movement of patient while ECG recording. It is a high frequency noise of above 100 Hz and hence, it may be removed by using low-pass filter of an appropriate cut-off frequency. The power line interference (PLI) is centered at 50 Hz or 60 Hz with a bandwidth of less than 1 Hz. Notch filter is used to remove PLI. However, the baseline wander and other wideband noises are easy to be suppressed by using the software scheme instead of using analog circuits. Thus, de-noising of ECG signals is very important for further processing.

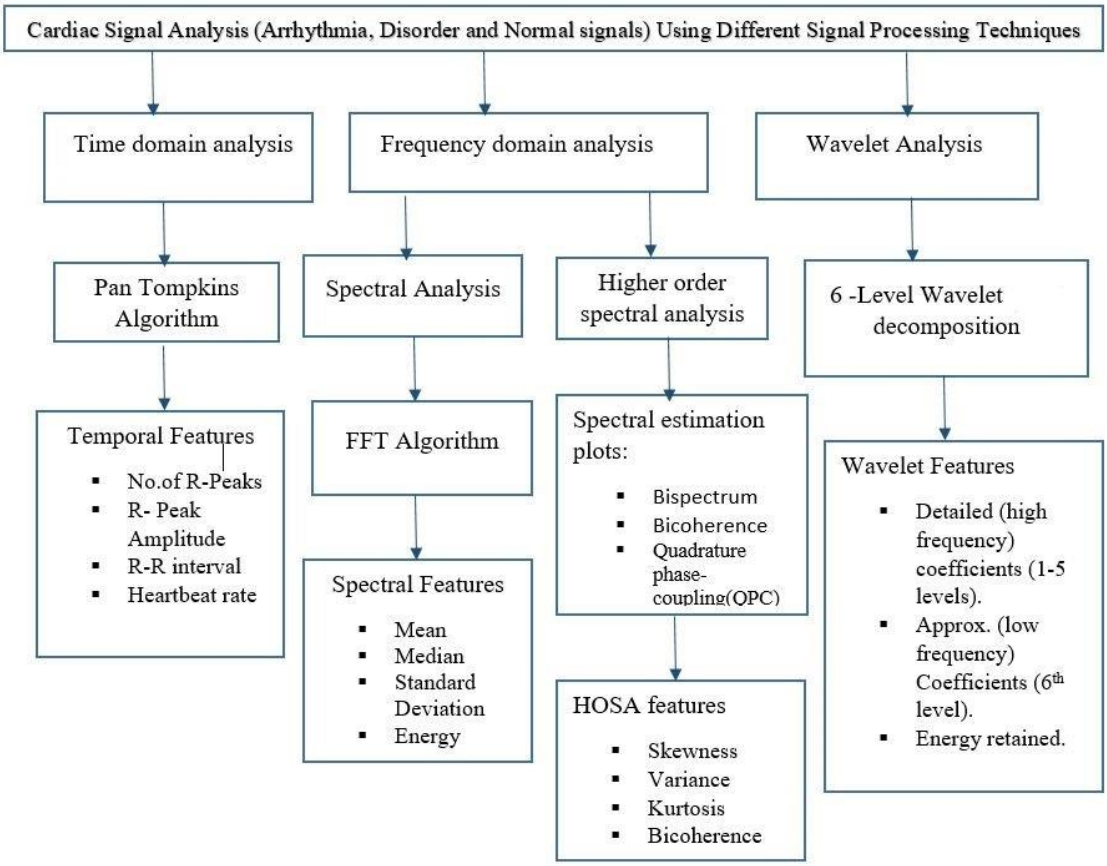

Fig 1.20 Cardiac signal analysis using signal processing techniques for feature extraction

In ECG signal processing stage, four different signal processing techniques have been used for cardiac signal analysis for feature extraction as shown in Fig 1.20. In time domain, temporal features are extracted using Pan Tompkins's algorithm. Temporal features are number of R-peaks, R-R intervals, amplitude of R-peaks and heartbeat rate. In spectral domain, spectral features are extracted using FFT algorithm. Frequency spectrum is divided into five regions i.e., Region R1: 0-2 Hz, Region R2: 2-8 Hz, Region R3: 8-16 Hz, Region R4: 16-22 Hz and Region R5: 22-32 Hz. In each region, spectral features such as mean, median, standard deviation and energy are computed. In higher order spectral domain, higher order spectral features such as skewness, variance and kurtosis are computed and in wavelet domain, using 6 level wavelet decomposition technique wavelet features are extracted. Wavelet based features are high frequency detailed coefficients (min and max) and standard deviation from 1 to 5 levels and low frequency approximation coefficients (min and max) & standard deviation from 6^{th} level. Later, the proposed work aims at classification of 7 types of cardiac signals using these selected features. These features are fed to different supervised classifiers such as Multi-Layer

Perceptron (MLP), Random Basis Function (RBF) and Random Forest (RF). In this work, 66% of ECG data is used for training purpose and 34% of data is used for testing purpose. The training to testing dataset split ratio is selected based on prediction and accuracy. Specific ratio approximately 2:1 is selected to overcome the problem of data under fit and over fit.

All the four signal processing methods and classifiers used in this work are better compared to the existing methods. However, the wavelet based feature scheme with MLP classifier proposed in the last approach is superior in terms of number of cardiac arrhythmias classification and enhancement of classification accuracy, sensitivity and specificity. This efficient wavelet based feature scheme is used to develop an experimental set up for a cardiac alert system.

1.6 Database details

The MIT-BIH Arrhythmia Database [1] was the first generally available set of standard test material for evaluation of arrhythmia detectors and it has been used for that purpose as well as for basic research into cardiac dynamics at about 500 sites worldwide since 1980. Together with the American Heart Association (AHA) Database, it played an interesting role in stimulating manufacturers of arrhythmia analysers to compete on the basis of objectively measurable performance and much of the current appreciation of the value of common databases, both for basic research and for medical device development and evaluation. In this research work, annotated databases of ECG are used [1]. NSR data has been collected from MIT-BIH Normal Sinus Rhythm data base (nsrdb), SVT has been collected from MIT-BIH Supraventricular arrhythmia data base (svdb) and AF data has been collected from MIT-BIH atrial fibrillation data base (afdb),VT data has been collected from Ventricular Tachyarrhythmia Database (CUDB) [40], VF data has been collected from Malignant Ventricular Ectopy Database (VFDB) [55], CI data has been collected from European ST_T database [39] and SCA data has been collected from sudden cardiac death holter data base [55]. ECG data of 1-minute duration and a sampling frequency of 250 Hz has been collected and used directly except NSR and SVT data. These two data bases have been resampled with 250 Hz as their available sampling frequency is 128 Hz. For each one minute data 15000 discrete samples are available.

The following Table1.2 shows, ECG data types and their record numbers used in the proposed research work.

Table 1.2 ECG data records

S.No	ECG signal	Record Numbers	No. of records
1.	CI	e0104, e0105 e0106,e0107,e0108 , e0110, e0111, e0112,e0113, e0114 ,e0118, e0119, e0121, e0123, e0125	15
2.	SCA	30,31,32,33,34,36,37,38,39,41,42,43,44,45,46	15
3.	AF	04043,04048,04126,04746,04936,05091,06426,06453,07162, 07859, 7879,07910,08215,08219,08434	15
4.	VF	418,419,421,425,427,428,429,430,602,605,607,609,610,611, 612	15
5.	VT	cu01, cu03, cu05, cu06, cu07, cu08, cu09, cu11, cu12, cu13, cu14, cu15, cu16, cu18, cu19	15
6.	SVT	801,802,803,807,808,809,810,811,812,820,821,822,823,824, 825	15
7.	NSR	16265,16272,16273,16420,16483,16539,16773,16786,16795, 17052, 17453,18177,18184,19093,19830	15
		Total no. of records	**105**

1.7 Tools used for ECG analysis and classification

In this research work, Matlab R2017a tool box is used Cardiac Signal Analysis. MATLAB, the language of technical computing, is a programming environment for algorithm development, data analysis, visualization, and numeric computation. Engineers and scientists worldwide rely on these product families to accelerate the pace of discovery, innovation, and development in automotive, aerospace, electronics, financial services, biotech-pharmaceutical, and other industries. It is the leading developer of mathematical computing software Millions of engineers and scientists worldwide use MATLAB to analyse and design the systems and products transforming our world. The matrix-based MATLAB language is the world's most

natural way to express computational mathematics. Built-in graphics make it easy to visualize and gain insights from data. The desktop environment invites experimentation, exploration, and discovery.

In this research work, Waikato Environment for Knowledge Analysis (Weka) tool is used for Cardiac signals classification, Weka tool is developed at the University of Waikato, New Zealand, is free software licensed under the GNU General Public License, and the companion software to the book "Data Mining: Practical Machine Learning Tools and Techniques". [59] WEKA is a collection of different machine learning and neural network algorithms which are used for data mining tasks. The machine learning algorithms such as Random Forest (RF) and neural network algorithms such as Multi-Layer Perceptron (MLP) and Random Basis Function (RBF) can be applied directly to a given dataset. It contains tools for data processing, classification, regression, clustering, association rules and visualization.

1.8 Thesis Organization

The research work carried out in this thesis is organized in to seven chapters. The chapter wise description of the thesis is outlined below.

First chapter: This first chapter introduces anatomy and electrical functioning of heart, need of arrhythmias analysis and classification, motivation, objectives, overview of the research work, data base details, tools used for feature extraction and classification and thesis organisation.

Second chapter: In this chapter, the literature is reviewed in detail. Various researchers' contributions have been understood and presented briefly. The remarks and limitations on their contributions are highlighted and motivation for the proposed research work has been concluded.

Third chapter discusses cardiac arrhythmias analysis and classification in time domain. For that purpose temporal features are extracted using Pan Tompkin's algorithm for different cardiac arrhythmias. The machine learning algorithms such as Random Forest (RF) and neural network algorithms such as Multi-Layer Perceptron (MLP) and Random Basis Function (RBF). Performance comparison of cardiac arrhythmias classification and conclusion are given.

Fourth chapter describes cardiac arrhythmias analysis and classification in spectral domain.

For that purpose spectral features are extracted using FFT algorithm for different cardiac arrhythmias. The machine learning algorithms such as Random Forest (RF) and neural network algorithms such as Multi-Layer Perceptron (MLP) and Random Basis Function (RBF). Performance comparison of cardiac arrhythmias classification and conclusion are given.

Fifth chapter discusses cardiac arrhythmias analysis and classification in higher order spectral domain. For that purpose, bispectral features are extracted from bispectrum, bicoherence and quadrature phase coupling plots for different cardiac arrhythmias. The machine learning algorithms such as Random Forest (RF) and neural network algorithms such as Multi-Layer Perceptron (MLP) and Random Basis Function (RBF). Performance comparison of cardiac arrhythmias classification and conclusion are given.

Sixth chapter narrates cardiac arrhythmias classification in wavelet domain. For that purpose, wavelet features are extracted using discrete wavelet transform for different cardiac arrhythmias. The machine learning algorithms such as Random Forest (RF) and neural network algorithms such as Multi-Layer Perceptron (MLP) and Random Basis Function (RBF). Performance comparison of cardiac arrhythmias classification and conclusion are given.

Seventh chapter presents the conclusion of the research work done and future scope for the research work.

Appendix presents an experimental setup of cardiac alert system for remote monitoring of cardiac patients which has been application of wavelet based feature scheme.

Chapter 2

Literature Review

This chapter presents a literature review on the work done by various researchers for identification and classification of normal and cardiac arrhythmias. Different signal processing techniques have been used by different researchers for feature extraction and classification. Some existing contributions that have been made by researchers are explained and their limitations are given in this chapter. Some improvements are aimed in the proposed work for overcoming these limitations. Further, few more cardiac arrhythmias and disorders are considered for analysis and classification in the proposed work.

2.1 Introduction

In the last two decades, this field of cardiac arrhythmias classification has attracted the attention of researchers because of its importance in early diagnosis of severe cardiac problems. The different research areas in this field include cardiac signal (normal, arrhythmias and disorders) analysis, identification and classification. The need for the automatic classification of cardiac arrhythmia arises in different contexts. Identifying cardiac disorders belonging to a different ventricular arrhythmias and atrial arrhythmias. Classification of cardiac arrhythmias in time domain [2], [3], [4], [5], [6], [7] ,[8] and [9]; spectral domain [18] and [19]; higher order spectral domain [21], [25], [27], [30], [33], [74] and [89] and wavelet domain [20], [29], [42], [43], [44], [45], [46], [70] and [72].The cardiac arrhythmias classification field attracted the attention of researchers to enhance classification accuracy and for accurate detection of severe cardiac arrhythmias and disorders to save the life of heart patients. Since, last two decades this field has attracted the attention of investigators to use artificial intelligence application in biomedical field. A review of literature related to cardiac arrhythmias and disorders identification and classification is solely focused in this chapter.

2.2 Cardiac arrhythmias analysis and classification in time domain

A review of literature related to cardiac arrhythmias and disorders identification and classification in time domain is focused in this literature.

Pan-Tompkins et al [2] have developed a real time QRS detection algorithm based on slope, amplitude, and width of the QRS complex. This method used band pass filter to reduce the influence of muscle noise, 60 Hz power line interference. QRS detection algorithm correctly detected 99.3% of the QRS complexes.

Limitations/remarks: Many researchers extracted morphological features using this QRS detection and classified normal and cardiac arrhythmias. This method may not be sufficient to describe the complex changes that take place in ECG as heart beat rate increases or decreases. These dynamics are important to be explored further to identify different types of cardiac arrhythmias.

M. Vijayavanan et al. [5] used an efficient technique for automatic classification of normal and cardiac arrhythmia signals on MIT-BIH arrhythmia database. Sampling rate has been used as 360 Hertz .Wavelet analysis to extract morphological features such as P, Q, R, S, T peak points, QRS complex duration, PR interval, ST interval, QT interval, RR interval, ST segment and PR segment and these 12 features were fed to Probabilistic Neural Network (PNN) classifier for classification Normal Sinus Rhythm and cardiac arrhythmia (which is abnormal). So, in this work, normal and abnormal categories only were considered. About 150 records of each category were given for training and 50 untrained records were given for testing by using the Probabilistic Neural Network (PNN). They used data durations of 5, 10, 15 and 20 minutes for observing classification accuracy. Classification accuracy varied with changing data duration of the ECG signal. For 20 minutes data duration, 96.5% classification accuracy was obtained.

Limitations/remarks: Only normal and arrhythmia categories were classified. The type of arrhythmia was not known. Some more dynamics are to be explored further to classify different arrhythmias.

Mujeeb Rahman et al. [6] extracted potential biomarkers of arrhythmia using two algorithms i.e, Pan-Tompkins Algorithm and Wavelet based algorithm. ECG signals used in in this work were downloaded from the MIT-BIH arrhythmia database. These signals were then imported to MATLAB tool and pre-processed for noise removal, four temporal features such as QRS duration, RR interval and PR interval were extracted. Heartbeat rate was calculated. Based on

these features performance of the two algorithms was compared and it was proven that the Pan-Tompkins algorithm was more accurate than the wavelet transform based algorithm.

Limitations/remarks: This work shows the importance of certain temporal features such as QRS complex, R-R interval, P-R interval and heart beat rate. This work did not classify different types of cardiac arrhythmias.

.

V. Vijaya et al. [4] used modified Pan Tompkins algorithm to extract two temporal features (number of R-peaks and R-R interval). These two temporal features are used to distinguish sudden cardiac arrest and normal sinus rhythm. For this work, NSR data for records (16265, 16273, 16539, 16773 and 16775) has been collected from MIT BIH Normal Sinus Rhythm data base (nsrdb) and SCA data for records (30, 31, 32, 33, 34, 36 and 38) has been collected from Sudden cardiac death holter data base[55]. The duration of signal was selected as 4 seconds only. Sampling frequency (fs) of cardiac signal has been selected as 200 samples/sec and window size is considered as 30 samples. They computed No. of R-peaks and R-R interval using Pan Tompkins algorithm for NSR and SCA using 1000 samples. They found out that No. of R-peaks for SCA is found to be less compared to NSR and R-R interval for SCA is found to be compared to NSR.

Limitations/remarks: Only normal and sudden cardiac arrest (cardiac disorder) signals were analysed based on two temporal features. These two features may not be sufficient to describe the other types of arrhythmias.

Rathnakara et al. [37] used an efficient algorithm to differentiate normal and arrhythmia ECG signals. The arrhythmia signals are classified with variation in heartbeat rate. Heartbeat rate below 60bpm is considered as bradycardia and Heartbeat rate above 80bpm is considered as tachycardia. The steps used by the algorithm are QRS peak detection by Pan-Tompkins algorithm, Baseline wandering noise removal and differentiating ECG signal into NSR and arrhythmia. Compared the obtained values with threshold values and classified into normal and arrhythmia signals.

Limitations/remarks: The analysis of the signal is done based on hear beat rate variabaility. Further, it can also be deeply implemented using various temporal features like RR intervals, No. of R peaks/sample, R peak amplitude, etc. and classification can be done using various machine learning techniques.

2.3 Cardiac arrhythmias analysis and classification in spectral domain

A review of literature related to cardiac arrhythmias & disorders identification and classification in spectral domain is focused in this literature.

Usman Rashed et al. [19] In this work, 4 to 5 min of ECG data was used instead of 24 hours to detect the possibility of Sudden Cardiac Arrest. For this work, NSR data for records (16272, 16273, 16539, 16773, 16483, 16795, 16786 and 16420) and SCA data for records (30, 31, 33, 35, 39, 41, 46 and 52) has been collected from MIT BIH database. In the data base, NSR signals were originally sampled at 128Hz and SCA signals at 256Hz. Before spectral analysis, each signal was pre-processed. In order to apply the signal processing techniques equally to each record signal and preserve most of the information, each signal was re-sampled to 500Hz. After re-sampling, the mean was removed from each ECG signal and then signals were passed through a 3rd order low-pass Butterworth filter by setting cut of frequency 32 Hz for preprocessing. For spectral analysis, Fast Fourier Transform (FFT) model using the Discrete Fourier Transform was considered and implemented it using Matlab. Fast Fourier Transform (FFT) on QRS complex was used to extract time and frequency information from the ECG signals.

The obtained frequency spectrum was divided into five regions (R1 to R5):

Region R1: 0-2 Hz
Region R2: 2-8 Hz
Region R3: 8-16 Hz
Region R4: 16-22 Hz
Region R5: 22-32 Hz

Spectra in the above regions were plotted to gain the information regarding the variation and energy localization. Then spectral parameters including mean, median, standard deviation, energy and power were selected to represent the spectra in the respective region. Hence, they discovered that the normal ECG rhythm of patient suffering from Sudden Cardiac Death has:

1) Lower spectral energy.
2) Low frequency range of first lobe.
3) Negligible energy in region 4 (16-22 Hz).

Classification can be done on basis of these above three findings. Further authors concluded that less than 5-minutes ECG data will be sufficient to detect possibility of SCA in spectral domain.

Limitations/remarks: From their work, it is noticed that ECG data of 24 hours may not be required for identification of sudden cardiac arrest in spectral domain as spectrum of ECG data of 24 hours or 1hour or 1min was same. Only normal and sudden cardiac arrest (cardiac disorder) signals were distinguished based on 5 spectral features analysis. In this work, energy difference of both signals observed in Region4 (16-22 Hz) region, instead of Region3 (8-16 Hz) region. This work distinguished two signals only. They did not use these spectral parameters for cardiac arrhythmias classification.

Glenn A. Myers et al. [18] described a method of power spectrum analysis on 24 hours ambulatory ECG's. This method was used to segregate three groups of people of normal, heart patients with history of SCD and without history of SCD. In this work, compared power spectrum results with non-power spectrum results.

Limitations/remarks: This work distinguished only three groups of cardiac signals (NSR, SCD and Non SCD) based on heart rate variability using power spectral method and non-power spectral method. In their work, arrhythmias classification was not addressed.

2.4 Cardiac arrhythmias analysis and classification in higher order spectral domain

A review of literature related to cardiac arrhythmias and disorders identification and classification in higher order spectral domain is focused in this literature.

L. Khadra et al. [21] used high order spectral analysis technique for quantitative analysis and classification of cardiac arrhythmias. They classified four types of cardiac signals such as AF, VT, VF and NSR. A total of 8 -NSR, 12- AF, 11 -VT and 12 -VF (total 43 records) were considered for this work. Using bispectral analysis, bispectrum and bicoherence plots of above signals were evaluated with different bicoherence values. The classification results revealed the importance of higher order spectral analysis in identifying the life threatening arrhythmia which

is an important tool in ICU that enables online monitoring of the cardiac activities. The results showed a significant difference in parameter values for different arrhythmias.

Limitations/remarks: The medical statistics obtained by using HOSA technique were Sensitivity(S) as 89.2% and Specificity (Sp) as 93.55%. The sensitivity and specificity obtained can be enhanced further by using different classifiers.

I. A. Karaye et al. [26] analysed cardiac signals such as NSR, RBBB, LBBB, paced beat and atrial premature beats using higher order spectral analysis to reveal the complex dynamics of ECG signals. General characteristics for each of these classes in the bispectrum and bicoherence plot for visual observation have been presented and also extracted higher order statistical parameters (skewness, kurtosis and variance) using HOSA and temporal features (RR interval) using Pan Tompkins algorithm were used for classification of five different types of signals and obtained average classification accuracy as 94.9%.

Limitations/remarks: Authors used both morphological and higher order statistical parameters (hybrid) to classify 5 types of cardiac signals and obtained an average classification accuracy as 94.9% and this work can be extended to identify other types of cardiac arrhythmias.

K. Sharmila et al. [25] used higher order statistics (HOS) analysis to identify sudden cardiac arrest. Estimation of higher order spectra on the basis of cumulants is more useful for the analysis of stochastic signals whereas estimation of higher order spectra on the basis of moments is more useful for the analysis of deterministic signals.

Limitations/remarks: Authors have used both spectral and higher order statistical parameters to distinguish two types of cardiac signals (NSR and SCA). This work can be extended to identify other types of cardiac arrhythmias and disorders.

2.5 Cardiac arrhythmias analysis and classification in Wavelet Domain

A review of literature related to cardiac arrhythmias and disorders classification in wavelet domain is focused in this literature.

H.M. Rai et al. [44] used DWT based feature extraction scheme and BPNN Classifier to classify normal and abnormal signals. Normal class 25 files and abnormal class 20 files of

1minute duration were collected from MIT-BIH arrhythmia database (out of 48 files, 45 files have been considered).

The extracted DWT based features are shown below

1. Mean of the absolute values of the details and approximation coefficients at each level.
2. Standard deviation of the details and approximation coefficients in each sub band.
3. Variance values of the details and approximation coefficients at each level.

48 wavelet features and 16 statistical and morphological features such as standard deviation of RR interval, PR interval, PT interval, ST interval, TT interval, QT interval, maximum values of P, Q, R, S, T peaks and number of R peaks count are used. Total 64 hybrid features are considered and fed to the Back Propagation Neural Network (BPNN) classifier and the system performance was measured on the basis of accuracy. The average classification accuracy obtained as 97.8 %.

Limitations/remarks: The limitation of this work is that it has used 64 features and for classification of two types of signals. The classification can be performed for different number of ECG signals.

Maedeh Kiani Sarkaleh et al. [45] used discrete wavelet transform for processing ECG recordings. They classified both normal and two types of cardiac disorders using 10 files of ECG records. It produced results with classification accuracy of 96.5%. Extracted 24 wavelet features using 8 level wavelet decomposition and these features were fed to MLP classifier and produced results with 24 input neurons and 2 linear output neurons. The performance of this MLP neural network was tested using the Mean Squared Error (MSE) parameter. This error is computed using the differences between the actual outputs and the outputs obtained by the trained NN.

Limitation: The limitation of this work is that it has only used 10 records out of 48 available records in the ECG Arrhythmia database. So, the training set obtained after extracting features from the samples those records suffers from lack of diversity. Also, this work classified only three types of cardiac signals, while it ignores the other classes of severe arrhythmias. This work results are showing 24 input neurons 2 output neurons but aimed to classify three types of cardiac signals

N. K. Dewangan et al. [106] Used four morphological features i.e. R peak amplitude, QRS duration, RR interval and PR interval along with eight wavelet based features i.e. variance of detail coefficients obtained after eight level wavelet decomposition of each ECG beats. LM Back propagation algorithm was used to train the multilayer feed-forward back propagation networks. 5 types of arrhythmias were detected by this system.

Limitations/remarks: This existing neural network based global classifier obtained sensitivity as 65%, specificity as 92%, positive predictive value as 63% and classification accuracy as 87%.

E. D. Ubeyli et al. [50] classified four types of cardiac disorders and NSR using Mixture of expert algorithm and produced results with an accuracy of 96.88%. The ECG signals were decomposed into time–frequency representations using discrete wavelet transforms (DWT) and statistical features were calculated to depict their distribution. The ME network structure was implemented for cardiac disorders classification using the statistical features as inputs. To improve classification accuracy, the outputs of expert networks were combined by a gating network simultaneously trained in order to stochastically select the expert that is performing the best at solving the problem. Five types of ECG beats (normal beat, congestive heart failure beat, ventricular tachyarrhythmia beat, atrial fibrillation beat and partial epilepsy beat) obtained from the Physio bank database were classified with an accuracy of 96.89% by the ME network structure.

Limitations/remarks: Five types of ECG signals were classified with an accuracy of 96.89%.

Ali Sadr et.al [51] distinguished performance of MLP and RBF algorithms based on available training data set. RBF algorithm is giving more accuracy when the size of training data set is relatively small whereas MLP algorithm is giving more accuracy when the size of training data set size is relatively large. Further, in literature survey, it has been reported that finding optimum and efficient feature set is a major challenge for arrhythmias classification. Selection of a suitable classifier also plays a significant role in improving the classification accuracy [94], [95]. The classification accuracy obtained using RBF classifier as 94% and MLP classifier as 92% for 50 number records.

Limitations/remarks: In this work, they compared of performance of MLP and RBF based on number records. MLP algorithm is being more accurate than RBF when the size of training data set size is relatively large.

Monalisa Mohanty et al. [47] used multi-domain features and supervised classifiers to classify VF, VT and NSR. The ventricular arrhythmia detection algorithm that combines ECG features with C4.5 classifier has been used in this work. The Ventricular Tachyarrhythmia Database (cudb) and MIT-BIH Malignant Ventricular Ectopy Database (vfdb) are used from physionet database. A total combination of 13 temporal, spectral and statistical features were considered. Further, the extracted features have been ranked in Gain Ratio Attribute Evaluation in order to improve the classification accuracy. Classification of selected features for VF, VT and normal sinus rhythm (NSR) was done by using two classifiers namely cubic support vector machine (SVM) and the C4.5 classifier .The obtained medical statistics were sensitivity as 90.97%, specificity as 97.86% and accuracy as 97.02% using C4.5 classifier. The obtained medical statistics were sensitivity as 79.43%, specificity as 81% and accuracy as 92.23% using SVM classifier.

Limitations/remarks: This work compared the classification results of SVM and C4.5 classifiers and proved that C4.5 was the better classifier. But the sensitivity of this classifier was very low to classify three types of signals. Sensitivity of the classification can be enhanced by using efficient feature schemes**.**

Pooja Bhardwaj et al. [49] successfully classified NSR and 4 types of cardiac disorders by using support vector machine (SVM) algorithm and obtained results with a total performance accuracy of 95.21%. The wavelet based temporal features were obtained by using Acq Knowledge software. This software is used for pre-processing and feature extraction. 18 wavelet based temporal features were extracted from ECGs and fed to SVM classifier. This method used 3,003 beats from the MIT-BIH Arrhythmia database. In this study, 70% data has been taken for training purpose and 30% data has been taken for testing purpose and achieved total average accuracy as 95.21% and average sensitivity as 85.43% for 5 types of cardiac signals (one normal and four arrhythmic beats).

Limitations/remarks: They might have taken unequal records of ECG signals and classified the ECG beats of 5 categories. Their sensitivity is very low which can be enhanced further using different classifiers and more number of features.

A summary of literature review has been presented in Table 2.1 and Table 2.2. It gives the summary of features, the classifiers, number of diseases and the classification accuracy obtained.

Table 2.1 Summary of literature review using time and spectral analysis

Time domain and Spectral domain Analysis			
Study by	**Records and Features**	**Algorithm**	**Cardiac Arrhythmia Analysis**
Pan and Tompkin [2] (1985)	Morphological features(slope, amplitude and width of the QRS complex)	Pan-Tompkins Algorithm	QRS detection has been done with 99.3% accuracy
V. Vijaya et al. (2012) [4]	Features-2 Temporal features (No. of R-peaks/1000 samples and R-R interval)	Pan-Tompkins Algorithm	Distinguished NSR and SCA
M. Vijayavanan et al. (2014) [5]	300 Records 12 -Morphological features	PNN classifier	Distinguished Normal and Arrhythmia with accuracy of 96.5%
Mujeeb Rahman K et al. (2019) [6]	8 records Features-4 temporal features (R-R interval, P-R interval, Q-T interval and QRS complex duration)	Pan-Tompkins Algorithm (PTA) and Wavelet based Algorithm (WBA)	PTA accuracy (99.95%) more than WBA (97.75%) accuracy.
Rathnakara et al. (2018) [37]	Temporal Features (RR intervals, No. of R peaks and R peak amplitude)	Modified Pan-Tompkins Algorithm	Distinguished Normal and Arrhythmia
Pooja Bhardwaj et al. (2012) [49]	Features-18 Morphological Features	SVM using LibSVM3	NSR, 4 types of Arrhythmias (5-Types)
Usman Rashed et al.(2008) [19]	8 Records, Features -5 Spectral features	FFT Algorithm	NSR and SCA(two types)

Table 2.2 Summary of literature review using HOSA and wavelet analysis has been presented

Higher Order Spectral domain Analysis				
Study by	**Records and Features**	**Classifier**	**Cardiac Arrhythmias**	**Classification Performance**
Ibrahim Abdullahi Karaye et al. (2012) [26]	47 records, Temporal and HOSA features	Feed forward ANN	NSR, LBBB,RBBB, PB and APB (5 types)	Sensitivity-88.4% Specificity-96.2% Accuracy- 94.9%.
L. Khadra et al. (2012) [21]	43-records (AF-12, VT-11, VF-12 and NSR-08) HOSA features	Bispectral contour analysis	NSR, VT, VF and AF (4 types)	Sensitivity - 89.2% Specificity - 93.55%
Wavelet Analysis				
Study by	**Records and Features**	**Classifier**	**Cardiac Arrhythmia**	**Classification Performance**
Ayad Mousa (2012) [42]	38 records (17-NSR and 21-VT) Features-wavelet, morphological and both wavelet and morphological	BPNN	NSR and VT (2-Types of signals)	Using wavelet features-84.21%, Using Morphological features-76.32%, Using both Wavelet and Morphological features -100%
H.M.Rai et al. (2012) [44]	45 Records (25 arrhythmia and 20 normal) Features-16 morphological and 48 wavelet features (Total: 64 features)	BPNN	Normal and Arrhythmia class (2-Types of signals)	Accuracy- 97.8%
Maedeh Kiani Sarkaleh et al. (2012) [45]	10 Records Features- wavelet features	MLP	Normal and 2-Arrhythmias (3-Types of signals)	Accuracy-96.5%
Mangesh Singh Tomar et al. [46]	62 Records ,25 features (14-NSR and 48-Arrhythmia) (20- wavelet and 5 statistical features)	BPNN	Normal and Arrhythmia classes (2-Types of signals)	Accuracy-98.4%

Jose Antonio Gutierrez-Gnecch el al. [109]	Features-wavelet and morphological features	PNN classifier	5 Arrhythmia types	AF-91.5%, Avg : 84.54%
Naser Safdarian et al. (2012) [24]	57 records Features-2 Temporal features	Fuzzy classifier using Genetic algorithm	NSR, VT and VF	Sensitivity - 95.22% Specificity - 96.0% Accuracy - 93.33%
Monalisa Mohanty et al. (2018) [47]	57 Records Features-13 Temporal and Statistical features	SVM and C4.5 classifier	NSR, VT and VF (3-Types)	SVM classifier: Sensitivity - 79.43%, Specificity - 81.44%, Accuracy - 92.23% C4.5 classifier: Sensitivity - 90.97%, Specificity - 97.86%, Accuracy - 97.02%
E. D. Ubeyli et al. (2009) [50]	Statistical parameters and ROC curves	Recurrent Neural Networks (RNN)	NSR and 4 diseases	Accuracy - 96.89%
Ali Sadr et al.(2011) [51]	50 records Wavelet features	Compared MLP and RBF classifiers	Normal and Arrhythmia (2types)	Average Accuracy using MLP classifier - 94% and Average Accuracy using RBF classifier - 96%

2.6 Concluding remarks

Due to wide variation in the number of cardiac signals and variation in number of features, it is difficult to draw the meaningful conclusions about the merits of any one approach over another. Some of studies have used recordings from clinical data collections, some of them used MIT-BIH database, European ST data base, SCD Holter database and some others have used AHA database. Further, it has been observed that, experiments were performed on different databases of different records and different classifiers. Therefore without applying each of these approaches to the same training and testing data, there appears to be no metric that can be applied to equate their results.

There is a lack of standardization of cardiac signal features. Feature extraction method temporally selects ECG features. So, the accuracy of any classifier depends on these selected features. A small variations in these selected features may cause a misclassification. Heart beat rate of the individuals is changing due to physiological conditions and the mental condition such as stress, excitement and other working activities. For ECG classification, no optimal classification rules exist which can help in the classification process. [53]

It has been found that classification accuracy depends on many parameters such as type of cardiac arrhythmia, diversity in arrhythmia, type of cardiac disorder, selected arrhythmia database, selected number of records, selected feature extraction technique and selected neural network classifier etc., It has been consistently observed that finding efficient feature scheme and classifier are very important for cardiac arrhythmias classification and has enormous scope for research work.

From the literature review it is identified that novel feature scheme and improving the classification accuracy are active research topics in this area which have been taken up in this proposed research work.

Chapter 3

Cardiac arrhythmias analysis and classification in time domain

3.1 Introduction

From the literature review, it has been consistently observed that temporal features have proved their significance in cardiac signal analysis. Most of the works distinguished normal and cardiac arrhythmias. In this work, a novel approach is proposed to analyse and classify 7 types of cardiac signals (4-arrhythmias, 2-cardiac disorders and 1-normal) using Pan Tomkins algorithm and artificial intelligence algorithms.

This chapter has been organized as follows. Section 3.2 describes briefly the overview of existing works. Cardiac arrhythmia analysis using temporal features is explained in section 3.3, different classification algorithms has been explained in section 3.4, cardiac arrhythmias classification based on proposed temporal features is explained in section 3.5, conclusions based on classification results have mentioned in section 3.6 and performance comparison has been done with the existing works is given in section 3.7.

3.2 Overview of existing works

In this section, the work done by some researchers was presented briefly. Pan-Tompkins et al. [2] peak detection algorithm correctly detected 99.3% of QRS complexes accurately. V. Vijaya et al. [4] used Pan Tompkins Algorithm to extract two temporal features (number of R-peaks and R-R interval) to distinguish sudden cardiac arrest from normal sinus rhythm. But, classification of arrhythmias was not done. M. Vijayavanan et al. [5] used 8 level wavelet decomposition for extraction of 12 morphological features (P, Q, R, S, T peak points, QRS complex duration, PR interval, QT interval, ST interval, ST segment, RR interval and PR segment). Only normal (NSR) and arrhythmia (abnormal) signals were distinguished by using Probabilistic Neural Network (PNN) classifier with a classification accuracy of 96.5%. Mujeeb Rahman et al. [6] used Pan-Tompkins Algorithm and Wavelet based algorithm for extraction of four temporal features (QRS duration, RR interval, heartbeat rate and PR interval). In this work, it has been proven that Pan-Tompkins algorithm is more accurate than wavelet transform based algorithm. In this work, classification of arrhythmias has not been addressed.

Rathnakara et al. [37] used a modified Pan Tompkins algorithm to extract temporal features such as RR intervals, No. of R peaks and R peak amplitude. This work used Turning point knot algorithm to remove base line wander noise. The analysis of ECG signal was done based on heartbeat rate variability. In this work, heartbeat rate below 60bpm was considered as bradycardia and heartbeat rate above 80bpm is considered as tachycardia. In this work, only normal (NSR) and arrhythmia signals were distinguished based on heartbeat rate.

3.3 Cardiac arrhythmia analysis using temporal features

In this work, existing Pan Tompkins algorithm has been used for feature extraction. Pan Tompkins algorithm identifies the QRS complexes based upon digital analysis of slope, amplitude, and width of the ECG data. The algorithm implements a special digital band pass filter. It can reduce false detection caused by the various types of interferences present in the ECG signal. The algorithm automatically adjusts the thresholds and parameters periodically to adapt the changes in QRS morphology and heart rate.

The processing steps in the Pan Tompkins algorithm as shown in Fig 3.1 are as follows,

1. In the first stage, ECG data of seven types of cardiac signals has been collected from standard ECG data bases.

2. In the second stage of pre-processing, the noise is eliminated from input ECG signals.

Base line wander (BW) noise (0.5Hz-2Hz) is observed in ECG signals, though it's filtered standard base. BW noise is present in the ECG signal during recording due to movement and respiration of the patients. So, BW removal is an important step in ECG signal processing. Otherwise important diagnostic information present in the ECG may be corrupted

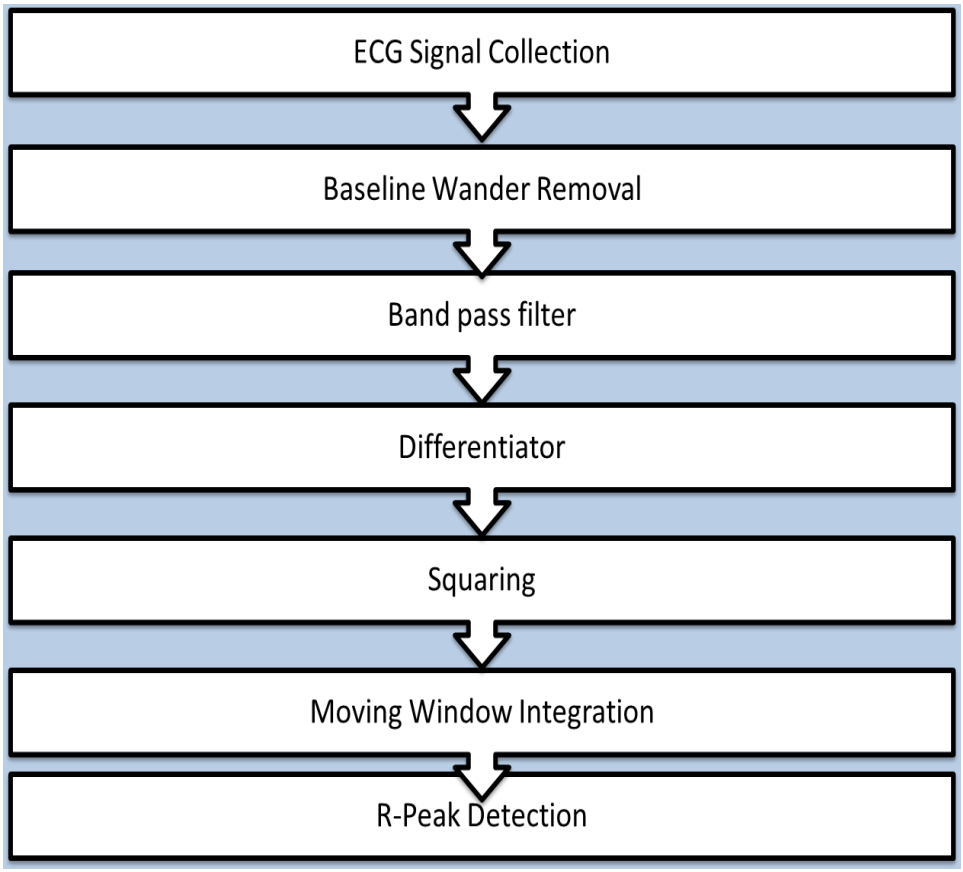

Fig 3.1 Pan Tompkins algorithm

So, a 3rd order Butterworth low pass filter is used to remove baseline wander noise from ECG signal by selecting cut off frequency 2Hz. The block diagram of Base line wander removal from the ECG signal is shown in Fig 3.2.

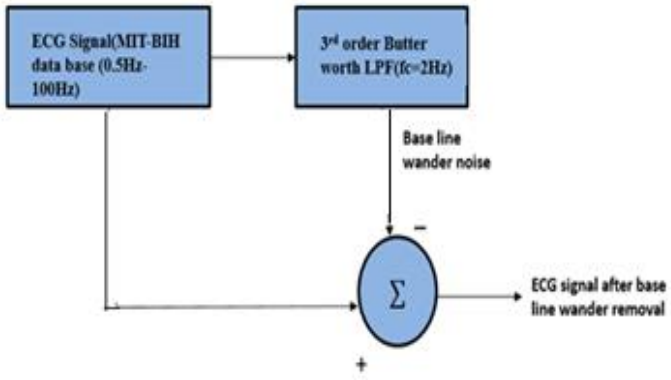

Fig 3.2 Base line wander removal

3. After removal of baseline wander noise from the main ECG signal, the signal is passed through band pass filter (BPF) for the extraction of QRS complex (5-15Hz). The QRS complex detection from the ECG signal is shown in Fig 3.3

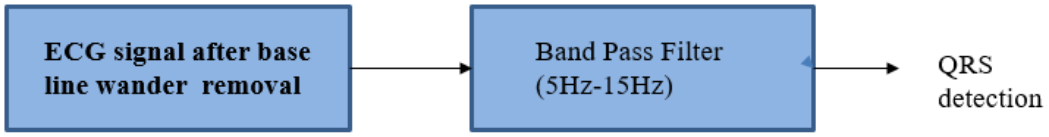

Fig 3.3 QRS detection

4. The next processing step is differentiation, it is a standard technique for finding the high slopes that normally distinguish the QRS complexes in ECG waves. ECG signal is differentiated by using 4th order high pass Butterworth filter with cut-off frequency of 30 HZ. The derivative procedure suppresses, the low frequency components of P and T waves and provides a large gain to the high-frequency components arising from the high slopes of the QRS Complex.

5. Next squaring operation makes the result positive and emphasizes large differences resulting from QRS complexes. The small differences arising from P and T waves are suppressed. The high frequency components in the signal related to the QRS complex are further enhanced. This is a nonlinear transformation that consists of point by point squaring of the signal samples.

6. Next squared waveform passes through a moving window integrator. This integrator sums the area under the squared waveform over a suitable interval, advances one sample interval, and integrates the new predefined interval window.

After differentiation and squaring operation, multiple peaks appear within the duration of a single QRS complex. Smoothing of the output of the preceding operation is done by using moving-window integration filter. Moving window integration is performed by the following equation.

$$y(n) = \frac{1}{N}\left[x(n-(N-1)) + x(n-(N-2)) + \cdots + x(n)\right] \tag{3.1}$$

The choice of the window width N is to be made with the following considerations: too large a value will result in the outputs due to the QRS and T waves being merged, whereas too small a value could yield several peaks for a single QRS complex. The choice of the duration of the sliding window results in a trade-off between false and missed detections. The ability to detect the presence of disorder of concern and percentage of detection peaks that are actually present. A window width of N = 50 was found to be suitable for fs = 250 Hz.

7. After moving window integration, R-peak detection is done by using fixed thresholding. Threshold is set as mean of the data.

8. Later R-R interval is computed from these results. With R-R intervals heartbeat rate has been calculated using the following expression

$$\text{Heartbeat rate} = \frac{60}{\text{RR Interval}} \tag{3.2}$$

7 types of ECG signals (four types arrhythmias- SVT, VT, VF and AF, two types of cardiac disorders-SCA & CI and normal signal-NSR) are analysed in time domain by using Pan Tomkins Algorithm. Ventricular Arrhythmias lead to serious disorder SCA. If neglected, it leads to sudden cardiac death. CI is also a serious disorder if neglected, it leads to heart attack will arise. Both disorders treatment is different. Similarly, different cardiac arrhythmias need different treatment. Early diagnosis is also important to save life of heart patients. Therefore, there is a need to classify these different cardiac signals. Using time domain analysis, the following four temporal features are extracted and used for classification purpose.

- R-Peak Amplitude
- No.of R-Peaks
- R-R Interval
- Heartbeat rate

The Simulation results of Pan Tompkins algorithm are shown below step wise from Fig 3.4 to Fig 3.9.

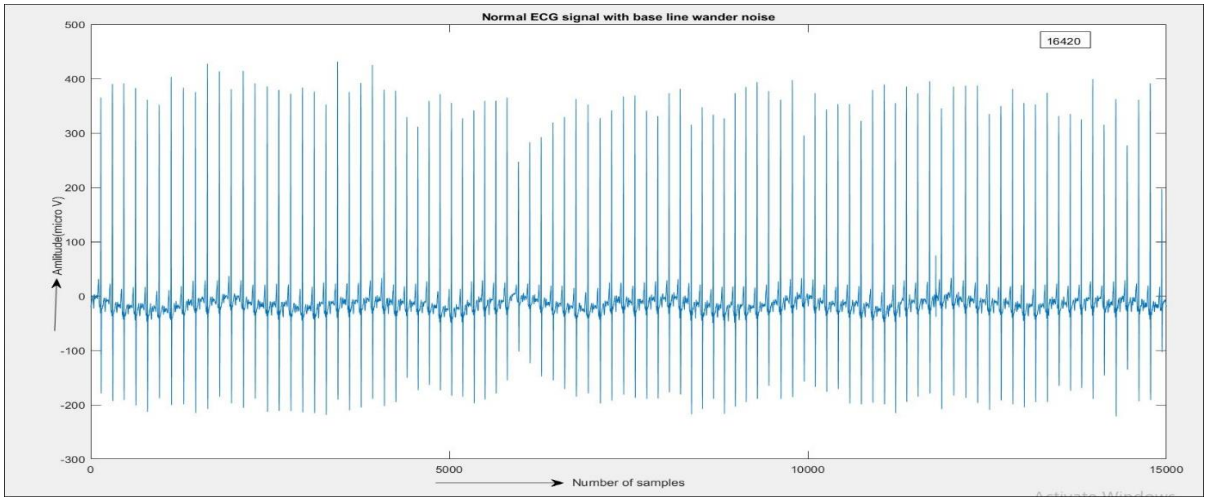

Fig 3.4 Normal ECG signal (record no 16420) with base line wander noise.

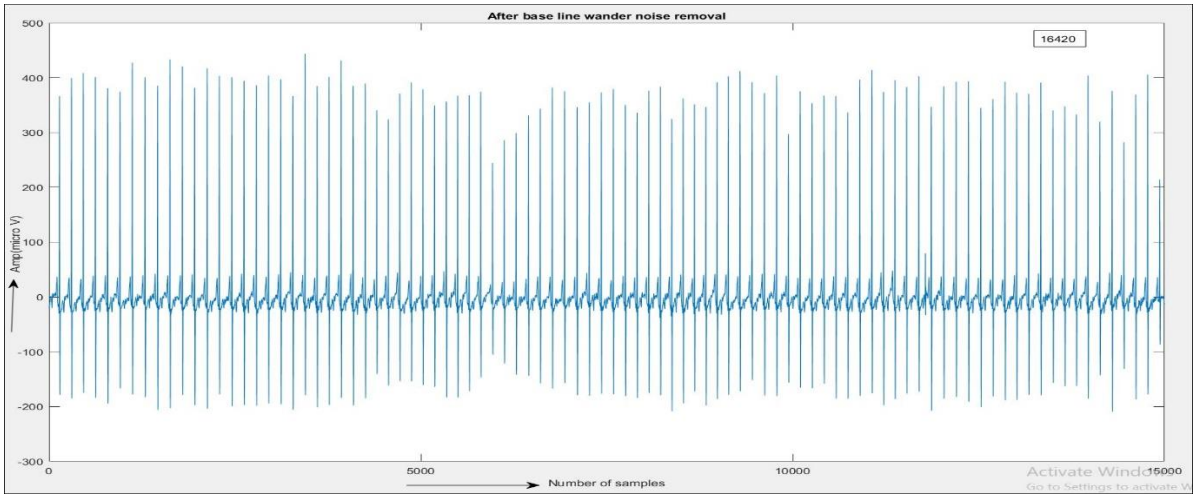

Fig 3.5 Normal ECG signal (record no 16420) after removal of base line wander noise

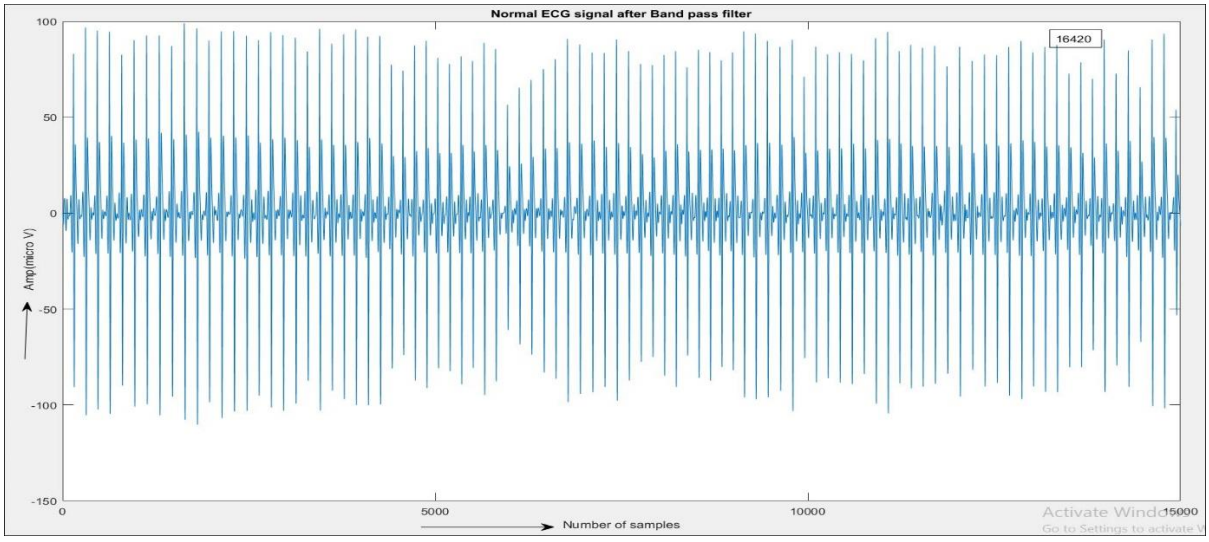

Fig 3.6 Normal ECG signal (record no 16420) after band pass filter

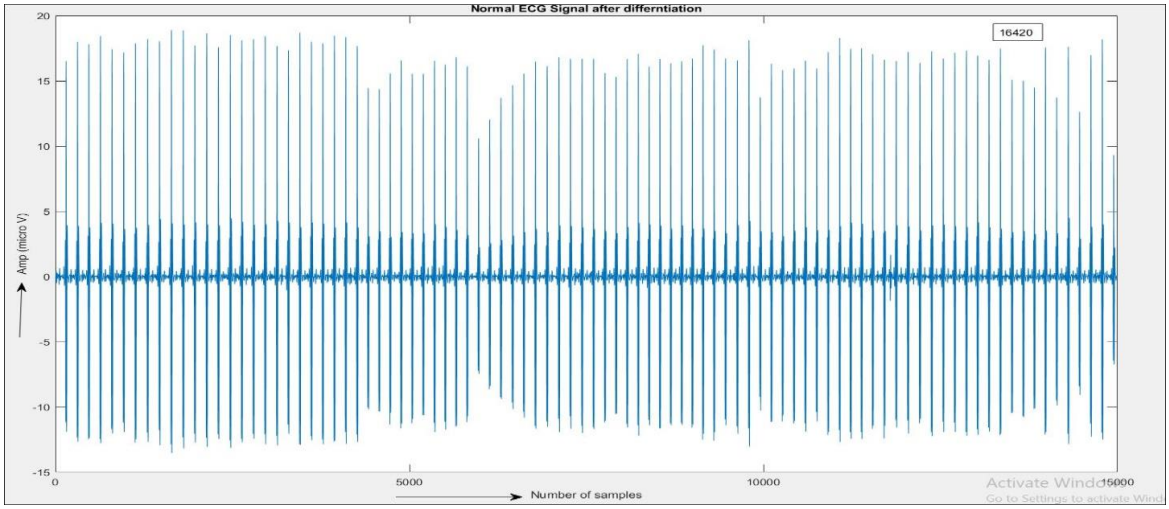

Fig 3.7 Normal ECG signal (record no 16420) after differentiation

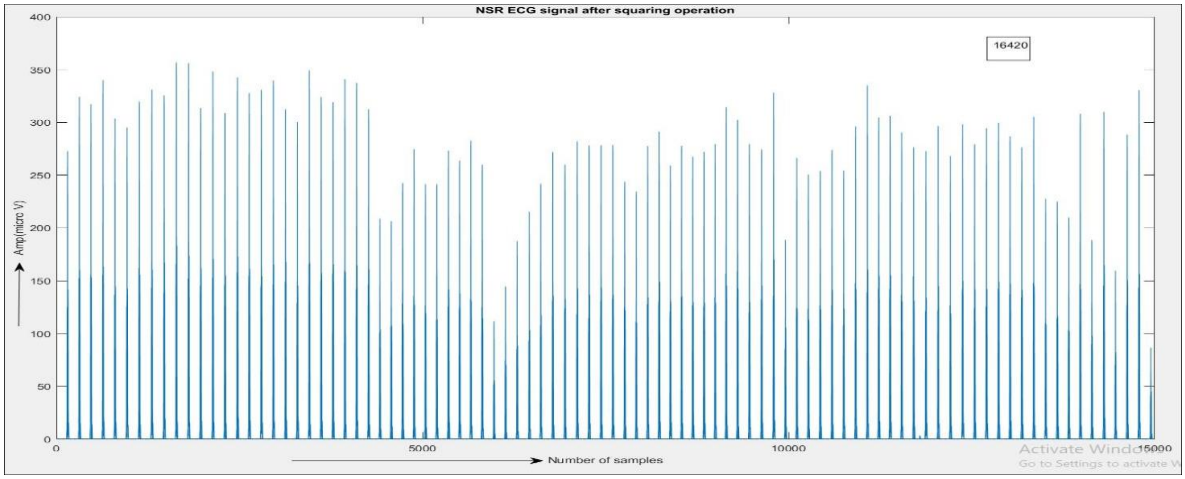

Fig 3.8 Normal ECG signal (record no 16420) after squaring operation

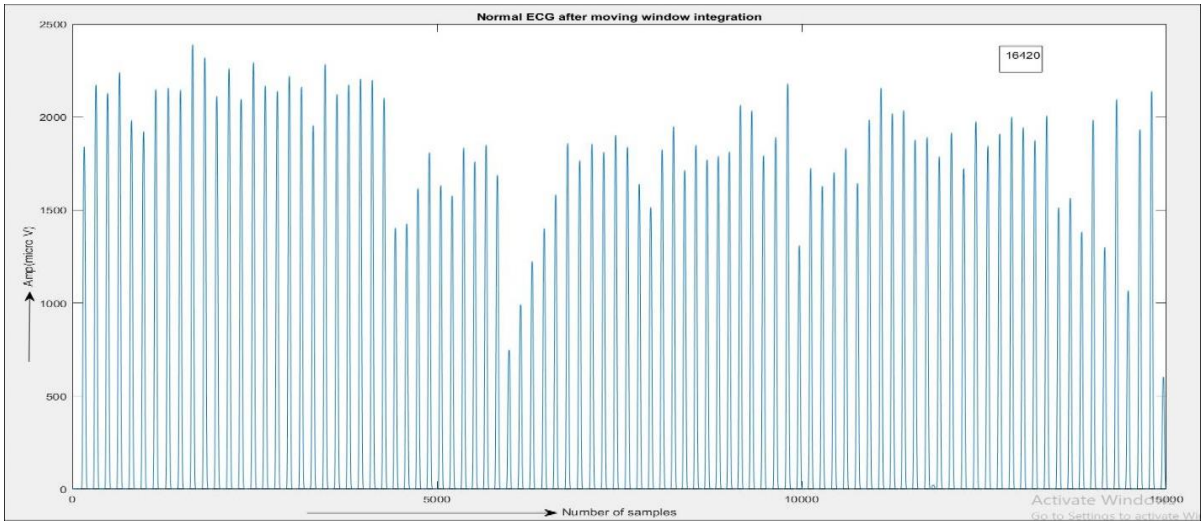

Fig 3.9 Normal ECG signal (record no 16420) after moving integration

The simulation results of a few records of Normal ECG signal (16265, 16273 and 16773) after implementing Pan Tompkins algorithm for 1minute (15000 samples) is shown in fig 3.10. From these simulation results, computed temporal features of NSR records.

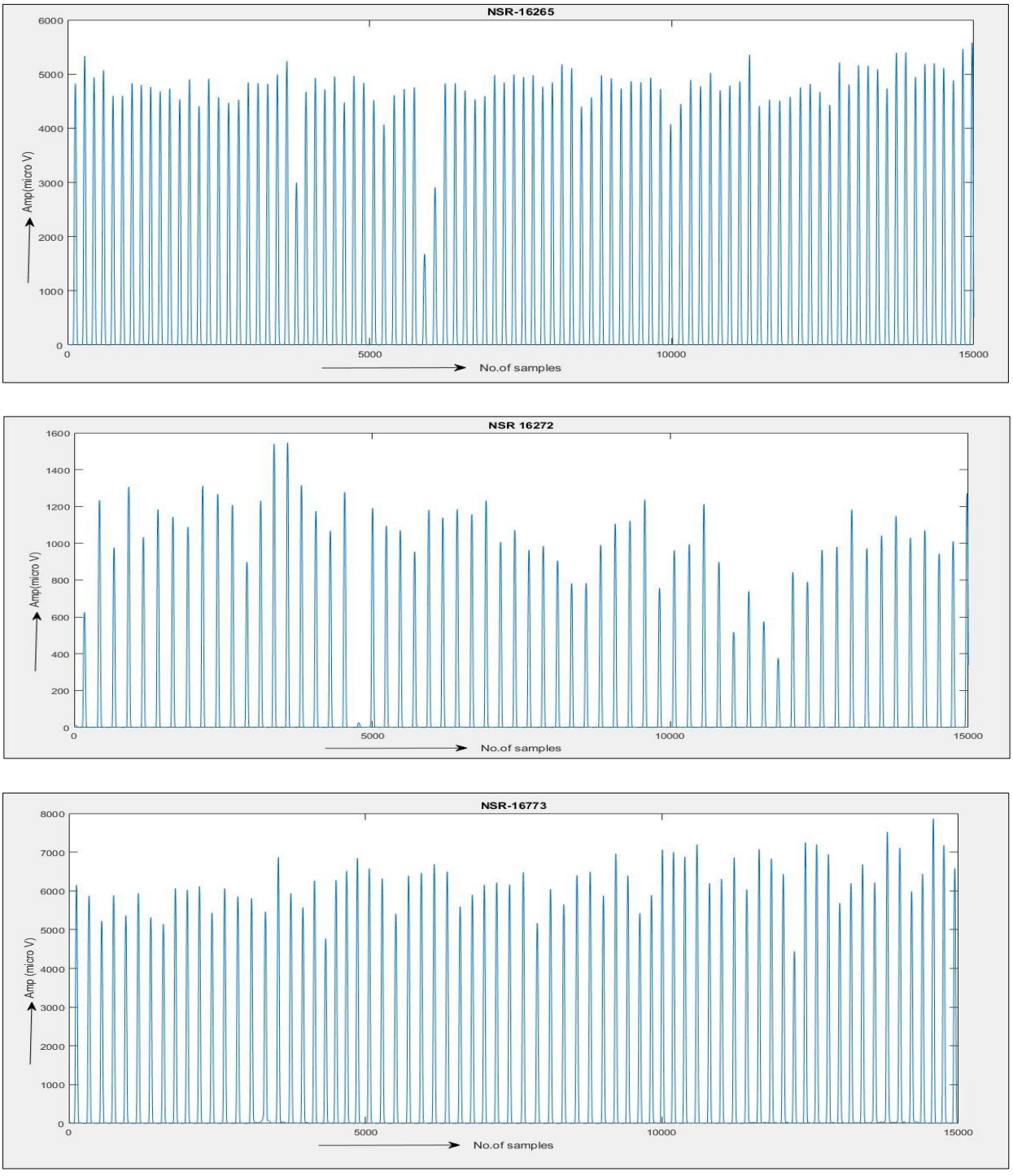

Fig 3.10 Simulation results of NSR records [16265, 16273 and 16773]

The simulation results of a few records of SVT (820, 823 and 800) for after implementing Pan Tompkins algorithm for 1 minute (15000 samples) is shown in Fig 3.11. From these simulation results, computed temporal features of SVT records.

Fig 3.11 Simulation results of SVT records [820,823 and 800]

The simulation results of a few records (cu01, cu15 and cu12) for Ventricular Tachycardia ECG signal after implementing Pan Tompkins algorithm for 1minute (15000 samples) is shown in Fig 3.12. From these simulation results, computed temporal features of VT records.

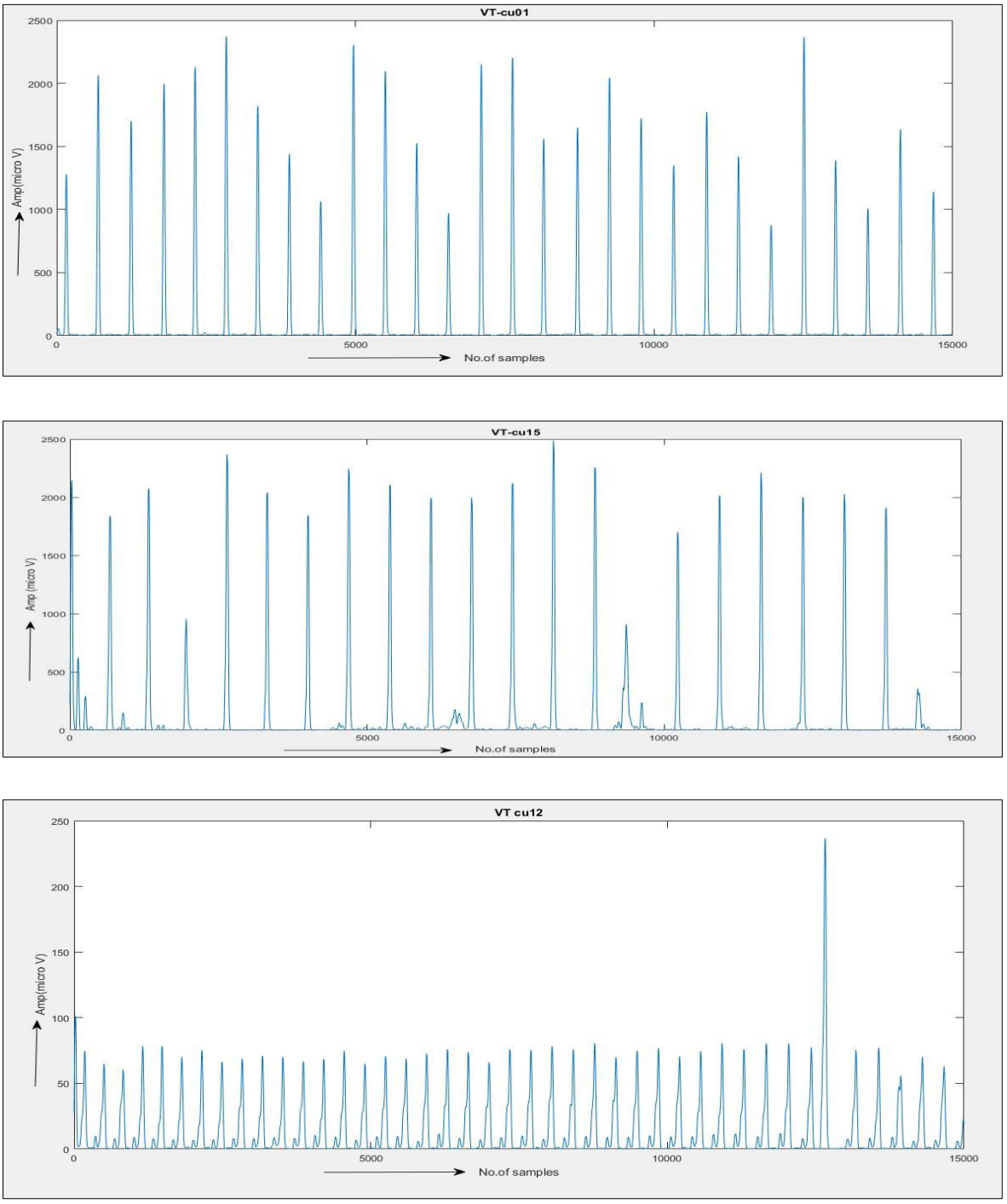

Fig 3.12 Simulation results of VT records [cu01, cu15 and cu12]

The simulation results of a few records (602, 609 and 430) for Ventricular Fibrillation ECG signal after implementing Pan Tompkins algorithm for 1minute (15000 samples) is shown in Fig 3.13. From these simulation results, computed temporal features of VF records.

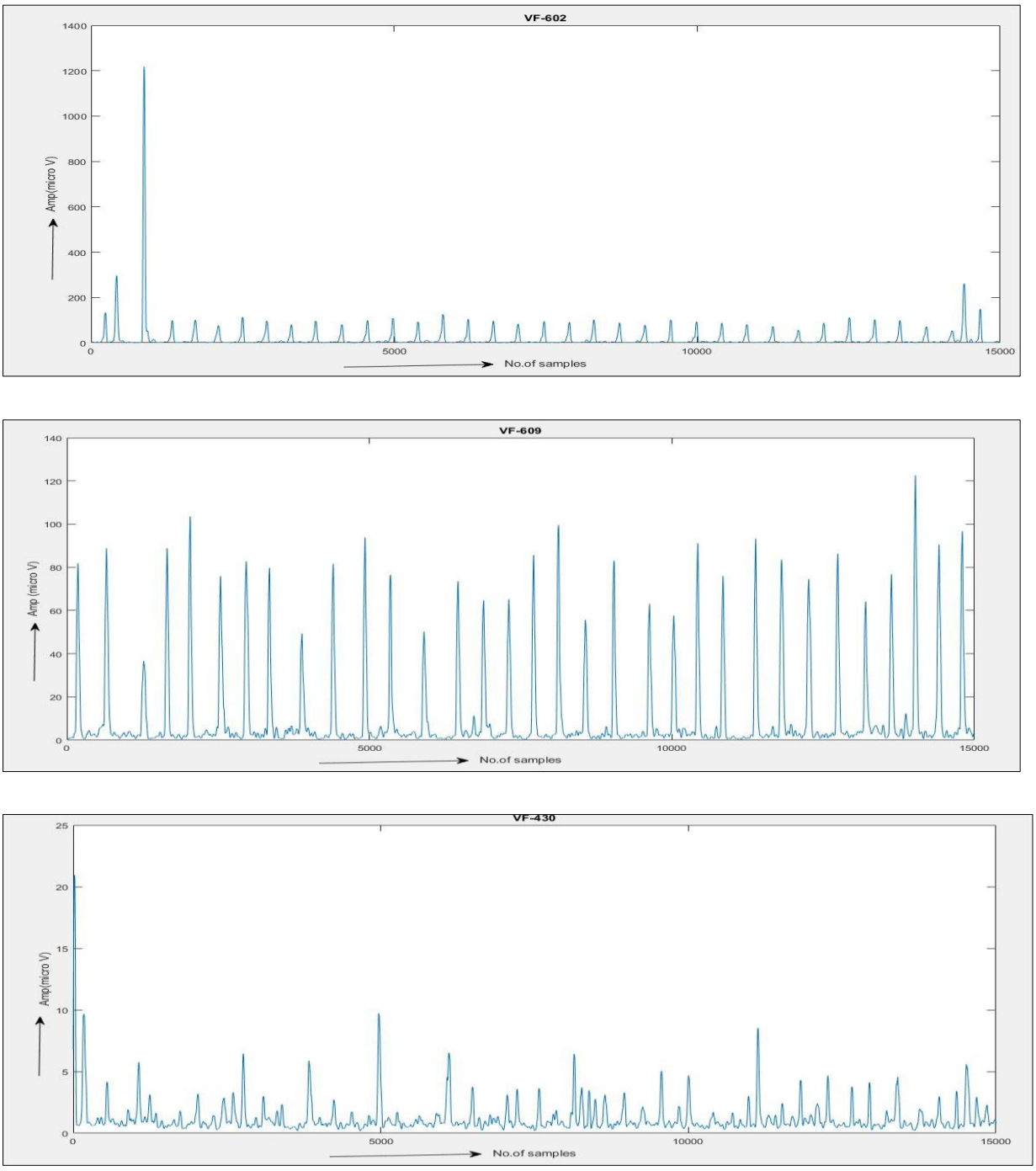

Fig 3.13 Simulation results of VF records [602,609 and 430]

The simulation results of a few records (e0104, e0105 and e01017) for Cardiac Ischemia (CI) signal after implementing Pan Tompkins algorithm for 1minute (15000 samples) is shown in Fig 3.14. From these simulation results, computed temporal features of CI records.

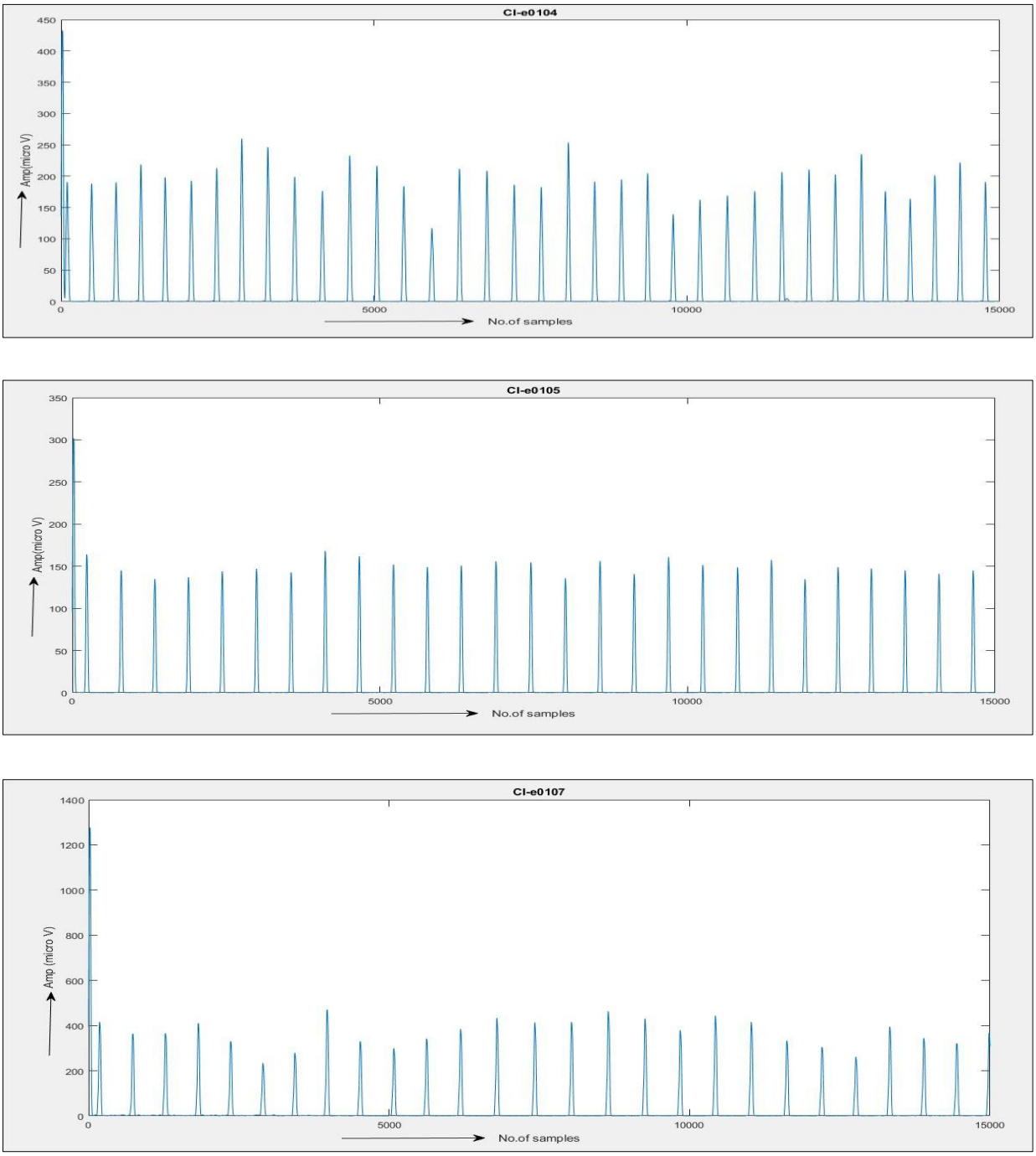

Fig 3.14 Simulation results of CI records [e0104, e0105 and e0107]

The simulation results of a few records (42, 43 and 41) for sudden cardiac arrest signal after implementing Pan Tompkins algorithm for 1minute (15000 samples) is shown in Fig 3.15. From these simulation results, computed temporal features of SCA records. The simulation results of a few AF records (04043, 08215 and 08434) is shown in Fig 3.16.

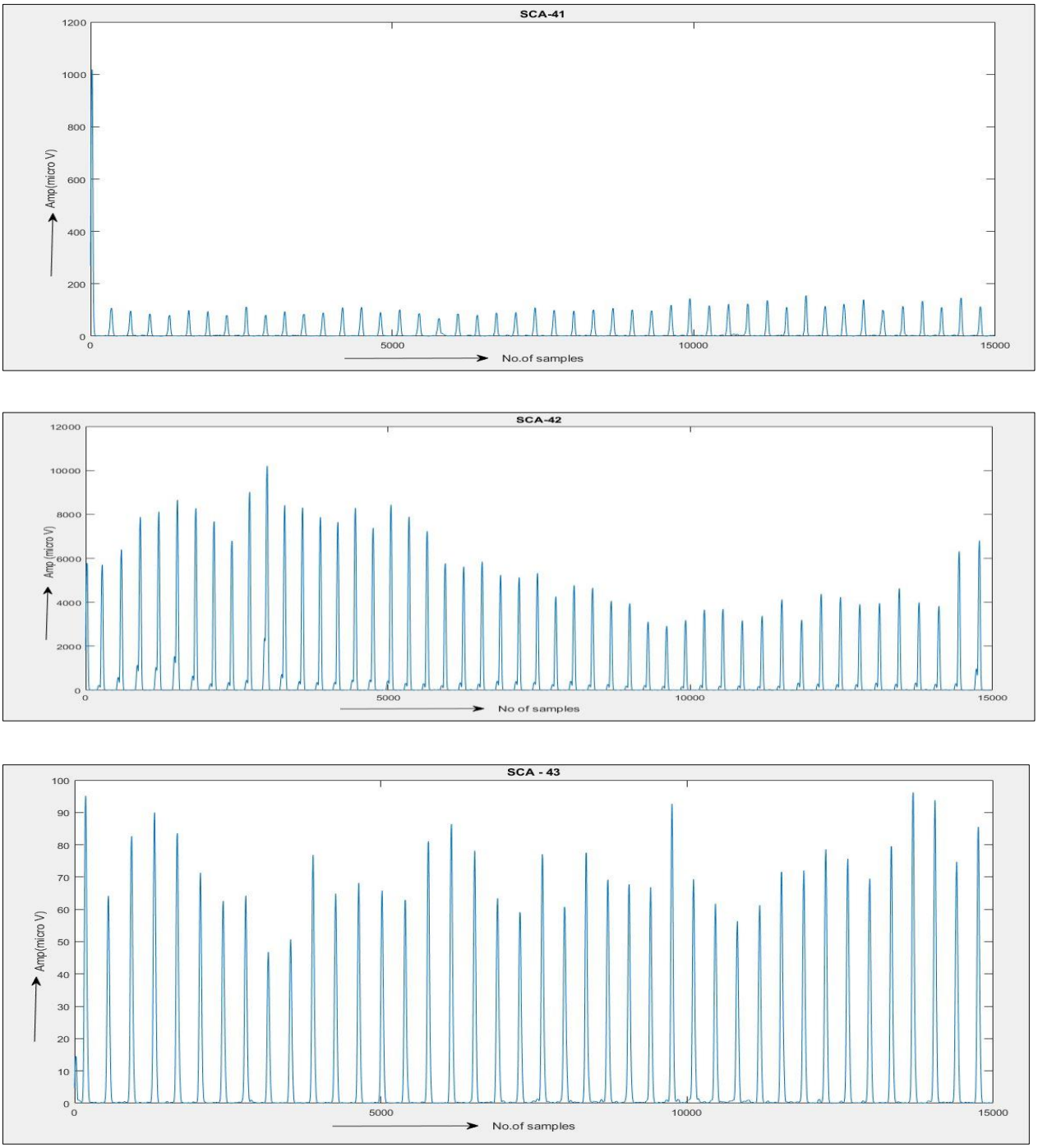

Fig 3.15 Simulation results of SCA records [42, 43 and 41]

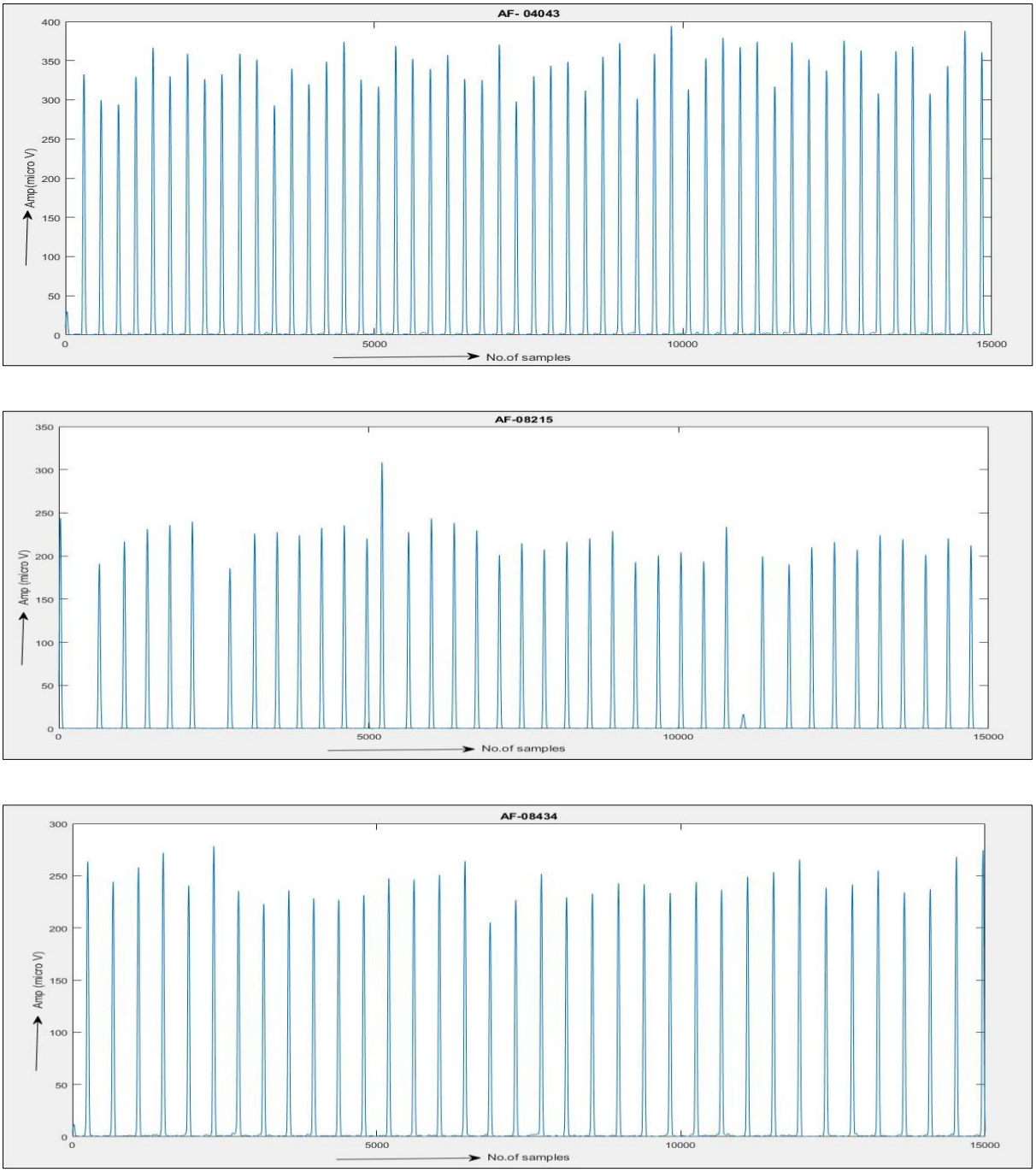

Fig 3.16 Simulation results of AF records [04043, 08215 and 08434]

Temporal features such as No. of R-peaks, R peak amplitude, R-R interval and heartbeat rate of 7 types of cardiac signals (NSR, Cardiac Arrhythmias-SVT, VT, VF and AF and cardiac disorders-SCA and CI) of each 15 records. Temporal features of total 105 records are shown in Table 3.1

Table 3.1 Temporal features of different cardiac signals

No. of R-peaks/minute	R peak Amplitude (mV)	R-R interval (secs)	Heartbeat rate(bpm)	Signal?
41	0.195675	0.7827	76.65772327	VF
63	0.127919355	0.511677419	117.2613794	VF
40	0.202846154	0.811384615	73.9476678	VF
53	0.151153846	0.604615385	99.23664122	VF
22	0.368095238	1.472380952	40.75032342	VF
44	0.18227907	0.729116279	82.29140087	VF
55	0.145537037	0.582148148	103.0665479	VF
43	0.186404762	0.745619048	80.47004726	VF
24	0.332913043	1.331652174	45.05681076	VF
57	0.141589286	0.566357143	105.9402194	VF
36	0.223428571	0.893714286	67.13554987	VF
25	0.315625	1.2625	47.52475248	VF
34	0.237060606	0.948242424	63.27495846	VF
25	0.323541667	1.294166667	46.36188023	VF
56	0.141945455	0.567781818	105.6743948	VF
32	0.159901472	0.974580645	61.56494108	VT
73	0.972875472	0.604461538	99.2618987	VT
75	0.031811855	0.417567568	143.6893204	VT
24	0.0005856	1.368347826	43.84850025	VT
76	0.031955662	0.414293333	144.8249228	VT
36	0.143324647	0.8792	61.56494108	VT
46	0.000695974	0.706133333	144.5396146	VT
42	0.000455776	0.773560976	143.6893204	VT
47	0.058796857	0.668782609	89.71525159	VT
47	0.121282677	0.69173913	144.8249228	VT
29	0.246977028	1.106428571	68.24385805	VT
38	0.137871937	0.830918919	84.96978852	VT
23	0.001140161	1.354363636	77.56337495	VT
38	0.0029195	0.844216216	48.6886523	VT

23	0.001505313	1.390909091	86.73790069	VT
52	0.854975	0.617960784	54.22853454	SVT
32	1.955584375	1.962580645	72.20921155	SVT
44	0.958168182	0.723348837	71.07184018	SVT
40	1.49194	0.801025641	74.90396927	SVT
32	1.656490625	0.997677419	60.13967926	SVT
43	1.7546	0.728761905	82.33141662	SVT
35	1.625905714	0.933529412	64.27221172	SVT
25	0.6304737	1.295166667	46.32608416	SVT
28	1.298521429	1.151703704	52.0967327	SVT
40	0.21319754	0.797230769	75.26051717	SVT
54	0.142973048	0.587698113	102.0932323	SVT
41	0.27527253	0.7825	76.67731629	SVT
54	1.245340741	0.590188679	101.6624041	SVT
41	1.010692683	0.7675	78.17589577	SVT
50	0.558014608	0.649877551	92.32508479	SVT
23	0.149586735	1.367636364	43.87131082	SCA
29	0.101811814	1.071	56.02240896	SCA
23	0.235015752	1.425636364	42.08646856	SCA
24	0.042966113	1.370782609	43.77061659	SCA
24	0.003038279	1.342086957	44.70649216	SCA
18	0.08510885	1.837411765	32.65462927	SCA
8	0.085488825	4.554857143	13.17275122	SCA
32	0.0917072	1.006580645	59.6077426	SCA
31	0.098433552	1.0532	56.96923661	SCA
26	0.000126904	1.27568	47.03373887	SCA
30	0.00067424	1.06937931	56.1073133	SCA
25	0.063374748	1.328833333	45.15238931	SCA
22	0.001336595	1.467619048	40.8825438	SCA
26	0.00075585	1.26384	47.47436384	SCA
22	0.417294723	1.505142857	39.86332574	SCA
31	1.150783871	0.149586735	60.3378922	NSR

49	5.529473469	0.101811814	93.0833872	NSR
50	5.507928	0.235015752	92.7327782	NSR
49	1.891016327	0.042966113	92.69988413	NSR
50	1.758144	0.003038279	93.34518669	NSR
40	1.79936	0.372409457	75.99376461	NSR
38	5.969310526	0.08510885	71.42857143	NSR
37	4.3836	0.085488825	70.07526603	NSR
34	1.267570588	0.091707288	63.43713956	NSR
36	0.992038889	0.098433552	66.66666667	NSR
43	3.451974419	0.000711936	81.29032258	NSR
58	0.610459962	0.000126904	74.57479285	NSR
43	2.0547	0.00067424	80.66581306	NSR
57	0.609691228	0.00075585	109.517601	NSR
60	0.112759242	0.198319587	111.7424242	NSR
20	0.001611579	1.611578947	37.23056826	CI
15	0.002124857	2.124857143	28.23719242	CI
16	0.002090667	2.090666667	28.69897959	CI
15	0.002114857	2.114857143	28.37071062	CI
14	0.002198462	2.198461538	27.29181246	CI
18	0.001763529	1.763529412	34.02268179	CI
17	0.00193125	1.93125	31.06796117	CI
10	0.002975111	2.975111111	20.16731401	CI
18	0.001869882	1.869882353	32.08758022	CI
13	0.002682667	2.682666667	22.36580517	CI
18	0.001818824	1.818823529	32.98835705	CI
16	0.002013067	2.013066667	29.80527222	CI
21	0.0015494	1.5494	38.72466761	CI
21	0.0015456	1.5456	38.81987578	CI
24	0.0013434	1.343478	44.66019	CI
28	0.336032521	1.344130086	44.63853658	AF
19	0.1203049	0.4812196	124.6832008	AF
20	0.11645225	0.465809	128.8081596	AF

19	0.028093468	0.112373874	533.9319366	AF
19	0.269214163	1.076856653	55.71772237	AF
16	0.298580794	1.194323175	50.23765866	AF
19	0.243727268	0.974909074	61.54420101	AF
33	0.125365379	0.501461515	119.6502587	AF
22	0.026578409	0.106313636	564.3678652	AF
19	0.005267116	0.021068463	2847.85841	AF
62	0.062670811	0.250683245	239.3458724	AF
18	0.047963394	0.191853578	312.7384993	AF
15	0.279369273	1.117477093	53.69237576	AF
21	0.227674081	0.910696324	65.88365236	AF
30	0.11149009	0.44596036	134.5411059	AF

Table 3.2 Average values of temporal features of cardiac signals

Cardiac Signal	**R peak average amplitude (mV)**	**Average no. of R- peaks**	**Average R-R interval (secs)**	**Average heart-beat rate (bpm)**
NSR	2.4726	90	0.09774	82.5060
CI	0.00198	34.1	1.97554	31.6359
AF	0.15325	48	0.61300	355.843
SVT	1.04481	81.4	0.89245	73.5850
VT	0.12747	86.4	0.86836	96.2485
VF	0.21840	82.4	0.87360	76.9767
SCA	0.09178	48.4	1.52931	44.6250

Average values of temporal features such as R-peak amplitude, number of R-peaks, R-R intervals and heartbeat rate of 7 types of cardiac signals are shown in Table 3.2. There is a variation in number of R-Peaks, amplitude of R peaks, R-R intervals and heartbeat rate of different cardiac signals. These temporal features will determine the functioning of heart [61].

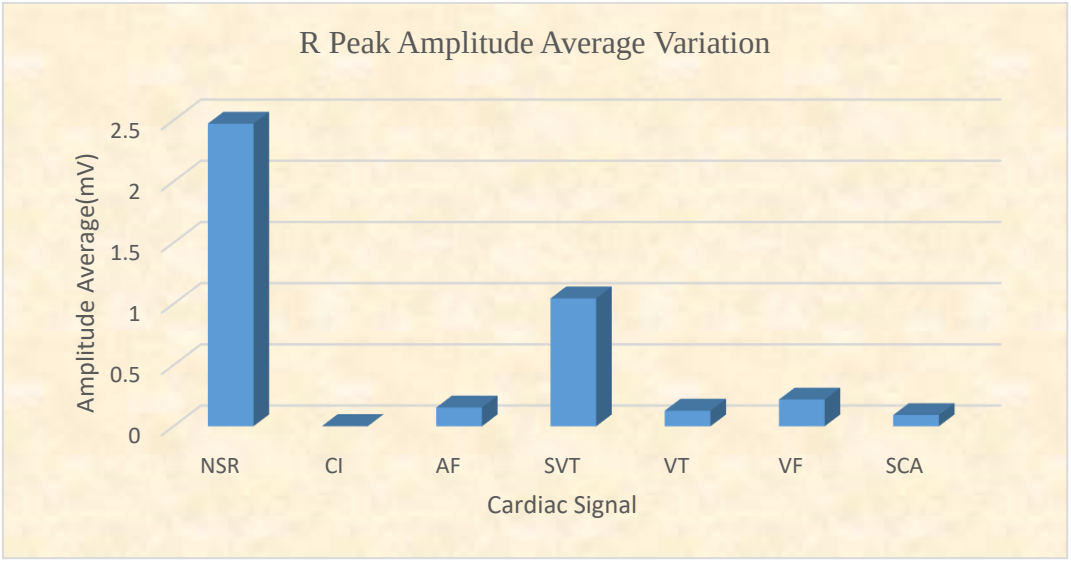

Fig 3.17 R-peak amplitude variation of different cardiac signals

As shown in Fig 3.17, NSR and SVT signals amplitudes are very high. Severe ventricular arrhythmias such as VT and VF, the average amplitudes are 0.1 mV to 0.2 mV respectively. For cardiac disorders such as SCA and CI, the amplitudes are almost reaching to zero (0.09 mV and 0.001 mV).

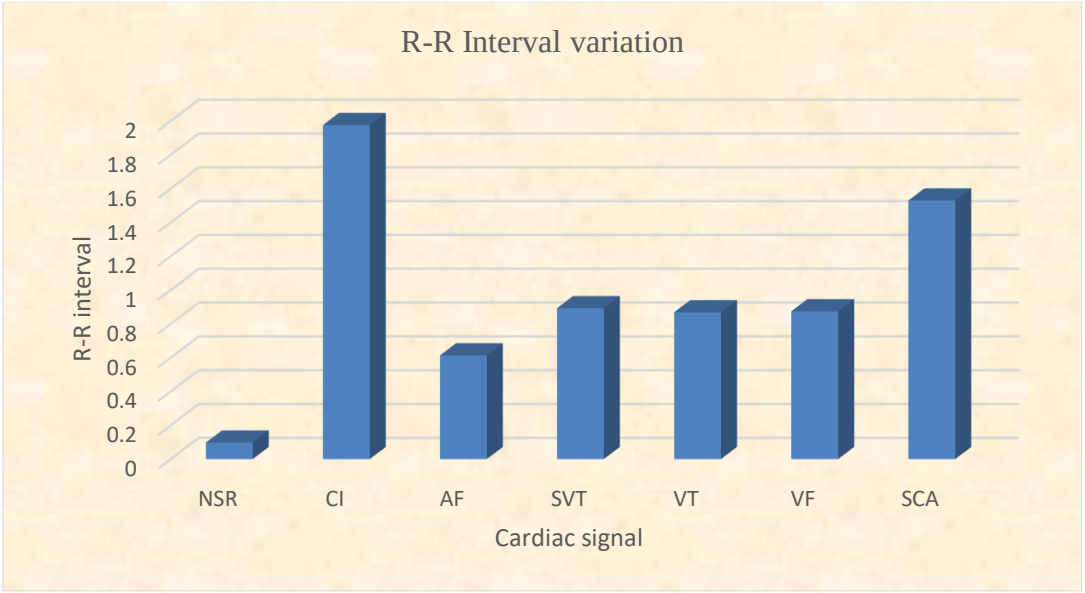

Fig 3.18 R-R Interval variation of different cardiac signals

R-R interval variation in NSR is very less (0.09s) whereas it is very high (1.5s to 1.9s) in cardiac disorders (CI and SCA) and in all ventricular arrhythmias it is 0.8s and in AF, the R-R interval is 0.6s. The R-R interval variation of different cardiac signals is shown in Fig 3.18

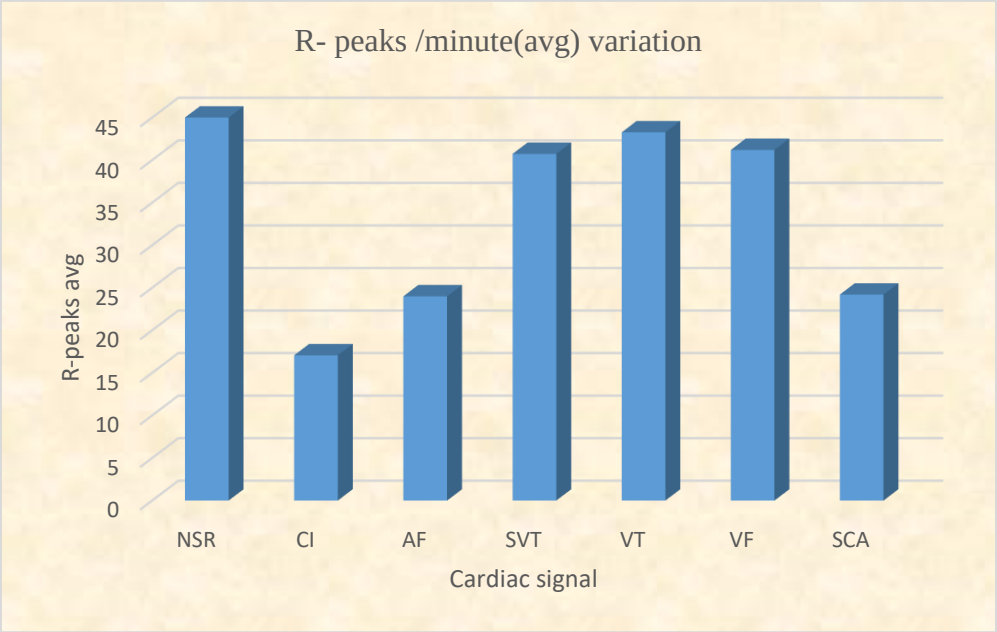

Fig 3.19 Average number of R-Peaks/minute in different cardiac signals

Number of R-Peaks/minute variation in NSR is very high (90) whereas it is very low (34.13 to 48.4) in cardiac disorders (CI and SCA) and in all ventricular arrhythmias (VT and VF) it is 86.4 and 82.4 respectively and in AF, it is 48. The number of R-Peaks variation of different cardiac signals is shown in Fig 3.19

Table 3.3 Standard Deviation (SD) of R-R intervals of cardiac signals

Cardiac Signal	SD for R-R intervals (milliseconds)
CI	429.8072
SCA	863.8298
NSR	105.9631
VF	319.3791
VT	317.8802
SVT	359.1926
AF	447.8123

The standard deviation (σ) gives information about the spread of data values from the mean value. If σ is small, the data values are close to the mean value. Standard Deviation (SD) of R-R intervals of cardiac signals is shown in Table 3.3. R-R standard deviation varitation is shown in Fig 3.20. If σ is high, the data values are widely spread out from the mean value. R-R interval

standard deviation of less than 105.9ms for NSR had a relative risk 4 times higher than those with R-R interval standard deviation of 429.8ms for CI and relative risk 8.5 times higher than those with R-R interval standard deviation of 863.8ms for SCA. R-R interval standard deviation of Ventricular arrhythmias (VT, SVT and VF) is approximately 319ms to 359ms having a relative risk of 3.5 times higher compared to NSR. R-R interval standard deviation of atrial fibrillation (AF) is approximately 447ms having a relative risk of 4.5 times higher compared to NSR.

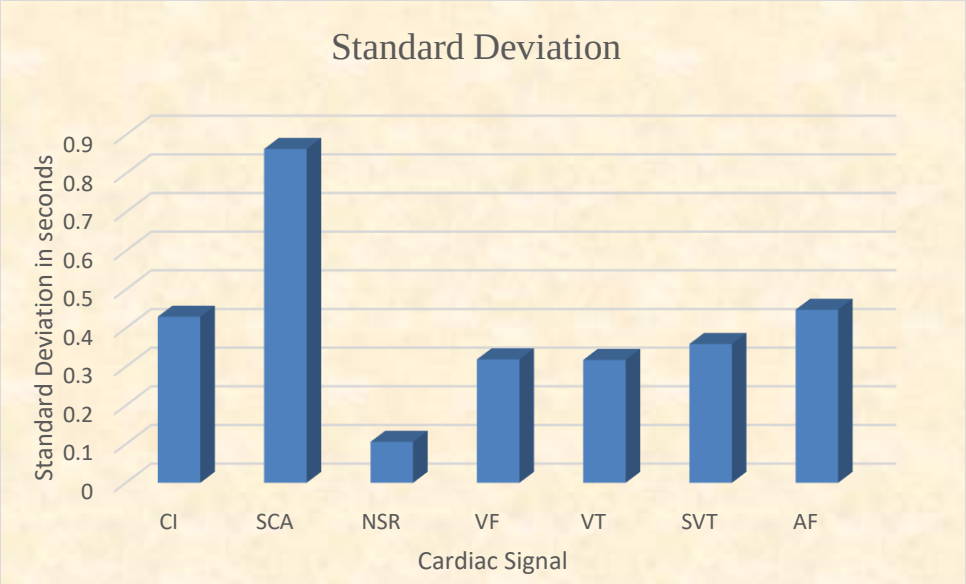

Fig 3.20 Standard Deviation of R-R intervals of cardiac signals

Heartbeat rates of various signals are calculated from R-R intervals and the variation of heartbeat rate of cardiac signals is shown in Fig 3.21.The heartbeat rate of 4 signals (NSR, CI, AF and SCA) out of 7 signals are found to be accurate with reference to existing works [56].

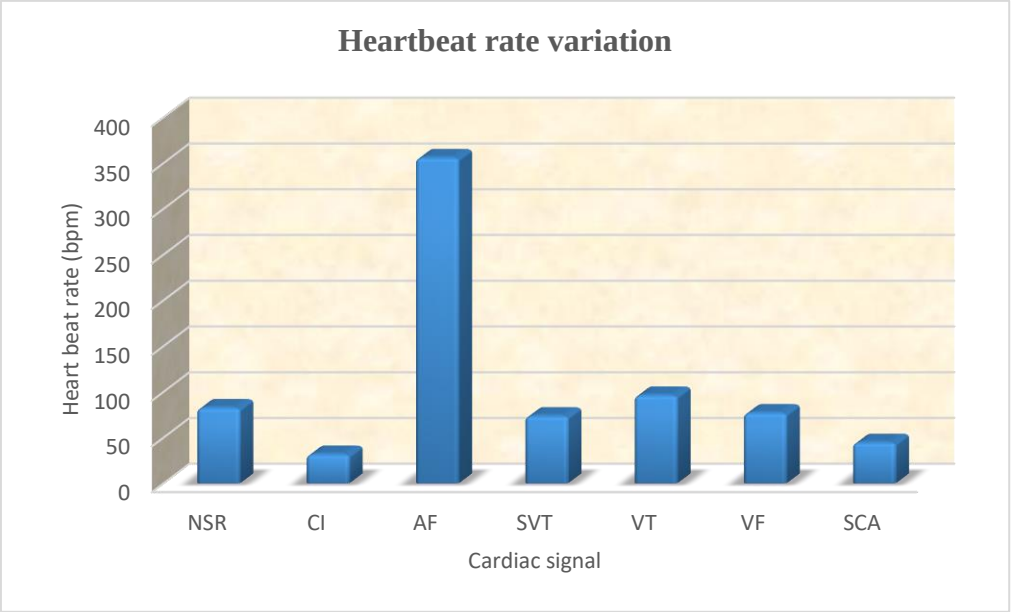

Fig 3.21 Heartbeat rate variation of cardiac signals

Atrial Fibrillation Heartbeat Rate: 355 bpm, Irregular R-R interval; SCA Heartbeat Rate: 20-50bpm, Irregular R-R interval; CI Heartbeat Rate: 20-40bpm, NSR Heartbeat Rate; 60-100bpm, Regular R-R interval; SVT Heartbeat Rate: Above 100bpm; VT Heartbeat Rate: 170bpm (wide QRS complex (120ms)); VF Heartbeat Rate: above 400bpm (narrow QRS complex (80ms)).

3.4 Introduction to Artificial Intelligence Algorithms

3.4.1 Introduction

Artificial neural networks are computational models that work similarly to the functioning of a human nervous system. Neural Networks are organized in layers made up of interconnected nodes which contain an activation function that computes the output of the network. Both Neural networks and Random Forest are different techniques that learn differently but can be used in similar domains. Neural Networks are exclusive to Deep Learning while Random Forest is a technique of Machine Learning.

Machine learning based classifier (RF) and Artificial neural networks (MLP and RBF) are implemented based on the mathematical operations and a set of features is required as input to determine the output. The literature survey shows that selection of a suitable classifier plays an important role in any classification problem [59], [66].

3.4.2 Random Forest (RF) Classifier

The random forest is a classification algorithm consisting of many decisions trees. Decision trees are a popular method for various machine learning tasks. Both the Random Forest and Neural Networks are different techniques that learn differently but can be used in similar domains. Random forests is an ensemble learning method for classification, regression and other tasks, in which a number of decision tress are created at the training time and a class is given as output which is the mode of the classes[20]. In order to create number of decision trees, data and variables are selected randomly from the available set of data and variables. To build a tree during training time a finite set of thresholds is used. While constructing a tree separation of classes is being done and probability of data point to be of any class is different for each node. The newly arrived data point go down in tree and it ends at leaf and the class with highest probability for that node shows the actual class of data point in that tree. Single random tree is not a good classifier but if we combine a number of random trees then it becomes a very good classifier.

Let a dataset of N data points be X = x_1, x_2, x_3 ..., x_n with responses C= c_1, c_2, c_3 ..., c_n. Every input has some features. The algorithm of random forest classifier is shown in Fig 3.22

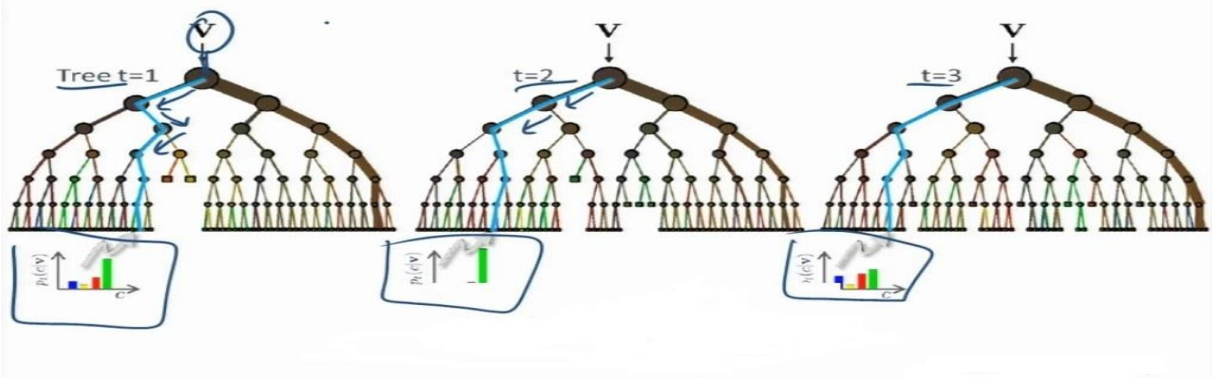

Fig 3.22 Random Forest Classifier [110]

In order to create more randomness among these data points every time some data points are selected and from these data inputs some features are selected randomly in order to make a decision tree. If one or few features are very strong predictors for the target output, these features will be selected in many of the decision trees. Typically, for a classification problem with f features, $\sqrt{f}$ features are used in each split.

- Sample, with replacement, n training examples from X, C; call these Xt, Ct.
- Train a decision or regression tree ft on Xt, Ct.

In the forest with T trees where t ∈ {1, 2, 3, . . , T}. All the decision trees are trained independently. During testing case, each test point V is simultaneously pushed through all the trees starting at root node until it reaches to corresponding leaves. For different trees, the data point will follow different path when it goes to leaf. The class probabilities for that point V is different in each tree. For the output prediction, bagging method is used which leads to better model performance because it decreases the variance of the model, without increasing the bias. It can be made by averaging the predictions from all individual decision trees given by the following equation 3.4.

$$p(c|v) = \frac{1}{T}\sum_{t=1}^{T} p_t\,(c|v) \tag{3.4}$$

Where c represents the class of V.

3.4.3 Multilayer perceptron (MLP) Classifier

Multilayer perceptron is a feed-forward neural network model that takes feature vectors from the given dataset as input and map them onto outputs or appropriate classes[14][20]. In MLP there are several layers such as input layer, an output layer and one or more hidden layers. The weighted sum of the inputs produces the activation signal that is passed to the activation function to obtain one output from the neuron. The commonly used activation functions are linear, step, sigmoid, tanh and rectified linear unit (ReLu) functions. The MLP neural network structure is shown below in Fig 3.23.

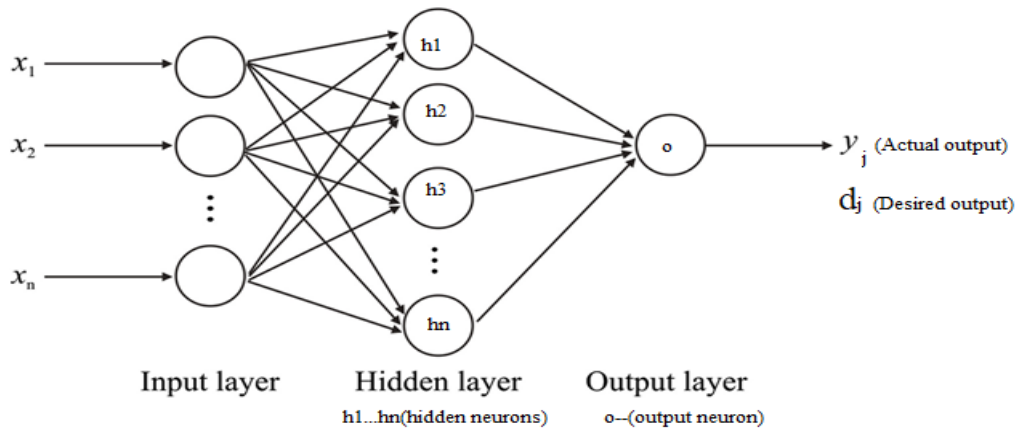

Fig 3.23 MLP general neural network structure [66]

All other nodes expect the input nodes have an activation function (E.g., sigmoid function). The input layer consists of the same number of nodes as the size of the input feature vector. The output layer has the same number of nodes that the input data should be classified. Each node in one layer is connected to all other nodes in the next layer through different weights [20]. Weights are initialized randomly at the beginning of training phase. MLP performs the gradient descent search to reduce the mean square error between the actual output and the desired output through the adjustment of the weights. It is highly accurate for most classification problems because of the property of the generalized data rule. In MLP training, the weights are adapted using a recursive algorithm starting at the output nodes and working back to the first hidden layer.

The entire process of classification consists of two phases.

- MLP is used to learn the behavior of the input data using back-propagation. This step is called the training phase.
- Trained MLP is used to test using unknown input data. The back propagation algorithm compares the result that is obtained in this step with the result that was expected. This kind of classification is called supervised classification.

The MLP computes the error signal using the obtained output and desired output. The computed signal error is then fed back to the neural network and used to adjust the weights such that with each iteration the error decreases and the neural model gets closer and closer to produce the desired output. During the training phase, the perceptron first processes the given data through feed forward propagation. The error in output node j in the nth data point is represented in equation 3.5.

$$E_j(n) = d_j(n) - y_j(n) \tag{3.5}$$

Where d_j is the desired output of node j and y_j is the actual output produced by the perceptron.

Using gradient descent weights will be adjusted to minimize error in the entire output, given by E (n) = 1,

$$E(n) = \frac{1}{2}\sum_j e_j^2\,(n) \tag{3.6}$$

The change in each weight will be given by,

$$\Delta w_t = -\eta \frac{\partial E(w)^T}{\partial w}\Big|_{w_t} \tag{3.7}$$

Where η is the learning rate which should be chosen carefully so that the cost function converges to a global minimum. If the learning rate is too large, then the algorithm may never converge and if it is very low, the algorithm may take a long time to converge. Generally learning rate is kept between 0 and 1[20].

3.4.4 Radial Basis Function (RBF) Classifier

RBF neural networks are also a type of feed-forward network trained using a supervised training algorithm. The main advantage of RBF network is that it has only one hidden layer and it uses radial basis function as the activation function. These functions are very powerful in approximation. The training of the RBF model is terminated once the calculated error reached the desired values or number of training iterations. An RBF network with a specific number of nodes in its hidden layer is formed. It is typically observed that the RBF network required less time to reach the end of training compared to MLP. The fig 3.24 shows the RBF neural network structure.

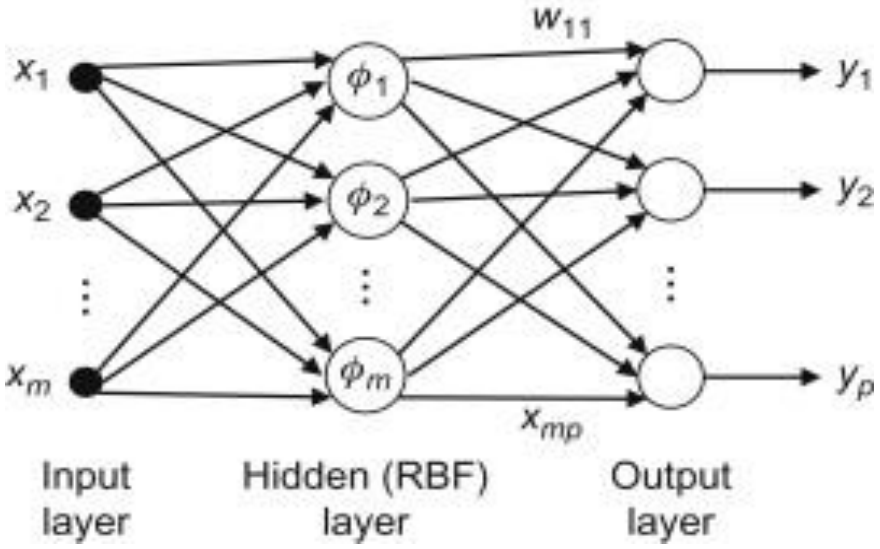

Fig 3.24 RBF general neural network structure [66]

The procedure in training the RBF is faster than that we use in MLP. This can be given by internal representation formed by the hidden units, and leads to a two stage training procedure.

- In first stage, the parameters governing the basis function are determined using relatively fast, unsupervised learning methods.
- The second stage of training then involves the determination of the final layer weights, which requires the solution of a linear problem, and which is therefore also faster.

If it is considered the Gaussian function as basis function. The Gaussian radial basis function will be considered as follows

$$Gaussian\ function:\ H_{j(x)} = \exp\left(\frac{\|x-c_j\|^2}{\sigma^2}\right) \tag{3.8}$$

It is remarked that MLP NNs perform global matching to the input–output data, whereas in RBF NNs, this is done only locally, of course with better accuracy. The above two neural network algorithms, MLP and RBF networks, have different structures and characteristics, so they have different performances in classification tasks depending on the available training data sets. Experiments using the two real world data sets with the above two neural network algorithms show that multilayer perceptrons have relatively better performance for larger number of data sets and radial basis function networks have relatively better performance for smaller number of data sets. [52]

3.4.5 Choice of a classifier

The choice of a classifier is a crucial step in any classification problem. The classifier's evaluation is mostly based on prediction accuracy (the percentage of correct prediction divided by the total number of predictions), sensitivity, specificity and precision. Classifier's accuracy is examined by splitting the data set in to two-thirds for training and one third for testing. Tenfold cross-validation is used to improve classification accuracy. To decrease error rate, the following points are to be considered,

- Relevant features
- Training and testing of data
- 10 fold cross validation
- Appropriate classifier

A common method for comparing supervised algorithms is to perform statistical comparisons of the accuracies of trained classifiers on specific features. Training of ANN is very time-

consuming and computationally intensive. In addition to the learning process itself, a large amount of preparatory work is also necessary to bring the inputs into the required form. The inputs must be in number format and normalized. RF classifier can be trained with a relative small amount of data. MLP and RBF Neural Networks need more data to achieve the same level of accuracy. Random Forests require much less input preparation. They can handle binary features, categorical features as well as numerical features and there is no need for feature normalization. Random Forests are quick to train and to optimize according to their hyper parameters. Thus, the computational cost and time of training a Random Forest are comparatively low.

3.4.6 Medical statistics

RF, MLP and RBF classifiers classification performance can be evaluated using medical statistics such as sensitivity, specificity, classification accuracy, mean squared error (MSE) and receiver operating characteristics (ROC).

Sensitivity (S) measures how often a test correctly generates a positive result for people who have the condition that are being tested. It is also known as the true positive rate (TPR). It is the percentage of persons with the disease who are identified correctly by the medical test. 'S' can be calculated by using the equation 3.9,

$$S = \frac{TP}{TP+FN} \tag{3.9}$$

Specificity (Sp) measures a test's ability to correctly generate a negative result for people who don't have the condition that are being tested. It is also known as the true negative rate (TNR). It is the percentage of persons without the disease who are correctly excluded by the test. 'Sp' can be calculated by using the equation 3.10,

$$Sp = \frac{TN}{TN+FP} \tag{3.10}$$

Precision (P) is the proportion of the predicted positive cases that are correct. It is also known as the Positive Predictivity (Pp). It is given in the following equation 3.11,

$$Pp = \frac{TP}{TP+FP} \tag{3.11}$$

Accuracy (Acc) is the ability to differentiate all cases correctly. To estimate the accuracy of the test, we should calculate the proportion of true positive and true negative in all evaluated cases. It is given in the following equation 3.12,

$$\text{Acc} = \frac{\text{TP+TN}}{\text{TP+TN+FP+FN}} \tag{3.12}$$

Where; TP is True positive, FP is False positive, TN is True negative and FN is False negative.

3.5 Results and Discussion

3.5.1 MLP classifier results

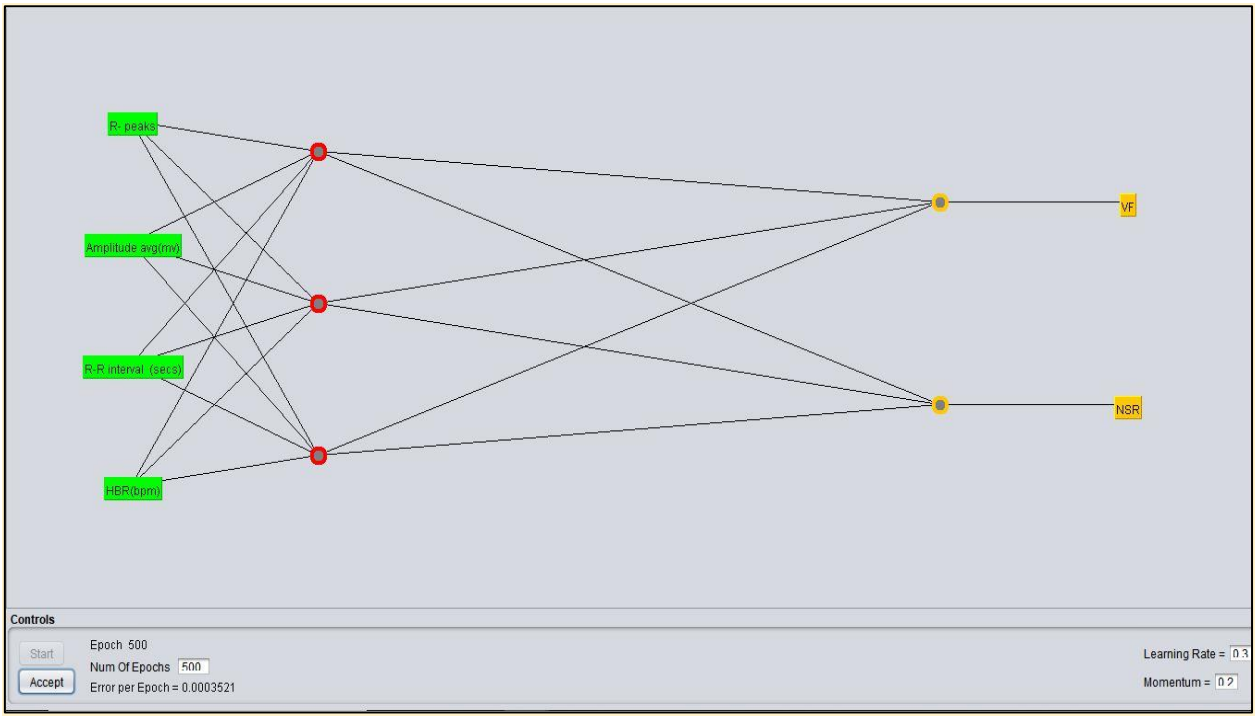

Fig 3.25 ANN Structure for classification of NSR and VF using temporal features

The above Fig 3.25 shows neural network architecture of MLP results obtained for 2 types of signals (NSR and VF). It has one input layer, one output layer and one hidden layer. Input layer has four neurons represented as Number of R-Peaks, Amplitude of R-Peaks, R-R interval and Heartbeat rate are used in this work. The output layer has two neurons represented as NSR and VF. The error per epoch obtained as 0.0003521 and Learning rate obtained as 0.3.

```
Time taken to build model: 0.11 seconds

=== Stratified cross-validation ===
=== Summary ===

Correctly Classified Instances          30               100      %
Incorrectly Classified Instances         0                 0      %
Kappa statistic                          1
Mean absolute error                      0.0306
Root mean squared error                  0.0887
Relative absolute error                  6.0465 %
Root relative squared error             17.522  %
Total Number of Instances               30

=== Detailed Accuracy By Class ===

                 TP Rate   FP Rate   Precision   Recall  F-Measure  MCC      ROC Area  PRC Area  Class
                 1.000     0.000     1.000       1.000   1.000      1.000    1.000     1.000     VF
                 1.000     0.000     1.000       1.000   1.000      1.000    1.000     1.000     NSR
Weighted Avg.    1.000     0.000     1.000       1.000   1.000      1.000    1.000     1.000

=== Confusion Matrix ===

  a  b   <-- classified as
 15  0 |  a = VF
  0 15 |  b = NSR
```

Fig 3.26 Simulation Results for Classification of NSR and VF using MLP

The above Fig 3.26 shows the simulation results for classification of NSR and Ventricular fibrillation using MLP classifier. Time to build the model is 0.11 Seconds. Correctly classified instances are 30 out of 30 instances. RMSE value is 0.0887. The classification accuracy for classifying NSR and VF is obtained as 100%.

```
Time taken to build model: 0.44 seconds

=== Stratified cross-validation ===
=== Summary ===

Correctly Classified Instances          29               96.6667 %
Incorrectly Classified Instances         1                3.3333 %
Kappa statistic                          0.9333
Mean absolute error                      0.087
Root mean squared error                  0.1754
Relative absolute error                 17.2087 %
Root relative squared error             34.659  %
Total Number of Instances               30
Ignored Class Unknown Instances                 1

=== Detailed Accuracy By Class ===

                 TP Rate   FP Rate   Precision   Recall  F-Measure  ROC Area  Class
                   1         0.067     0.938       1         0.968      1        SCA
                   0.933     0         1           0.933     0.966      0.983    NSR
Weighted Avg.      0.967     0.033     0.969       0.967     0.967      0.992

=== Confusion Matrix ===

   a  b   <-- classified as
  15  0 |  a = SCA
   1 14 |  b = NSR
```

Fig 3.27 Simulation Results for Classification of NSR and SCA using MLP

The above Fig 3.27 shows the simulation results for classification of NSR and SCA using MLP classifier. Time to build the model is 0.44 Seconds. Correctly classified instances are 29 out of

30 instances. RMSE value is 0.1754. The classification accuracy for classifying NSR and SCA is obtained as 96.67%.

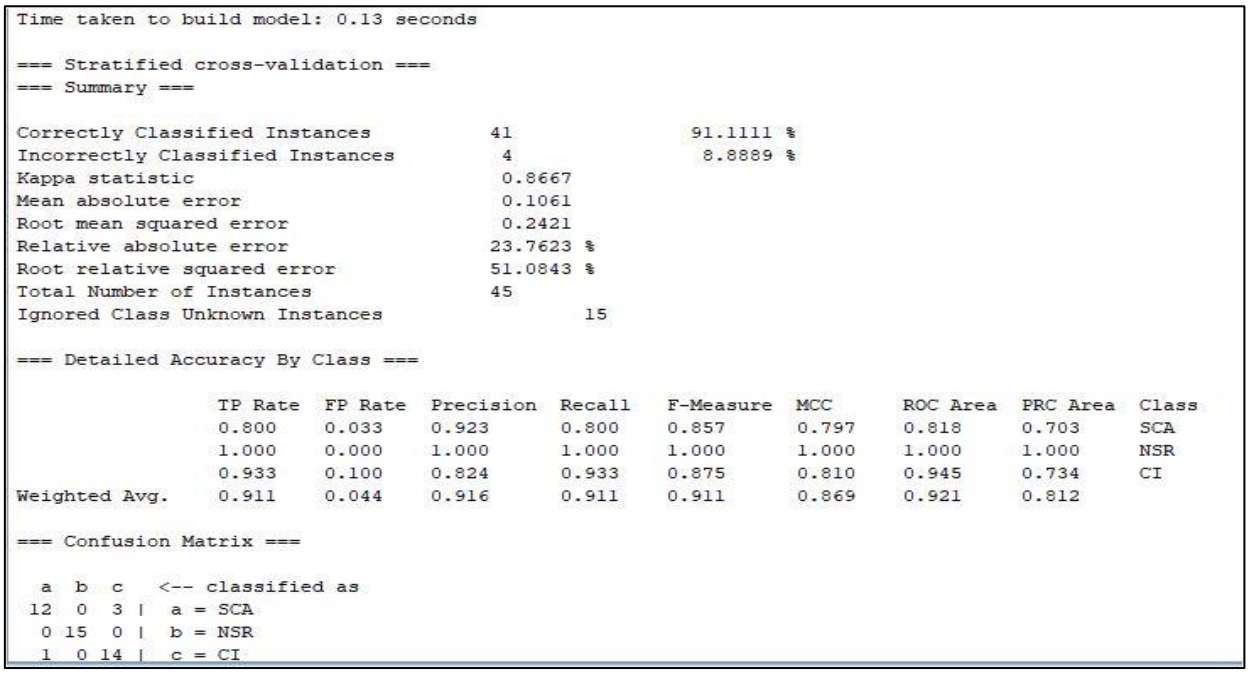

```
Time taken to build model: 0.13 seconds

=== Stratified cross-validation ===
=== Summary ===

Correctly Classified Instances          41               91.1111 %
Incorrectly Classified Instances         4                8.8889 %
Kappa statistic                          0.8667
Mean absolute error                      0.1061
Root mean squared error                  0.2421
Relative absolute error                 23.7623 %
Root relative squared error             51.0843 %
Total Number of Instances               45
Ignored Class Unknown Instances                 15

=== Detailed Accuracy By Class ===

                 TP Rate  FP Rate  Precision  Recall   F-Measure  MCC      ROC Area  PRC Area  Class
                 0.800    0.033    0.923      0.800    0.857      0.797    0.818     0.703     SCA
                 1.000    0.000    1.000      1.000    1.000      1.000    1.000     1.000     NSR
                 0.933    0.100    0.824      0.933    0.875      0.810    0.945     0.734     CI
Weighted Avg.    0.911    0.044    0.916      0.911    0.911      0.869    0.921     0.812

=== Confusion Matrix ===

  a  b  c   <-- classified as
 12  0  3 |  a = SCA
  0 15  0 |  b = NSR
  1  0 14 |  c = CI
```

Fig 3.28 Simulation Results for Classification of NSR, SCA and CI using MLP

The above Fig 3.28 shows the simulation results for classification of NSR, SCA and CI using MLP classifier. Time to build the model is 0.13 Seconds. Correctly classified instances are 41 out of 45 instances. RMSE value is 0.2421. The classification accuracy for classifying NSR, SCA and CI is obtained as 91.11%.

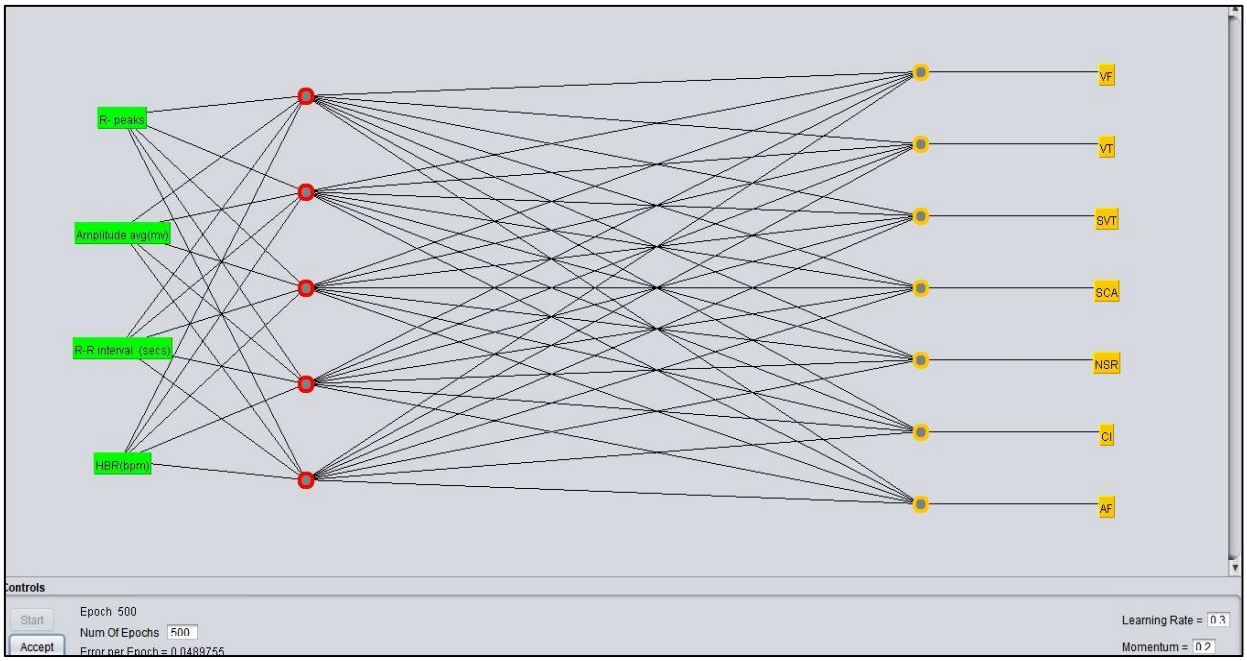

Fig 3.29 ANN Structure for classification of 7 types using temporal features

The above Fig 3.29 shows neural network architecture of MLP results obtained for 7 types of signals (NSR, SVT, VT, VF, AF, CI and SCA). It has one input layer, one output layer and one hidden layer. Input layer has four temporal features(Number of R-Peaks, Amplitude of R-Peaks, R-R interval and Heartbeat rate) used in this work. The output layer has 7 neurons represented as NSR, VT, VF, SVT, AF, CI and SCA. The error per epoch obtained as 0.0489755 and Learning rate obtained as 0.3.

```
Time taken to build model: 0.26 seconds

=== Stratified cross-validation ===
=== Summary ===

Correctly Classified Instances          74               70.4762 %
Incorrectly Classified Instances        31               29.5238 %
Kappa statistic                          0.6556
Mean absolute error                      0.1225
Root mean squared error                  0.2423
Relative absolute error                 49.9192 %
Root relative squared error             69.1076 %
Total Number of Instances              105

=== Detailed Accuracy By Class ===

                 TP Rate   FP Rate   Precision   Recall  F-Measure   MCC      ROC Area  PRC Area  Class
                 0.533     0.111     0.444       0.533   0.485       0.392    0.860     0.423     VF
                 0.200     0.067     0.333       0.200   0.250       0.167    0.788     0.338     VT
                 0.800     0.011     0.923       0.800   0.857       0.838    0.979     0.922     SVT
                 0.733     0.111     0.524       0.733   0.611       0.544    0.899     0.535     SCA
                 0.933     0.000     1.000       0.933   0.966       0.961    0.996     0.983     NSR
                 0.867     0.044     0.765       0.867   0.813       0.781    0.970     0.749     CI
                 0.867     0.000     1.000       0.867   0.929       0.921    0.908     0.892     AF
Weighted Avg.    0.705     0.049     0.713       0.705   0.701       0.658    0.914     0.692
```

Fig 3.30 Simulation Results for Classification of 7 types of signals using MLP

The above Fig 3.30 shows the simulation results for classification of 7 types of signals using MLP classifier. Time to build the model is 0.26 Seconds. Correctly classified instances are 74 out of 105 instances. RMSE value is 0.2423. The classification accuracy for classifying 7 types is obtained as 70.47%.

3.5.2 RBF classifier results

```
Time taken to build model: 0.02 seconds

=== Stratified cross-validation ===
=== Summary ===

Correctly Classified Instances          30               100      %
Incorrectly Classified Instances         0                 0      %
Kappa statistic                          1
Mean absolute error                      0.0158
Root mean squared error                  0.0868
Relative absolute error                  3.1331 %
Root relative squared error             17.1519 %
Total Number of Instances               30

=== Detailed Accuracy By Class ===

               TP Rate   FP Rate   Precision   Recall  F-Measure   ROC Area  Class
                 1         0          1          1          1          1        VF
                 1         0          1          1          1          1        NSR
Weighted Avg.    1         0          1          1          1          1

=== Confusion Matrix ===

  a  b   <-- classified as
 15  0 |  a = VF
  0 15 |  b = NSR
```

Fig 3.31 Simulation Results for Classification of NSR and VF using RBF

The above Fig 3.31 shows the simulation results for classification of NSR and VF using RBF classifier. Time to build the model is 0.02 Seconds. Correctly classified instances are 30 out of 30 instances. RMSE value is 0.0868. The classification accuracy for classifying NSR and VF is obtained as 100%.

```
Time taken to build model: 0.03 seconds

=== Stratified cross-validation ===
=== Summary ===

Correctly Classified Instances          29               96.6667 %
Incorrectly Classified Instances         1                3.3333 %
Kappa statistic                          0.9333
Mean absolute error                      0.0333
Root mean squared error                  0.1826
Relative absolute error                  6.5909 %
Root relative squared error             36.0813 %
Total Number of Instances               30
Ignored Class Unknown Instances                 1

=== Detailed Accuracy By Class ===

               TP Rate   FP Rate   Precision   Recall  F-Measure   ROC Area  Class
                 0.933     0          1         0.933     0.966      0.963    SCA
                 1         0.067      0.938     1         0.968      0.988    NSR
Weighted Avg.    0.967     0.033      0.969     0.967     0.967      0.975

=== Confusion Matrix ===

  a  b   <-- classified as
 14  1 |  a = SCA
  0 15 |  b = NSR
```

Fig 3.32 Simulation Results for Classification of NSR and SCA using RBF

The above Fig 3.32 shows the simulation results for classification of NSR and SCA using RBF classifier. Time to build the model is 0.03 Seconds. Correctly classified instances are 29 out of 30 instances. RMSE value is 0.1826. The classification accuracy for classifying NSR and SCA is obtained as 96.67%.

```
Time taken to build model: 0.05 seconds

=== Stratified cross-validation ===
=== Summary ===

Correctly Classified Instances          38               84.4444 %
Incorrectly Classified Instances         7               15.5556 %
Kappa statistic                          0.7667
Mean absolute error                      0.1077
Root mean squared error                  0.2632
Relative absolute error                 24.1075 %
Root relative squared error             55.5331 %
Total Number of Instances               45
Ignored Class Unknown Instances                 15

=== Detailed Accuracy By Class ===

               TP Rate   FP Rate   Precision   Recall  F-Measure   ROC Area  Class
                 0.733     0.1         0.786     0.733     0.759      0.89     SCA
                 1         0           1         1         1          0.986    NSR
                 0.8       0.133       0.75      0.8       0.774      0.785    CI
Weighted Avg.    0.844     0.078       0.845     0.844     0.844      0.887

=== Confusion Matrix ===

  a  b  c   <-- classified as
 11  0  4 |  a = SCA
  0 15  0 |  b = NSR
  3  0 12 |  c = CI
```

Fig 3.33 Simulation Results for Classification of NSR, SCA and CI using RBF

The above Fig 3.33 shows the simulation results for classification of NSR, SCA and CI using RBF classifier. Time to build the model is 0.05 Seconds. Correctly classified instances are 38 out of 45 instances. RMSE value is 0.2632. The classification accuracy for classifying NSR, SCA and CI is obtained as 84.4%.

```
Time taken to build model: 7.07 seconds

=== Stratified cross-validation ===
=== Summary ===

Correctly Classified Instances          74               70.4762 %
Incorrectly Classified Instances        31               29.5238 %
Kappa statistic                          0.6556
Mean absolute error                      0.0932
Root mean squared error                  0.2825
Relative absolute error                 37.9892 %
Root relative squared error             80.5724 %
Total Number of Instances              105

=== Detailed Accuracy By Class ===

               TP Rate   FP Rate   Precision   Recall  F-Measure   ROC Area  Class
                 0.667    0.089      0.556     0.667     0.606      0.89     VF
                 0.4      0.044      0.6       0.4       0.48       0.824    VT
                 0.8      0.078      0.632     0.8       0.706      0.883    SVT
                 0.667    0.078      0.588     0.667     0.625      0.872    SCA
                 0.867    0          1         0.867     0.929      0.925    NSR
                 0.8      0.022      0.857     0.8       0.828      0.973    CI
                 0.733    0.033      0.786     0.733     0.759      0.83     AF
Weighted Avg.    0.705    0.049      0.717     0.705     0.705      0.885
```

Fig 3.34 Simulation Results for Classification of 7 types of signals using RBF

The above Fig 3.34 shows the simulation results for classification of 7 types using RBF classifier. Time to build the model is 7.07 Seconds. Correctly classified instances are 74 out of 105 instances. RMSE value is 0.2825. The classification accuracy for classifying NSR and VF is obtained as 70.47%.

3.5.3 RF classifier results

The above Fig 3.35 shows the simulation results for classification of NSR and VF using RF classifier. Time to build the model is 0.06 Seconds. Correctly classified instances are 29 out of 30 instances. RMSE value is 0.1389. The classification accuracy for classifying NSR and VF is obtained as 96.67%.

```
Time taken to build model: 0.06 seconds

=== Stratified cross-validation ===
=== Summary ===

Correctly Classified Instances          29               96.6667 %
Incorrectly Classified Instances         1                3.3333 %
Kappa statistic                          0.9333
Mean absolute error                      0.0467
Root mean squared error                  0.1389
Relative absolute error                  9.2273 %
Root relative squared error             27.455  %
Total Number of Instances               30

=== Detailed Accuracy By Class ===

               TP Rate   FP Rate   Precision   Recall  F-Measure   ROC Area  Class
                 1         0.067      0.938     1         0.968      1         VF
                 0.933     0          1         0.933     0.966      1         NSR
Weighted Avg.    0.967     0.033      0.969     0.967     0.967      1

=== Confusion Matrix ===

  a  b   <-- classified as
 15  0 |  a = VF
  1 14 |  b = NSR
```

Fig 3.35 Simulation results for classification of VF and NSR using RF Classifier

```
Time taken to build model: 0.05 seconds

=== Stratified cross-validation ===
=== Summary ===

Correctly Classified Instances          28               93.3333 %
Incorrectly Classified Instances         2                6.6667 %
Kappa statistic                          0.8667
Mean absolute error                      0.2295
Root mean squared error                  0.2743
Relative absolute error                 45.3772 %
Root relative squared error             54.2126 %
Total Number of Instances               30
Ignored Class Unknown Instances                 1

=== Detailed Accuracy By Class ===

               TP Rate   FP Rate   Precision   Recall  F-Measure   ROC Area  Class
                 1         0.133      0.882     1         0.938      0.946     SCA
                 0.867     0          1         0.867     0.929      0.938     NSR
Weighted Avg.    0.933     0.067      0.941     0.933     0.933      0.942

=== Confusion Matrix ===

  a  b   <-- classified as
 15  0 |  a = SCA
  2 13 |  b = NSR
```

Fig 3.36 Simulation results for classification of NSR and SCA using RF Classifier

The Fig 3.36 shows the simulation results for classification of NSR and SCA using RF classifier. Time to build the model is 0.05 Seconds. Correctly classified instances are 28 out of 30 instances. RMSE value is 0.2743. The classification accuracy for classifying NSR and SCA is obtained as 93.33%.

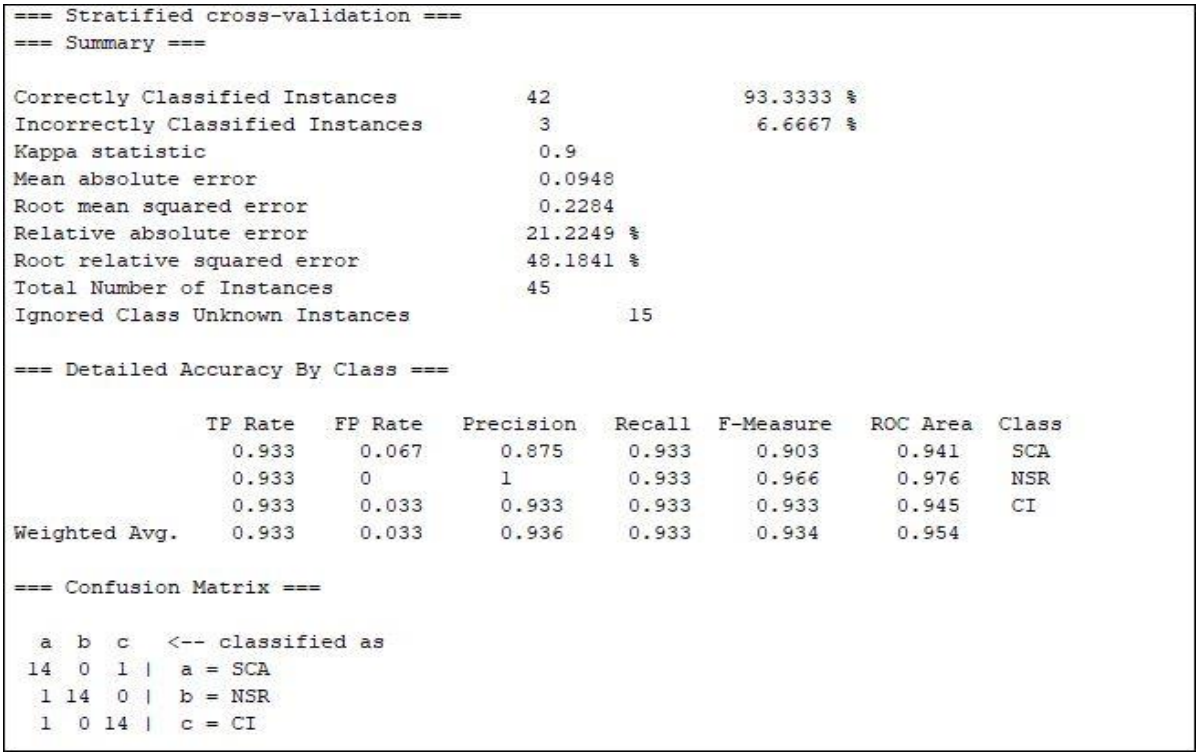

```
=== Stratified cross-validation ===
=== Summary ===

Correctly Classified Instances          42               93.3333 %
Incorrectly Classified Instances         3                6.6667 %
Kappa statistic                          0.9
Mean absolute error                      0.0948
Root mean squared error                  0.2284
Relative absolute error                 21.2249 %
Root relative squared error             48.1841 %
Total Number of Instances               45
Ignored Class Unknown Instances                 15

=== Detailed Accuracy By Class ===

               TP Rate   FP Rate   Precision   Recall  F-Measure   ROC Area  Class
                 0.933     0.067      0.875     0.933      0.903      0.941    SCA
                 0.933     0          1         0.933      0.966      0.976    NSR
                 0.933     0.033      0.933     0.933      0.933      0.945    CI
Weighted Avg.    0.933     0.033      0.936     0.933      0.934      0.954

=== Confusion Matrix ===

  a  b  c   <-- classified as
 14  0  1 |  a = SCA
  1 14  0 |  b = NSR
  1  0 14 |  c = CI
```

Fig 3.37 Simulation results for classification of NSR, SCA and CI using RF Classifier

The above Fig 3.37 shows the simulation results for classification of NSR, SCA and CI using RF classifier. Time to build this model is 0.01 Seconds. Correctly classified instances are 42 out of 45 instances. RMSE value is 0.2284. The classification accuracy for classifying NSR, SCA and CI is obtained as 86.67%.

The following Fig 3.38 shows Classification results of 7 types of cardiac signals using RF classifier. It's built by using random forest of 10 trees, each constructed while considering 3 random features. Out of bag error is 0.2952 and time taken to build the model is 0.02sec. RMSE value is 0.2303. The classification accuracy for 7 types of cardiac signals is obtained as 78.09%.

```
Time taken to build model: 0.02 seconds

=== Stratified cross-validation ===
=== Summary ===

Correctly Classified Instances          82               78.0952 %
Incorrectly Classified Instances        23               21.9048 %
Kappa statistic                          0.7444
Mean absolute error                      0.0893
Root mean squared error                  0.2303
Relative absolute error                 36.3762 %
Root relative squared error             65.6817 %
Total Number of Instances              105

=== Detailed Accuracy By Class ===

               TP Rate   FP Rate   Precision   Recall  F-Measure   ROC Area  Class
                 0.8       0.1       0.571     0.8       0.667      0.909    VF
                 0.533     0.033     0.727     0.533     0.615      0.828    VT
                 0.8       0.022     0.857     0.8       0.828      0.91     SVT
                 0.667     0.044     0.714     0.667     0.69       0.916    SCA
                 0.933     0         1         0.933     0.966      0.999    NSR
                 0.933     0.033     0.824     0.933     0.875      0.961    CI
                 0.8       0.022     0.857     0.8       0.828      0.916    AF
Weighted Avg.    0.781     0.037     0.793     0.781     0.781      0.92

=== Confusion Matrix ===

  a  b  c  d  e  f  g   <-- classified as
 12  0  1  1  0  0  1 |  a = VF
  4  8  1  2  0  0  0 |  b = VT
  3  0 12  0  0  0  0 |  c = SVT
  1  1  0 10  0  3  0 |  d = SCA
  0  0  0  0 14  0  1 |  e = NSR
  0  0  0  1  0 14  0 |  f = CI
  1  2  0  0  0  0 12 |  g = AF
```

Fig 3.38 Simulation results for classification of 7 types of cardiac signals using RF Classifier

The following Table 3.4, shows classification results of different cardiac signals in time domain. It has been observed that classification accuracy of NSR and VF is 100%. NSR and SCA is 96.67%; NSR, SCA and CI is 91.11% and NSR, VT, VF, SVT, AF, CI and SCA is 70.47% using MLP classifier. As, less number of features (4 temporal) are used machine learning algorithm, RF has produced better accuracy for classification of three and seven types as 93.33% and 78.09% respectively.

Table 3.4 Classification of cardiac arrhythmias and disorders in time domain

Features used	**Cardiac Signals**	**Classifier**	**Accuracy**
No. of R peaks, R peak amplitude, R-R interval & Heartbeat rate (4 temporal features)	NSR and Ventricular Arrhythmia(VF)	MLP	100%
		RBF	100%
		RF	96.67%
	NSR and SCA (2 types)	MLP	96.67%
		RBF	96.67%
		RF	93.33%
	NSR, SCA and CI (3 types)	MLP	91.11%
		RBF	84.44%
		RF	93.33%
	NSR,SVT,VT,VF,AF,CI and SCA (7 types)	MLP	70.47%
		RBF	70.05%
		RF	78.09%

3.6 Performance comparison of cardiac arrhythmias analysis and Classification

Summary of performance analysis and classification of cardiac signals is shown in Table 3.5

Table 3.5 Summary of performance analysis of cardiac signals

Study by	Records and Features	Algorithm	Cardiac Arrhythmia Analysis
Pan and Tompkin[2]	Morphological features(slope, amplitude and width of the QRS complex)	Real time QRS detection algorithm	QRS detection has been done with 99.3% accuracy
M. Vijayavanan et al. [5]	300 Records 12 -Morphological features	PNN classifier	Distinguished Normal and Arrhythmia with accuracy of 96.5%
Rathnakara et al. [37]	Temporal Features (RR intervals, No. of R peaks and R peak amplitude)	Modified Pan-Tompkins Algorithm	Distinguished Normal and Arrhythmia
V. Vijaya et al.[4]	Features-2 Temporal features (No. of R-peaks/1000 samples and R-R interval)	Pan-Tompkins Algorithm	Distinguished NSR and SCA
Mujeeb Rahman K et al. [6]	8 records Features-4 temporal features (R-R interval, P-R interval, Q-T interval and QRS complex duration)	Pan-Tompkins Algorithm (PTA) and Wavelet based Algorithm (WBA)	PTA accuracy (99.95%) more than WBA (97.75%) accuracy.
Proposed	30 Records (NSR-15 and VF-15), 4 temporal features	Pan-Tompkins Algorithm	Distinguished and classified Normal and Arrhythmia with 100% accuracy.
	105 records, Each cardiac signal 15 records, 4-temporal features	Pan-Tompkins Algorithm, RF classifier	Classified 7 types of cardiac signals with classification accuracy of 78.09%

3.7 Conclusion

Cardiac arrhythmias analysis has been done using PTA, temporal features have been extracted and analysed 7 types of cardiac signals. For two types of cardiac signals (Normal and Ventricular Arrhythmia) obtained classification accuracy as 100% using MLP classifier.

V. Vijaya et al. [4] analysed and compared only two types of cardiac signals - normal and SCA based on the two temporal features (No. of R- peaks and R-R interval) on 10sec data of 1000 samples. Whereas, in proposed work classified NSR and SCA using four temporal features - No. of R-Peaks, R-R Interval, R-Peak Amplitude and Heartbeat rate on 1minute data for 15000 samples and obtained 96.6% accuracy using MLP classifier, Later, extended the work to classify three types of ECG signals (NSR, SCA and CI) and obtained classification accuracy as 91.11% using MLP and also evaluated the results with other classifiers as shown in Table 3.4, Fig 3.28, Fig 3.33 and Fig 3.37. The reason to classify is treatment for SCA is different from CI. The temporal features extracted was on 1min data of 15000 samples. The proposed work also classified 7 types of cardiac signals (1- normal, 4- arrhythmias and 2- cardiac disorders) and obtained an accuracy of 78.09% using Random Forest classifier and also evaluated the results with other classifiers (MLP and RBF) as shown in Table 3.4 The performance of RBF networks are good when the size of training data set is relatively small, but the performance of MLPs are good when the size of training data set size is relatively large [52].

Whereas Random Forest classifier performance is not depending on data size and also less computationally expensive. Use of Pan-Tompkins algorithm to extract temporal features may not be sufficient to describe complex changes that take place in ECG signal due to heartbeat rate variation. These dynamics are to be explored to improve classification accuracy. So, spectral analysis is preferred to get more information about different cardiac signals to improve classification accuracy.

Chapter 4

Cardiac Arrhythmias Analysis and Classification in Spectral Domain

In the previous chapter, it has been observed that the proposed temporal features improved the discriminating capability of the cardiac arrhythmias and the overall classification accuracy of seven types of cardiac signals. In this chapter, hybridization of temporal and spectral features have been proposed and compared with the existing works.

4.1 Introduction

In this chapter, spectral analysis and classification of cardiac signals have been described. Significant work has been done in time domain analysis; however, the spectral analysis gives frequency information. In time domain, detection of a condition would involve monitoring the ECG for over 24 hours which is not at all feasible. Therefore, in this work spectral features are extracted and analysed. This concept provided the motivation to perform this work in frequency domain to help enable physicians in future to identify diseases. Time-domain analysis represents how a signal varies with time, while spectral analysis shows how the signal's energy is distributed over the range of frequency components. To extract ECG spectral features, Fourier transform analysis is used to convert a signal from time domain to frequency domain.

The spectral parameters give a unique representation of signal that helps to understand the activity of the heart [36]. FFT algorithm has been proposed to extract spectral features (Mean, Median, Standard Deviation and Energy in Regions R1 to R5) to distinguish seven types of cardiac signals. In this research work, total number of 105 data records (7 types of cardiac signals, 15 records of each type, one minute duration and sampling frequency of 250 Hz) are considered. The spectral features (Mean, Median, Standard Deviation and Energy in only Region R3) along with temporal features (No. of R peaks, R peak amplitude, R-R interval and Heart beat rate) are fed to three types of supervised classifiers and medical statistics are computed. Further, performance comparison has been done with the existing works [19]

4.2 Overview of existing works

In this section, the work done by some researchers has been presented briefly.

Glenn A. Myers et al. **[18]** describes a method of power spectrum analysis of HRV applied to 24 hours ambulatory ECGs. In this method, two groups of patients with known heart disease: one with and one without a history of SCD have been analysed. The power spectral method provides excellent separation between the two groups of cardiac patients. The separation appears to be superior to that afforded by other indexes of heart rate variability.

Usman Rashed et al. [19] used spectral analysis to identify NSR and SCA. Further he mentioned time-domain analysis may not be sufficient when the signal changes over time and added spectral analysis gives how the ECG signal's energy distributed over a wide range of frequencies.

K. Minami et al. [15] developed a method to discriminate life-threatening ventricular arrhythmias by observing the QRS complex of the electrocardiogram (ECG) in each heartbeat. Changes in QRS complexes due to rhythm origination and conduction path were observed with the Fourier transform and classified three types of rhythms using neural networks. The method achieved high sensitivity as 98%.

Fast Fourier Transform on the ECG has been providing the basis with which a signal suggesting predisposition of the patient to suffer a cardiac arrest can be differentiated from a normal signal. In this way, it is proposed that instead of waiting for over 24 hours, few minutes of any cardiac patient ECG data is enough to detect possibility of sudden cardiac arrest.

4.3 Methodology for Spectral Domain Analysis

The main aim of spectral analysis on ECG is to diagnose the type of cardiac arrhythmias and disorders to enable doctors for proper treatment.

Fast Fourier Transform (FFT) algorithm shown in Fig 4.1 has been used to extract ECG signal information.

One ECG data record is taken for a duration of 1 minute using sampling frequency of 250Hz (250 samples /sec, no. of samples are 15000 in single data record). 15 data records are considered for each category (i.e., NSR, VT, SVT, VF, AF, CI, SCA and CI) resulting in total of 105 records. The processing steps of spectral analysis of ECG are shown below in Fig 4.1.

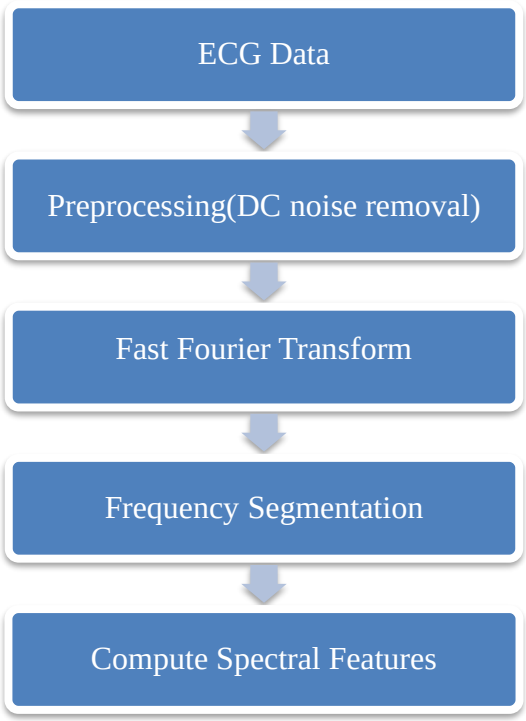

Fig 4.1 Spectral Analysis of ECG

For pre-processing, mean is removed from ECG data, so that DC noise can be removed. Frequency spectrum appeared up to 32 Hz. So, there is no effect on ECG due to power line interference 50Hz/60Hz.

Fourier transform decomposes a function into the sum of different frequency components. The inverse fourier transform converts the signal from frequency domain to time domain.

Fourier Transform decomposes the signal to complex exponential functions of different frequencies. This Transformation can be given by below equations,

The Fourier transform of time domain signal x (t) is given as

$$X(f) = \int_{-\infty}^{\infty} x(t)e^{-2j\pi ft}dt \quad (4.1)$$

The Inverse Fourier transform of X (f) is given as

$$x(t) = \int_{-\infty}^{\infty} X(f)e^{2\pi ft}\,df \quad (4.2)$$

Discrete Fourier Transform (DFT), is a special kind of discrete transform that converts the time domain signal into frequency domain. The input to the DFT is a finite sequence of real or complex numbers making the DFT ideal for processing information stored in computers. In particular, the DFT is widely employed in signal processing and related fields to analyse the frequencies contained in a sampled signal. A DFT decomposes a sequence of values into

components of different frequencies. This operation is useful in many fields but computing it directly from the definition is often too slow to be practical. Fast Fourier Transform, (FFT) is a way to compute the same result more quickly [67].

A sequence of N complex numbers X_0, X_{N-1} can be transformed into a sequence of N complex numbers by the DFT according to the following equation (3.5).The DFT of x_n is given by X_k as

$$X_k = \sum_{n=0}^{N-1} x_n e^{-\frac{2\pi i k n}{N}} \quad where\ k = 0,1,2 \dots \dots \dots, N-1 \tag{4.3}$$

The difference in speed can be substantial, especially for long data sets where N may be in the thousands or millions in practice, the computation time can be reduced by several orders of magnitude in such cases, and the improvement is roughly proportional to *N /log (N)*. This huge improvement made many DFT-based algorithms practical. FFT technique (RADIX 2 FFT) is applied to distinguish NSR, 4 types of cardiac arrhythmias and 2 cardiac disorders.

The obtained frequency spectrum is divided into five regions (R1 to R5):

Region R1: 0-2 Hz

Region R 2: 2-8 Hz

Region R 3: 8-16 Hz

Region R 4: 16-22 Hz

Region R 5: 22-32 Hz

Absolute values of DFT is used to compute spectral features such as Mean (μ), Median, Standard deviation (σ) and Energy (ϵ_x) can be calculated in each region by using the following equations 4.4, 4.5, 4.6 and 4.7 respectively.

$$\mu = \frac{1}{N}\sum_{i=0}^{N-1} x_i \tag{4.4}$$

$$Median = \begin{cases} \frac{(N+1)th\ term}{2}, & when\ N\ is\ odd \\ \frac{\frac{N}{2}th\ term + \left(\frac{N}{2}+1\right)th\ term}{2}, & when\ N\ is\ \text{even} \end{cases} \tag{4.5}$$

$$\sigma = \sqrt{\frac{1}{N-1}\sum_{i=0}^{N-1}(x_i - \mu)^2} \tag{4.6}$$

$$\epsilon_x \triangleq \sum_{n=0}^{N-1} |x_n|^2 \tag{4.7}$$

4.4 Classification of Arrhythmias using Neural Networks and Machine Learning Algorithms

Frequency-domain analysis shows how the signal's energy is distributed over a range of frequencies. The spectrum of frequency components is the frequency domain representation of the signal. For each segment, applied FFT to extract spectral parameters such as Mean, Median, Standard deviation and Energy as shown in Table 4.1 to Table 4.7.

Table 4.1 Spectral features in different regions of NSR records

NSR Record Number	Regions	Mean	Median	Standard Deviation	Energy(μJ)
16265	R1	2.271759999	0.798958935	4.228627392	1502.902796
	R2	4.62274717	2.197159464	5.059316499	9226.79886
	R3	3.069773132	2.273440434	2.36611201	**3930.163713**
	R4	0.679883614	0.59315605	0.450642343	130.1996903
	R5	0.121916507	0.091916047	0.101290169	4.939036918
16272	R1	5.892062306	2.92664164	6.639619605	5156.777935
	R2	4.679667747	4.122259314	3.141053869	6247.939179
	R3	2.587070164	1.996687945	2.035269876	**2834.694617**
	R4	0.260691612	0.172579399	0.218597018	22.63819078
	R5	0.030916149	0.024670065	0.022866737	0.290780214
16273	R1	3.082669328	1.80496069	3.460109316	1405.391283
	R2	4.634336637	3.313052952	3.472296536	6594.125258
	R3	2.943485958	2.281973785	2.098412458	**3419.267106**
	R4	0.644597202	0.516006507	0.459748398	122.6559633
	R5	0.133046688	0.103076814	0.101299729	5.498460467
16420	R1	1.859126363	1.044979552	2.725868698	711.0925653
	R2	4.723454518	3.377616127	4.094499651	7681.197218
	R3	3.328344126	2.723233865	2.417013475	**4427.153182**
	R4	0.413316452	0.324554894	0.329465442	54.64953399
	R5	0.085645731	0.073374042	0.04991913	1.933448886
16483	R1	5.595256276	2.360897158	9.924433408	8468.389525
	R2	3.805035101	1.177835958	7.295562554	13284.36921
	R3	2.462858069	1.175585063	3.070945134	**4050.619254**
	R4	0.989137537	0.744574874	0.985107593	381.0002502
	R5	0.326572392	0.222626935	0.280916704	36.477139
16539	R1	4.47882866	3.442214475	3.581039445	2157.503635
	R2	5.087040628	4.68472902	2.679169591	6504.840665
	R3	2.673598757	1.902471844	2.258605822	**3204.24951**
	R4	0.190420789	0.132504538	0.164638922	12.39264015
	R5	0.032109078	0.025631529	0.023572073	0.312011551

16773	R1	5.041315759	2.993751431	5.828602024	3885.600164
	R2	4.061962893	3.47885802	2.972347855	4982.040828
	R3	2.872988556	2.326710561	2.149705053	**3368.706073**
	R4	0.630875989	0.486812081	0.468974855	120.8966807
	R5	0.112963599	0.083479945	0.090345932	4.113700551
16786	R1	4.212371593	1.944382934	5.127796401	2880.238148
	R2	6.021601694	5.396827209	3.673486364	9788.080736
	R3	2.034667443	1.303892172	2.000554421	**2129.225256**
	R4	0.086485695	0.073952701	0.050357576	1.960533638
	R5	0.044364864	0.039302891	0.023712194	0.497948067
16795	R1	6.984080504	5.374971381	5.329401055	5065.470626
	R2	4.101522086	3.331237243	3.285756487	5430.083589
	R3	2.427299927	2.096758724	1.597049591	**2209.345743**
	R4	0.565528878	0.443734418	0.410541707	95.55146684
	R5	0.129880741	0.098860429	0.100217045	5.291711759
17052	R1	4.248374873	2.718428658	4.185850897	2330.10108
	R2	5.416539104	5.162773335	3.227715988	7821.719984
	R3	2.481611082	1.942629148	1.992187334	**2649.358621**
	R4	0.181172588	0.116329153	0.183849612	13.02453985
	R5	0.025204438	0.022331925	0.014537053	0.166566823
17453	R1	2.710424748	1.67579378	3.05833702	1092.835199
	R2	4.350176918	4.114782016	2.64597176	5100.264371
	R3	3.187020376	2.706260704	2.146591435	**3863.810006**
	R4	0.700644459	0.550838999	0.487632795	142.5851409
	R5	0.153721283	0.12634524	0.11385552	7.195919442
18177	R1	8.568895593	3.383656129	13.5702569	16815.98584
	R2	4.06120458	2.162014352	5.730714853	9686.050554
	R3	2.314183825	1.19072864	3.47979221	**4563.564005**
	R4	0.147768018	0.092115798	0.149939799	8.663714833
	R5	0.063532091	0.061769325	0.015856451	0.844436024
18184	R1	4.642562393	3.796132519	3.80397542	2363.088332
	R2	4.356981367	3.883999051	3.016144075	5522.743982
	R3	2.681022387	2.250020583	1.898995544	**2824.438877**
	R4	0.696126712	0.586660555	0.439403484	132.6298173
	R5	0.164625127	0.134312912	0.120482324	8.184116357
19093	R1	11.71653499	1.453846151	63.0632295	267563.4042
	R2	2.972286828	1.31234217	9.935013458	21086.47484
	R3	1.334766437	0.929448988	2.538321717	**2148.42271**
	R4	0.505930254	0.416572589	0.479034544	94.91667108
	R5	0.290309391	0.275624291	0.095746749	18.39988806
19830	R1	17.50244296	8.411157094	20.3037016	47013.76304
	R2	2.919917015	2.004995906	3.77474681	4472.353171
	R3	0.991418041	0.666821428	1.184211206	**623.537313**
	R4	0.195516503	0.146287257	0.175609314	13.50596686
	R5	0.054762108	0.039684968	0.053698625	1.155955311

Table 4.2 Spectral features in different regions of SCA records

SCA Record Number	Regions	Mean(μ)	Median	Standard Deviation	Energy(μJ)
SCA 30m	R1	16.1703691	12.21735374	17.70543813	37634.1003
	R2	3.746058567	3.162439612	2.558040516	4047.032065
	R3	0.626090103	0.382938423	0.619019828	**202.7124979**
	R4	0.093221863	0.088711695	0.026808491	1.843447457
	R5	0.068001971	0.066929536	0.006024733	0.918095099
SCA 31m	R1	15.19551187	12.3731859	12.55670601	25488.24263
	R2	4.688224808	3.093082561	4.762720315	8775.918956
	R3	0.425739357	0.224785701	0.448520318	**99.99404215**
	R4	0.038553069	0.03376915	0.019262649	0.363677142
	R5	0.026901324	0.026572077	0.004991049	0.147447677
SCA 32m	R1	11.62489197	6.783394671	13.68061617	21084.46729
	R2	5.162139058	3.375418898	5.920794168	12120.53039
	R3	0.88234104	0.709683089	0.733048154	**344.2245905**
	R4	0.091871731	0.069755038	0.074351862	2.732320215
	R5	0.019941755	0.018527899	0.007866617	0.090470894
SCA 33m	R1	20.79393389	12.97355374	29.36933162	84603.83389
	R2	3.549181322	1.326285873	4.570716445	6576.271515
	R3	0.229368956	0.184770073	0.156002167	**20.13572344**
	R4	0.056531619	0.052945814	0.01922596	0.698460823
	R5	0.026475339	0.026440288	0.005254445	0.143497289
SCA 34m	R1	11.54275773	6.209648512	18.52704132	31104.8588
	R2	4.341932582	3.664368885	2.884840035	5345.089772
	R3	1.224409378	0.767286603	1.207169171	**773.1289045**
	R4	0.127390264	0.110996735	0.065299846	4.012236378
	R5	0.092611117	0.090601537	0.007533197	1.700756138
SCA 36m	R1	12.38812578	9.799323191	12.07105023	19599.90007
	R2	5.082829784	4.196997196	3.451066793	7423.859202
	R3	0.572979712	0.358887522	0.557918739	**167.258443**
	R4	0.126614191	0.114447204	0.070129019	4.101131522
	R5	0.063115618	0.059598346	0.015867005	0.834110816
SCA 37m	R1	26.98089565	16.60674423	50.39186962	213103.0702
	R2	1.454921923	0.886127605	1.656954738	955.1269718
	R3	0.250137685	0.198120695	0.145294739	**21.90289818**
	R4	0.129064511	0.124817069	0.016327827	3.316885611
	R5	0.099075846	0.098829795	0.006857323	1.94297305
SCA 38m	R1	11.99031595	4.917130197	19.74903711	34840.25698
	R2	5.173977729	3.126707366	6.438263335	13398.14099
	R3	0.650384431	0.275602946	0.765030377	**263.5818316**

	R4	0.093993835	0.089377376	0.02854338	1.890500126
	R5	0.059593836	0.057910632	0.006915488	0.709004271
SCA 39m	R1	15.36695901	12.10168776	12.50537448	25750.45173
	R2	4.00454862	2.977799755	3.900568434	6141.201787
	R3	0.869937054	0.554571729	0.80373526	**366.8825913**
	R4	0.090753733	0.068947583	0.073936647	2.680295478
	R5	0.027606516	0.025615662	0.009214411	0.166779038
SCA 41m	R1	16.32727585	9.80208581	20.71343231	45482.28391
	R2	4.155438844	2.212914226	6.563688962	11845.80589
	R3	0.49597694	0.372989878	0.346165426	**95.7259598**
	R4	0.083281284	0.076211673	0.031466877	1.552493411
	R5	0.030722008	0.029904444	0.00844642	0.19991987
SCA 43m	R1	10.45411892	4.164355242	17.56094034	27258.17842
	R2	4.417565634	2.301328041	5.665379661	10135.3518
	R3	1.553610053	1.178256733	1.429477971	**1165.719797**
	R4	0.122133331	0.099833767	0.075010566	4.020827973
	R5	0.062345877	0.060602304	0.008326913	0.779330789
SCA 44m	R1	13.47484363	10.34722644	8.670549012	16870.31043
	R2	3.46965355	2.303458894	3.121247637	4281.052279
	R3	0.582272431	0.517254859	0.203343926	**99.62081449**
	R4	0.348334047	0.345135659	0.03201942	23.98189764
	R5	0.26911952	0.268425416	0.016588018	14.32171907
SCA 45m	R1	13.24140417	6.153349547	29.16757857	66870.69233
	R2	4.435085656	3.535302183	3.061452067	5711.994797
	R3	1.297025899	0.778638331	1.357418518	**921.6710534**
	R4	0.090931589	0.079725459	0.05617475	2.23597905
	R5	0.045244275	0.044329154	0.012941767	0.436095667
SCA 46m	R1	12.96235939	8.219017681	12.46762654	21193.21348
	R2	4.687005488	2.599705747	5.716800272	10733.33388
	R3	0.662703922	0.403043553	0.673264233	**233.3715538**
	R4	0.132908087	0.126957066	0.024696525	3.581187777
	R5	0.088955192	0.088146987	0.008864894	1.574269082

Table 4.3 Spectral features in different regions of VF records

VF Record Number	Regions	Mean	Median	Standard Deviation	Energy(μJ)
418	R1	21.6421982	17.3682233	12.75305666	41485.02256
	R2	2.657841326	1.671900979	3.171434387	3362.998972
	R3	0.343176495	0.193789448	0.365996093	**65.81753739**
	R4	0.039058856	0.035647286	0.019316011	0.371772583
	R5	0.031017737	0.030591979	0.006419558	0.197611007
419	R1	25.29862888	14.98218592	28.14687518	93737.389
	R2	1.532244392	0.949186749	1.695739581	1026.115671
	R3	0.188104717	0.126906742	0.163526924	**16.24986212**
	R4	0.04740008	0.045306999	0.024490342	0.557322931
	R5	0.0403885	0.040433307	0.009638768	0.339562048
421	R1	12.46081469	7.332522515	13.80471665	22635.00869
	R2	5.237752847	3.671006568	5.225500769	10756.45704
	R3	0.590171121	0.327730482	0.601270162	**185.6133474**
	R4	0.058108623	0.05516179	0.020580371	0.744408543
	R5	0.042752917	0.042813759	0.005629346	0.366290088
425	R1	16.46240456	6.49111613	40.22589318	123064.6718
	R2	3.838136747	3.13202819	2.4423628	4071.231522
	R3	0.64813082	0.52953411	0.445384347	**161.833116**
	R4	0.179176651	0.166746071	0.073303778	7.340258942
	R5	0.134737483	0.132364071	0.012413704	3.606578887
427	R1	19.53849955	3.969056208	90.74892069	560494.5251
	R2	2.703663306	2.272004347	1.752023598	2041.668659
	R3	0.891079244	0.695898754	0.51789543	**278.0381127**
	R4	0.394678498	0.380011834	0.061664173	31.27262061
	R5	0.28679114	0.284049456	0.02118902	16.29108309
428	R1	27.17923013	3.301971466	164.3733349	1804963.455
	R2	1.913272813	1.489124461	1.685193477	1277.756636
	R3	0.800647123	0.75161153	0.262899141	**185.9906486**
	R4	0.396364474	0.386293835	0.060751653	31.51223885
	R5	0.279680148	0.278691095	0.023830219	15.52083843
429	R1	14.81694734	9.304580153	20.12280883	40810.05055
	R2	4.622811979	3.588443351	4.645714263	8440.168506
	R3	0.823908052	0.521058458	0.953832261	**415.3087647**
	R4	0.060140258	0.052046447	0.039259362	1.009455736
	R5	0.01757476	0.014970599	0.011862279	0.088427697
430	R1	20.97574716	13.39638217	24.72592168	68777.93813
	R2	3.275228276	1.95707469	3.712156415	4814.143321
	R3	0.299906974	0.216334948	0.252590171	**40.21764699**
	R4	0.065603257	0.061559332	0.034609005	1.077110055

	R5	0.02654114	0.023472394	0.016136954	0.189811774
602	R1	11.69758294	9.245687317	8.302292924	13511.33188
	R2	5.456304414	4.610219388	4.055289077	9088.23022
	R3	0.651541569	0.399401455	0.634269402	**216.2203742**
	R4	0.059647886	0.046720102	0.047522402	1.137726421
	R5	0.023066789	0.022446488	0.010275423	0.125513652
605	R1	14.76248149	12.29173152	10.14855284	21077.98985
	R2	4.139842243	3.161534639	3.621358916	5946.634997
	R3	0.821253876	0.530039829	0.755675688	**325.7509168**
	R4	0.108134008	0.0737037	0.093926102	4.012132855
	R5	0.043747989	0.041964778	0.016005211	0.427244339
607	R1	14.93094213	8.832009292	18.86044321	37835.14085
	R2	4.214002565	2.368749011	6.078040266	10739.03447
	R3	0.616601174	0.421790914	0.659471153	**213.1210906**
	R4	0.091828314	0.083656124	0.042688154	2.00810241
	R5	0.063698666	0.061520028	0.014635722	0.841315507
609	R1	23.75976707	17.48949524	20.89761552	65644.92279
	R2	1.956294254	1.077010545	2.447313574	1927.847551
	R3	0.230681085	0.180910845	0.172279574	**21.68855155**
	R4	0.05227533	0.041263594	0.038640449	0.826762619
	R5	0.026398017	0.025530118	0.006852379	0.146483693
610	R1	13.98241565	14.43435674	7.512833621	16572.29801
	R2	4.951727948	4.111135572	3.669706075	7469.84467
	R3	0.451626015	0.309122598	0.44615283	**105.3917698**
	R4	0.0543282	0.044371407	0.03565577	0.826414555
	R5	0.02350978	0.023185306	0.010501775	0.130500126
611	R1	10.17293981	5.548994231	13.07439042	17941.334
	R2	4.708764258	2.255272238	6.711476674	13196.58294
	R3	0.622177989	0.524727448	0.374499102	**138.0267676**
	R4	0.308509311	0.301598607	0.048631143	19.11605966
	R5	0.236761107	0.235282895	0.016928898	11.0991681
612	R1	10.73748135	6.497433432	16.32652733	24935.47852
	R2	4.785607329	4.099542729	3.07525231	6365.308037
	R3	1.334080198	0.981739164	1.135449522	**802.7928393**
	R4	0.182035592	0.146697144	0.130635195	9.822626571
	R5	0.049913612	0.044006714	0.03261872	0.699339895

Table 4.4 Spectral features in different regions of VT records

VT Record Number	Regions	Mean	Median	Standard Deviation	Energy(μJ)
cu01	R1	8.936889	4.599143	11.12743934	13319.58087
	R2	5.428527	4.641444	3.750013288	8561.643145
	R3	1.344726	0.861307	1.496466881	**1058.258574**
	R4	0.062318	0.04963	0.049738739	1.243592034
	R5	0.02678	0.026181	0.006078761	0.148524781
cu03	R1	19.65029	8.125646	29.53443922	82183.2383
	R2	2.991765	1.429753	5.222057886	7108.177744
	R3	0.573815	0.508414	0.436440222	**135.9822574**
	R4	0.107755	0.100314	0.041513458	2.611849749
	R5	0.063727	0.061417	0.011495404	0.825940411
cu05	R1	9.836789	9.198354	7.459985348	10003.65988
	R2	5.527864	4.706349	3.59317076	8550.315626
	R3	0.935075	0.549974	1.013270139	**497.0568659**
	R4	0.079075	0.068316	0.033100839	1.439220385
	R5	0.051576	0.050303	0.005112007	0.529148433
cu06	R1	22.16736	11.12872	36.66617514	119818.3976
	R2	1.979216	0.989676	2.924808899	2448.390976
	R3	0.263549	0.187291	0.228463873	**31.82114939**
	R4	0.136695	0.13573	0.012221412	3.691500706
	R5	0.109426	0.108667	0.00660933	2.367466886
cu07	R1	9.407328	4.140272	19.69806585	31061.75283
	R2	5.785841	2.915512	9.427121472	24013.40421
	R3	0.758157	0.398361	1.130145647	**483.9549854**
	R4	0.107779	0.097003	0.06340265	3.060666198
	R5	0.072942	0.070989	0.014419194	1.088886601
cu08	R1	16.2912	7.665769	20.71946336	45420.86435
	R2	3.967017	3.167332	3.210610584	5120.604716
	R3	0.309582	0.227301	0.206630672	**36.25399969**
	R4	0.132359	0.126899	0.020102045	3.512481711
	R5	0.094101	0.0937	0.007300861	1.75486676
cu09	R1	12.9903	10.76637	9.927517795	17543.47967
	R2	5.07379	3.613214	4.678606082	9361.751644
	R3	0.627606	0.42699	0.623114374	**204.5377588**
	R4	0.070653	0.05833	0.050097859	1.467813785
	R5	0.014692	0.012348	0.009511457	0.060254514
cu11	R1	14.81571	5.017268	28.06204025	65673.41468
	R2	4.897827	1.966762	8.013240199	17311.33102
	R3	0.324433	0.250492	0.279963158	**48.03429504**
	R4	0.03037	0.024845	0.018486709	0.2474213
	R5	0.016	0.015468	0.003300277	0.052566243
cu12	R1	22.81135	9.589894	34.66012292	112429.6794
	R2	2.39268	1.408434	3.384660369	3373.170535

	R3	0.234756	0.138707	0.27098823	**33.60530409**
	R4	0.026754	0.023973	0.011192288	0.16471684
	R5	0.017467	0.016988	0.002784975	0.061621322
cu13	R1	8.168212	4.737276	10.68695027	11827.20854
	R2	5.689958	4.143276	4.727758636	10758.93212
	R3	0.767574	0.433227	0.724567901	**291.3870252**
	R4	0.207597	0.196776	0.0441103	8.826365398
	R5	0.155328	0.153566	0.011850521	4.780523246
cu14	R1	18.01342	14.96994	14.81328478	35679.073
	R2	4.079908	1.576585	6.139701502	10667.59681
	R3	0.17004	0.09864	0.183271033	**16.34192485**
	R4	0.018945	0.018948	0.007647649	0.081751634
	R5	0.019402	0.01925	0.001974868	0.07492071
cu15	R1	9.699953	6.694202	9.914310009	12598.96017
	R2	5.25086	3.970961	4.324193297	9096.526648
	R3	1.248266	0.718208	1.304581805	**852.4445921**
	R4	0.131913	0.110532	0.089826248	4.983998026
	R5	0.031449	0.026353	0.019798956	0.271671704
cu16	R1	13.33278	8.575741	14.87798209	26120.39631
	R2	4.481799	2.430601	5.572065831	10042.43696
	R3	0.761745	0.445096	0.84894489	**340.1317386**
	R4	0.106052	0.094937	0.046278385	2.622062846
	R5	0.069931	0.067706	0.007446334	0.974257194
cu18	R1	7.216714	5.529683	6.677489101	6335.619357
	R2	6.355227	4.751198	5.157453358	13170.08232
	R3	1.18689	0.729922	1.23232208	**765.4405948**
	R4	0.035332	0.029382	0.025117143	0.367696482
	R5	0.007569	0.004772	0.00708484	0.021125245
cu19	R1	14.71691	6.295317	20.77634195	42352.4339
	R2	4.285156	3.364854	4.498307966	7583.440695
	R3	0.800514	0.52684	0.788647374	**330.2283074**
	R4	0.084955	0.077173	0.050480514	1.911505172
	R5	0.043108	0.041777	0.009395592	0.383394218

Table 4.5 Spectral features in different regions of CI records

CI Record Number	Regions	Mean	Median	Standard Deviation	Energy(μJ)
e0104	R1	6.224571347	4.3316303	6.179685401	5039.442296
	R2	4.036887254	3.452007739	2.569577437	4504.537092
	R3	2.885351525	2.414558603	2.136657282	**3372.76083**
	R4	0.244424598	0.172574149	0.20118409	19.60233568
	R5	0.063205395	0.058501208	0.038371822	1.075589383
e0105	R1	13.11656921	7.634283379	16.33761145	28704.57022
	R2	5.14786454	4.014827822	4.179175615	8643.840065
	R3	0.504295612	0.441304021	0.362612291	**100.9485676**
	R4	0.064113071	0.057967327	0.03673315	1.06877347
	R5	0.041184558	0.039371025	0.016461207	0.387255442
e0106	R1	11.71943395	6.375735447	14.09490526	21978.09175
	R2	4.106738354	2.83141927	4.025564601	6498.677472
	R3	1.640080089	1.471114307	1.027970657	**980.5489049**
	R4	0.236965406	0.166771672	0.215507098	20.06235566
	R5	0.033732784	0.03106635	0.019493198	0.298643462
e0107	R1	11.57106471	7.840111988	12.43629546	18889.70346
	R2	4.992893248	4.235382276	3.122353579	6821.831655
	R3	0.790575858	0.571629937	0.678642681	**283.957756**
	R4	0.124721473	0.110385024	0.05995315	3.749771541
	R5	0.086432025	0.085004498	0.012789236	1.503746171
e0108	R1	7.52696724	4.424436168	9.317855812	9382.703965
	R2	5.356180145	5.206140241	2.956701427	7365.115484
	R3	1.752235477	1.342213559	1.573688331	**1450.791427**
	R4	0.091210229	0.072191177	0.068534967	2.54650707
	R5	0.026248225	0.023291977	0.014013022	0.174214451
e0110	R1	12.26217992	8.29023474	11.89540111	19121.36663
	R2	5.409103687	4.772016766	3.74559937	8513.690201
	R3	0.650119562	0.541112444	0.500344999	**176.0758024**
	R4	0.083586773	0.072722622	0.052451423	1.905877343
	R5	0.022016772	0.019604628	0.014092671	0.134419693
e0111	R1	11.21412732	4.462179115	14.82540749	22586.46497
	R2	4.043657503	3.199515612	3.465822036	5575.51649
	R3	1.622444209	1.109021431	1.489856059	**1269.003356**
	R4	0.308368149	0.299933756	0.148077736	22.91358754
	R5	0.179903822	0.159686899	0.114121083	8.928610735
e0112	R1	15.83414366	7.656411502	22.57310018	49667.94232
	R2	3.930439347	3.670043714	1.885249415	3739.942041
	R3	0.711171017	0.524868524	0.676697859	**252.0273427**
	R4	0.134981301	0.103984546	0.100598923	5.544538446
	R5	0.047380054	0.045473993	0.016767895	0.49734711

e0113	R1	4.663794092	1.768583241	5.783190343	3609.508257
	R2	5.309471829	4.816027066	3.20888639	7571.729312
	R3	2.462965807	1.902764283	1.982871285	**2615.538745**
	R4	0.205410385	0.142152478	0.18576066	14.99878098
	R5	0.034871837	0.032133848	0.019355449	0.312989007
e0114	R1	11.11198238	9.394851666	7.406155187	11714.74982
	R2	5.852932914	5.227536261	3.859770576	9668.568732
	R3	0.579076971	0.319004892	0.607764454	**184.2640583**
	R4	0.058178888	0.049352487	0.038325741	0.949845645
	R5	0.02353672	0.019630909	0.016698726	0.163787607
e0118	R1	6.687339414	4.550802716	8.010843051	7122.837972
	R2	4.932756694	4.354062595	3.278516636	6900.161037
	R3	2.23089934	1.919574945	1.572481619	**1949.325202**
	R4	0.182815001	0.112954884	0.172344389	12.34258437
	R5	0.031697209	0.02921854	0.010498439	0.219531051
e0119	R1	8.973698745	5.217432953	10.23013272	12117.41478
	R2	5.509519195	4.996418253	3.110615986	7876.378582
	R3	0.618181032	0.353900962	0.633388037	**204.8308064**
	R4	0.234160155	0.229735352	0.028714528	10.90765396
	R5	0.179506494	0.176812176	0.013122936	6.381601992
e0121	R1	4.75555293	1.924499825	6.748927216	4453.229929
	R2	5.202203206	3.765187218	4.310552766	8973.244453
	R3	2.517190337	1.942987187	1.932972115	**2635.292257**
	R4	0.176042341	0.106011034	0.168665366	11.62157863
	R5	0.016223375	0.015109309	0.006445473	0.059992633
e0123	R1	3.878976268	1.835117708	5.138191746	2709.132092
	R2	5.045328115	2.8165154	6.910202999	14373.87863
	R3	2.809716005	1.790503023	3.306812445	**4922.397286**
	R4	0.250148511	0.17450113	0.232285457	22.78608245
	R5	0.028288698	0.02165188	0.022788946	0.259439196
e0125	R1	3.753819783	2.485846196	3.856937926	1896.954816
	R2	5.562471631	4.087958476	5.193219991	11381.4235
	R3	2.484130986	1.639679739	2.447887724	**3180.729845**
	R4	0.187049072	0.141903884	0.160262952	11.86594328
	R5	0.022577633	0.019548755	0.013840011	0.137963652

Table 4.6 Spectral features in different regions of AF records

AF Record Number	Regions	Mean	Median	Standard Deviation	Energy(μJ)
4043	R1	8.791477075	3.434375906	13.68072753	17266.69443
	R2	4.600405675	2.546918516	7.576096647	15419.1144
	R3	1.863173759	1.28318622	1.840807063	**1793.92805**
	R4	0.269090615	0.208446708	0.219873538	23.61946551
	R5	0.057709668	0.051494637	0.029943137	0.831821858
4048	R1	12.04343788	5.311591809	27.65047717	59268.60783
	R2	5.786380531	4.46653026	5.128309157	11750.70607
	R3	0.599683797	0.366050522	0.729848186	**233.2496678**
	R4	0.091615496	0.082162441	0.048692148	2.107436643
	R5	0.054054261	0.053090707	0.014474455	0.616670965
4126	R1	6.738400269	3.703377694	7.902242774	7055.752176
	R2	4.997457725	4.222352695	3.211711608	6941.750917
	R3	2.096010931	1.438612462	1.872814443	**2066.474856**
	R4	0.13926702	0.113006507	0.108443398	6.094673644
	R5	0.055889558	0.05520152	0.015632401	0.663254523
4746	R1	13.99838492	8.236119204	21.10094687	41874.26283
	R2	4.61450111	4.009152341	3.056206915	6025.561776
	R3	0.707721786	0.499259719	0.635160898	**236.5230379**
	R4	0.099388919	0.081346016	0.065400867	2.77018714
	R5	0.039797772	0.036881091	0.020684773	0.395881478
4936	R1	9.764157776	7.614398013	8.989275196	11544.81874
	R2	4.938602729	3.962142729	3.722119149	7520.207501
	R3	0.618950913	0.52011311	0.380995904	**138.2584672**
	R4	0.289086343	0.282942859	0.037111321	16.64846285
	R5	0.224727186	0.222921227	0.015964474	9.998908091
5091	R1	4.172207711	2.514492993	4.520641034	2477.235632
	R2	5.682646971	4.389743356	4.65574529	10610.10687
	R3	2.406674155	1.659720539	2.510528576	**3162.543812**
	R4	0.1074084	0.074768722	0.105568357	4.434378817
	R5	0.021183413	0.020256655	0.010823141	0.1113607
6426	R1	14.99431678	12.07274347	10.29632565	21729.68028
	R2	4.383250736	3.650715073	3.114824693	5686.556785
	R3	0.714531254	0.481163044	0.634622491	**238.8820166**
	R4	0.045504005	0.031415691	0.043035144	0.766985042
	R5	0.009397078	0.008864684	0.005540495	0.023412729
6453	R1	19.63547728	15.76326161	14.65703368	39410.29126
	R2	3.329484908	2.568548525	2.921495375	3856.724045
	R3	0.214499143	0.138294331	0.221297233	**24.8364027**
	R4	0.055335395	0.051700676	0.019688442	0.675741946
	R5	0.039545982	0.038479317	0.006009032	0.315162541
7162	R1	7.179106082	5.73420745	6.005103371	5745.593556
	R2	6.148699962	5.494669425	3.746141887	10198.4642

	R3	0.782883734	0.440018326	0.833499873	**341.9040705**
	R4	0.199524728	0.194121372	0.033752191	8.024928998
	R5	0.147509108	0.145070636	0.013597255	4.322748096
7859	R1	8.607069128	7.310383075	6.92923297	8010.315693
	R2	4.401817859	4.278234203	2.207220925	4771.949636
	R3	1.952965786	1.689704062	1.216979953	**1385.839239**
	R4	0.431898325	0.362222146	0.293115046	53.31479176
	R5	0.117732854	0.093045639	0.088111874	4.252307558
7879	R1	7.748171924	5.7355769	8.413222528	8563.105463
	R2	4.632338029	3.672807115	3.482241949	6604.033218
	R3	2.191718167	1.470137734	1.867326042	**2168.633282**
	R4	0.213191329	0.158599169	0.177276386	15.03655523
	R5	0.041328084	0.034018823	0.027989689	0.490028924
7910	R1	10.2639232	6.233147975	10.75435893	14470.63122
	R2	6.156414806	4.416361626	6.760017942	16423.36147
	R3	0.538266317	0.33006051	0.578316339	**163.2008191**
	R4	0.058985846	0.053255795	0.030450301	0.862756737
	R5	0.029265873	0.028205161	0.009819391	0.1876272
8215	R1	13.28129618	5.3343696	24.43005376	50435.71589
	R2	3.27653426	2.482733927	3.263796952	4202.792947
	R3	1.676378761	1.096473412	1.861163403	**1640.369911**
	R4	0.206518977	0.176682392	0.125014051	11.40697726
	R5	0.121274423	0.117105787	0.021075319	2.984431825
8219	R1	11.76724608	8.978260064	11.26153721	17382.33761
	R2	5.935758169	4.70372603	4.284149285	10538.31661
	R3	0.468749739	0.279027042	0.475990614	**116.702299**
	R4	0.05815897	0.04847598	0.04191533	1.005557793
	R5	0.016851483	0.015329665	0.0095356	0.0737644
8434	R1	10.17033428	4.637813454	17.50851915	26752.39194
	R2	5.84087899	4.359842797	4.673143824	11001.12742
	R3	0.807342739	0.572978123	0.707357661	**301.3648207**
	R4	0.110443025	0.104523805	0.06043918	3.103056163
	R5	0.058340657	0.056256507	0.018026601	0.734207387

Table 4.7 Spectral features in different regions of SVT records

SVT Record Number	Regions	Mean	Median	Standard Deviation	Energy(µJ)
801	R1	8.548464447	6.662520703	6.548879552	7610.740651
	R2	5.347888337	3.449964847	5.61237839	11807.94528
	R3	1.284755984	0.954643589	1.3706721	**922.8083234**
	R4	0.184270958	0.158597776	0.122125083	9.563668506
	R5	0.065352686	0.061775346	0.024677491	0.960741606
802	R1	5.875767562	3.691352863	6.167206382	4750.864779
	R2	6.332293465	5.54393566	3.897586073	10876.76501
	R3	1.406694075	0.76059695	1.684764015	**1259.272688**
	R4	0.152534959	0.103532333	0.137321225	8.237453261
	R5	0.037195869	0.032207299	0.023613357	0.381843699
803	R1	5.93457559	5.322307519	3.85404847	3289.956195
	R2	5.004416108	4.068369277	3.457823821	7277.186507
	R3	2.041766299	1.686428025	1.42496883	**1622.19806**
	R4	0.536940574	0.451173847	0.345468436	79.78076115
	R5	0.133087175	0.108558029	0.09226893	5.157959528
807	R1	3.637518276	2.295342805	3.39927554	1624.361411
	R2	5.393814232	3.078747919	6.157956801	13163.77136
	R3	2.415489951	1.633947547	2.360666606	**2983.149948**
	R4	0.273533798	0.170012126	0.256551492	27.49950508
	R5	0.063392292	0.061454095	0.01906618	0.862910548
808	R1	9.320557706	4.595154358	12.57266445	16008.27748
	R2	6.190045648	5.261460306	4.789875781	12045.19339
	R3	0.695216425	0.267691965	0.952971949	**363.6599748**
	R4	0.107306737	0.090750825	0.073948562	3.323224265
	R5	0.024630816	0.023171753	0.013498948	0.15523082
	R2	4.183626279	2.853144322	3.865862056	6377.235911
	R3	3.14531286	2.382033112	2.658553969	**4436.688465**
	R4	0.536514424	0.40968903	0.452833643	96.4045247
	R5	0.099588094	0.090450376	0.04243225	2.30670151
810	R1	6.130120523	3.367850741	6.843267115	5524.142736
	R2	5.755825369	4.82964631	4.11598402	9847.016152
	R3	1.745578657	0.854327858	1.876596541	**1717.467155**
	R4	0.170337925	0.116829047	0.157336987	10.51415258
	R5	0.036283181	0.033475034	0.01935863	0.332796731
811	R1	5.255009955	3.294793103	6.224990469	4341.381468
	R2	5.239298586	4.354250244	3.66041097	8033.826446
	R3	2.163124373	1.96362805	1.475519858	**1794.164507**
	R4	0.414684035	0.34829802	0.28799777	49.8785479
	R5	0.08032323	0.066984962	0.05827641	1.936652207
812	R1	9.930117707	7.726080286	6.997423103	9690.733142
	R2	6.147904466	5.851210819	3.796131552	10270.43617
	R3	0.589033374	0.259593173	0.748515428	**237.1354681**

	R4	0.075919626	0.070626714	0.042500358	1.481927444
	R5	0.025070501	0.022180314	0.015075438	0.168365105
820	R1	3.570503786	2.45898661	5.310073043	2674.197743
	R2	5.30348675	3.753226052	5.026153075	10492.40751
	R3	2.575538813	1.868117067	2.20042468	**3001.678597**
	R4	0.400918606	0.279075038	0.36007227	56.78635062
	R5	0.047505238	0.038968727	0.034443871	0.67710982
821	R1	8.979605089	6.483835074	9.822648962	11593.28642
	R2	4.265512717	3.182940472	4.040310364	6783.861087
	R3	2.009598095	1.373932641	1.859384776	**1960.441306**
	R4	0.157159664	0.116469585	0.13462801	8.375352063
	R5	0.071890397	0.067340831	0.037568008	1.294766775
822	R1	5.715663405	4.505362985	4.161820901	3281.990298
	R2	5.810570139	5.159302934	3.440221549	8970.941255
	R3	1.600992447	0.970112797	1.514160317	**1269.942188**
	R4	0.147990932	0.133168721	0.078682792	5.499899385
	R5	0.088274225	0.087271087	0.030024405	1.711777867
823	R1	3.573375035	1.932115644	5.582048134	2868.106592
	R2	4.626262631	2.505673395	6.5178309	12542.74972
	R3	2.766229348	1.453469546	3.786006217	**5745.963541**
	R4	0.642936907	0.514274813	0.522531504	134.2627404
	R5	0.178710129	0.130899303	0.14634182	10.48917209
824	R1	5.715663405	4.505362985	4.161820901	3281.990298
	R2	5.810570139	5.159302934	3.440221549	8970.941255
	R3	1.600992447	0.970112797	1.514160317	**1269.942188**
	R4	0.147990932	0.133168721	0.078682792	5.499899385
	R5	0.088274225	0.087271087	0.030024405	1.711777867
825	R1	6.388175318	3.793541512	9.141787578	8125.577945
	R2	5.311253474	3.949137426	5.26799017	10996.59166
	R3	1.918725628	1.404131456	1.698144487	**1717.199421**
	R4	0.265046304	0.219998211	0.208228708	22.2239535
	R5	0.066126476	0.057029828	0.038203491	1.147487358

In spectral analysis of spectral features in all 5-regions, energy in R3 region appeared as significant parameter to distinguish all 7 types of cardiac signals (1- normal, 4- arrhythmias and 2- cardiac disorders) as shown in Fig 4.2 to Fig 4.8,

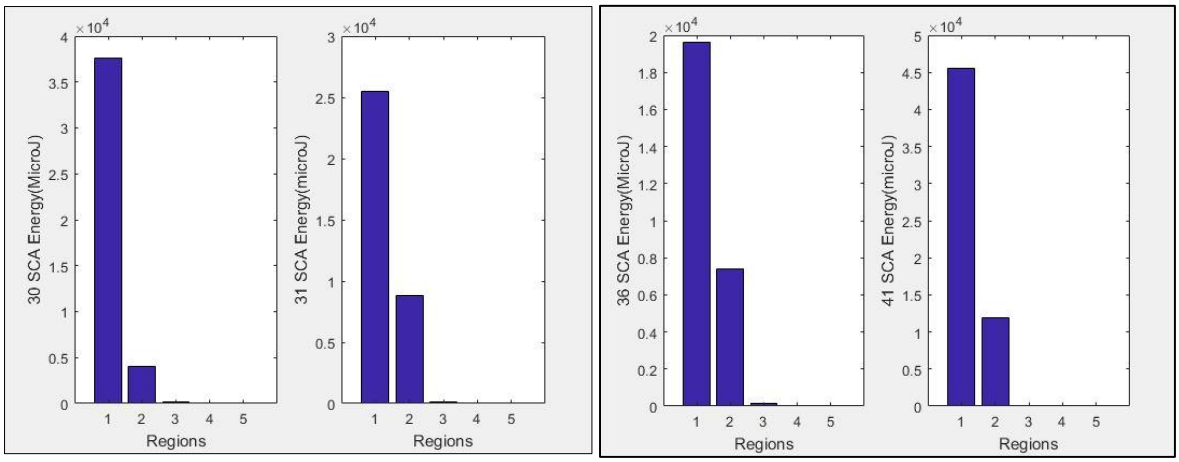

Fig 4.2 Energy at different regions of SCA Records (30, 31, 36 and 41)

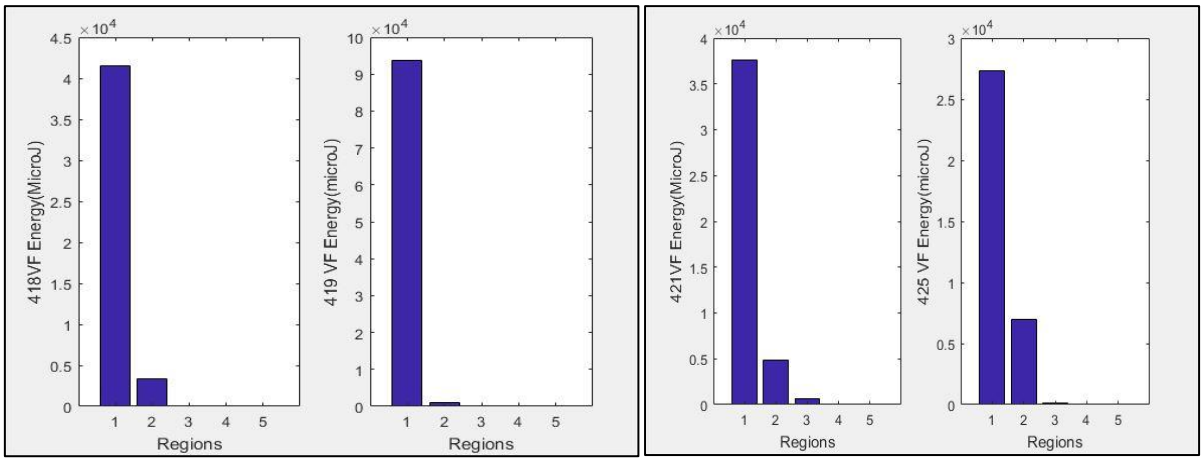

Fig 4.3 Energy at different of VF Records (418, 419, 421 and 425)

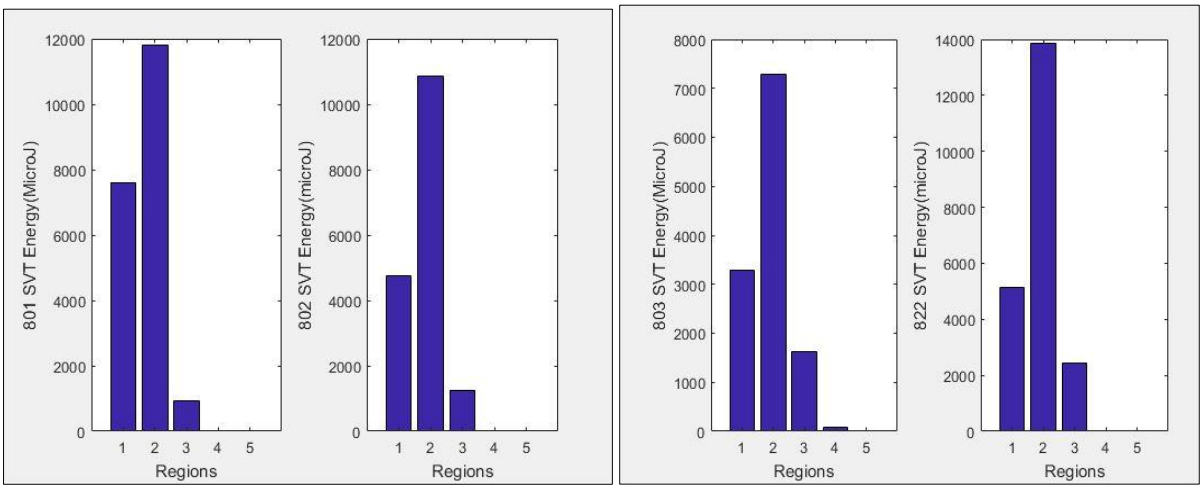

Fig 4.4 Energy at different regions of SVT Records (801, 802, 803 and 822)

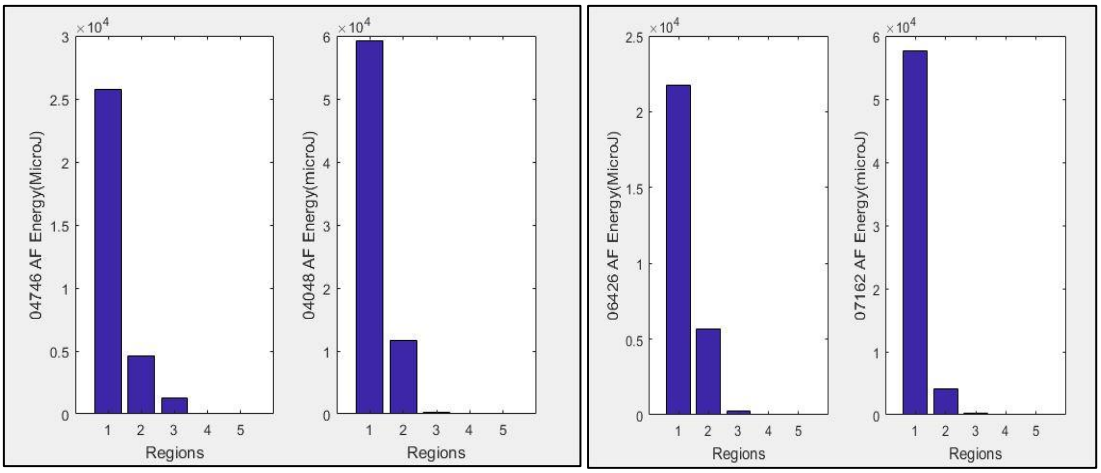

Fig 4.5 Energy at different regions of AF Records (04746, 04748, 06426 and 07162)

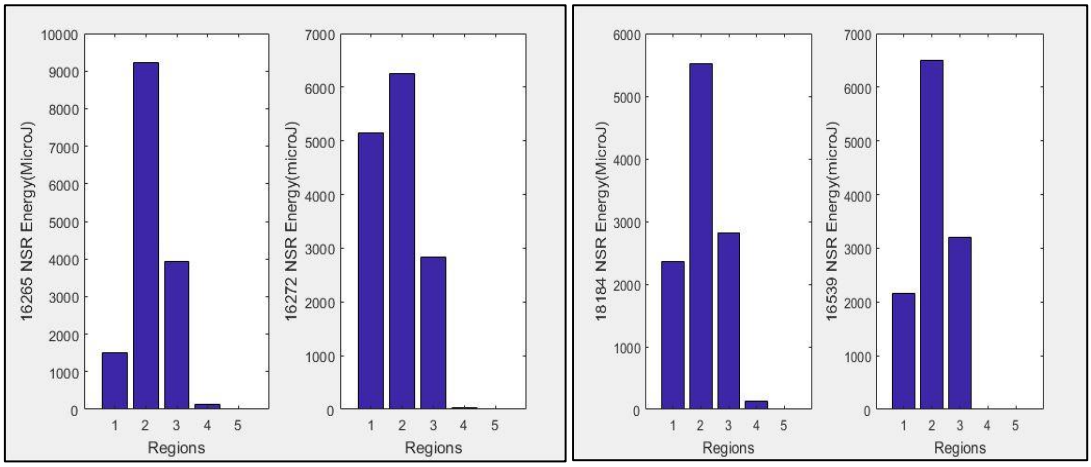

Fig 4.6 Energy at different regions of NSR Records (16265, 16272, 16184 and 16539)

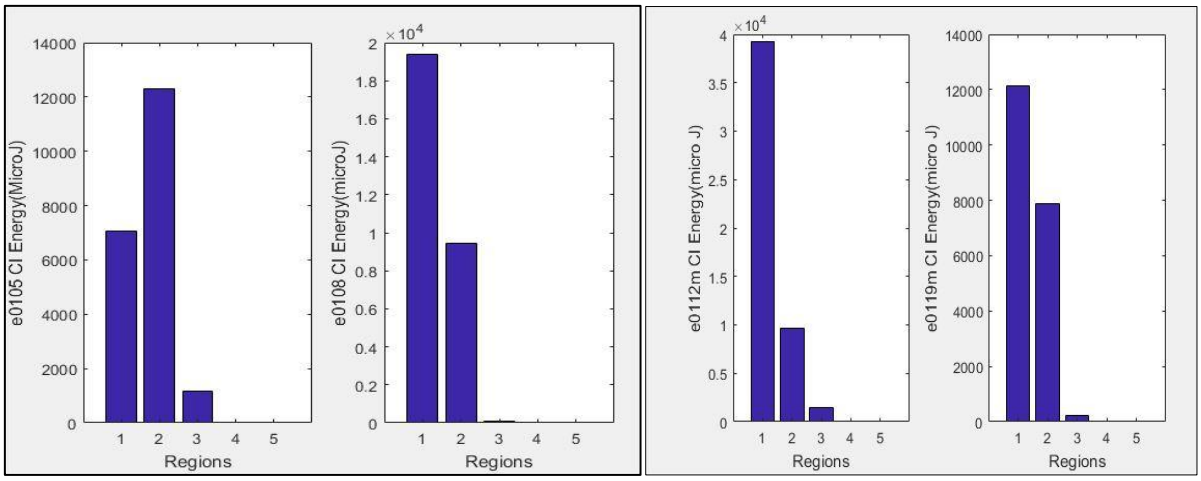

Fig 4.7 Energy at different regions of CI Records (e0105, e0106, e0112 and e0119)

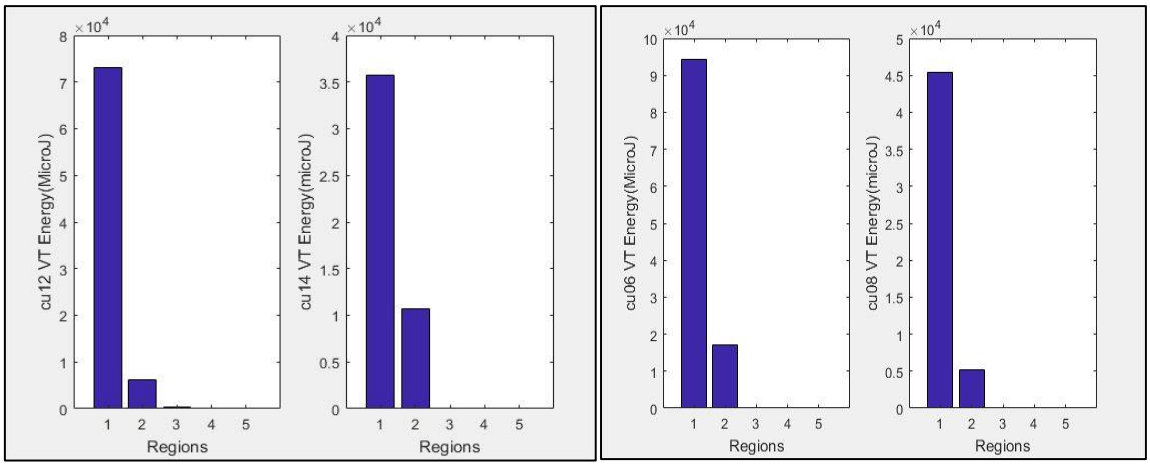

Fig 4.8 Energy at different regions of VT Records (cu12, cu14, cu06 and cu08)

Spectral and Temporal features (hybrid features) of 7 types of cardiac Signals for each record are shown in Table 4.8

Table 4.8 Spectral and Temporal features (hybrid features) of different cardiac Signals

Mean R3	Median R3	SD R3	Energy R3	No. of R-peaks	Amplitude average (mv)	R-R interval (secs)	HBR (bpm)	Signal
1.284756	0.9546436	1.370672	922.80832	52	0.854975	0.617960784	54.2285345	SVT
1.4066941	0.760597	1.684764	1259.2727	32	1.955584	1.962580645	72.2092116	SVT
2.0837691	1.4072656	2.002424	2184.1606	44	0.958168	0.723348837	71.0718402	SVT
2.41549	1.6339475	2.360667	2983.1499	40	1.49194	0.801025641	74.9039693	SVT
0.6952164	0.267692	0.952972	363.65997	32	1.656491	0.997677419	60.1396793	SVT
3.1453129	2.3820331	2.658554	4436.6885	43	1.7546	0.728761905	82.3314166	SVT
1.7455787	0.8543279	1.876597	1717.4672	35	1.625906	0.933529412	64.2722117	SVT
2.1631244	1.9636281	1.47552	1794.1645	25	0.630474	1.295166667	46.3260842	SVT
0.5890334	0.2595932	0.748515	237.13547	28	1.298521	1.151703704	52.0967327	SVT
2.5755388	1.8681171	2.200425	3001.6786	40	0.213198	0.797230769	75.2605172	SVT
2.0095981	1.3739326	1.859385	1960.4413	54	0.142973	0.587698113	102.093232	SVT
2.7662293	1.4534695	3.786006	5745.9635	41	0.275273	0.7825	76.6773163	SVT
2.7662293	1.4534695	3.786006	5745.9635	54	1.245341	0.590188679	101.662404	SVT
1.6009924	0.9701128	1.51416	1269.9422	41	1.010693	0.7675	78.1758958	SVT
1.9187256	1.4041315	1.698144	1717.1994	50	0.558015	0.649877551	92.3250848	SVT
0.3431765	0.1937894	0.365996	65.817537	41	0.195675	0.7827	76.6577233	VF
0.1881047	0.1269067	0.163527	16.249862	63	0.127919	0.511677419	117.261379	VF
0.5901711	0.3277305	0.60127	185.61335	40	0.202846	0.811384615	73.9476678	VF
0.6481308	0.5295341	0.445384	161.83312	53	0.151154	0.604615385	99.2366412	VF
0.8910792	0.6958988	0.517895	278.03811	22	0.368095	1.472380952	40.7503234	VF
0.8006471	0.7516115	0.262899	185.99065	44	0.182279	0.729116279	82.2914009	VF
0.8239081	0.5210585	0.953832	415.30876	55	0.145537	0.582148148	103.066548	VF
0.299907	0.2163349	0.25259	40.217647	43	0.186405	0.745619048	80.4700473	VF
0.6515416	0.3994015	0.634269	216.22037	24	0.332913	1.331652174	45.0568108	VF
0.8212539	0.5300398	0.755676	325.75092	57	0.141589	0.566357143	105.940219	VF
1.8631738	1.2831862	1.840807	1793.9281	28	0.336033	1.344130086	44.6385366	AF
0.5996838	0.3660505	0.729848	233.24967	19	0.120305	0.4812196	124.683201	AF
2.0960109	1.4386125	1.872814	2066.4749	20	0.116452	0.465809	128.80816	AF
0.7077218	0.4992597	0.635161	236.52304	19	0.028093	0.112373874	533.931937	AF
0.6189509	0.5201131	0.380996	138.25847	19	0.269214	1.076856653	55.7177224	AF
2.4066742	1.6597205	2.510529	3162.5438	16	0.298581	1.194323175	50.2376587	AF
2.1917182	1.4701377	1.867326	2168.6333	19	0.243727	0.974909074	61.544201	AF
0.5382663	0.3300605	0.578316	163.20082	33	0.125365	0.501461515	119.650259	AF
0.7828837	0.4400183	0.8335	341.90407	22	0.026578	0.106313636	564.367865	AF
0.2144991	0.1382943	0.221297	24.836403	19	0.005267	0.021068463	2847.85841	AF
0.7145313	0.481163	0.634622	238.88202	62	0.062671	0.250683245	239.345872	AF
0.8073427	0.5729781	0.707358	301.36482	18	0.047963	0.191853578	312.738499	AF
2.1155531	1.5827104	1.991601	2207.8479	15	0.279369	1.117477093	53.6923758	AF
0.6540064	0.4870057	0.536112	187.07937	21	0.227674	0.910696324	65.8836524	AF
1.604149	1.1548549	1.371871	1165.4131	30	0.11149	0.44596036	134.541106	AF
0.5042956	0.441304	0.362612	100.94857	20	0.001612	1.611578947	37.2305683	CI

1.6400801	1.4711143	1.027971	980.5489	15	0.002125	2.124857143	28.2371924	CI
0.7905759	0.5716299	0.678643	283.95776	16	0.002091	2.090666667	28.6989796	CI
0.7905759	0.5716299	0.678643	283.95776	15	0.002115	2.114857143	28.3707106	CI
1.7522355	1.3422136	1.573688	1450.7914	14	0.002198	2.198461538	27.2918125	CI
0.6501196	0.5411124	0.500345	176.0758	18	0.001764	1.763529412	34.0226818	CI
1.6224442	1.1090214	1.489856	1269.0034	17	0.001931	1.93125	31.0679612	CI
0.711171	0.5248685	0.676698	252.02734	10	0.002975	2.975111111	20.167314	CI
2.4629658	1.9027643	1.982871	2615.5387	18	0.00187	1.869882353	32.0875802	CI
0.579077	0.3190049	0.607764	184.26406	13	0.002683	2.682666667	22.3658052	CI
2.2308993	1.9195749	1.572482	1949.3252	18	0.001819	1.818823529	32.9883571	CI
0.618181	0.353901	0.633388	204.83081	16	0.002013	2.013066667	29.8052722	CI
2.5171903	1.9429872	1.932972	2635.2923	21	0.001549	1.5494	38.7246676	CI
2.809716	1.790503	3.306812	4922.3973	21	0.001546	1.5456	38.8198758	CI
2.484131	1.6396797	2.447888	3180.7298	24	0.001343	1.343478	44.66019	CI
0.6166012	0.4217909	0.659471	213.12109	36	0.223429	0.893714286	67.1355499	VF
0.2306811	0.1809108	0.17228	21.688552	25	0.315625	1.2625	47.5247525	VF
0.451626	0.3091226	0.446153	105.39177	34	0.237061	0.948242424	63.2749585	VF
0.6166012	0.4217909	0.659471	213.12109	25	0.323542	1.294166667	46.3618802	VF
1.3340802	0.9817392	1.13545	802.79284	56	0.141945	0.567781818	105.674395	VF
0.6260901	0.3829384	0.61902	202.7125	23	0.149587	1.367636364	43.8713108	SCA
0.4257394	0.2247857	0.44852	99.994042	29	0.101812	1.071	56.022409	SCA
0.882341	0.7096831	0.733048	344.22459	23	0.235016	1.425636364	42.0864686	SCA
0.229369	0.1847701	0.156002	20.135723	24	0.042966	1.370782609	43.7706166	SCA
0.4600767	0.346358	0.366678	90.549786	24	0.003038	1.342086957	44.7064922	SCA
0.5729797	0.3588875	0.557919	167.25844	18	0.085109	1.837411765	32.6546293	SCA
0.2501377	0.1981207	0.145295	21.902898	8	0.085489	4.554857143	13.1727512	SCA
0.6503844	0.2756029	0.76503	263.58183	32	0.091707	1.006580645	59.6077426	SCA
0.8699371	0.5545717	0.803735	366.88259	31	0.098434	1.0532	56.9692366	SCA
0.4959769	0.3729899	0.346165	95.72596	26	0.000127	1.27568	47.0337389	SCA
0.7749418	0.5252367	0.659912	271.00142	30	0.000674	1.06937931	56.1073133	SCA
0.2610245	0.1190362	0.379342	55.409041	25	0.063375	1.328833333	45.1523893	SCA
0.5822724	0.5172549	0.203344	99.620814	22	0.001337	1.467619048	40.8825438	SCA
1.2970259	0.7786383	1.357419	921.67105	26	0.000756	1.26384	47.4743638	SCA
0.9416736	0.7225081	0.798269	398.64632	22	0.417295	1.505142857	39.8633257	SCA
1.3447264	0.8613069	1.496467	1058.2586	32	0.159901	0.974580645	61.5649411	VT
0.5738146	0.5084143	0.43644	135.98226	73	0.972875	0.604461538	99.2618987	VT
0.9350754	0.5499737	1.01327	497.05687	75	0.031812	0.417567568	143.68932	VT
0.2635493	0.1872905	0.228464	31.821149	24	0.000586	1.368347826	43.8485003	VT
0.7581571	0.3983612	1.130146	483.95499	76	0.031956	0.414293333	144.824923	VT
0.3095816	0.2273011	0.206631	36.254	36	0.143325	0.8792	61.5649411	VT
0.6276057	0.4269904	0.623114	204.53776	46	0.000696	0.706133333	144.539615	VT
0.324433	0.2504925	0.279963	48.034295	42	0.000456	0.773560976	143.68932	VT
0.2347556	0.1387072	0.270988	33.605304	47	0.058797	0.668782609	89.7152516	VT
0.7675737	0.4332266	0.724568	291.38703	47	0.121283	0.69173913	144.824923	VT
0.1700403	0.0986396	0.183271	16.341925	29	0.246977	1.106428571	68.2438581	VT
1.2482658	0.7182084	1.304582	852.44459	38	0.137872	0.830918919	84.9697885	VT

0.7617454	0.4450964	0.848945	340.13174	23	0.00114	1.354363636	77.563375	VT
0.345285	0.3049168	0.133518	35.888929	38	0.00292	0.844216216	48.6886523	VT
1.4167591	1.1481852	1.088397	835.07078	23	0.001505	1.390909091	86.7379007	VT
3.0697731	2.2734404	2.366112	3930.1637	31	1.150784	0.149586735	60.3378922	NSR
2.5870702	1.9966879	2.03527	2834.6946	49	5.529473	0.101811814	93.0833872	NSR
2.943486	2.2819738	2.098412	3419.2671	50	5.507928	0.235015752	92.7327782	NSR
3.3283441	2.7232339	2.417013	4427.1532	49	1.891016	0.042966113	92.6998841	NSR
2.4628581	1.1755851	3.070945	4050.6193	50	1.758144	0.003038279	93.3451867	NSR
2.6735988	1.9024718	2.258606	3204.2495	40	1.79936	0.372409457	75.9937646	NSR
2.8729886	2.3267106	2.149705	3368.7061	38	5.969311	0.08510885	71.4285714	NSR
2.0346674	1.3038922	2.000554	2129.2253	37	4.3836	0.085488825	70.075266	NSR
2.4272999	2.0967587	1.59705	2209.3457	34	1.267571	0.091707288	63.4371396	NSR
2.4816111	1.9426291	1.992187	2649.3586	36	0.992039	0.098433552	66.6666667	NSR
3.1870204	2.7062607	2.146591	3863.81	43	3.451974	0.000711936	81.2903226	NSR
2.3141838	1.1907286	3.479792	4563.564	58	0.61046	0.000126904	74.5747929	NSR
2.6810224	2.2500206	1.898996	2824.4389	43	2.0547	0.00067424	80.6658131	NSR
1.4178385	1.1669999	1.49963	1113.65	57	0.609691	0.00075585	109.517601	NSR
1.1935218	0.7480308	2.465748	1960.0749	60	0.112759	0.198319587	111.742424	NSR

4.5 Results and Discussion

4.5.1 MLP classifier

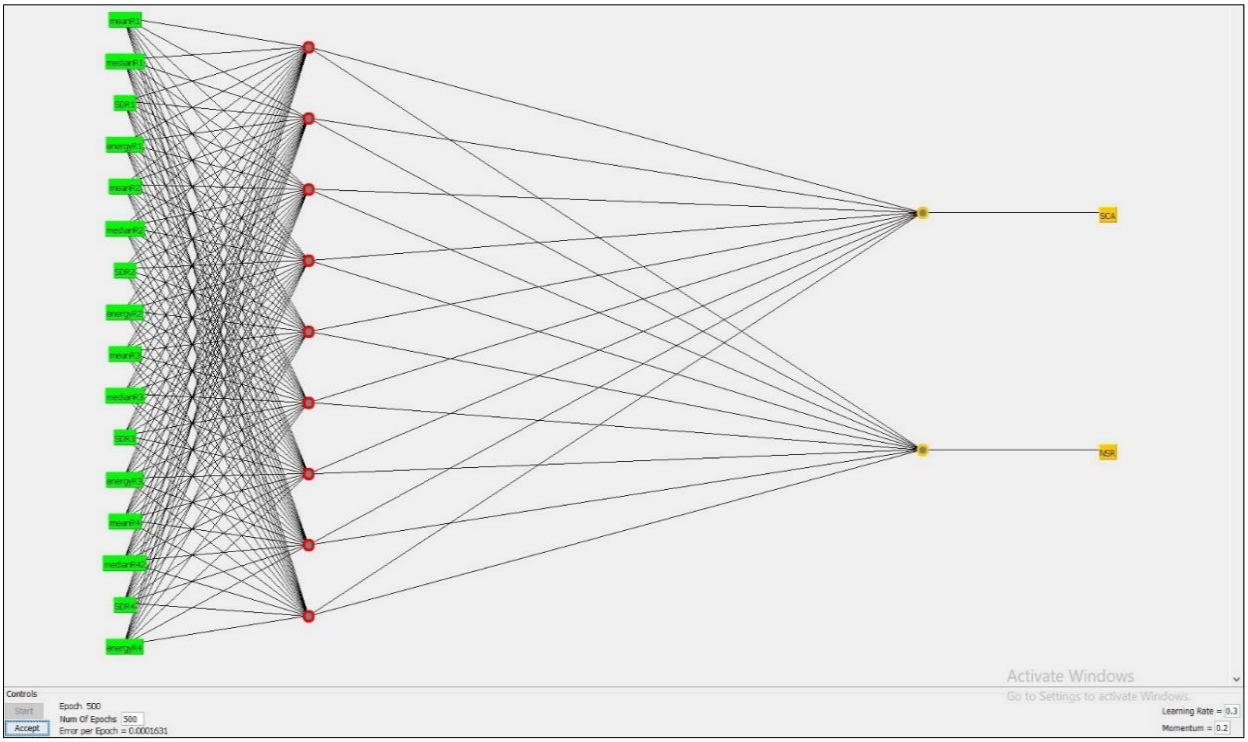

Fig 4.9 ANN Structure for classification of NSR and SCA using spectral features

The Fig 4.9 shows neural network architecture of MLP results obtained for 2 types of signals (NSR and SCA). It has one input layer, one output layer and one hidden layer. Input layer has 16 neurons represented as mean, median, standard deviation and energy for each region (4features*4regions) are used in this work. The output layer has two neurons represented as NSR and SCA. The error per epoch obtained as 0.0001631 and Learning rate obtained as 0.3

```
Time taken to build model: 0.04 seconds

=== Stratified cross-validation ===
=== Summary ===

Correctly Classified Instances          30               100      %
Incorrectly Classified Instances         0                 0      %
Kappa statistic                          1
Mean absolute error                      0.017
Root mean squared error                  0.0433
Relative absolute error                  3.3676 %
Root relative squared error              8.5496 %
Total Number of Instances               30

=== Detailed Accuracy By Class ===

               TP Rate   FP Rate   Precision   Recall  F-Measure   ROC Area  Class
                 1         0          1         1         1          1        VF
                 1         0          1         1         1          1        NSR
Weighted Avg.    1         0          1         1         1          1

=== Confusion Matrix ===

  a  b   <-- classified as
 15  0 |  a = VF
  0 15 |  b = NSR
```

Fig 4.10 MLP Simulation Results for classification of NSR and VF using spectral features

The Fig 4.10 shows the simulation results for classification of NSR and VF using MLP classifier. Time to build the model is 0.04 Seconds. Correctly classified instances are 30. RMSE value is 0.0433. The classification accuracy for classifying NSR and VF is obtained as 100%.

```
Time taken to build model: 0.03 seconds

=== Stratified cross-validation ===
=== Summary ===

Correctly Classified Instances          28               93.3333 %
Incorrectly Classified Instances         2                6.6667 %
Kappa statistic                          0.8667
Mean absolute error                      0.0563
Root mean squared error                  0.1858
Relative absolute error                 11.1289 %
Root relative squared error             36.7109 %
Total Number of Instances               30

=== Detailed Accuracy By Class ===

               TP Rate   FP Rate   Precision   Recall  F-Measure   ROC Area  Class
                 0.933     0.067      0.933     0.933      0.933      0.996    SCA
                 0.933     0.067      0.933     0.933      0.933      0.996    NSR
Weighted Avg.    0.933     0.067      0.933     0.933      0.933      0.996

=== Confusion Matrix ===

  a  b   <-- classified as
 14  1 |  a = SCA
  1 14 |  b = NSR
```

Fig 4.11 MLP Simulation Results for classification of NSR and SCA using temporal and spectral features

The Fig 4.11 shows the simulation results for classification of NSR and SCA using MLP classifier. Time to build the model is 0.03 Seconds. Correctly classified instances are 28 out of 30 instances. RMSE value is 0.1858. The classification accuracy for classifying NSR and SCA is obtained as 100%.

```
Time taken to build model: 0.06 seconds

=== Stratified cross-validation ===
=== Summary ===

Correctly Classified Instances          32               71.1111 %
Incorrectly Classified Instances        13               28.8889 %
Kappa statistic                          0.5667
Mean absolute error                      0.2177
Root mean squared error                  0.3718
Relative absolute error                 48.7431 %
Root relative squared error             78.4499 %
Total Number of Instances               45

=== Detailed Accuracy By Class ===

               TP Rate   FP Rate   Precision   Recall  F-Measure   ROC Area  Class
                 0.733     0.267      0.579     0.733      0.647      0.78     VF
                 0.533     0.167      0.615     0.533      0.571      0.798    VT
                 0.867     0          1         0.867      0.929      1        NSR
Weighted Avg.    0.711     0.144      0.731     0.711      0.716      0.859

=== Confusion Matrix ===

  a  b  c   <-- classified as
 11  4  0 |  a = VF
  7  8  0 |  b = VT
  1  1 13 |  c = NSR
```

Fig 4.12 MLP Simulation Results for classification of NSR, VT and VF using temporal and spectral features

The Fig 4.12 shows the simulation results for classification of NSR, VT and VF using MLP classifier. Time to build the model is 0.06 Seconds. Correctly classified instances are 32 out of 45 instances. RMSE value is 0.3718. The classification accuracy for classifying NSR, VT and VF is obtained as 71.11%.

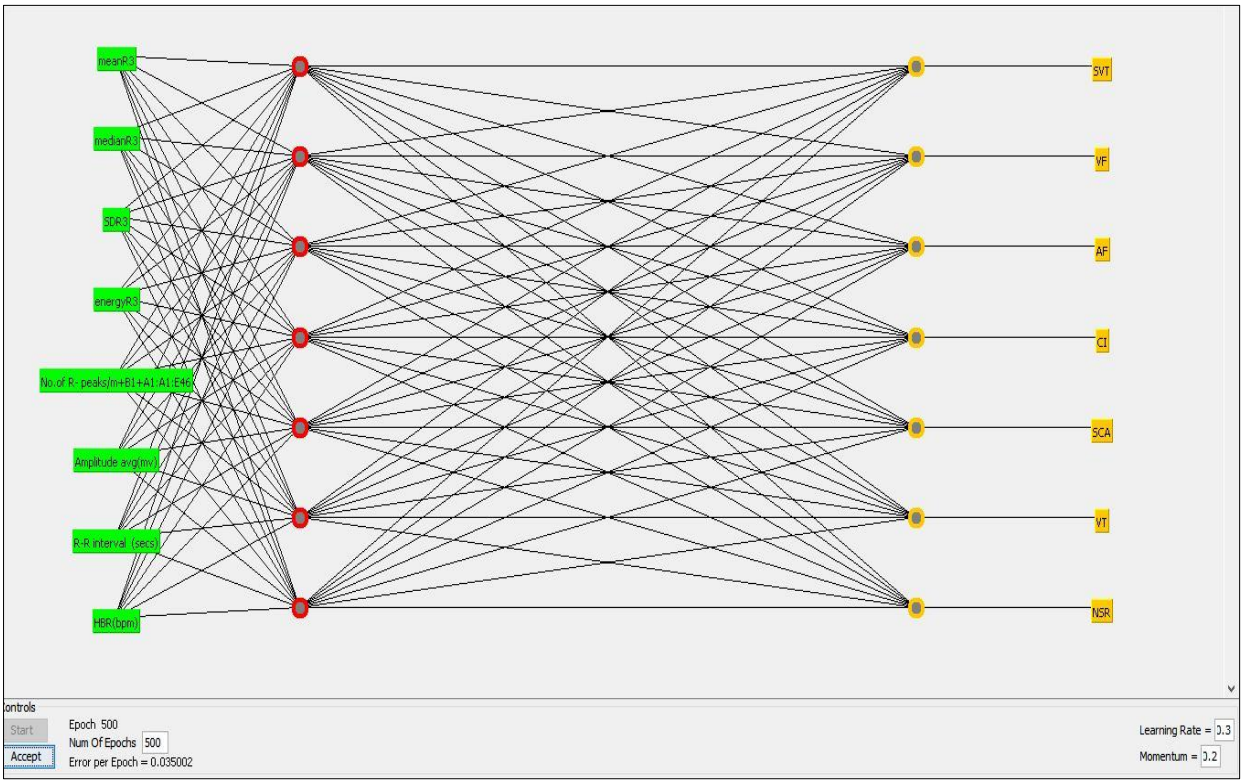

Fig 4.13 ANN Structure for classification of 7 types using temporal and spectral features

The Fig 4.13 shows neural network architecture of MLP results obtained for 7 types of signals (NSR, SVT, VT, VF, AF, CI and SCA). It has one input layer, one output layer and one hidden layer. Input layer has hybrid features (temporal and spectral features) represented as mean, median, standard deviation and energy for R3 region from spectral features; Number of R-Peaks, Amplitude of R-Peaks, R-R interval and Heart beat rate from temporal features are used in this work The output layer has 7 neurons represented as NSR, VT, VF, SVT, AF, CI and SCA. The error per epoch obtained as 0.035002 and Learning rate obtained as 0.3.

```
Time taken to build model: 0.22 seconds

=== Stratified cross-validation ===
=== Summary ===

Correctly Classified Instances          75               71.4286 %
Incorrectly Classified Instances        30               28.5714 %
Kappa statistic                          0.6667
Mean absolute error                      0.1108
Root mean squared error                  0.2404
Relative absolute error                 45.1671 %
Root relative squared error             68.575  %
Total Number of Instances              105

=== Detailed Accuracy By Class ===

               TP Rate   FP Rate   Precision   Recall  F-Measure   ROC Area  Class
                 0.8       0          1         0.8       0.889      0.984    SVT
                 0.6       0.111      0.474     0.6       0.529      0.87     VF
                 0.733     0          1         0.733     0.846      0.943    AF
                 0.867     0.056      0.722     0.867     0.788      0.982    CI
                 0.667     0.111      0.5       0.667     0.571      0.888    SCA
                 0.333     0.056      0.5       0.333     0.4        0.803    VT
                 1         0          1         1         1          1        NSR
Weighted Avg.    0.714     0.048      0.742     0.714     0.718      0.924

=== Confusion Matrix ===

  a  b  c  d  e  f  g   <-- classified as
 12  2  0  1  0  0  0 |  a = SVT
  0  9  0  0  3  3  0 |  b = VF
  0  2 11  1  0  1  0 |  c = AF
  0  0  0 13  2  0  0 |  d = CI
  0  2  0  2 10  1  0 |  e = SCA
  0  4  0  1  5  5  0 |  f = VT
  0  0  0  0  0  0 15 |  g = NSR
```

Fig 4.14 MLP Simulation Results for classification of 7 Types using temporal and spectral features.

The Fig 4.14 shows the simulation results for classification of 7 types of signals using MLP classifier. Time taken to build the model is 0.22 Seconds. Correctly classified instances are 75 out of 105 instances. RMSE value is 0.2404. The classification accuracy for classifying 7 types is obtained as 71.42%.

4.5.2 RBF classifier

```
Time taken to build model: 0.02 seconds

=== Stratified cross-validation ===
=== Summary ===

Correctly Classified Instances          27               90      %
Incorrectly Classified Instances         3               10      %
Kappa statistic                          0.8
Mean absolute error                      0.1
Root mean squared error                  0.3162
Relative absolute error                 19.7727 %
Root relative squared error             62.4944 %
Total Number of Instances               30

=== Detailed Accuracy By Class ===

               TP Rate   FP Rate   Precision   Recall  F-Measure   ROC Area  Class
                 0.867     0.067      0.929     0.867     0.897      0.987    SCA
                 0.933     0.133      0.875     0.933     0.903      0.987    NSR
Weighted Avg.    0.9       0.1        0.902     0.9       0.9        0.987

=== Confusion Matrix ===

  a  b   <-- classified as
 13  2 |  a = SCA
  1 14 |  b = NSR
```

Fig 4.15 RBF Simulation Results for classification of NSR and SCA using Spectral features

The Fig 4.15 shows the simulation results for classification of NSR and SCA using RBF classifier. Time taken to build the model is 0.02 Seconds. Correctly classified instances are 27 out of 30 instances. RMSE value is 0.3162. The classification accuracy for classifying NSR and SCA is obtained as 90%.

```
Time taken to build model: 0.08 seconds

=== Stratified cross-validation ===
=== Summary ===

Correctly Classified Instances          30               100      %
Incorrectly Classified Instances         0                 0      %
Kappa statistic                          1
Mean absolute error                      0
Root mean squared error                  0
Relative absolute error                  0      %
Root relative squared error              0.0001 %
Total Number of Instances               30

=== Detailed Accuracy By Class ===

               TP Rate   FP Rate   Precision   Recall  F-Measure   ROC Area  Class
                 1         0          1         1         1          1        SCA
                 1         0          1         1         1          1        NSR
Weighted Avg.    1         0          1         1         1          1

=== Confusion Matrix ===

  a  b   <-- classified as
 15  0 |  a = SCA
  0 15 |  b = NSR
```

Fig 4.16 RBF Simulation Results for classification of NSR and SCA using temporal and spectral features.

The Fig 4.16 shows the simulation results for classification of NSR and SCA using hybrid features using RBF classifier. Time taken to build the model is 0.08 Seconds. Correctly classified instances are 30 out of 30 instances. RMSE value is 0.00. The classification accuracy for classifying NSR and SCA is obtained as 100%.

```
Time taken to build model: 0.03 seconds

=== Stratified cross-validation ===
=== Summary ===

Correctly Classified Instances          34               75.5556 %
Incorrectly Classified Instances        11               24.4444 %
Kappa statistic                          0.6333
Mean absolute error                      0.1909
Root mean squared error                  0.3915
Relative absolute error                 42.7276 %
Root relative squared error             82.6056 %
Total Number of Instances               45

=== Detailed Accuracy By Class ===

               TP Rate   FP Rate   Precision   Recall  F-Measure   ROC Area  Class
                 0.667     0.133      0.714     0.667      0.69       0.838    VF
                 0.733     0.233      0.611     0.733      0.667      0.778    VT
                 0.867     0          1         0.867      0.929      0.96     NSR
Weighted Avg.    0.756     0.122      0.775     0.756      0.762      0.859

=== Confusion Matrix ===

  a  b  c   <-- classified as
 10  5  0 |  a = VF
  4 11  0 |  b = VT
  0  2 13 |  c = NSR
```

Fig 4.17 RBF Simulation Results for classification of NSR, VT and VF using temporal and spectral features

The Fig 4.17 shows the simulation results for classification of NSR, VT and VF using RBF classifier. Time taken to build the model is 0.03 Seconds. Correctly classified instances are 34 out of 45 instances. RMSE value is 0.3915. The classification accuracy for classifying NSR, VT and VF is obtained as 75.55%.

The Fig 4.18 shows the simulation results for classification of 7 types of signals using RBF classifier. Time taken to build the model is 2.97 Seconds. Correctly classified instances are 70 out of 105 instances. RMSE value is 0.2868. The classification accuracy for classifying 7 types is obtained as 66.66%.

The Fig 4.19 shows the simulation results for classification of NSR and SCA using RF classifier. Time taken to build the model is 0.01 Seconds. Correctly classified instances are 28 out of 30 instances. RMSE value is 0.177. The classification accuracy for classifying NSR and SCA is obtained as 93.33%.

```
Time taken to build model: 2.97 seconds

=== Stratified cross-validation ===
=== Summary ===

Correctly Classified Instances          70               66.6667 %
Incorrectly Classified Instances        35               33.3333 %
Kappa statistic                          0.6111
Mean absolute error                      0.0924
Root mean squared error                  0.2868
Relative absolute error                 37.6454 %
Root relative squared error             81.7925 %
Total Number of Instances              105

=== Detailed Accuracy By Class ===

               TP Rate   FP Rate   Precision   Recall  F-Measure   ROC Area  Class
                 0.933     0.033      0.824     0.933      0.875      0.96     SVT
                 0.467     0.033      0.7       0.467      0.56       0.95     VF
                 0.533     0.067      0.571     0.533      0.552      0.776    AF
                 0.867     0.1        0.591     0.867      0.703      0.936    CI
                 0.4       0.067      0.5       0.4        0.444      0.824    SCA
                 0.533     0.089      0.5       0.533      0.516      0.77     VT
                 0.933     0          1         0.933      0.966      0.947    NSR
Weighted Avg.    0.667     0.056      0.669     0.667      0.659      0.88
```

Fig 4.18 RBF Simulation Results for classification of 7 Types using temporal and spectral features.

4.5.3 RF classifier results

```
Time taken to build model: 0.01 seconds

=== Stratified cross-validation ===
=== Summary ===

Correctly Classified Instances          28               93.3333 %
Incorrectly Classified Instances         2                6.6667 %
Kappa statistic                          0.8667
Mean absolute error                      0.0667
Root mean squared error                  0.177
Relative absolute error                 13.1818 %
Root relative squared error             34.9821 %
Total Number of Instances               30

=== Detailed Accuracy By Class ===

               TP Rate   FP Rate   Precision   Recall  F-Measure   ROC Area  Class
                 0.933     0.067      0.933     0.933      0.933      0.991    SCA
                 0.933     0.067      0.933     0.933      0.933      0.991    NSR
Weighted Avg.    0.933     0.067      0.933     0.933      0.933      0.991

=== Confusion Matrix ===

  a  b   <-- classified as
 14  1 |  a = SCA
  1 14 |  b = NSR
```

Fig 4.19 RF Simulation Results for classification of NSR and SCA using Spectral features

```
=== Stratified cross-validation ===
=== Summary ===

Correctly Classified Instances          28               93.3333 %
Incorrectly Classified Instances         2                6.6667 %
Kappa statistic                          0.8667
Mean absolute error                      0.0633
Root mean squared error                  0.1889
Relative absolute error                 12.5227 %
Root relative squared error             37.3227 %
Total Number of Instances               30

=== Detailed Accuracy By Class ===

               TP Rate   FP Rate   Precision   Recall  F-Measure   ROC Area  Class
                 0.933     0.067      0.933     0.933     0.933      0.996    SCA
                 0.933     0.067      0.933     0.933     0.933      0.996    NSR
Weighted Avg.    0.933     0.067      0.933     0.933     0.933      0.996

=== Confusion Matrix ===

  a  b   <-- classified as
 14  1 |  a = SCA
  1 14 |  b = NSR
```

Fig 4.20 RF Simulation Results for classification of NSR and SCA using temporal and spectral features

The Fig 4.20 shows the simulation results for classification of NSR and SCA using RF classifier. Time taken to build the model is 0.01 Seconds. Correctly classified instances are 28 out of 30 instances. RMSE value is 0.1889. The classification accuracy for classifying NSR and SCA is obtained as 93.33%.

The following Fig 4.21 shows the simulation results for classification of NSR, VT and VF using RF classifier. Time taken to build the model is 0.01 Seconds. Correctly classified instances are 36 out of 45 instances. RMSE value is 0.3188. The classification accuracy for classifying NSR, VT and VF is obtained as 80%.

```
Correctly Classified Instances          36               80      %
Incorrectly Classified Instances         9               20      %
Kappa statistic                          0.7
Mean absolute error                      0.163
Root mean squared error                  0.3188
Relative absolute error                 36.4803 %
Root relative squared error             67.2659 %
Total Number of Instances               45

=== Detailed Accuracy By Class ===

               TP Rate   FP Rate   Precision   Recall  F-Measure   ROC Area  Class
                 0.867     0.167      0.722     0.867      0.788      0.904    VF
                 0.667     0.1        0.769     0.667      0.714      0.853    VT
                 0.867     0.033      0.929     0.867      0.897      0.993    NSR
Weighted Avg.    0.8       0.1        0.807     0.8        0.8        0.917

=== Confusion Matrix ===

  a  b  c   <-- classified as
 13  2  0 |  a = VF
  4 10  1 |  b = VT
  1  1 13 |  c = NSR
```

Fig 4.21 RF Simulation Results for classification of NSR, VT and VF using temporal and spectral features

```
Time taken to build model: 0.17 seconds

=== Stratified cross-validation ===
=== Summary ===

Correctly Classified Instances          82               78.0952 %
Incorrectly Classified Instances        23               21.9048 %
Kappa statistic                          0.7444
Mean absolute error                      0.1092
Root mean squared error                  0.2198
Relative absolute error                 44.5165 %
Root relative squared error             62.683  %
Total Number of Instances              105

=== Detailed Accuracy By Class ===

               TP Rate   FP Rate   Precision   Recall  F-Measure   ROC Area  Class
                 0.933     0.022      0.875     0.933      0.903      0.992    SVT
                 0.867     0.1        0.591     0.867      0.703      0.943    VF
                 0.733     0.011      0.917     0.733      0.815      0.974    AF
                 0.8       0.011      0.923     0.8        0.857      0.993    CI
                 0.667     0.067      0.625     0.667      0.645      0.948    SCA
                 0.533     0.044      0.667     0.533      0.593      0.844    VT
                 0.933     0          1         0.933      0.966      1        NSR
Weighted Avg.    0.781     0.037      0.8       0.781      0.783      0.956
```

Fig 4.22 RF Simulation Results for classification of 7 Types using temporal and spectral features

The Fig 4.22 shows the simulation results for classification of 7 types of signals using RF classifier. It is built by using random forest of 10 trees, each constructed while considering 4 random features. Out of bag error is 0.3429. Time taken to build the model is 0.17 Seconds. Correctly classified instances are 82 out of 105 instances. RMSE value is 0.2198. The classification accuracy for classifying 7 types is obtained as 78.09%.

4.6 Performance comparison of cardiac arrhythmias classification

The performance of cardiac signals classification in terms of number of ECG records, the number of features, type of neural network classifier, classification accuracy and number of arrhythmias/disorders/normal signals classification reported in the literature have been compared with the proposed classification system as shown in Table 4.9

Usman Rashed et al. [19] used FFT algorithm to distinguish SCA and NSR using spectral features. In the proposed work, classified 7 types of cardiac signals (normal, cardiac arrhythmias and disorders) using Machine learning RF classifier and ANN based MLP and RBF classifiers. These two techniques are different that they can learn differently but can be used in similar domains for classification.

From the results it's identified that RF classifier gives more accuracy irrespective of data size. MLP classifier works better when data size is more. RBF works better when data size is less. with less computation time.

Table 4.9 Summary of performance comparison of cardiac arrhythmias classification

Study by	Records and Features	Classifier	Cardiac Signals	Classification Accuracy
Usman Rashed et al. [19]	8 Records, Features - 5 Spectral features	-	NSR and SCA (2 types)	Distinguished NSR and SCA using spectral parameters
Proposed [FDA]	30 Records (NSR-15 and SCA-15), 16- Spectral features(R1-R4)	MLP,RF and RBF	NSR and SCA	MLP-93.33% RF-93.33% RBF-90%
	30 Records, 4- Spectral features(R3)	MLP,RF and RBF	NSR and SCA	MLP-93.33% RF-93.33% RBF-96.6%
Proposed [TDA+FDA]	Temporal and Spectral Features (Hybrid)	MLP,RF and RBF	NSR and SCA	MLP-100% RBF-100% RF-93.33%
			NSR and VF	MLP-100% RF-90% RBF-100%
			NSR,VT and VF	MLP-73.33% RBF-71.11% RF-75.55%
			NSR, SVT, VT, VF, AF, CI and SCA (seven types)	MLP–71.4% RBF-66.6% RF-78.09%

4.7 Conclusion

In this chapter, a spectral feature extraction scheme has been proposed for analysis of seven types of cardiac signals based on the spectral features. A significant change in Energy was observed in 3rd segment, (QRS complex duration 5Hz to 15Hz). It was found from the Fig 4.2, 4.3, 4.4, 4.5, 4.6, 4.7 and 4.8 the energy of NSR in Region3 region is more than that of other cardiac signals. Cardiac arrhythmias such as VT, VF and AF except SVT, energy is very less. Cardiac disorders such as CI and SCA, energy is also very less.

In existing works, Usman Rashed et al. [19] used spectral analysis to classify normal and sudden cardiac arrest signals (two types) based on energy in region R4 of different signals. But in the proposed work obtained Energy difference of 7 types in R3 region as QRS complex frequency lies in this R3 (8Hz-16Hz) region.

Using the regions (R1 to R4) spectral features classified NSR and SCA and obtained 93.3% and using only R3 features classified NSR and SCA obtained same classification accuracy as 93.3% and these results are evaluated with other classifiers as shown in Table 4.9. To improve classification accuracy this work used temporal features along with spectral using hybrid approach and obtained 100% accuracy. Similarly classified NSR and VF and obtained accuracy as 100% using MLP classifier and these results are evaluated with other classifiers as shown in Table 4.9. Later, the work extended to classify three types of signals NSR, VT and VF and obtained an accuracy as 77.77% using Random Forest Classifier and these results are evaluated with other classifiers as shown in Table 4.9

The proposed work also classified 7 types of cardiac signals (1- normal, 4- arrhythmias and 2- cardiac disorders) and obtained an accuracy of 74.2% using Random Forest classifier and also evaluated the results with other classifiers as shown in Table 4.9. It is observed that normal spectral analysis of ECG provides only energy within frequency components but does not provide any phase coupled information. ECG signal is characterised by time varying random process (Non Gaussian/Non stationary). This may be the reason to get a less classification accuracy. Hence, higher order spectral analysis (HOSA) proposed to provide supplementary information about non gaussianity and non-linearity of the ECG signal.

Chapter 5

Cardiac Arrhythmias Analysis and Classification in HOS Domain

5.1 Introduction

In the previous chapters, time domain and spectral domain analysis of ECG have been proposed to identify and classify cardiac arrhythmias and disorders. Spectral analysis is a good tool for the analysis of power distribution of linear and stationary signals. Whereas, this analysis may not be adequate to detect phase correlations among different frequency components of ECG signal as it is non-linear, non-stationary and quasi periodic in nature [22], [30], [97]. Hence, there is a need for phase related characteristics in identifying cardiac arrhythmias with better accuracy.

Bispectrum, Bicoherence and Quadratic phase coupling plots are used for analysis of ECG to distinguish different types of cardiac signals. Higher order spectral features (skewness, variance, kurtosis and bicoherence) are extracted using bispectral analysis. The bispectrum is estimated using an autoregressive model, and the frequency support of the bispectrum is extracted as a quantitative measure to classify atrial & ventricular arrhythmias. The bicoherence spectrum shows different bicoherence values for normal and arrhythmia signals. In general, the bicoherence indicates that the phase coupling decreases as arrhythmia kicks in. In this chapter, higher order spectral domain analysis of cardiac signals and their classification have been described.

5.2 Overview of existing works

Lot of research work has been done in the past to identify cardiac arrhythmias in higher order spectral domain. In this section, the work done by some of the researchers has been presented briefly.

L.Khadra et al.[21] used a higher order spectral analysis to distinguish cardiac arrhythmias (VT, VF and AF) and NSR. In this work, phase coupling information of ECG signals was found from bispectrum. This bispectral analysis is used to discriminate different types of arrhythmias. To quantify the differences between the various arrhythmias, a simple classification parameter

that was proportional to the area of the frequency support of the bispectrum was used. (a=f1*f2). In order to quantify the degree of phase coupling for arrhythmia cases, computed the bicoherence spectrum. It was identified that spectral estimation depends on signal energies in the bifrequency plane. The variance of the estimate will be high at high frequencies. Medical statistics were computed as Sensitivity(S) as 89.2% and Specificity (Sp) as 93.55%.

K. Sharmila et al. [25] used higher order spectral analysis to distinguish sudden cardiac arrest and normal sinus rhythm. Specifically, quadratic phase coupling techniques were applied on ECG to extract information. Higher order spectral parameter such as energy was computed and compared normal portion of QRS complex of SCD- ECG and are compared with that of the healthy person ECG. In this work, on the basis of cumulants, estimated higher order spectra for the analysis of non-stationary ECG signals. HOS are "resistant" to gaussian noise in the sense that all cumulants of order greater than two have value zero for a gaussian signal.

I. A. Karaye [26] used higher order spectral analysis to classify 5 types of cardiac signals (NSR, RBBB, paced beat, atrial premature beats and LBBB). In this work, bispectrum and bicoherence plots were used for identification of cardiac arrhythmias. This work extracted higher order spectral features (skewness, kurtosis and variance) and morphological features (no.of R-Peaks and R-R intervals) and these features were fed to back propagation neural network classifier. In this work, 70% of the data was used for training purpose and 30% of the data was used for testing purpose and obtained classification accuracy as 94.9%, Sensitivity as 88.4%, Specificity as 96.2% and positive prediction as 87.3%.

5.3 Methodology for Higher Order Spectral Analysis

From the literature survey, it is identified that ECG signals are non-linear and non-stationary in nature. Normal spectral analysis of ECG provides only power within the frequency components but does not provide any phase coupled information of different frequency components. Higher Order Spectral Analysis (HOSA) possesses the ability to suppress gaussian noise and preserves the true phase characteristics of the signal, from which signal reconstruction is possible. Phase correlations among rhythmic events at different frequencies are introduced only by non-linear interactions [99]. Thus, non-linear analysis methods have to be applied for the detection of non-linear correlations. One such method for the study of such non-linear effects is to quantify the deviation of the measured ECG signal from gaussianity by utilizing the bispectrum. This approach often detects important quadratic phase correlations present among the other higher

order correlations. So, higher order spectral (HOS) analysis is more suitable to identify different types of cardiac arrhythmias and disorders. Higher Order Spectral Analysis (HOSA) on ECG signal processing steps are shown in Fig 5.1

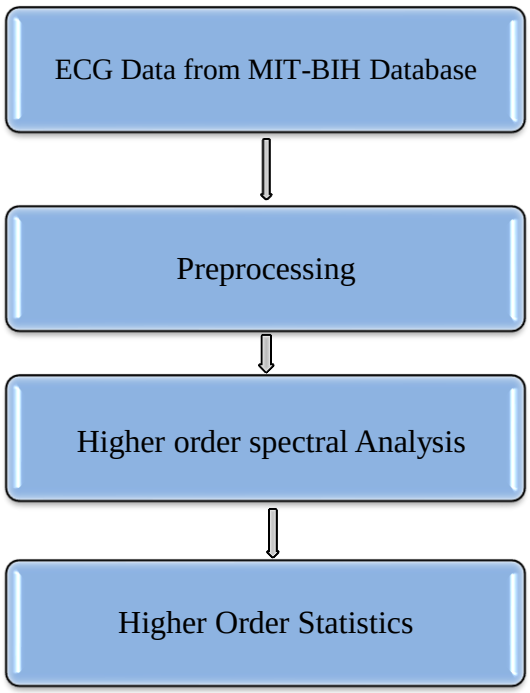

Fig 5.1 Processing steps of Higher order spectral analysis

For pre-processing, 3rd order Butterworth low pass filter is used to remove baseline wander noise from ECG signal by selecting cut off frequency 2Hz. HOS measures are extensions of second-order measures (such as autocorrelation function and the power spectrum) to higher orders. The second-order measures are good, if the signal has a gaussian probability density function, but cardiac signals are non-gaussian in nature. The gaussian function can be completely characterized by its mean and variance. Higher order measures are related to higher-order moments of the signal. For nonlinear signals such as ECG signal, second order statistics may not be sufficient for ECG analysis. Hence, third order and fourth order statistics are used in this analysis. Higher order spectra are defined to be spectral representations of higher order cumulants of a random process[26], [48], [62], [74], [98].

Let x(k) be a real, discrete time and n^{th}-order stationary random process. We use non-linear features such as higher order Cumulants(c) because they make efficient features as input to the classifier and provide higher discrimination to higher accuracy in classification of arrhythmias [22], [48].

The n^{th} order moment can be calculated by taking an expectation over the process multiplied by n-1 lagged versions of itself.

$$m_1^x = E[x(k)] \tag{5.1}$$

$$m_2^x(t) = E[x(k)x(k+t)] \tag{5.2}$$

$$m_3^x(t_1, t_2) = E[x(k)x(k+t_1)x(k+t_2] \tag{5.3}$$

$$m_4^x(t_1, t_2, t_3) = E[x(k)x(k+t_1)x(k+t_2)x(k+t_3)] \tag{5.4}$$

Where E denotes expectation function, $x(k)$ denotes zero mean process.

Using the moments, the cumulants can be computed. The second-order, third-order and fourth-order cumulants are represented by following equations 5.6 to 5.8.

$$c_1^x = m_1^x \tag{5.5}$$

$$c_2^x(t) = m_1^x(t) - m_1^x(t)^2 = m_2^x \tag{5.6}$$

$$c_3^x(t_1, t_2) = m_3^x(t_1, t_2) \tag{5.7}$$

$$c_4^x(t_1, t_2) = m_3^x(t_1, t_2) - m_2^x(t_1)m_3^x(t_2 - t_3) - m_2^x(t_3 - t_1) - m_2^x(t_3)m_2^x(t_1 - t_2) \tag{5.8}$$

Where $m_1, m_2, m_3 \, and \, m_4$ are corresponding first, second, third and fourth order moments of x(k) and $c_1, c_2, c_3 \, and \, c_4$ are the first four order cumulants. The second order cumulant is called the variance. The third order cumulant is called the skewness and the fourth order cumulant is called the kurtosis.

The Fourier transform of second order cumulants is the traditional power spectrum. The power spectrum is the frequency domain representation of second order moment. It can be calculated in two ways:

1. By taking Discrete Fourier Transform (DFT) of the autocorrelation function as shown in equation 5.1

$$P(k) = DFT[R(m)] \tag{5.9}$$

2. Multiply together the signal Fourier Transform X (k) with its complex conjugate as shown in equation 5.2,

$$P(k) = X(k)\, X^*(k) \tag{5.10}$$

The Fourier transform of third order cumulants is called bispectrum or bispectral density. Features related to third-order statistics namely, Bispectrum B (k, l) can be calculated in a similar way using Discrete Fourier Transform (DFT) as shown below,

Double Discrete Fourier Transform (DDFT) of the third-order cumulants is shown below in equation 5.3,

$$B(k, l) = DDFT[C3] \tag{5.11}$$

Where '*C3*' is third order cumulants.

To perform the work, 1-minute ECG data of 7-types has been collected from MIT-BIH database. The verification of results is done by using HOSA tool box. A set of higher order spectral features are obtained based on the existence of peaks in bi-frequency plane and the statistical parameters. Higher order statistics such as variance, skewness and kurtosis are computed.

5.3.1 Bispectrum

Bispectrum of a signal is defined as the second order Fourier transform of the third order cumulants of a signal [65]. The prefix bi- in bispectrum refers to two frequencies of a single signal. The bispectrum equation (5.12) shows that bispectrum is a function of two frequency variables (f_1 and f_2). Where f denotes frequency. The bispectrum (B) of a signal is given by the following equation 5.12

$$B(f_1, f_2) = \lim_{T\to\infty} E[X(f_1)\, X(f_2)\, X^*(f_1 + f_2)] \tag{5.12}$$

In this work, the bispectrum is computed by using direct FFT method. It is a function of two-frequency variables (*f1* and *f2)* and carries information about phase [38], [108]. Bispectrum is a complex quantity having both magnitude and phase. The bispectrum analyses the frequency components at f_1,f_2, f_1+f_2 , (f_1-f_2).

Bispectrum can be plotted against two independent frequency variables (f_1 and f_2) in three-dimensional plots. Bispectrum plots of NSR, cardiac arrhythmias and cardiac disorders are shown in Fig 5.2, 5.4, 5.6, 5.8, 5.10, 5.12, and 5.14 which provide additional information about the signal to classify cardiac arrhythmias.

5.3.2 Bicoherence

In statistical analysis, bicoherence is a squared normalised version of the bispectrum. The bicoherence takes values bounded between 0 and 1, which make it a convenient measure for quantifying the extent of phase coupling in a signal. It is also known as bispectral coherency. The prefix bicoherence refers two frequencies of a single signal. Bicoherence is given by the following equation 5.13,

$$\mathrm{B_{norm}}(f_1, f_2) = \frac{\mathrm{E[X}(f_1)\mathrm{X}(f_2)\mathrm{X}^*(f_1+f_2)]}{\sqrt{\mathrm{P}(f_1)\mathrm{P}(f_2)\mathrm{P}(f_1+f_2)}} \tag{5.13}$$

Where P (*f*) is the power spectrum. Theoretically, if the Fourier components at the frequenciesf_1, f_2 and f_1+f_2 are perfectly phase coupled, and the bicoherence will be 1. Due to the finite data length of processes, peaks may appear in the bispectrum at locations where there are no significant phase coupling. Bicoherence (or normalized bispectrum) is used to avoid incorrect interpretations. The magnitude of bicoherence quantifies the strength of phase correlation**.** Chaudhary et al. [23], calculated the value of bicoherence which is used to find linearity of a signal.

Using the above equation 5.13, bicoherence values are derived which are further used to know the linearity of signals. Bicoherence plots of NSR and cardiac disorders are shown in Fig 5.2, 5.4, 5.6, 5.8, 5.10, 5.12, and 5.14 which provide additional information about the signal to classify cardiac signals.

5.3.3 Quadratic phase coupling

Quadratic phase coupling occurs when two waves interact non-linearly and generate a third wave with a frequency equal to the sum or difference of the first two waves [101]. In a non-linear system, an interaction between two harmonic components causes contribution to the power as their sum or difference of frequencies. Since the power spectrum suppresses all phase information, it cannot be utilized to detect phase coupling. The bispectrum is capable of detecting and characterizing quadratic phase coupling. Harmonically related peaks in the power spectrum are necessary conditions for the presence of quadratic non-linearities in the data. The bispectrum preserves phase and is used to extract phase information quantitatively.

If a signal of frequency f_1, and phase φ_1 is passed through a nonlinear system results in a frequency component of $2f_1$ along with phase component $2\varphi_1$. This phenomenon of phases adding or subtracting along with frequencies can only be observed in a second order nonlinear systems. Such a phase relationship is termed as quadratic phase coupling (QPC).

Table 5.1 QPC

$f_1, f_2, 2f_1$	$\varphi_1, \varphi_2, 2\varphi_1$
$f_1, f_2, f_1 + f_2$	$\varphi_1, \varphi_2, \varphi_1 + \varphi_2$
$f_1, f_2, f_1 - f_2$	$\varphi_1, \varphi_2, \varphi_1 - \varphi_2$

Quadratic phase coupling occurs when two waves interact non-linearly and generate a third wave with a frequency equal to the sum/difference of the first two waves as shown in Table 5.1

The bispectrum is capable of detecting and characterizing quadratic phase coupling [65], [102]. Harmonically related peaks in the power spectrum are necessary conditions for the presence of quadratic non-linearities in the data. As ECG is a nonlinear signal, QPC can be used to give phase coupling information present in the ECG signal

5.3.4 Higher Order Statistics

The variance, skewness and kurtosis are three higher order statistics considered for analysis of ECG signal.

Variance: It is a measurement of the spread between numbers in a dataset from the mean. It is used to determine the measure of dispersion and the uncertainty in the given data set values. If a random variable (x) has the expected value or mean, μ = E[x], then the variance of the random variable(x) is given by the equation 5.14,

$$\mathrm{Var(x)} = \mathrm{E}[(x-\mu)]^2 \tag{5.14}$$

Skewness: Skewness is a measure of the asymmetry of the data around the sample mean. If the skewness is negative, the data are spread out more to the left of the mean. If skewness is positive, then the data are spread out more to the right of the mean. The skewness of the any perfectly symmetric distribution is zero.

The skewness (S) of a distribution is given by the following equation 5.15

$$S = \mathrm{E}\,\frac{(x-\mu)^3}{\sigma^3} \tag{5.15}$$

Where μ is the mean of random variable(x), σ is the standard deviation of random variable(x) and E (t) represents the expected value of the quantity t.

Kurtosis: Kurtosis is a measure of how outlier-prone a distribution is. The kurtosis of the normal distribution is 3. Distributions that are more outlier-prone than the normal distribution have kurtosis greater than 3, distributions that are less outlier-prone have kurtosis less than 3.

The kurtosis (K) of a distribution is given by the following equation 5.16

$$\mathrm{K} = \mathrm{E}\frac{(x-\mu)^4}{\sigma^4} \tag{5.16}$$

From using above equations 5.14, 5.15 and 5.16, HOSA features have been computed and listed in Table 5.3 to Table 5.6.

5.4 Classification of Arrhythmias using Neural Networks and Machine Learning Algorithms

This work has been done using HOSA tool box. HOSA plots are used as visual aids to distinguish normal and different types of cardiac arrhythmias. HOSA features are used to categorise different types of cardiac signals. Bispectrum and Bicoherence plots of NSR records (16786, 16420 and 16539) are as shown in Fig 5.2, NSR record 16539 exhibit peaks around +0.3 to -0.3 in bi-frequency plane, obtained 15 normal records average skewness value as 2.75789.

The bicoherence values appear to be scattered throughout the bifrequency plane in a random manner. Average Bicoherence value of NSR of 15 records is 5.125613 which indicates the strength of phase correlation as shown in Table 5.2. It can be further identified that bicoherence indicates the non-linearity present in cardiac signals. The corresponding QPC plot of NSR record 16539 is shown in Fig 5.3.

Bispectrum and Bicoherence plots of SCA records (30, 32 and 37) are shown in Fig 5.4 which exhibit peaks around -0.2 to +0.2 in bi-frequency plane, average skewness value is 0.19142. The bicoherence values appear to be scattered throughout the bifrequency plane in a random manner. Average Bicoherence value of SCA of 15 records is 5.2879 which indicates the strength of phase correlation and indicates the non-linearity present in cardiac signals as shown in Table 5.2. The corresponding QPC plot of SCA record 30 is shown in Fig 5.5.

Bispectrum and Bicoherence plots of VT records (cu06, cu13 and cu15) are as shown in Fig 5.6 exhibit peaks around -0.15 to +0.15 in bi-frequency plane, average skewness value is 0.92956. The bicoherence values appear to be scattered throughout the bifrequency plane in a random manner. Average Bicoherence value of VT of 15 records is 5.8385 which indicates the strength of phase correlation as shown in Table 5.2. The corresponding QPC plot of VT record cu06is shown in Fig 5.7.

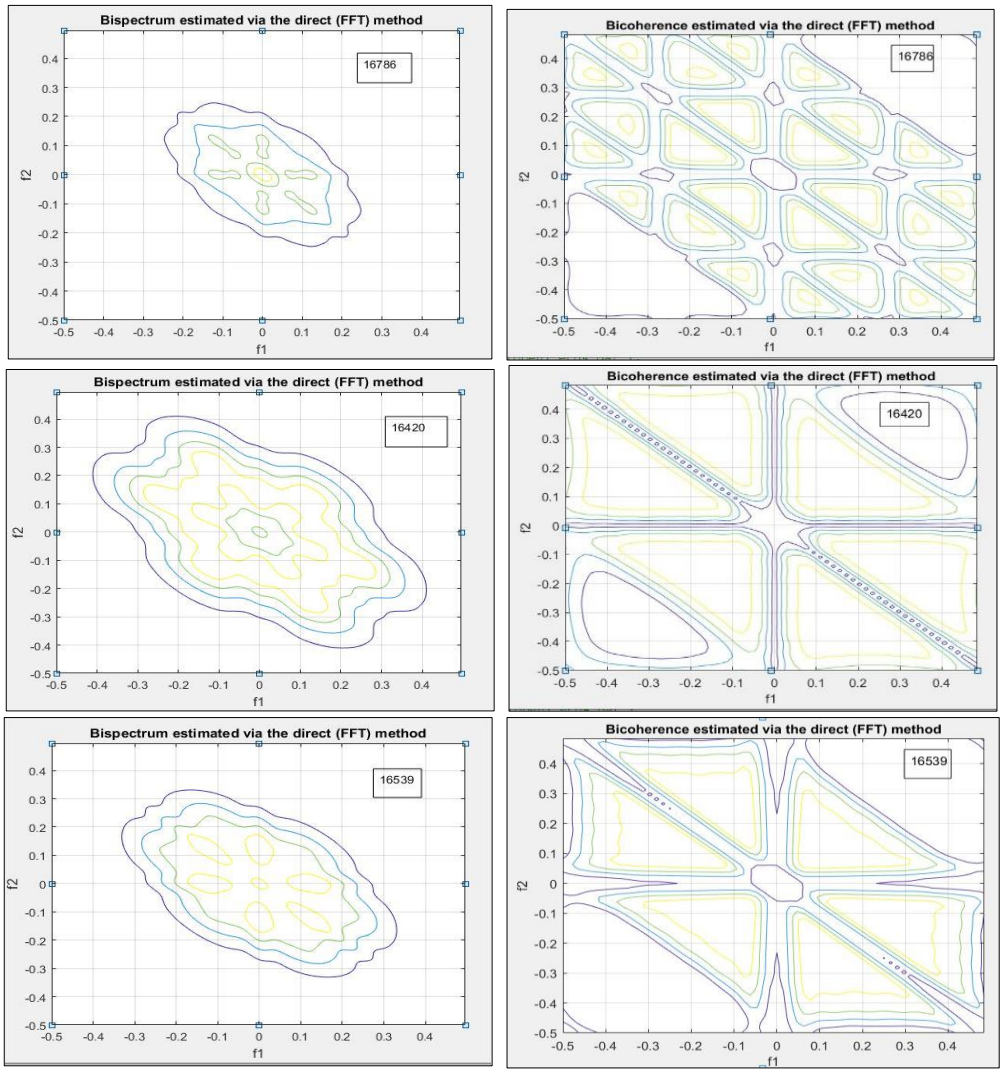

Fig 5.2 Bispectrum and Bicoherence plots of NSR records (16265, 16420 and 16539)

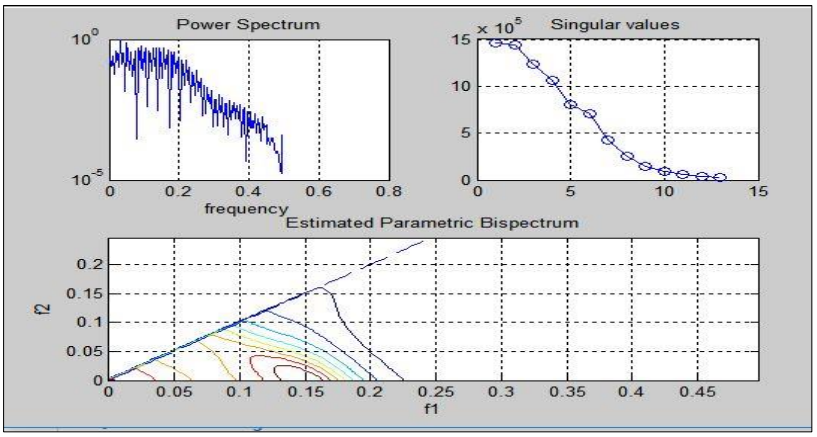

Fig 5.3 QPC plot of NSR record 16539

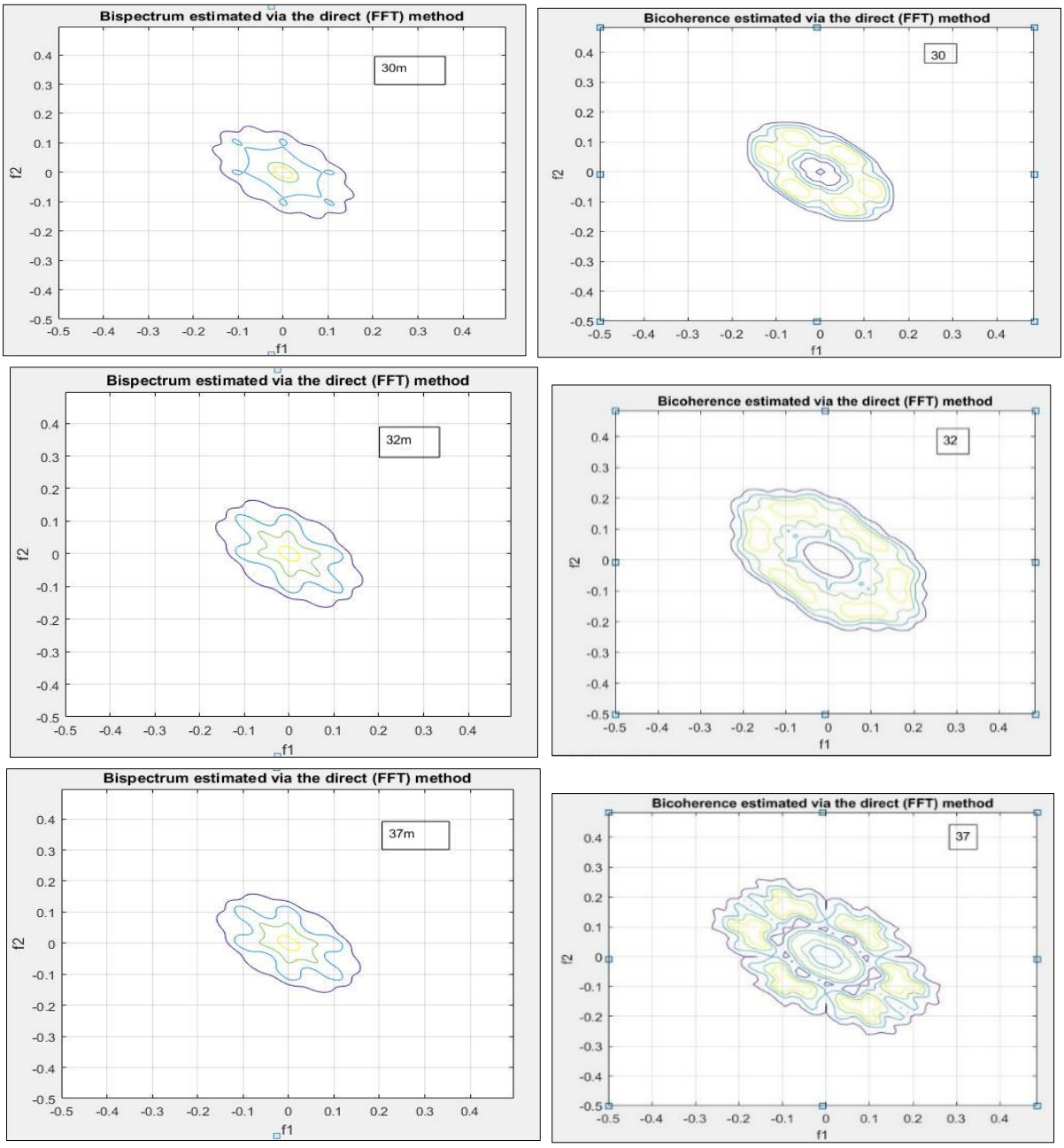

Fig 5.4 Bispectrum and Bicoherence plots of SCA records (30, 32 and 37)

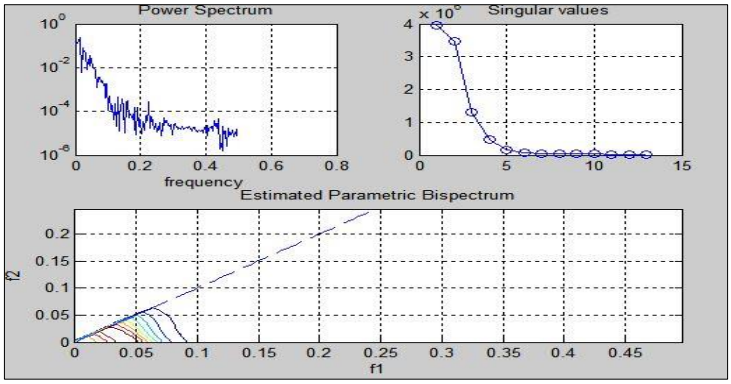

Fig 5.5 QPC plot of SCA (record 30)

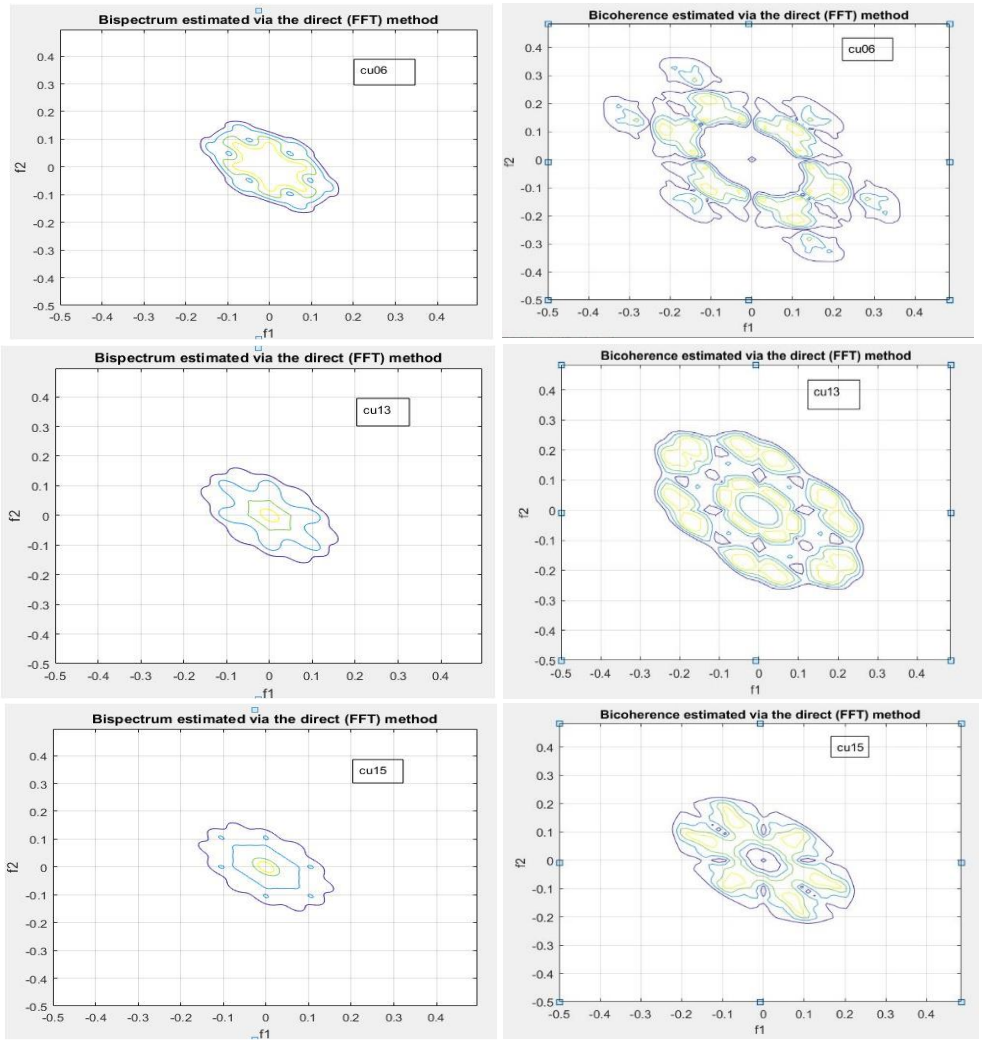

Fig 5.6 Bispectrum and Bicoherence plots of VT records (cu06, cu13 and cu15)

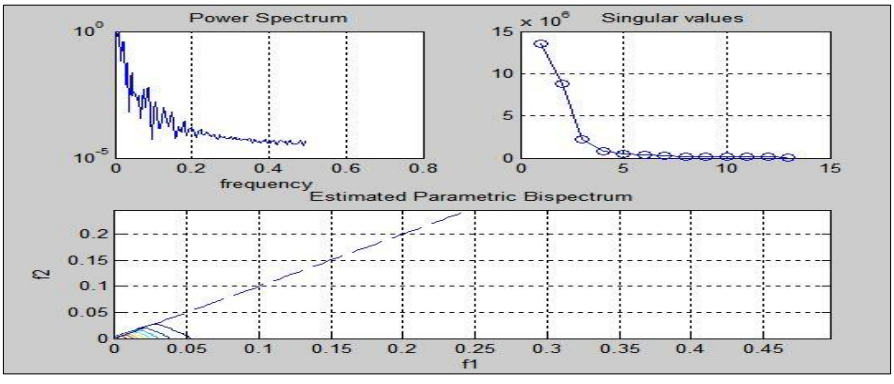

Fig 5.7 QPC plot of VT records (cu06)

Bispectrum and Bicoherence plots of AF records (04746, 07910 and 04048) are as shown in Fig 5.8 which exhibit peaks around -0.25 to +0.25 in bi-frequency plane, average skewness value is 0.3. The bicoherence values appear to be scattered throughout the bifrequency plane in a random manner. Average Bicoherence value of AF of 15 records is 7.4163 which indicates the strength of phase correlation as shown in Table 5.2. The corresponding QPC plot of AF record 04048 is shown in Fig 5.9.

Bispectrum and Bicoherence plots of CI records (e0112, e0123 and e0125)) are as shown in Fig 5.10 exhibit peaks around -0.3 to +0.3 in bi-frequency plane, average skewness value is 2.75. The bicoherence values appear to be scattered throughout the bifrequency plane in a random manner. Average Bicoherence value of CI of 15 records is 10.2520 which indicates the strength of phase correlation as shown in Table 5.2. The corresponding QPC plot of CI record e0123 is shown in Fig 5.11

Bispectrum and Bicoherence plots of VF records (418, 419 and 609) are as shown in Fig 5.12 exhibit peaks around -0.2 to +0.2 in bi-frequency plane, average skewness value is 0.63982. The bicoherence values appear to be scattered throughout the bifrequency plane in a random manner. Average Bicoherence value of VF of 15 records is 4.0090 which indicates the strength of phase correlation as shown in Table 5.2. The corresponding QPC plot of VF record 418 is shown in Fig 5.13.

Bispectrum and Bicoherence plots of SVT records (811, 812 and 824) are as shown in Fig 5.14 exhibit peaks around -0.2 to +0.2 in bi-frequency plane, average skewness value is 2.19287. The bicoherence values appear to be scattered throughout the bifrequency plane in a random manner. Average Bicoherence value of SVT of 15 records is 4.7224 which indicates the strength of phase correlation as shown in Table 5.2. The corresponding QPC plot of SVT record 812 is shown in Fig 5.15

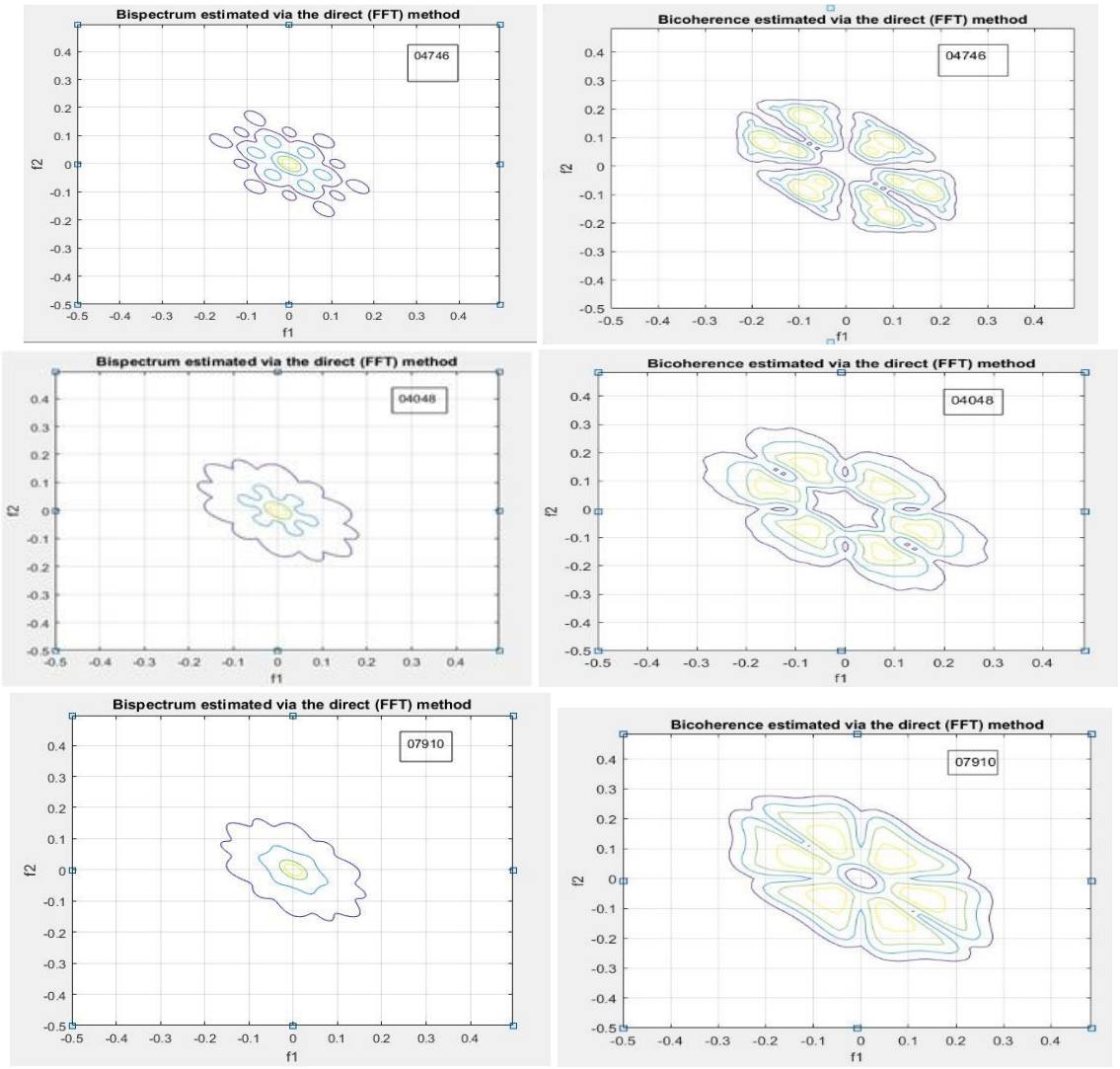

Fig 5. 8 Bispectrum and Bicoherence plots of AF records (04746, 07910 and 04048)

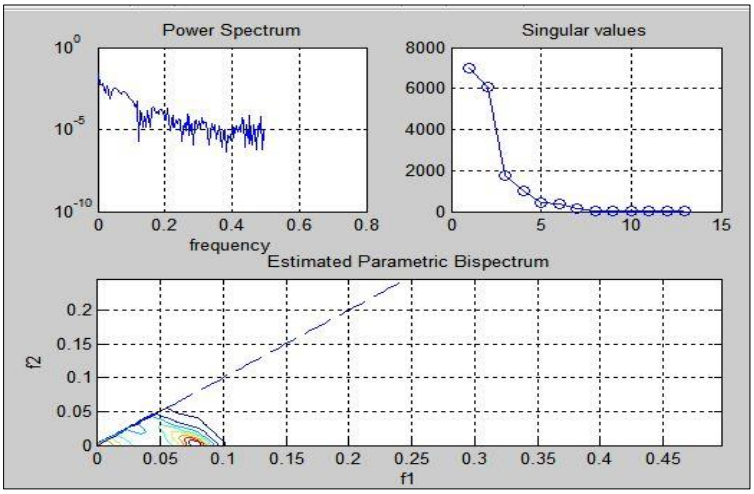

Fig 5.9 QPC plot of AF record (04048)

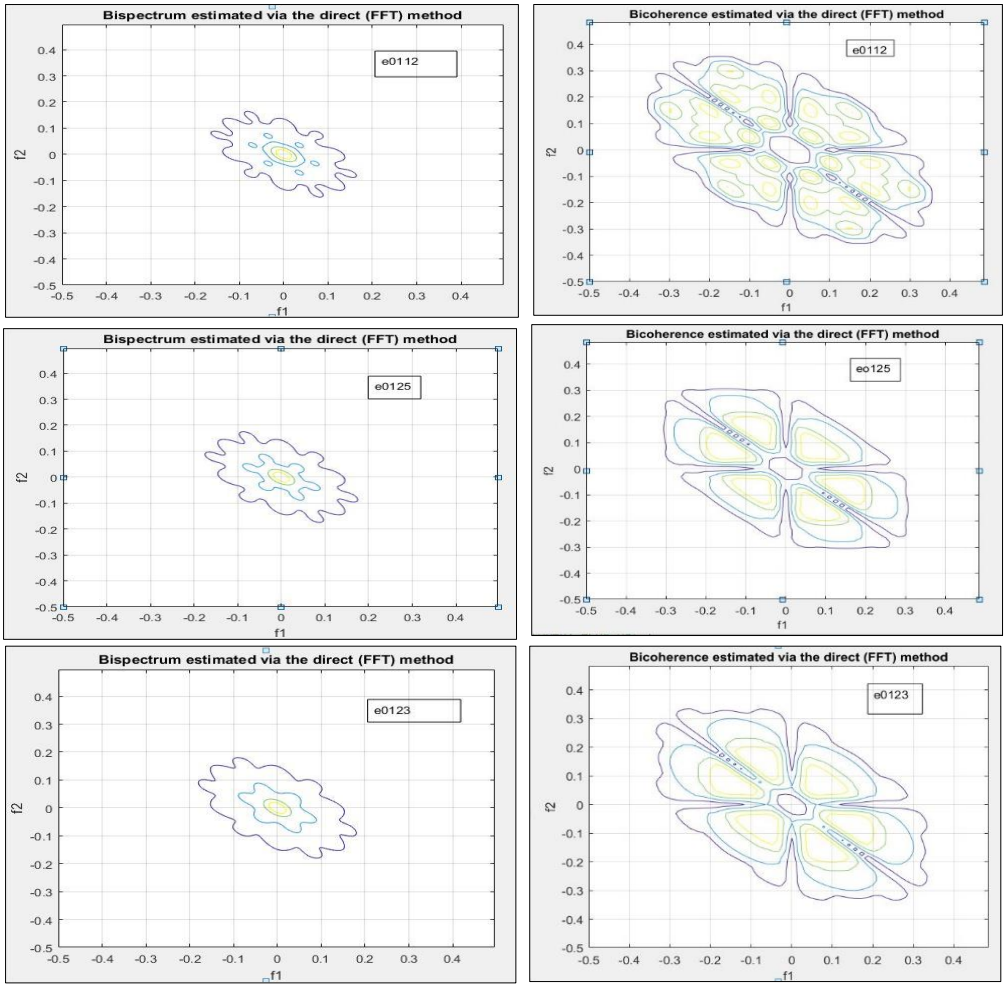

Fig 5. 10 Bispectrum and Bicoherence plots of CI records (e0112, e0123 and e0125)

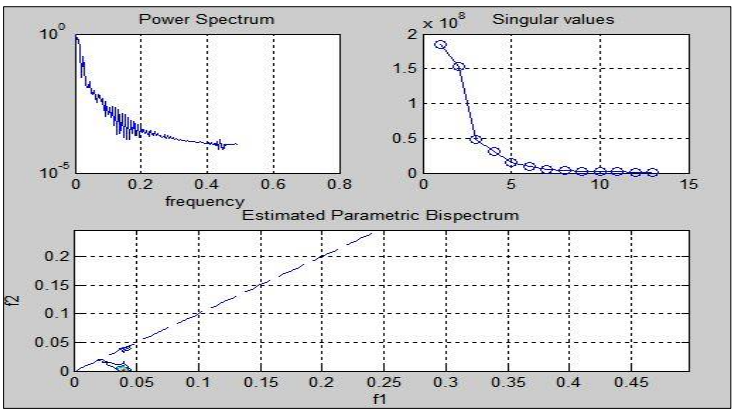

Fig 5.11 QPC plots of CI record (e0123)

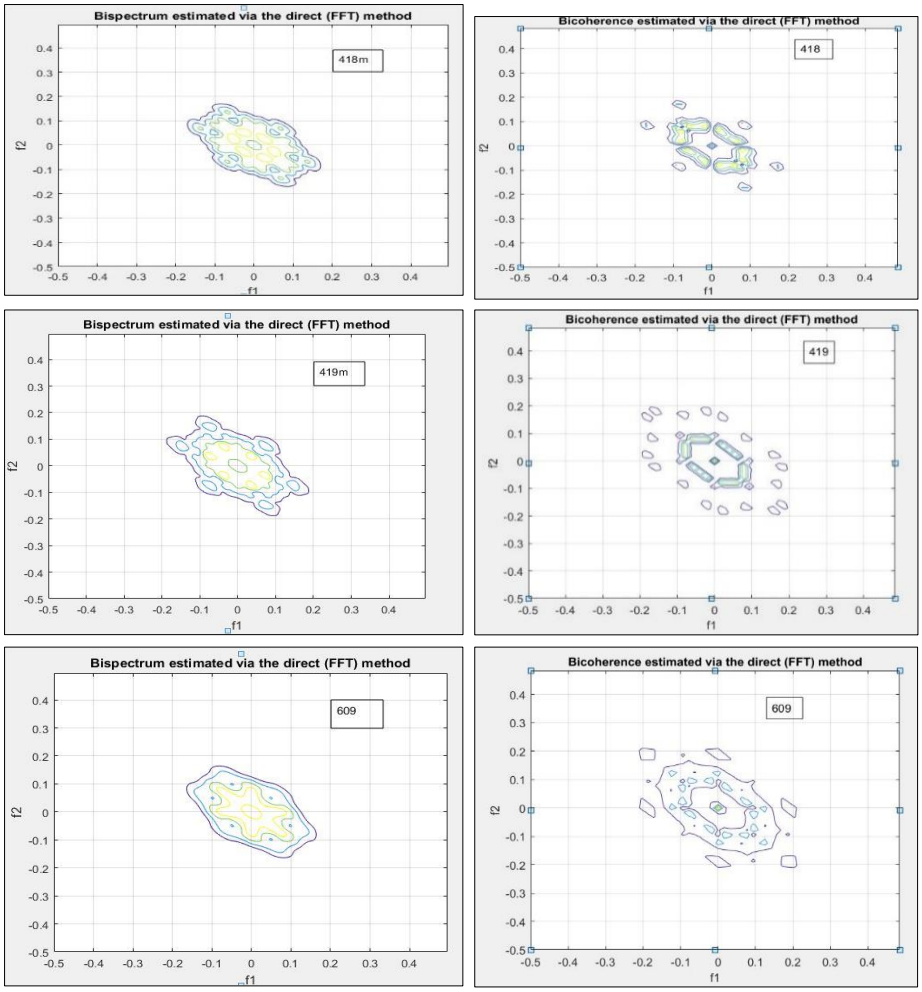

Fig 5.12 Bispectrum and Bicoherence plots of VF records (418, 419 and 609)

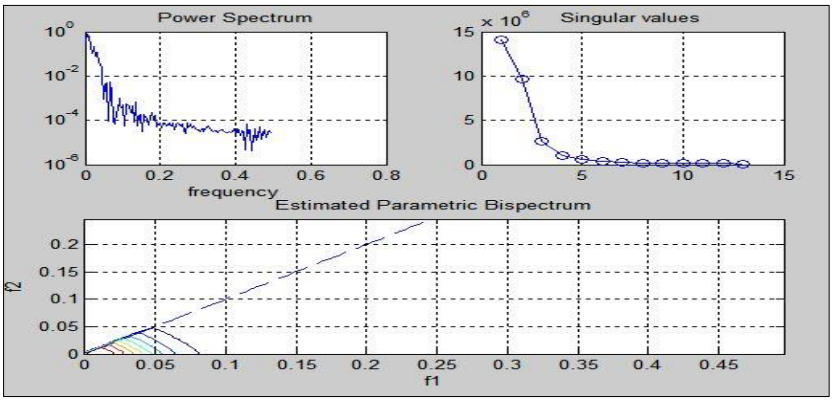

Fig 5. 13 QPC plot of VF record (418)

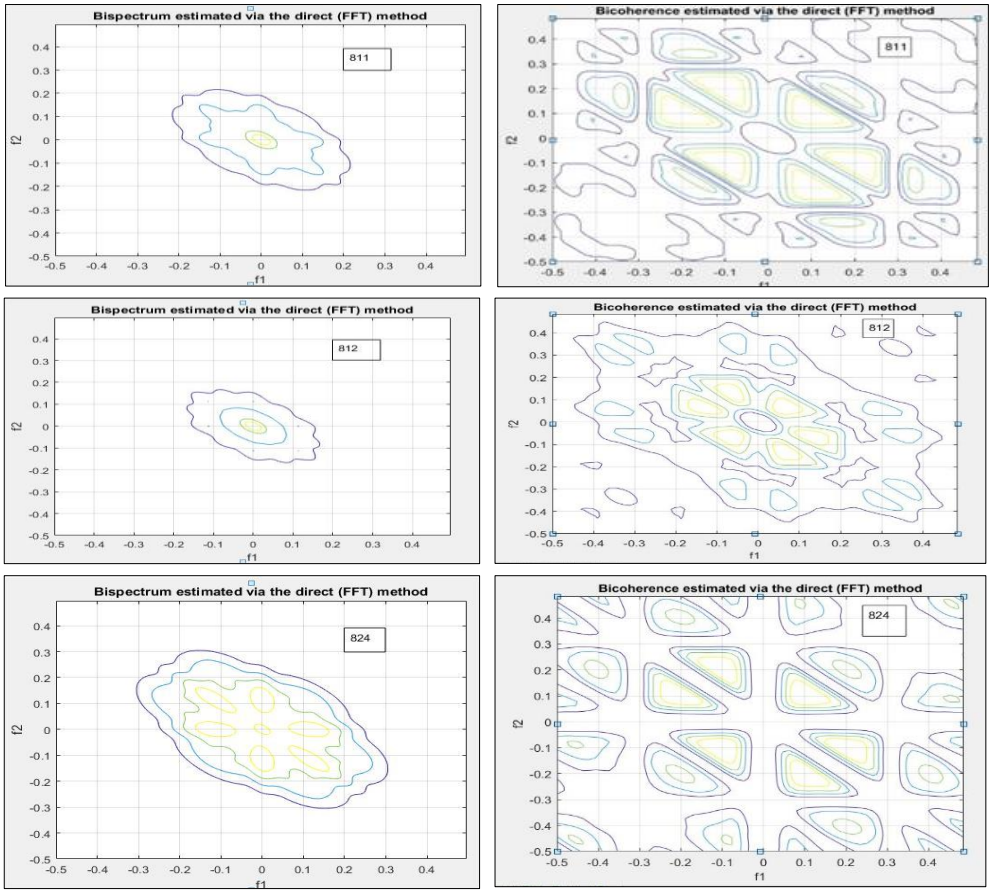

Fig 5.14 Bispectrum and Bicoherence plots of SVT records (811, 812 and 824)

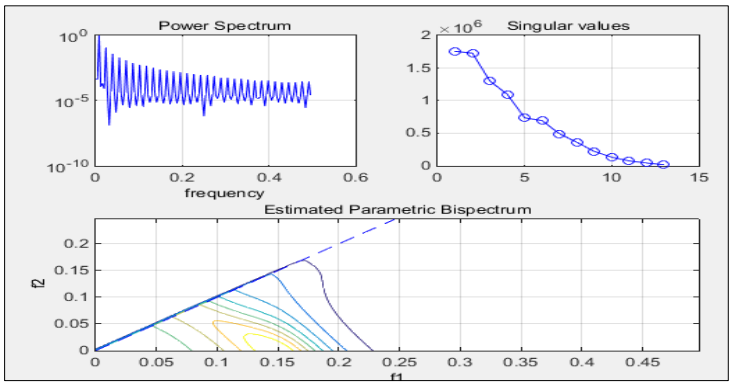

Fig 5. 15 QPC plots of SVT record (812)

Higher order spectral features such as skewness, kurtosis, variance and bicoherence are extracted using bispectrum and bicoherence plots. Average values of 15 records for different cardiac signals are shown in Table 5.2.

Table 5.2 Higher order spectral features of 7 types of cardiac signals

Cardiac Signal	Kurtosis (Avg)	Skewness (Avg)	Variance (Avg)	Bicoherence (Avg)
CI	18.6481	2.75664	2.06E+03	10.2520
AF	11.0441	-0.33311	2.48E+03	7.4163
NSR	16.8971	2.75789	5.86E+03	5.1256
SVT	16.7308	2.19287	6438.8	4.7224
VT	8.0496	0.92956	8.52E+04	5.8385
VF	6.5149	0.63982	2.47E+04	4.0090
SCA	6.7753	0.19142	93926	5.2879

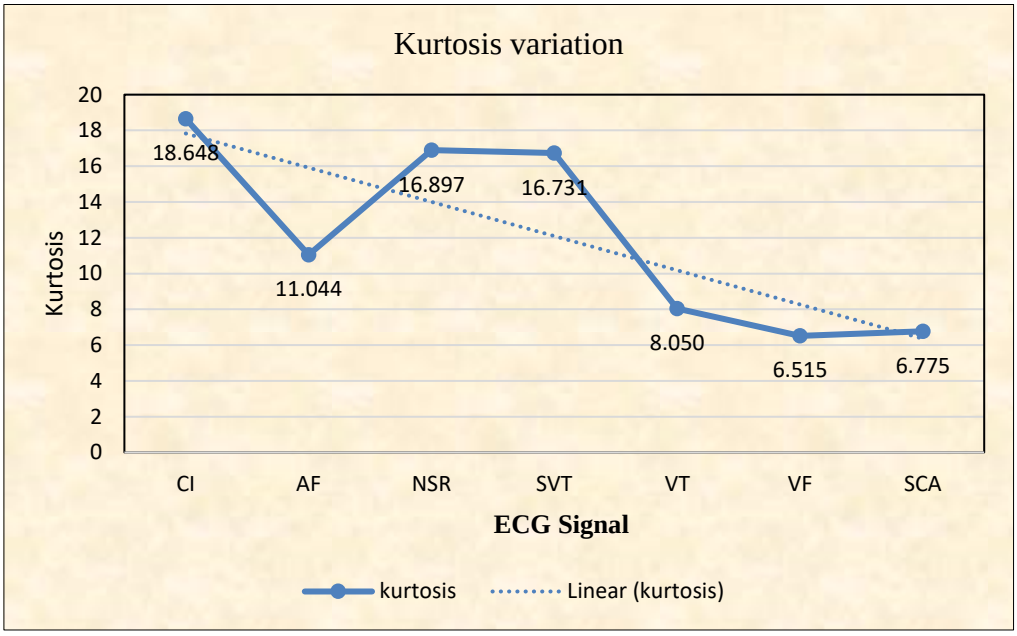

Fig 5.16 Kurtosis Variation in different signals

Higher values of kurtosis is the result of infrequent extreme deviations. The highest value of Kurtosis 18.6481 is observed in Cardiac Ischemia and the lowest value of kurtosis 6.5149 is observed in Ventricular fibrillation. The kurtosis variation (average value) of different cardiac signals is shown in Fig 5.16.

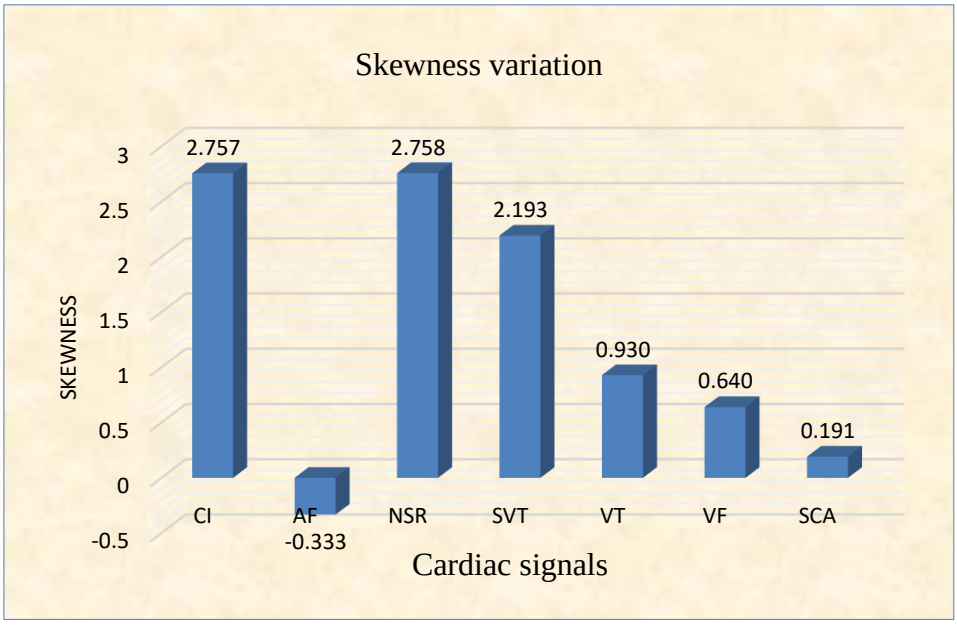

Fig 5.17 Skewness variation in different signals

The skewness variation of different cardiac signals is shown in Fig 5.17. Zero value of skewness indicates normal symmetric distribution. Skewness can be positive or negative. Here, it is observed that AF signal has average skewness value as -0.33311.

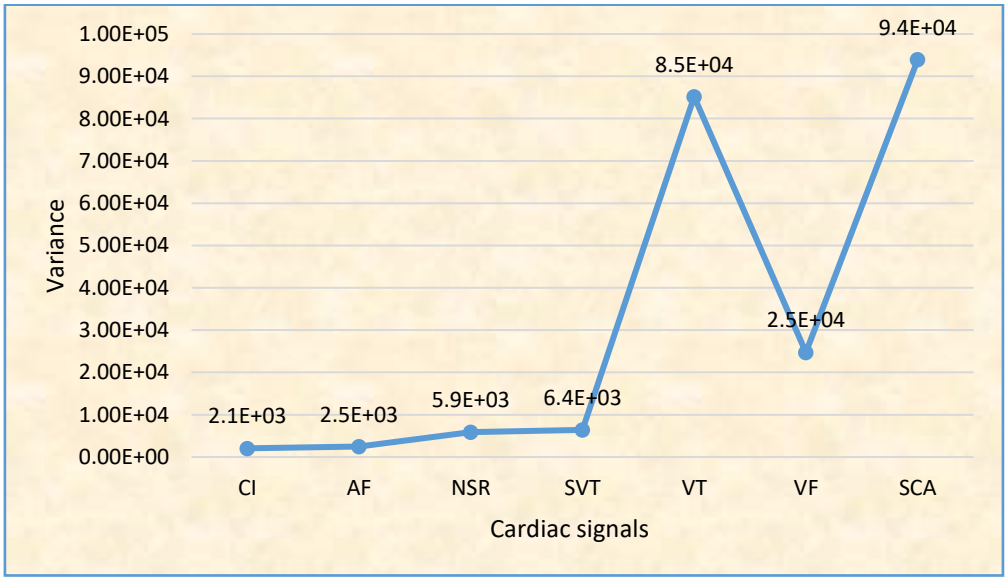

Fig 5.18 Variance variation in different signals

The average variance of 15 records of each category of 7 types of cardiac signals variation is shown in Fig 5.18. Highest variance value is observed in VT and SCA. Lowest variance is observed in AF and CI. Medium value of variance is observed in NSR, SVT and VF variance value is in between VT and SCA.

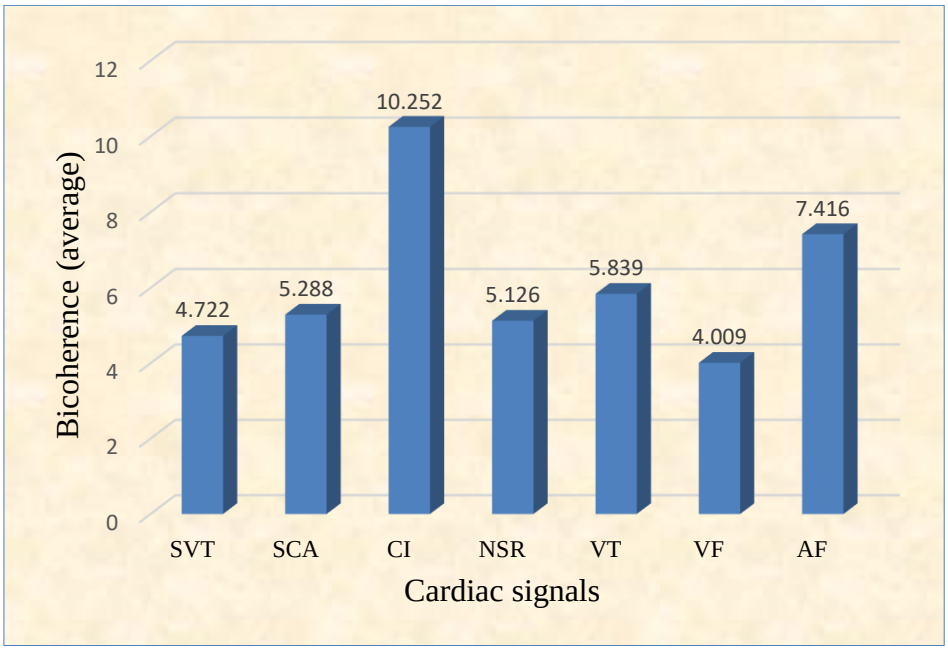

Fig 5.19 Bicoherence variation in different cardiac signals

Bicoherence indicates the strength of phase correlation. From the Fig 5.19, it is observed that bicoherence value is relatively less in NSR and VT. Bicoherence value is more in CI and AF. This result proves that high degree of phase correlation is existing in arrhythmia signals than NSR.

Spectral, Bispectral and Temporal features (hybrid features) of 7 types of cardiac signals for each record are shown in Table 5.3 Table 5.6 to are used for classification purpose using three supervised classifiers.

Table 5.3 HOSA features for different records of VF and VT signals

R- peaks	Amplitude	R-R	HBR(bpm)	kurtosis	skewness	variance	bicoherenc	Energy(mi	Signal?
41	0.195675	0.783	76.657723	2.7979	-0.173732	8.00E+03	0.96368	65.818	VF
63	0.1279194	0.512	117.26137	2.81973	-0.164595	9.63E+03	0.4833	16.25	VF
40	0.2028462	0.811	73.947667	5.19184	1.0175	2.57E+04	9.207	185.61	VF
53	0.1511538	0.605	99.236641	4.6537	1.025823	4.57E+04	2.8888	161.83	VF
22	0.3680952	1.472	40.750323	2.61687	-0.184986	2.07E+04	3.2975	278.04	VF
44	0.1822791	0.729	82.291400	1.71676	-0.089938	1.36E+05	5.58	185.99	VF
55	0.145537	0.582	103.06654	6.11141	-1.044052	3.47E+02	3.7358	415.31	VF
43	0.1864048	0.746	80.470047	3.6149	-0.150869	1.48E+03	3.2021	40.218	VF
24	0.332913	1.332	45.056810	9.82071	1.973202	1.48E+04	3.9841	216.22	VF
57	0.1415893	0.566	105.94021	4.59975	0.679012	1.56E+03	4.2673	325.75	VF
36	0.2234286	0.894	67.135549	9.33153	2.227323	8.74E+03	1.6224	213.12	VF
25	0.315625	1.263	47.524752	5.06922	1.306243	2.71E+04	5.6265	21.689	VF
34	0.2370606	0.948	63.274958	6.99069	-0.386476	2.57E+04	3.0103	105.39	VF
25	0.3235417	1.294	46.361880	13.7723	3.135424	3.19E+04	1.372	213.12	VF
56	0.1419455	0.568	105.67439	18.6163	0.427468	1.37E+04	4.4663	802.79	VF
32	0.1599015	0.975	61.564941	23.2254	3.7796	2.29E+04	11.7668	202.71	VT
73	0.9728755	0.604	99.261898	10.1039	2.0053	1.07E+05	11.7668	398.65	VT
75	0.0318119	0.418	143.68932	9.76475	0.115924	3.71E+04	2.8842	1058.3	VT
24	0.0005856	1.368	43.848500	3.02	-0.379572	1.08E+05	2.2751	135.98	VT
76	0.0319557	0.414	144.82492	4.62428	1.052646	3.75E+04	2.0668	497.06	VT
36	0.1433246	0.879	61.564941	4.91989	0.459662	3.17E+05	2.9665	31.821	VT
46	0.000696	0.706	144.53961	4.06572	-0.641717	8.25E+04	3.4592	483.95	VT
42	0.0004558	0.774	143.68932	3.41328	0.512979	1.12E+05	1.2539	36.254	VT
47	0.0587969	0.669	89.715251	3.33129	-0.464357	1.22E+05	22.441	204.54	VT
47	0.1212827	0.692	144.82492	7.87341	2.094548	4.43E+04	4.5837	48.034	VT
29	0.246977	1.106	68.243858	19.3454	2.894891	7.04E+04	3.0937	33.605	VT
38	0.1378719	0.831	84.969788	11.4482	-1.130091	4.71E+04	8.8448	291.39	VT
23	0.0011402	1.354	77.563375	4.42566	1.01947	6.37E+04	1.8913	16.342	VT
38	0.0029195	0.844	48.688652	6.72368	1.724641	5.35E+04	4.8939	852.44	VT
23	0.0015053	1.391	86.737900	4.45987	0.89949	5.24E+04	3.39	340.13	VT

Table 5.4 HOSA features for different records of NSR and AF signals

R- peaks	Amplitude	R-R	HBR(bpm	kurtosis	skewness	variance	bicoherenc	Energy(mi	Signal?
31	1.1507839	0.15	60.3378922	19.1923	4.0184	1.19E+04	4.3887	35.889	NSR
49	5.5294735	0.102	93.0833872	19.1236	3.0191	2.08E+03	7.1182	3930.2	NSR
50	5.507928	0.235	92.7327782	20.3318	4.0076	1.39E+04	4.4381	2834.7	NSR
49	1.8910163	0.043	92.6998841	27.1841	3.82289	3.24E+03	4.2992	3419.3	NSR
50	1.758144	0.003	93.3451867	11.4669	2.11016	3.66E+03	3.9847	4427.2	NSR
40	1.79936	0.372	75.9937646	25.3493	4.07809	2.74E+03	4.9182	4050.6	NSR
38	5.9693105	0.085	71.4285714	15.5557	3.03404	1.21E+04	5.0646	3204.2	NSR
37	4.3836	0.085	70.075266	24.812	4.44105	8.66E+03	5.7747	3368.7	NSR
34	1.2675706	0.092	63.4371396	7.76684	-0.2895	2.73E+03	5.8268	2129.2	NSR
36	0.9920389	0.098	66.6666667	32.3599	4.97377	1.60E+03	5.8643	2209.3	NSR
43	3.4519744	7E-04	81.2903226	24.082	4.18583	6.49E+03	5.1291	2649.4	NSR
58	0.61046	1E-04	74.5747929	4.04005	0.38992	2.50E+03	3.4824	3863.8	NSR
43	2.0547	7E-04	80.6658131	19.2133	3.53243	4.85E+03	4.8912	4563.6	NSR
57	0.6096912	8E-04	109.517601	1.54114	0.0581	6.12E+03	9.3307	2824.4	NSR
60	0.1127592	0.198	111.742424	1.43862	-0.01353	5.30E+03	2.3733	1113.7	NSR
28	0.3360325	1.344	44.6385366	9.18079	2.199079	3.13E+03	6.5968	1960.1	AF
19	0.1203049	0.481	124.683201	7.35514	0.666182	8.72E+02	8.1957	1793.9	AF
20	0.1164523	0.466	128.80816	9.73161	-0.57056	2.51E+03	8.0637	233.25	AF
19	0.0280935	0.112	533.931937	3.59298	0.241468	3.84E+02	5.977	2066.5	AF
19	0.2692142	1.077	55.7177224	23.4522	-4.186971	2.21E+03	9.817	236.52	AF
16	0.2985808	1.194	50.2376587	22.8318	-2.473967	1.30E+03	11.4552	138.26	AF
19	0.2437273	0.975	61.544201	5.71486	-1.336088	1.06E+04	4.6813	3162.5	AF
33	0.1253654	0.501	119.650259	5.46218	-1.424031	6.31E+03	3.4928	2168.6	AF
22	0.0265784	0.106	564.367865	4.16901	0.203298	1.74E+02	7.0904	163.2	AF
19	0.0052671	0.021	2847.85841	8.49625	-0.957753	4.90E+02	0.89883	341.9	AF
62	0.0626708	0.251	239.345872	5.88229	0.515044	3.35E+02	10.0928	24.836	AF
18	0.0479634	0.192	312.738499	29.6484	4.502998	1.31E+03	12.9355	238.88	AF
15	0.2793693	1.117	53.6923758	13.4884	-2.395023	1.53E+03	8.5302	301.36	AF
21	0.2276741	0.911	65.8836524	7.92083	0.972137	4.36E+03	4.5012	2207.8	AF
30	0.1114901	0.446	134.541106	8.73571	-0.952489	1.66E+03	8.9162	187.08	AF

Table 5.5 HOSA features for different records of SVT and SCA signals

R- peaks	Amplitud	R-R	HBR(bp	kurtosis	skewness	variance	bicoheren	Energy(m	Signal?
52	0.854975	0.618	54.228534	17.1615	2.883129	2.40E+03	1.6977	922.81	SVT
32	1.9555844	1.963	72.209211	5.87581	-0.992182	2.62E+04	4.7938	1259.3	SVT
44	0.9581682	0.723	71.071840	12.6778	-0.84985	4.64E+03	5.8349	2184.2	SVT
40	1.49194	0.801	74.903969	17.3634	2.990202	1.54E+03	4.4546	2983.1	SVT
32	1.6564906	0.998	60.139679	12.2866	1.894445	1.67E+04	3.5916	363.66	SVT
43	1.7546	0.729	82.331416	27.0406	4.566205	6.73E+02	4.2748	4436.7	SVT
35	1.6259057	0.934	64.272211	13.7693	3.025711	9.92E+03	4.6932	1717.5	SVT
25	0.6304737	1.295	46.326084	9.95861	2.005118	1.11E+04	5.3901	1794.2	SVT
28	1.2985214	1.152	52.096732	13.8017	1.961011	4.62E+03	3.9795	237.14	SVT
40	0.2131975	0.797	75.260517	30.7822	2.291805	7.47E+03	5.4145	3001.7	SVT
54	0.142973	0.588	102.09323	17.5698	3.35238	1.60E+03	8.3551	1960.4	SVT
41	0.2752725	0.783	76.677316	21.1762	4.003127	7.47E+03	6.7847	5746	SVT
54	1.2453407	0.59	101.66240	12.6579	2.687353	8.89E+02	5.0274	5746	SVT
41	1.0106927	0.768	78.175895	9.8282	-1.773114	6.38E+02	3.6685	1269.9	SVT
50	0.5580146	0.65	92.325084	29.0136	4.847777	7.22E+02	5.2366	1717.2	SVT
23	0.1495867	1.368	43.871310	8.9098	-1.003569	3.95E+04	5.8064	202.71	SCA
29	0.1018118	1.071	56.022409	6.51175	0.911851	6.04E+03	6.6024	99.994	SCA
23	0.2350158	1.426	42.086468	5.98922	0.961966	1.14E+04	5.3536	344.22	SCA
24	0.0429661	1.371	43.770616	5.40128	-1.073249	9.56E+03	3.7852	20.136	SCA
24	0.0030383	1.342	44.706492	3.76023	0.381738	1.43E+05	7.7219	90.55	SCA
18	0.0851089	1.837	32.654629	3.97686	0.133352	1.47E+04	3.7779	167.26	SCA
8	0.0854888	4.555	13.172751	9.93668	1.18076	1.48E+04	7.2184	21.903	SCA
32	0.0917073	1.007	59.607742	3.44263	-0.903982	5.80E+04	2.3668	263.58	SCA
31	0.0984336	1.053	56.969236	3.31139	0.197193	2.33E+03	1.8045	366.88	SCA
26	0.0001269	1.276	47.033738	7.99787	-1.703829	1.36E+04	4.8766	95.726	SCA
30	0.0006742	1.069	56.107313	2.79243	0.887277	9.62E+05	5.9199	271	SCA
25	0.0633747	1.329	45.152389	6.28482	-1.331848	2.61E+03	4.643	55.409	SCA
22	0.0013366	1.468	40.882543	15.6582	3.2326	4.97E+04	7.5185	99.621	SCA
26	0.0007559	1.264	47.474363	8.7388	-0.6861	7.39E+04	5.4856	921.67	SCA
22	0.4172947	1.505	39.863325	8.91766	1.687199	7.75E+03	6.4391	398.65	SCA

Table 5.6 HOSA features for different records of CI signals

R- peaks	Amplitud	R-R	HBR(bp	kurtosis	skewness	variance	bicoheren	Energy(m	Signal?
20	0.0016116	1.612	37.230568	21.6309	4.13376	1680	8.0981	100.95	CI
15	0.0021249	2.125	28.237192	30.2791	5.022827	1160	11.2365	980.55	CI
16	0.0020907	2.091	28.698979	18.0479	-1.300318	2190	12.9051	283.96	CI
15	0.0021149	2.115	28.370710	16.1192	3.021688	1970	7.8144	283.96	CI
14	0.0021985	2.198	27.291812	10.5262	2.430609	3320	11.7924	1450.8	CI
18	0.0017635	1.764	34.022681	9.27806	-1.089619	902	7.633	176.08	CI
17	0.0019313	1.931	31.067961	17.74	3.563465	3980	10.9664	1269	CI
10	0.0029751	2.975	20.167314	5.01326	1.579862	6270	7.2783	252.03	CI
18	0.0018699	1.87	32.087580	25.3376	3.4454	1510	11.0197	2615.5	CI
13	0.0026827	2.683	22.365805	26.2562	4.176393	867	14.8998	184.26	CI
18	0.0018188	1.819	32.988357	13.7981	2.778066	957	9.2354	1949.3	CI
16	0.0020131	2.013	29.805272	15.1468	2.990783	979	11.9167	204.83	CI
21	0.0015494	1.549	38.724667	20.7248	3.787391	2420	9.7889	2635.3	CI
21	0.0015456	1.546	38.819875	23.6687	3.358272	1220	8.9444	4922.4	CI
24	0.0013434	1.343	44.66019	26.1558	3.451057	1430	10.123	3180.7	CI

5.5 Results and Discussion

5.5.1 MLP classifier results

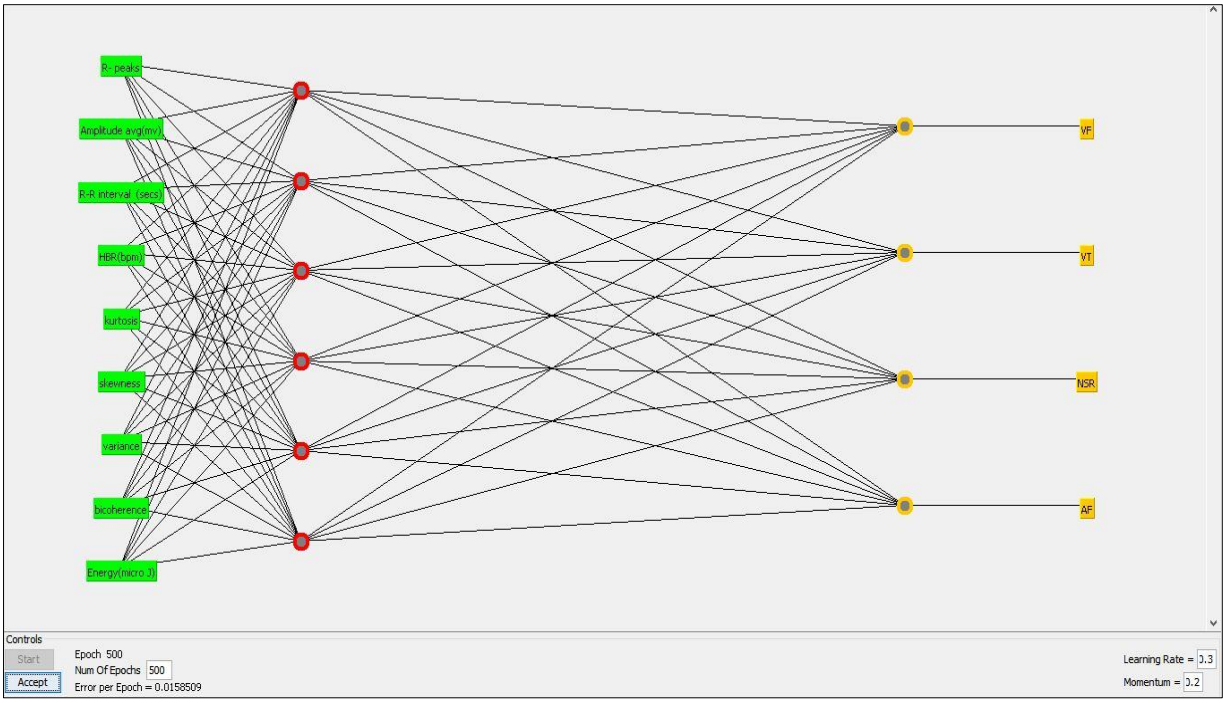

Fig 5.20 ANN structure for classification of NSR, VT, VF and AF using temporal, spectral and bispectral features

The Fig 5.20 shows MLP neural network architecture obtained for 4 types of signals (NSR, VT, AF and VF). It has one input layer, one output layer and one hidden layer. Input layer has nine neurons using temporal, spectral and bispectral features represented as number of R-peaks, amplitude of R-peaks, R-R interval, heart beat rate, kurtosis, skewness, variance, bicoherence and energy are used in this work. The output layer has four neurons represented as NSR, VT, AF and VF. The error per epoch obtained as 0.0158509 and Learning rate obtained as 0.3

```
Time taken to build model: 0.09 seconds

=== Stratified cross-validation ===
=== Summary ===

Correctly Classified Instances          50               83.3333 %
Incorrectly Classified Instances        10               16.6667 %
Kappa statistic                          0.7778
Mean absolute error                      0.1038
Root mean squared error                  0.25
Relative absolute error                 27.5804 %
Root relative squared error             57.5085 %
Total Number of Instances               60

=== Detailed Accuracy By Class ===

               TP Rate   FP Rate   Precision   Recall  F-Measure   ROC Area  Class
                 0.8       0.133      0.667      0.8       0.727      0.907    VF
                 0.8       0.067      0.8        0.8       0.8        0.96     VT
                 0.867     0          1          0.867     0.929      0.996    NSR
                 0.867     0.022      0.929      0.867     0.897      0.933    AF
Weighted Avg.    0.833     0.056      0.849      0.833     0.838      0.949

=== Confusion Matrix ===

  a  b  c  d   <-- classified as
 12  3  0  0 |  a = VF
  3 12  0  0 |  b = VT
  1  0 13  1 |  c = NSR
  2  0  0 13 |  d = AF
```

Fig 5.21 Simulation results of NSR,VT,VF and AF using MLP Classifier

The Fig 5.21 shows the simulation results for classification of NSR, VT, AF and VF using MLP classifier. Time taken to build the model is 0.09 seconds. Correctly classified instances are 50 out of 60 instances. RMSE value is 0.25. The classification accuracy for classifying NSR, and VF is obtained as 83.33%

```
Time taken to build model: 0.13 seconds

=== Stratified cross-validation ===
=== Summary ===

Correctly Classified Instances          63               84       %
Incorrectly Classified Instances        12               16       %
Kappa statistic                          0.8
Mean absolute error                      0.0932
Root mean squared error                  0.2371
Relative absolute error                 29.0335 %
Root relative squared error             59.1078 %
Total Number of Instances               75

=== Detailed Accuracy By Class ===

               TP Rate   FP Rate   Precision   Recall  F-Measure   ROC Area  Class
                 0.733     0.083      0.688     0.733      0.71       0.873    VF
                 0.733     0.05       0.786     0.733      0.759      0.916    VT
                 0.933     0          1         0.933      0.966      1        NSR
                 0.867     0.033      0.867     0.867      0.867      0.947    AF
                 0.933     0.033      0.875     0.933      0.903      0.991    SVT
Weighted Avg.    0.84      0.04       0.843     0.84       0.841      0.945

=== Confusion Matrix ===

  a  b  c  d  e   <-- classified as
 11  3  0  0  1 |  a = VF
  4 11  0  0  0 |  b = VT
  0  0 14  1  0 |  c = NSR
  1  0  0 13  1 |  d = AF
  0  0  0  1 14 |  e = SVT
```

Fig 5.22 Simulation results of NSR,SVT,VT,VF and AF using MLP Classifier

The Fig 5.22 shows MLP neural network architecture for classification of NSR, SVT, VT, AF and VF using MLP classifier. Time taken to build the model is 0.01 seconds. Correctly classified instances are 63 out of 75 instances. RMSE value is 0.2371. The classification accuracy for classifying NSR, SVT, VT, AF and VF is obtained as 84%.

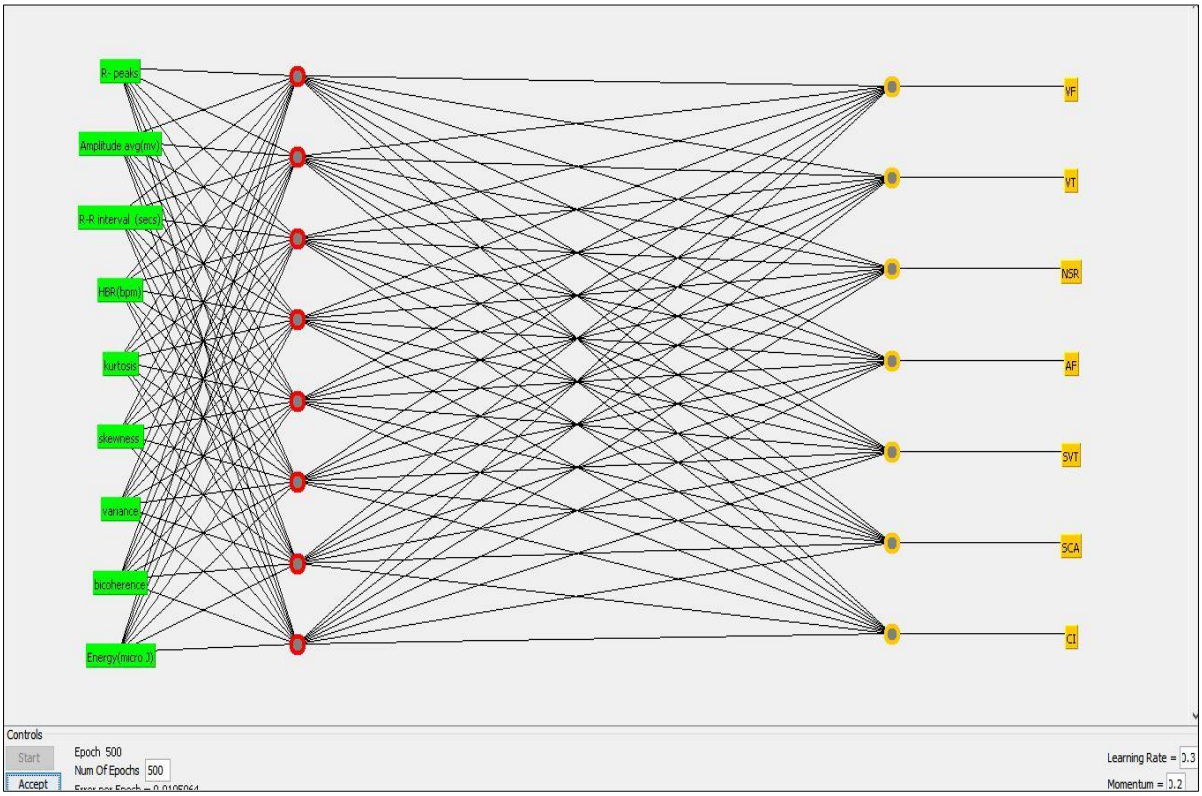

Fig 5.23 ANN structure for classification of 7 types using temporal, spectral and bispectral features

The Fig 5.23 shows neural network architecture of MLP results obtained for 7 types of signals (NSR, SVT, VT, VF, AF, CI and SCA). It has one input layer, one output layer and one hidden layer. Input layer has 9 features using temporal, spectral and bispectral features represented as Number of R-Peaks, Amplitude of R-Peaks, R-R interval, Heart beat rate, kurtosis, skewness, variance, bicoherence and energy are used in this work. The output layer has 7 neurons represented as NSR, VT, VF, SVT, AF, CI and SCA. The error per epoch obtained as 0.0105064 and Learning rate obtained as 0.3.

```
Time taken to build model: 0.25 seconds

=== Stratified cross-validation ===
=== Summary ===

Correctly Classified Instances          78               74.2857 %
Incorrectly Classified Instances        27               25.7143 %
Kappa statistic                          0.7
Mean absolute error                      0.0977
Root mean squared error                  0.2328
Relative absolute error                 39.8302 %
Root relative squared error             66.4041 %
Total Number of Instances              105

=== Detailed Accuracy By Class ===

               TP Rate   FP Rate   Precision   Recall  F-Measure   ROC Area  Class
                 0.533     0.067       0.571     0.533     0.552      0.898    VF
                 0.6       0.089       0.529     0.6       0.563      0.902    VT
                 0.867     0           1         0.867     0.929      0.996    NSR
                 0.8       0.033       0.8       0.8       0.8        0.907    AF
                 0.933     0.011       0.933     0.933     0.933      0.997    SVT
                 0.533     0.089       0.5       0.533     0.516      0.842    SCA
                 0.933     0.011       0.933     0.933     0.933      0.991    CI
Weighted Avg.    0.743     0.043       0.753     0.743     0.747      0.933

=== Confusion Matrix ===

  a  b  c  d  e  f  g   <-- classified as
  8  4  0  0  0  3  0 |  a = VF
  2  9  0  0  0  4  0 |  b = VT
  1  0 13  1  0  0  0 |  c = NSR
  1  1  0 12  1  0  0 |  d = AF
  0  0  0  1 14  0  0 |  e = SVT
  2  3  0  1  0  8  1 |  f = SCA
  0  0  0  0  0  1 14 |  g = CI
```

Fig 5.24 Simulation results of 7 types using MLP Classifier

The Fig 5.24 shows the classification results of 7 types cardiac signals using MLP classifier. Time taken to build the model is 0.25 seconds. Correctly classified instances are 78 out of 105 instances. RMSE value is 0.2328. The classification accuracy for classifying 7 types of ECG signals is obtained as 74.28%. The medical statistics of 7 types of signals are sensitivity as 74.3%, specificity as 95.71% and precision as 75.25% are shown in Table 5.7.

Table 5.7 Medical Statistics of MLP using confusion matrix for 7 types of signals

ECG	TP	FP	FN	TN	Sensitivity(S)	Specificity(S)	Precision(Pp)
VF	08	6	7	84	53.33%	93.33%	57.14%
VT	09	8	6	82	60.00%	91.11%	52.94%
NSR	13	0	2	90	86.66%	100%	100%
AF	12	3	3	87	80.00%	96.66%	82.00%
SVT	14	1	1	89	93.33%	98.88%	93.33%
SCA	08	8	7	82	53.33%	91.11%	50.00%
CI	14	1	1	89	93.33%	98.88%	93.33%
				Average	**74.28%**	**95.71%**	**75.25%**

5.5.2 RBF classifier results

```
Time taken to build model: 0.02 seconds

=== Stratified cross-validation ===
=== Summary ===

Correctly Classified Instances          48               80      %
Incorrectly Classified Instances        12               20      %
Kappa statistic                          0.7333
Mean absolute error                      0.1045
Root mean squared error                  0.314
Relative absolute error                 27.7486 %
Root relative squared error             72.2247 %
Total Number of Instances               60

=== Detailed Accuracy By Class ===

               TP Rate   FP Rate   Precision   Recall  F-Measure   ROC Area  Class
                 0.6       0.089      0.692     0.6       0.643      0.811    VF
                 0.733     0.156      0.611     0.733     0.667      0.857    VT
                 0.933     0          1         0.933     0.966      0.959    NSR
                 0.933     0.022      0.933     0.933     0.933      0.945    AF
Weighted Avg.    0.8       0.067      0.809     0.8       0.802      0.893

=== Confusion Matrix ===

  a  b  c  d   <-- classified as
  9  5  0  1 |  a = VF
  4 11  0  0 |  b = VT
  0  1 14  0 |  c = NSR
  0  1  0 14 |  d = AF
```

Fig 5.25 Simulation results of NSR,VT,VF and AF using RBF Classifier

The Fig 5.25 shows the simulation results for classification of NSR, VT, AF and VF using RBF classifier. Time taken to build the model is 0.02 seconds. Correctly classified instances are 48 out of 60 instances. RMSE value is 0.314. The classification accuracy for classifying NSR, VT, AF and VF is obtained as 80%.

```
Time taken to build model: 0.03 seconds

=== Stratified cross-validation ===
=== Summary ===

Correctly Classified Instances          55               73.3333 %
Incorrectly Classified Instances        20               26.6667 %
Kappa statistic                          0.6667
Mean absolute error                      0.1047
Root mean squared error                  0.3151
Relative absolute error                 32.6213 %
Root relative squared error             78.5458 %
Total Number of Instances               75

=== Detailed Accuracy By Class ===

               TP Rate   FP Rate   Precision   Recall  F-Measure   ROC Area  Class
                 0.533     0.1        0.571     0.533     0.552      0.831    VF
                 0.6       0.133      0.529     0.6       0.563      0.881    VT
                 0.733     0.017      0.917     0.733     0.815      0.913    NSR
                 0.8       0.033      0.857     0.8       0.828      0.867    AF
                 1         0.05       0.833     1         0.909      0.991    SVT
Weighted Avg.    0.733     0.067      0.742     0.733     0.733      0.897

=== Confusion Matrix ===

  a  b  c  d  e   <-- classified as
  8  6  1  0  0 |  a = VF
  6  9  0  0  0 |  b = VT
  0  0 11  2  2 |  c = NSR
  0  2  0 12  1 |  d = AF
  0  0  0  0 15 |  e = SVT
```

Fig 5.26 Simulation results of NSR,SVT,VT,VF and AF using RBF Classifier

The Fig 5.26 shows the simulation results for classification of NSR, SVT, VT, AF and VF using RBF classifier. Time taken to build the model is 0.03 seconds. Correctly classified instances are 55 out of 75 instances. RMSE value is 0.3151. The classification accuracy for classifying NSR, SVT, VT, AF and VF is obtained as 73.33%

```
Time taken to build model: 0.8 seconds

=== Stratified cross-validation ===
=== Summary ===

Correctly Classified Instances          78               74.2857 %
Incorrectly Classified Instances        27               25.7143 %
Kappa statistic                          0.7
Mean absolute error                      0.071
Root mean squared error                  0.2621
Relative absolute error                 28.9273 %
Root relative squared error             74.7656 %
Total Number of Instances              105

=== Detailed Accuracy By Class ===

               TP Rate   FP Rate   Precision   Recall  F-Measure   ROC Area  Class
                 0.533     0.078       0.533     0.533       0.533     0.816    VF
                 0.533     0.089       0.5       0.533       0.516     0.815    VT
                 0.867     0         1         0.867       0.929     0.949    NSR
                 0.867     0.044       0.765     0.867       0.813     0.884    AF
                 1         0.022       0.882     1           0.938     0.987    SVT
                 0.533     0.067       0.571     0.533       0.552     0.886    SCA
                 0.867     0         1         0.867       0.929     0.988    CI
Weighted Avg.    0.743     0.043       0.75      0.743       0.744     0.903

=== Confusion Matrix ===

  a  b  c  d  e  f  g   <-- classified as
  8  4  0  0  0  3  0 |  a = VF
  4  8  0  1  0  2  0 |  b = VT
  0  0 13  1  1  0  0 |  c = NSR
  0  1  0 13  1  0  0 |  d = AF
  0  0  0  0 15  0  0 |  e = SVT
  3  3  0  1  0  8  0 |  f = SCA
  0  0  0  1  0  1 13 |  g = CI
```

Fig 5.27 Simulation results of 7 types using RBF Classifier

The Fig 5.27 shows the simulation results for classification of 7 types using RBF classifier. Time taken to build the model is 0.8 seconds. Correctly classified instances are 78 out of 105 instances. RMSE value is 0.2621. The classification accuracy for classifying 7 types of ECG signals is obtained as 74.28% The medical statistics obtained using the confusion matrix of RBF for 7 types of signals are sensitivity as 74.28%, specificity as 95.71% and precision as 75.55% are shown in Table 5.8.

Table 5.8 Medical Statistics of RBF using confusion matrix for 7 types of signals

ECG	TP	FP	FN	TN	Sensitivity(S)	Specificity(S)	Precision(Pp)
VF	08	7	7	83	53.33%	92.22%	53.33%
VT	08	8	7	82	53.33%	91.11%	53.33%
NSR	13	0	2	90	86.66%	100%	100%
AF	13	4	2	86	86.66%	95.55%	76.47%
SVT	15	2	0	88	100%	97.77%	88.23%
SCA	08	6	7	84	53.33%	93.33%	57.14%
CI	13	0	2	90	86.66%	100%	100%
				Average	**74.28%**	**95.71%**	**75.55%**

5.5.3 RF classifier results

```
Time taken to build model: 0.01 seconds

=== Stratified cross-validation ===
=== Summary ===

Correctly Classified Instances          54               90       %
Incorrectly Classified Instances         6               10       %
Kappa statistic                          0.8667
Mean absolute error                      0.1267
Root mean squared error                  0.2306
Relative absolute error                 33.6489 %
Root relative squared error             53.0366 %
Total Number of Instances               60

=== Detailed Accuracy By Class ===

               TP Rate   FP Rate   Precision   Recall  F-Measure   ROC Area  Class
                 1         0.111      0.75       1         0.857      0.961    VF
                 0.8       0          1          0.8       0.889      0.958    VT
                 0.867     0          1          0.867     0.929      0.959    NSR
                 0.933     0.022      0.933      0.933     0.933      0.993    AF
Weighted Avg.    0.9       0.033      0.921      0.9       0.902      0.968

=== Confusion Matrix ===

  a  b  c  d   <-- classified as
 15  0  0  0 |  a = VF
  3 12  0  0 |  b = VT
  1  0 13  1 |  c = NSR
  1  0  0 14 |  d = AF
```

Fig 5.28 Simulation results of NSR,VT,VF and AF using RF Classifier

The Fig 5.28 shows the simulation results for classification of NSR, VT, AF and VF using RF classifier. Time taken to build the model is 0.01 seconds. Correctly classified instances are 54 out of 60 instances. RMSE value is 0.2306.The classification accuracy for classifying NSR, VT, AF and VF is obtained as 90%

```
Time taken to build model: 0.02 seconds

=== Stratified cross-validation ===
=== Summary ===

Correctly Classified Instances          64               85.3333 %
Incorrectly Classified Instances        11               14.6667 %
Kappa statistic                          0.8167
Mean absolute error                      0.1152
Root mean squared error                  0.217
Relative absolute error                 35.901  %
Root relative squared error             54.0958 %
Total Number of Instances               75

=== Detailed Accuracy By Class ===

               TP Rate   FP Rate   Precision   Recall  F-Measure   ROC Area  Class
                 0.8       0.05       0.8        0.8       0.8        0.972    VF
                 0.8       0.033      0.857      0.8       0.828      0.941    VT
                 0.867     0.017      0.929      0.867     0.897      0.986    NSR
                 0.867     0.033      0.867      0.867     0.867      0.988    AF
                 0.933     0.05       0.824      0.933     0.875      0.991    SVT
Weighted Avg.    0.853     0.037      0.855      0.853     0.853      0.975

=== Confusion Matrix ===

  a  b  c  d  e   <-- classified as
 12  2  0  1  0 |  a = VF
  2 12  0  0  1 |  b = VT
  1  0 13  0  1 |  c = NSR
  0  0  1 13  1 |  d = AF
  0  0  0  1 14 |  e = SVT
```

Fig 5.29 Simulation results of NSR, SVT, VT, VF and AF using RF Classifier

The Fig 5.29 shows the simulation results for classification of NSR, SVT, VT, AF and VF using RF classifier. Time taken to build the model is 0.02 seconds. Correctly classified instances are 64 out of 75 instances. RMSE value is 0.217. The classification accuracy for classifying NSR, SVT, VT, AF and VF is obtained as 85.33%.

```
Time taken to build model: 0.02 seconds

=== Stratified cross-validation ===
=== Summary ===

Correctly Classified Instances          78               74.2857 %
Incorrectly Classified Instances        27               25.7143 %
Kappa statistic                          0.7
Mean absolute error                      0.1001
Root mean squared error                  0.213
Relative absolute error                 40.8123 %
Root relative squared error             60.7444 %
Total Number of Instances              105

=== Detailed Accuracy By Class ===

               TP Rate   FP Rate   Precision   Recall  F-Measure   ROC Area  Class
                 0.733     0.144       0.458    0.733      0.564      0.954    VF
                 0.467     0.033       0.7      0.467      0.56       0.902    VT
                 0.933     0          1         0.933      0.966      0.994    NSR
                 0.733     0.044       0.733    0.733      0.733      0.982    AF
                 0.933     0.022       0.875    0.933      0.903      0.993    SVT
                 0.533     0.044       0.667    0.533      0.593      0.951    SCA
                 0.867     0.011       0.929    0.867      0.897      0.961    CI
Weighted Avg.    0.743     0.043       0.766    0.743      0.745      0.962

=== Confusion Matrix ===

  a  b  c  d  e  f  g   <-- classified as
 11  1  0  1  1  1  0 |  a = VF
  5  7  0  0  1  2  0 |  b = VT
  0  0 14  1  0  0  0 |  c = NSR
  4  0  0 11  0  0  0 |  d = AF
  1  0  0  0 14  0  0 |  e = SVT
  3  2  0  1  0  8  1 |  f = SCA
  0  0  0  1  0  1 13 |  g = CI
```

Fig 5.30 Simulation results of 7 types using Random Forest Classifier

The Fig 5.30 shows the simulation results for classification of 7 types using RF classifier. It's built by using random forest of 10 trees, each constructed while considering 4 random features. Out of bag error is 0.381. Time taken to build the model is 0.02 Seconds. Correctly classified instances are 78 out of 105 instances. RMSE value is 0.213. The classification accuracy for classifying 7 types is obtained as 74.28%. The medical statistics obtained using the confusion matrix for 7 types of signals are sensitivity as 74.3%, specificity as 95.71% and precision as 75.02% are shown in Table 5.9.

Table 5.9 Medical Statistics of RF using confusion matrix for 7 types of signals

ECG	TP	FP	FN	TN	Sensitivity(S)	Specificity(S)	Precision(Pp)
VF	08	7	7	83	73.33%	85.55%	53.33%
VT	08	8	7	82	46.7%	96.66%	50%
NSR	13	0	2	90	93.33%	100%	100%
AF	13	4	2	86	73.33%	95.55%	76.4%
SVT	15	2	0	88	93.33%	97.77%	88.23%
SCA	08	6	7	84	53.33%	95.55%	57.14%
CI	13	0	2	90	86.7%	98.88%	100%
				Average	**74.3%**	**95.71**%	**75.02**%

5.6 Performance comparison of arrhythmias classification

The performance of cardiac signals classification in terms of number of ECG records, the number of features, type of neural network classifier, classification accuracy and number of cardiac signals reported in the literature have been compared with the proposed classification system is shown in Table 5.10.

L. Khadra et al. [21] used higher order spectral analysis on 43-records of different cardiac signals (AF-12, VT-11, VF-12 and NSR-08 records). HOSA features are extracted using bispectral contour analysis and classified these four types of cardiac signals and obtained sensitivity as 89.2% and specificity as 93.55%.

Sharmila et al. [25] analysed two types of cardiac signals (NSR and SCA) using higher order spectral features. This work did not use classifiers to represent classification accuracy.

Compared to the existing work of I. A. Karaye et al. [26] and Sharmila et al. [25] the proposed research work has given more clarity in identifying important cardiac arrhythmias, cardiac disorders and normal signals using bispectral, spectral and temporal features(hybrid features) and using RF , MLP and RBF neural network classifiers.

Table 5.10 Summary of performance comparison of cardiac arrhythmias classification

Study by	Number of records and Features	Classifier	Diseases	Accuracy
Ibrahim Abdullahi Karaye et al. [26]	Higher order spectral features and Temporal features	MLP	NSR and 4 diseases (5 types)	Sensitivity-88.4% Accuracy-94.9%. Specificity-96.2%
L. Khadra et al. [21]	43-records (AF-12, VT-11, VF-12 and NSR-08) HOSA features	Bispectral contour analysis	NSR ,VT, VF and AF (4 types)	Sensitivity-89.2% Specificity-93.55%
Proposed [HOSA]	Spectral, Bispectral and Temporal features	RF	NSR ,VT, VF and AF (4 types)	Sensitivity-90 % Accuracy-90% Specificity-96.62%
	Spectral, Bispectral and Temporal features	RF	NSR,SVT,VT, VF and AF (5 types)	Sensitivity-85.33% Accuracy-85.33% Specificity-96.33%
	Spectral ,Bispectral and Temporal features 105-Records (AF-15, VT-15, VF-15, SVT-15, SCA-15, CI-15 and NSR-15)	RF	NSR,SVT,VT, VF, AF, CI and SCA	Sensitivity-74.28% Accuracy-74.2% Specificity-95.70% Precision-75.02%
		RBF	NSR,SVT,VT, VF, AF, CI and SCA	Sensitivity-74.28% Accuracy-74.2% Specificity-95.71% Precision-75.55%
		MLP	NSR,SVT,VT, VF, AF, CI and SCA	Sensitivity -74.2% Accuracy-74.2% Specificity-95.71% Precision-75.25%

5.7 Conclusion

HOSA presents bispectrum, bicoherence, quadratic phase coupling plots for visual interpretation to classify normal, cardiac arrhythmias and cardiac disorders. HOS based features (such as skewness, variance, kurtosis and bicoherence) along with spectral features and temporal features (hybrid) are fed to three classifiers. Random forest (RF) classifier has produced better results compared to MLP and RBF classifiers. The proposed work classified NSR, VT, VF and AF (4 types) using RF classifier and obtained classification accuracy as 90%, sensitivity as 90% and specificity as 96.62%. It is a novel approach to enhance classification accuracy, sensitivity and specificity with the existing work.

Later, the same work has been extended to classify 5 types of cardiac signals (NSR, SVT, VT, VF and AF) and obtained an accuracy as 85.33%, sensitivity as 85.33% and specificity as 96.33%. Later, work has been extended to classify 7 types of cardiac signals (1- normal, 4- arrhythmias and 2- cardiac disorders) using RF, MLP and RBF classifiers. RF and ANN learning techniques are different even though got same results as shown in Table 5.10. Finally, obtained an average classification accuracy as 74.2%, sensitivity as 74.2%, precision as 75% and specificity as 95.70%. It has been observed that specificity is higher than sensitivity.

In real time applications, the specificity is more important than the sensitivity, as no normal person should be defibrillated except sudden cardiac arrest. Otherwise it might cause cardiac arrest to normal healthy person due to error analysis.

It is observed that spectral estimation depends on the signal energies in the bi-frequency plane. This causes serious problem in the estimation. The variance of the estimate is high at high frequencies. This unsatisfactory property should be resolved by making variance independent against the frequency variation. When number of cardiac disorders increased, classification accuracy and sensitivity are decreased. So, multi resolution analysis (using discrete wavelet transform) is preferred to enhance classification accuracy in the next chapter.

Chapter 6

Cardiac Arrhythmias Classification in Wavelet domain

6.1 Introduction

In the previous chapters; time domain, spectral analysis and higher order spectral analysis of ECG have been proposed to analyse and classify cardiac arrhythmias and disorders. As ECG is a quasi-periodic, nonlinear and non-stationary signal, multiresolution analysis is required to enhance the classification accuracy of different cardiac signals. Further in the literature review, it has been reported that finding an efficient feature scheme and suitable neural network classifiers are important to enhance the classification accuracy of different cardiac arrhythmias [17],[44-45],[47], [50,51], [67]-[72], [9], [82], [83], [72] and [110]. So, it is proposed to use wavelet transform decomposition technique to extract wavelet features**.**

In this chapter, wavelet based feature extraction scheme and classification of cardiac arrhythmias & disorders have been described. With reference to medical statistics such as classification accuracy, sensitivity and specificity. Further, performance comparison with the existing works has been given.

6.2 Overview of existing works

In this section, the work done by some researchers has been presented briefly.

Nguyen et al. [17] used a novel shock advice algorithm (SAA) to classify Normal, Shockable rhythms (SH) and Non shockable rhythms (NSH) of ECG signal. In this work, ventricular fibrillation (VF) and ventricular tachycardia (VT) were considered as shockable (SH) rhythms which lead to sudden cardiac arrests (SCA). In SAA algorithm, convolutional neural network (CNN) was used for feature extraction and a Boosting (BS) was used for classification. 5-fold cross validation was used in CNN. The medical statistics obtained as classification accuracy of 99.26%, sensitivity of 97.07%, and specificity of 99.44%. This work obtained different values of sensitivity and accuracy as unequal number of data records are used to classify three types of cardiac signals.

H.M Rai et al. [44] employed wavelet (db4) based feature extraction scheme and back propagation neural network algorithm to classify normal and abnormal signals. In this work 25 NSR records and 20 abnormal records of 1minute duration are considered, 48 wavelet based features, 16 statistical and morphological features, total 64 hybrid features were extracted and fed to the neural network classifier and obtained classification accuracy as 97.8%

Maedeh Kiani Sarkaleh et al. [45] used 8-level wavelet decomposition technique on 10 ECG records and extracted 24 wavelet features. Three types of cardiac signals (normal and two types of arrhythmias) classified using MLP neural network classifier and obtained classification accuracy of 96.5%. It produced results with 24 input neurons and 2 linear output neurons. These two output neurons indicate that they have classified only two types of cardiac signals.

Sukanta & Mohanty et al. [47] classified three types of signals NSR, VT and VF (total 57 records).Time -frequency based hybrid features (13 features) are extracted and fed to the SVM classifier and C4.5 classifier . Obtained average classification accuracy - 92.23%, sensitivity - 79.43 % and specificity -81.44% with SVM classifier. Obtained average classification accuracy - 97.02%, sensitivity -90.97% and specificity -97.86% with C4.5 classifier. In this work, classified only3-types of cardiac signals. This work obtained different values of sensitivity and accuracy as it is used unequal number of data records.

E. D. Ubeyli et al. [50] classified five types of cardiac signals (NSR, CHF, VT, AF, Partial epilepsy). In this work, they extracted wavelet based features, statistical parameters and ROC curves and fed to Mixture of Expert (ME) network classifier and enhanced the classification accuracy to 96.89%.

Ali Sadr et al. [51] compared the performance of MLP and RBF neural network classifiers. In this work RBF algorithm produced more accuracy when training data size was relatively small, MLP algorithm produced more accuracy when the size of training data was relatively large. From this work, it is identified that selection of data set and selection of a suitable classifier play a crucial role in improving classification accuracy.

Sumathi et al.[110] used hybrid approach of Adaptive Neuro-Fuzzy Inference System (ANFIS) model for classification of 6 types of arrhythmias including normal signals(Normal Sinus Rhythm (NSR), Atrial Fibrillation (AF), Pre-Ventricular Contraction (PVC), Ventricular Fibrillation (VF), and Ventricular Flutter (VFLU) Myocardial Ischemia(MI)). Feature

extraction is done by using Symlet wavelet transform. The classification accuracy was obtained as 98.24 %

6.3 Methodology for wavelet analysis

Several signal processing algorithms have been proposed to classify ECG arrhythmias and disorders. Existing feature extraction methods may not be sufficient to detect the possibility of more number of cardiac arrhythmias and disorders with high accuracy as ECG is a quasi-periodic, nonlinear and non-stationary signal. Hence, in this work, it is proposed to use Daubechies wavelet transform (db4). Six-level wavelet decomposition technique is used to extract wavelet features and are fed to three different supervised classifiers to classify 7 types of cardiac signals (normal, 4 types of cardiac arrhythmias and 2 types of cardiac disorders). This automatic classification of cardiac arrhythmias and disorders will enable the doctors for early diagnosis of cardiac problem. The block diagram of automatic classification of cardiac signals using wavelet features is shown in Fig 6.1

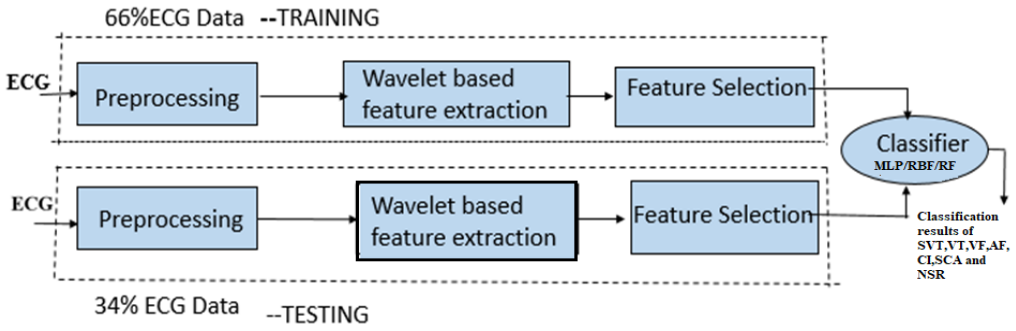

Fig 6.1 Automatic classification of cardiac signals using wavelet features

6.3.1 Pre-processing

Baseline wander or DC noise is usually occurs during the recording of the ECG signal. It is due to improper bias and chest movement while breathing. This DC noise frequency will be below 2Hz. This DC noise has been removed from ECG data in pre-processing stage through mean correction code. The statistical mean of the signal vector is computed and subtracted from each sample so that the distribution of the samples is along the axis.

6.3.2 Discrete Wavelet Transform

Fourier transform deals with transforming the time domain components to frequency domain

components and the wavelet transform deals with scale analysis, that is, by creating mathematical structures that provide varying time/frequency/amplitude slices for analysis. This transform is a portion of a complete waveform, hence the term wavelet. Wavelet is a fast decaying oscillating waveform, with average value is zero. Generally, the continuous wavelet transform can be expressed by the following equation (6.3),

$$\boldsymbol{CWT_x^{\psi}(T,S) = \psi_x^{\psi}(T,S) = \frac{1}{\sqrt{|s|}} \int x(t)\, \psi^{*}\left(\frac{t-T}{s}\right) dt} \qquad (6.1)$$

Where x (t) represents signal, ψ is the basis function, s is scaling factor, t is time and * is symbol for complex conjugate.

The wavelet transform has the ability to identify frequency (or scale) components, simultaneously with their location(s) in time. Additionally, computations are directly proportional to the length of the input signal. They require only N multiplications (times a small constant) to convert the waveform.

In wavelet analysis, the scale that one uses in looking at data plays a special role. Wavelet algorithms process data at different scales or resolutions. If we look at a signal with a large "window," we would notice gross features. Similarly, if we look at a signal with a small "window," we would notice small discontinuities as shown in Figure. The result in wavelet analysis is to "see the forest and the trees." A way to achieve this is to have short high-frequency fine scale functions and long low-frequency ones. This approach is known as multi-resolution analysis.

Wavelets are a family of basis functions Symlet, Coiflet, Daubechies, Biorthogonal and Reverse biorthogonal wavelets are different types of the wavelet families are shown in Fig 6.2.

One of the key advantages of wavelets is their ability to spatially adapt to features of a function such as discontinuities and varying frequency behaviour. They vary in various properties of wavelets like compactness, smoothness, fast implementation and orthonormality.

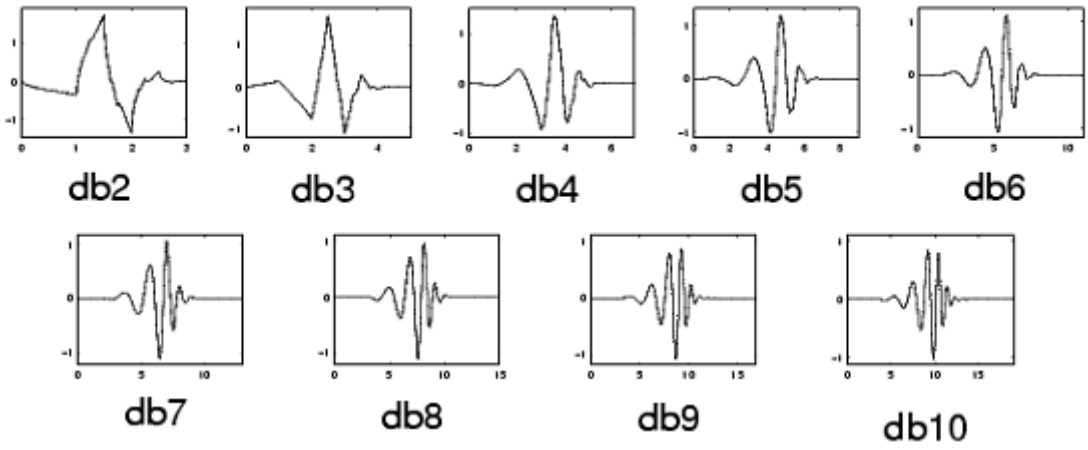

Fig 6.2 Types of Daubechies wavelets [100]

The compactness means the localization of wavelets i.e. a region of the data can be processed without affecting the data outside this region. Discrete Wavelet Transforms (DWT) are widely used for feature extraction which transforms a discrete time signal to a discrete wavelet representation. The DWT is also used for de-noising the signals. Daubechies wavelets are the most popular wavelets[85] and db4 wavelet has been chosen as the mother wavelets as it resembles the shape of ECG waveform.

The DWT utilizes two set of functions Φ (t) and Ψ (t), each associated with the low pass and the high pass filters respectively. These functions have a property that they can be obtained as the weighted sum of the scaled (dilated) and shifted version of the scaling function itself.

DWT is given by the following equations (5.2) and (5.3)

$$\varphi(t) = \sum_{n=1}^{\infty} h[n]\varphi(2t - n) \tag{6.2}$$

$$\Psi(t) = \sum_{n=1}^{\infty} g[n]\varphi(2\mathrm{t} - \mathrm{n}) \tag{6.3}$$

Here, h[n] and g[n] is the half band low pass filter and high pass filter respectively.

6.3.3 Wavelet based Feature Extraction using Wavelet Decomposition

Wavelet analysis consists of decomposing a signal into a hierarchical set of low frequency (approximation) and high frequency (detailed) coefficients. Wavelets are the essentially filter banks. Each filter splits a given signal into two non-overlapping independent high frequency and low frequency sub-bands such that it can then be reconstructed by the means of an inverse transform. When such filters are applied continually, you get a tree of filters with output of one fed into the next.

The wavelet representation of a discrete signal, X consisting of N samples can be computed by convolving the discrete signal, X with the Low-Pass Filters (LPF) and High-Pass Filters (HPF) and down-sampling the output signal by 2, so that the two frequency bands each contains N/2 samples. This technique is based on the use of wavelets as the basis functions for representing other functions. These basis functions have a finite support in time and frequency domain. Multi-resolution analysis is achieved by using the mother wavelet and a family of wavelets generated by translations and dilations of it. The convolutional algorithms apply filtering by multiplying the filter coefficients with the input samples and accumulating the results. These algorithms are implemented by using finite impulse response filter banks. The lifting scheme has been proposed for the efficient implementation of the wavelet transform. This approach has three phases namely: split, predict, and update. In 1D-DWT, at each decomposition level, the HPF associated with scaling function produces detail coefficients(DC) while the LPF associated with scaling function produces approximation coefficients(AC) of the signal. The approximation part can be iteratively decomposed. Wavelet transform decomposes a signal into a set of basis functions using 6 level decomposition technique as shown in Fig 6.3 to extract wavelet features.

- High frequency detailed coefficients (minimum and maximum) and standard deviation in 1-5 levels.
- Low frequency approximation coefficients (minimum and maximum) and standard deviation in the 6th level.
- Energy retained for each record,

Total 19 wavelet features are provided as inputs to RF, MLP and RBF and classifiers.

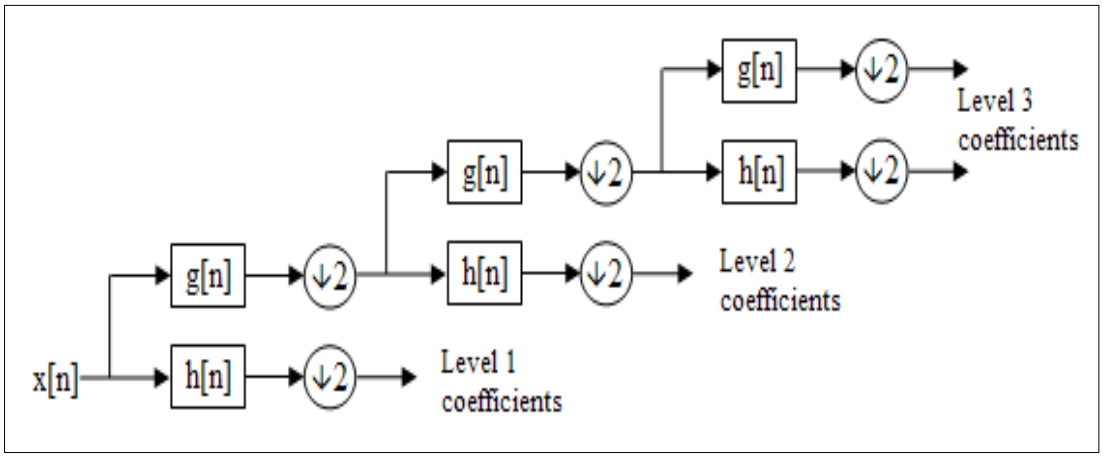

Fig 6.3 Wavelet decomposition [88]

The statistical features extracted using wavelet transform techniques are given below

- **Maximum value of coefficient:** It is the extreme of largest value of all the given samples.
- **Minimum value of coefficient:** It is the extreme of smallest value of all the given samples.
- **Energy ($\boldsymbol{\varepsilon_x}$):** The energy of the signal is sum of squared moduli of samples and is given by the equation 6.4,

$$\boldsymbol{\varepsilon_x \triangleq \sum_{n=0}^{N-1} |x_n|^2} \quad (6.4)$$

- **Standard deviation**($\boldsymbol{\sigma}$)**:** It is a measure of dispersion of set of samples from its mean. It can be calculated by the equation 6.5,

$$\boldsymbol{\sigma = \sqrt{\frac{1}{N-1}\sum_{i=0}^{N-1}(x_i - \mu)^2}} \quad (6.5)$$

6.4 Classification of Arrhythmias using Artificial Intelligence Algorithms

In the proposed work, db4 6-level wavelet decomposition technique is used to extract wavelet features so 19 extracted wavelet features are provided as inputs to neural network classifiers. Simulation Results of wavelet analysis are shown in Fig 6.4, Fig 6.5 and Fig 6.6.

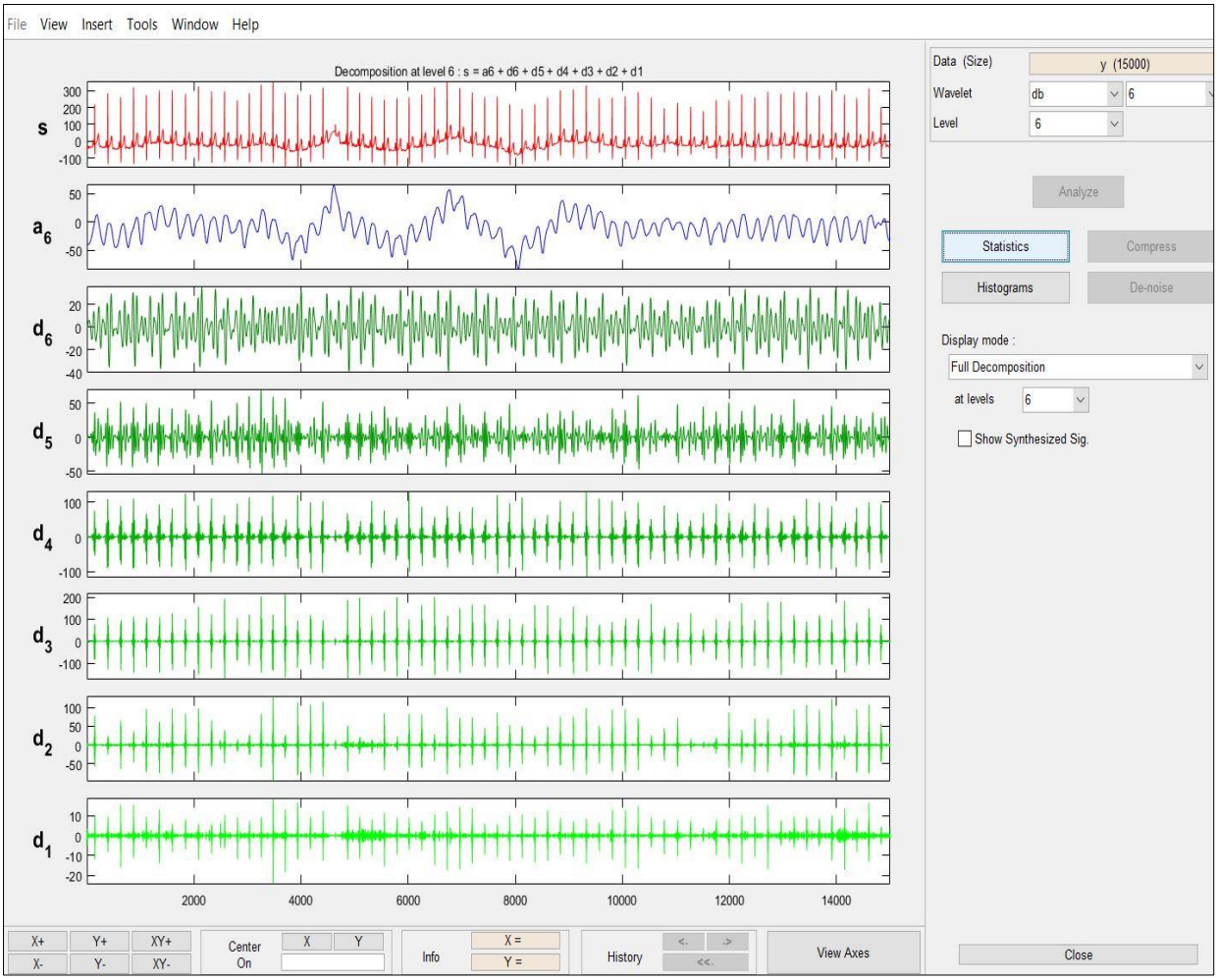

Fig 6.4 Six level wavelet decomposition of NSR Signal (165272)

As shown in Fig 6.4, six level wavelet decomposition on NSR signal is provided detailed and approximation information of the signal. Detailed and approximation statistics of normal signal are shown in Fig 6.5. Retained energy of NSR Signal is shown in Fig 6.6. Extracted wavelet features of 7 types of cardiac signals are shown in Table 6.1 to Table 6.4.

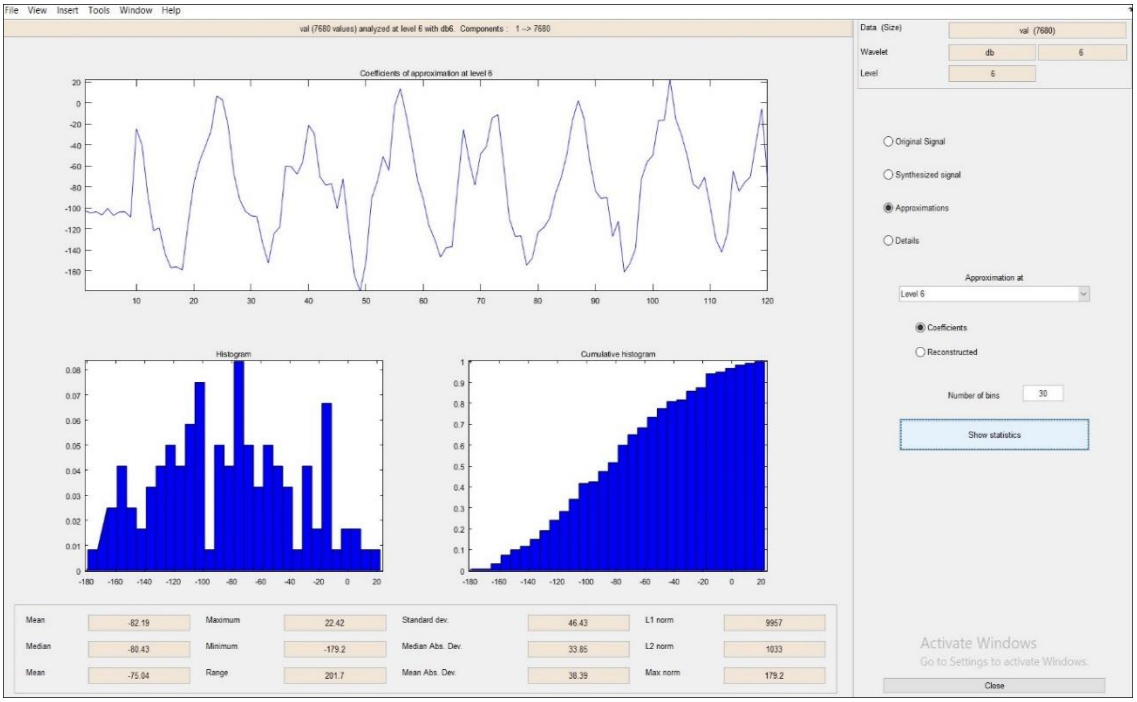

Fig 6.5 Detailed and approximation statistics of NSR signal

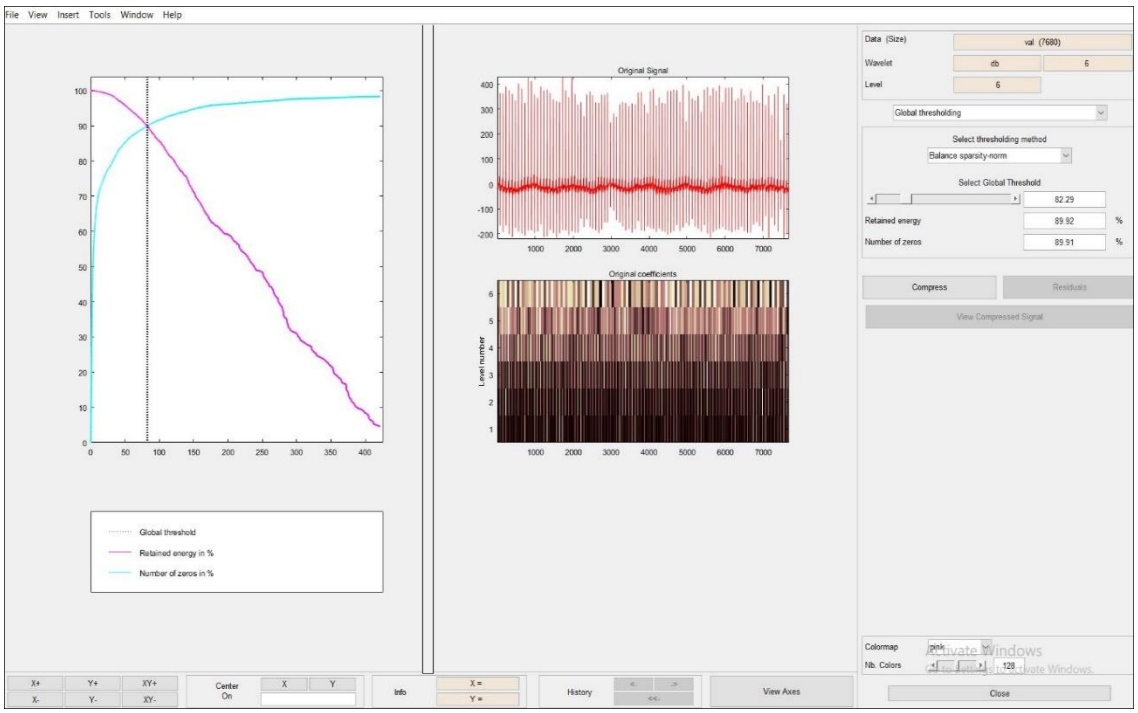

Fig 6.6 Retained energy of NSR Signal

Table 6.1 Wavelet based features - CI, VT

max1	min1	sd1	max2	min2	sd2	max3	nin3	sd3	max4	min4	sd4	max5	min5	sd5	max6	min6	sd6	energy	signal?
720	-426.6	106.6	1024	-347.9	149.5	976.8	-304.4	198.7	994.7	-391.7	236.6	854.5	-338	233.1	507.9	-453.1	213.9	94.56	CI
193.6	-307.3	43.78	285.6	-369.6	60.47	288.4	-360.8	71.78	207.7	-292.5	69.73	194.9	-225.2	75.67	131.3	-139.2	63.54	94.34	CI
486.3	-117.8	72.07	654.7	-203.4	100.8	659.3	-324.5	126.2	483.3	-332	132.2	284.7	-286.9	114.3	323.4	-206.6	112.6	94.28	CI
558.9	-130.9	85.33	795.9	-788.8	120.4	914.4	-327.7	162.1	783.8	-358.8	193.6	753.5	-473.6	221.9	450.9	-467.9	186.1	95.43	CI
251.2	-231.2	70.53	339.1	-305.3	98.42	284.4	-403.4	127.4	339	-395	147.4	335.9	-419	169.2	401.6	-371	192.9	92.04	CI
459.6	-106.3	77.86	636.4	-154.5	109	653.1	-266.7	137.4	498.7	-276	140.2	284.5	-200.1	99.28	288.5	-281.5	124.2	93.48	CI
609.4	-169.7	88.38	794.9	-223.2	122.8	795.5	-390.1	153.2	578.3	-379.3	160.6	337.3	-328.5	143.4	360.1	-358	158.2	93.43	CI
588.8	-490.3	82.26	864	-596.6	114.2	785.9	-715.8	134.4	915.1	-753.7	141.8	973.8	-694.2	143.7	652.1	-703.5	151.6	94.05	CI
814.3	-225.9	151.4	1165	-318.7	212.5	1260	-444.6	277	1119	-597.5	310	957.4	-746.5	319.4	578	-650.4	303.5	93.7	CI
529.2	-235.3	72.3	709.6	-325.5	101.3	790.5	-443.2	132.4	662.6	-583.3	156.3	602.7	-776.3	170.9	390	-408.5	158.1	94.49	CI
709	-561.9	129.5	926.8	-779.2	181.2	1196	-958.4	235.5	1391	-1180	280.8	1835	-1534	361.9	466.1	-681.1	189.1	94.31	CI
439.6	-131.8	70.18	623.4	-181.3	98.59	663.6	-259	130.3	536.4	-361.7	156.5	410.9	-494.4	188.1	288.2	-270.6	150.9	94.78	CI
604.4	-306	77	759	-354.8	105.7	708.9	-360.6	121.3	463.2	-400.4	124.3	460.1	-509.3	128.5	328.4	-316.7	131.7	93.81	CI
732.3	-134.3	103.4	958	-179.7	144.3	848	-358.9	177.8	664.5	-382.9	191.5	445.6	-360.5	176.1	395.3	-353.2	174.7	93.55	CI
125.5	-183.3	30.48	176	-258.9	43	239.7	-290.7	59.68	316.6	-344.5	79.65	399.2	-403.3	105.3	168.7	-167.1	62.01	95.72	CI
4.356	-5.096	1.456	20.4	-19.55	5.299	59.33	-79.05	11.52	1110	-1078	23.15	48	-85.84	18.47	55.85	-43.82	19.72	99.99	VT
7.778	-6.364	2.397	11.5	-13	4.042	12.02	-17.32	3.595	24.5	-22.5	6.423	57.28	-59.93	14.85	61.38	-36.75	26.61	100	VT
5.797	-7.656	1.803	34.66	-37.19	8.776	77	-103.1	24.44	175.8	-181	53.08	287.6	-357.6	123	342.1	-275.2	123.5	99.91	VT
3.417	-3.41	1.05	7.997	-13.06	2.198	61.86	-46.99	10.38	82.56	-94.02	17.9	50.26	-66.83	18.88	43.84	-49.15	26.03	99.99	VT
9.321	-8.114	1.601	55.62	-31.95	6.235	125.4	-94.9	17.38	161	-237.3	45.43	461.1	-453.7	126.7	632.1	-537.6	213.2	99.88	VT
7.808	-6.364	2.397	11.5	-13	4.042	12.02	-17.32	3.595	24.5	-22.5	6.423	57.28	-59.93	14.85	61.38	-36.75	26.61	100	VT
5.797	-7.656	1.803	34.66	-37.19	8.776	77	-103.1	24.44	175.8	-181	53.08	287.6	-357.6	123	342.1	-275.2	123.5	99.91	VT
4.108	-5.538	1.353	12.62	-12.46	3.464	38.29	-49.15	8.293	82.17	-116.4	22.86	232.8	-251.8	58.26	244.4	-291.1	77.29	99.98	VT
6.868	-5.316	1.398	42.53	-45.43	8.59	173.6	-228.1	45.8	504.6	-636.3	164.7	659.2	-978.3	318.1	738.3	994.8	438.2	99.23	VT
4.667	-4.401	1.355	39.68	-31.28	5.865	129.3	-136.2	25.93	159.5	-126.7	34.38	122.5	-98.19	39.72	92.31	-88.21	50.18	99.98	VT
4.447	-4.434	1.213	34.84	-29.93	5.7	198.8	-193.7	40.68	529.8	-664.6	148	649.1	-850.6	253	592.3	-905.9	365.5	99.6	VT
3.417	-3.41	1.05	7.997	-13.06	2.198	61.86	-46.99	10.38	82.56	-94.02	17.9	50.26	-66.83	18.88	43.84	-49.15	26.03	99.99	VT
4.108	-5.538	1.353	12.62	-12.46	3.464	38.29	-49.15	8.293	82.17	-116.4	22.86	232.8	-251.8	58.26	244.4	-291.1	77.29	99.98	VT
7.778	-6.364	2.397	11.5	-13	4.042	12.02	-17.32	3.595	24.5	-22.5	6.423	57.28	-59.93	14.85	61.38	-36.75	26.61	100	VT
4.565	-4.269	1.21	19.23	-28.18	3.77	113.7	-137	23.1	290.2	-356.6	83	380.9	-433.7	139.7	353.9	-416.7	177	99.87	VT

Table 6.2 Wavelet based features – AF, SCA

max1	min1	sd1	max2	min2	sd2	max3	nin3	sd3	max4	min4	sd4	max5	min5	sd5	max6	min6	sd6	energ	signal
27.14	-27.1	4.556	96.3	-199	21.27	422.7	-322	90.62	791.3	-1004	271.8	762.8	-1088	371.3	862.9	-844.7	461.4	93.85	AF
23.41	-35.6	4.142	134.6	-181.8	27.99	425.5	-542.9	105.2	579.8	-602.5	141.8	256.3	-322.1	137.4	392.6	-388	166.9	94.65	AF
13.35	-16	2.775	100.6	-117.1	16.89	256.1	-417.4	84.01	493.6	-656.6	191.7	833.6	-1087	327.6	879.3	-1577	751.7	94.73	AF
9.06	-10.8	2.111	47.7	-54.65	7.708	140.2	-192.6	35.46	173.5	-260.5	53.83	140.5	-173.2	46.05	83.77	-123.6	48.12	94.74	AF
11.43	-12.2	2.331	96.39	-63.55	12.99	283.1	-276.4	47.93	310	-334.4	86.59	317	-404.7	131.4	317.4	-366.3	157.3	94.53	AF
13.96	-37.9	3.05	83.43	-107.6	17.8	221.7	-243.6	49.66	317.2	-330	102.1	440.4	-360.3	173.4	279.4	-319.2	192	92.81	AF
7.592	-25.3	2.179	29.85	-28.84	5.251	64.9	-90.93	14.17	112.9	-95.97	23.93	81.97	-95.2	34.45	82.71	-61.33	39.12	96.03	AF
12.22	-33.6	2.274	44.36	-66.62	8.892	160.3	-151.8	29.11	240.7	-229.3	58.09	173.1	-186.2	65.15	50.9	-131.2	76.22	96.6	AF
45.57	-60.3	80235	164.4	-247.9	32.32	508.2	-554.6	93.54	573.3	-394	111.5	337.6	-238.1	112.2	342.3	-316.1	165	93.3	AF
15.12	-11.7	2.451	84.21	-67.76	11.99	244.1	-319.2	59.33	231.5	-430.6	83.49	167.4	-254.4	72.03	125.8	-127.1	58.5	94.53	AF
7.592	-25.3	2.179	29.85	-28.84	5.251	64.9	-90.93	14.17	112.9	-95.97	23.93	81.97	-95.2	34.45	82.71	-61.33	39.12	96.03	AF
9.06	-10.8	2.111	47.7	-54.65	7.708	140.2	-192.6	35.46	173.5	-260.5	53.83	140.5	-173.2	46.05	83.77	-123.6	48.12	94.74	AF
13.96	-37.9	3.05	83.43	-107.6	17.8	221.7	-243.6	49.66	317.2	-330	102.1	440.4	-360.3	173.4	279.4	-319.2	192	92.81	AF
27.14	-27.1	4.556	96.3	-199	21.27	422.7	-322	90.62	791.3	-1004	271.8	762.8	-1088	371.3	862.9	-844.7	461.4	93.85	AF
11.43	-12.2	2.331	96.39	-63.55	12.99	283.1	-276.4	47.93	310	-334.4	86.59	317	-404.7	131.4	317.4	-366.3	157.3	94.53	AF
6.236	-4.66	0.835	1.964	-1.109	0.335	2.672	-1.485	0.472	3.777	-2.035	0.657	5.456	-2.38	0.903	1.043	-1.158	0.419	83.92	SCA
11.58	-11.5	1.533	0.595	-0.592	0.123	0.596	-0.772	0.169	0.662	-0.85	0.226	0.824	-1.142	0.293	0.553	-0.535	0.134	85.47	SCA
2.94	-2.98	1.025	0.331	-0.557	0.124	0.448	-0.662	0.171	0.663	-0.733	0.22	0.731	-0.651	0.259	0.573	-0.56	0.262	74.48	SCA
5.332	-5.52	0.744	0.412	-0.502	0.124	0.558	-0.677	0.173	0.606	-0.786	0.217	0.69	-0.949	0.263	0.461	-0.421	0.161	79.08	SCA
11.24	-10.9	0.984	2.117	-2.577	0.688	2.985	-3.193	0.958	4.204	-3.927	1.322	5.777	-4.983	1.824	1.065	-1.184	0.523	86.53	SCA
17.27	-17.1	1.981	0.524	-1.174	0.321	0.729	-1.629	0.452	1.029	-2.001	0.609	1.345	-2.047	0.709	1.522	-2.222	0.808	89.28	SCA
15.72	-15.6	2.026	0.675	-0.941	0.190	0.891	-1.133	0.266	1.136	-1.659	0.356	1.418	-1.641	0.465	0.616	-0.758	0.275	82.09	SCA
5.715	-5.65	0.963	0.899	-1.05	0.211	1.258	-1.435	0.293	1.452	-1.471	0.398	1.367	-1.722	0.538	0.646	-0.899	0.202	77.45	SCA
7.694	-7.88	0.72	1.105	-0.89	0.357	1.538	-1.245	0.502	2.083	-1.712	0.682	2.164	-2.203	0.835	1.427	-0.942	0.477	81.55	SCA
4.941	-4.77	1.109	0.3	-0.315	0.085	0.399	-0.396	0.119	0.53	-0.538	0.161	0.629	-0.652	0.221	0.225	-0.259	0.107	80.45	SCA
13.59	-13.2	1.987	1.229	-0.759	0.307	1.663	-0.891	0.429	1.632	-1.16	0.566	1.616	-1.581	0.675	1.784	-1.369	0.809	83.59	SCA
10.72	-10.7	0.996	0.791	-0.617	0.172	1.086	-0.859	0.239	1.273	-1.207	0.31	1.584	-1.622	0.387	0.457	-0.482	0.25	86.73	SCA
32.24	-32.6	4.858	2.563	-2.848	1.22	3.595	-4.212	1.711	5.304	-6.112	2.366	7.85	-6.852	2.973	5.317	-6.157	2.649	87.49	SCA
1.372	-1.41	0.24	0.308	-0.231	0.078	0.402	-0.319	0.109	0.481	-0.443	0.147	0.611	-0.572	0.193	0.277	-0.38	0.146	79.14	SCA
6.599	-6.1	0.952	0.589	-1.449	0.315	0.736	-1.534	0.422	1.076	-1.513	0.498	1.387	-1.311	0.532	1.337	-1.85	0.617	82.97	SCA

Table 6.3 Wavelet based features – NSR, AF

max1	min1	sd1	max2	min2	sd2	max3	nin3	sd3	max4	min4	sd4	max5	min5	sd5	max6	min6	sd6	energy	signal?
9.54	-8.83	2.11	0.28	-0.3	0.08	0.44	-0.31	0.15	0.42	-0.44	0.18	0.2	-0.17	0.09	0.08	-0.09	0.04	90.1	NSR
14.5	-14.1	2.72	0.34	-0.41	0.09	0.48	-0.49	0.15	0.46	-0.47	0.16	0.29	-0.31	0.11	0.98	-1.42	0.31	91.5	NSR
11.4	-11.1	2.35	0.26	-0.26	0.06	0.22	-0.18	0.07	0.16	-0.17	0.06	0.04	-0.05	0.02	0.09	-0.08	0.04	90.4	NSR
22.9	-30.2	3.61	0.25	-0.24	0.06	0.2	-0.15	0.06	0.2	-0.15	0.07	0.14	-0.11	0.06	0.18	-0.18	0.08	90.5	NSR
12.9	-12.4	1.19	0.41	-0.37	0.05	0.38	-0.25	0.06	0.24	-0.16	0.06	0.16	-0.19	0.07	0.13	-0.12	0.05	87.7	NSR
23.6	-19.4	3.43	0.5	-0.67	0.09	0.87	-0.66	0.14	0.56	-0.4	0.14	0.32	-0.33	0.13	0.54	-0.42	0.21	90	NSR
7.81	-8.02	1.8	0.38	-0.39	0.07	0.74	-0.48	0.11	0.56	-0.4	0.13	0.41	-0.35	0.14	0.22	-0.18	0.1	90.5	NSR
45.4	-24.4	3.03	0.2	-0.22	0.04	0.21	-0.27	0.06	0.12	-0.14	0.05	0.22	-0.17	0.07	1.08	-0.39	0.21	90.9	NSR
3.97	-4.33	1.97	0.21	-0.3	0.04	0.28	-0.21	0.05	0.24	-0.15	0.05	0.15	-0.14	0.05	0.13	-0.13	0.06	91.5	NSR
9.64	-6.16	1.08	0.35	-0.54	0.07	0.54	-0.48	1.11	0.39	-0.32	0.1	0.26	-0.23	0.1	0.37	-0.13	0.08	91.3	NSR
6.36	-9.07	0.94	0.41	-0.52	0.02	0.1	-0.1	0.02	0.11	-0.1	0.01	0.03	-0.05	0.01	0.63	-0.53	0.21	90.8	NSR
9.27	-11	1.87	0.34	-0.26	0.06	0.52	-0.36	0.09	0.39	-0.3	0.1	0.16	-0.22	0.05	0.4	-0.49	0.15	89.6	NSR
8.41	-6.06	1.45	0.12	-0.11	0.02	0.12	-0.09	0.03	0.11	-0.12	0.04	0.11	-0.19	0.03	0.87	-2.21	0.38	90.2	NSR
12.1	-8.54	1.81	0.16	-0.19	0.03	0.2	-0.17	0.04	0.15	-0.17	0.05	0.12	-0.09	0.04	1.24	-0.79	0.36	94.8	NSR
20.6	-20.3	4.37	0.44	-0.36	0.06	0.36	-0.39	0.08	0.19	-0.23	0.08	0.25	-0.36	0.1	0.75	-0.99	0.42	93.1	NSR
19.3	-38	1.99	34.7	-14.6	4.82	71.5	52.6	13.1	152	-197	42.6	455	-395	158	1381	-972	484	96.1	VF
22.2	-7.08	1.96	16.3	-15.8	4.53	53.4	-42.9	12.2	138	-123	42.9	608	-636	182	1348	-1232	507	96.3	VF
6.89	-7.84	1.94	64.8	-59.2	7.43	266	-223	38.6	301	-400	79.8	285	-268	73.4	1540	-1409	683	97	VF
6.21	-10.8	1.92	38.3	-29.4	5.67	100	-127	18.8	142	-166	35.5	188	-164	64	345	-397	163	94.4	VF
7.17	-9.46	1.95	33.9	-34.5	6.37	93.3	-72.1	15	129	-171	25.3	237	-206	45.2	683	-664	304	96.1	VF
26.9	-7.48	1.97	32.1	-24.9	5.39	77.5	-99.9	15.4	188	-223	45.5	282	-221	72.3	5130	-3447	1672	99.1	VF
20.6	-6.99	1.93	29.6	-25.3	4.55	66.8	-87.3	15.3	150	-181	43.2	223	-233	79.6	706	-455	194	95.5	VF
39.5	-27.9	2.04	39.3	-44.2	3.87	104	-80.9	14.2	127	-274	36.8	191	-216	59.4	2377	-2498	1143	98.4	VF
5.48	-21	1.21	15	-10.5	2.93	52.9	-46.7	8.32	132	-77	23.6	159	-165	40.3	519	-301	132	94.9	VF
19.3	-38	1.99	34.7	-14.6	4.82	71.5	52.6	13.1	152	-197	42.6	455	-395	158	1381	-972	484	96.1	VF
22.2	-7.08	1.96	16.3	-15.8	4.53	53.4	-42.9	12.2	138	-123	42.9	608	-636	182	1348	-1232	507	96.3	VF
6.89	-7.84	1.94	64.8	-59.2	7.43	266	-223	38.6	301	-400	79.8	285	-268	73.4	1540	-1409	683	97	VF
6.21	-10.8	1.92	38.3	-29.4	5.67	100	-127	18.8	142	-166	35.5	188	-164	64	345	-397	163	94.4	VF
15.9	-16.3	3.14	57.9	-49	11.3	108	-119	24.5	237	-336	64.8	360	-325	100	589	-574	211	96.1	VF
7.17	-9.46	1.95	33.9	-34.5	6.37	93.3	-72.1	15	129	-171	25.3	237	-206	45.2	683	-664	304	96.1	VF

Table 6.4 Wavelet based feature - SVT

max1	min1	sd1	max2	min2	sd2	max3	nin3	sd3	max4	min4	sd4	max5	min5	sd5	max6	min6	sd6	energy	signal?
46.25	-51.5	6.924	179	-214	33.72	414.1	-386	85.91	383.1	-357	99.24	24.3	-225	105	101.8	-810	150	92.09	SVT
60.07	-93.2	15.03	238.7	-229	50.25	469.7	-546	112	398	-390	124	688.9	-614	131.8	632.7	-474	153.6	90.72	SVT
57.1	-58.2	8.532	183.5	-210	33.86	265.1	-190	53.53	450.6	-266	72.02	481.6	-396	93.19	136.2	-346	84.97	92.07	SVT
57.61	-65.2	10.74	208	-231	42.94	609.3	-495	127.5	733	-494	198.7	480.2	-355	206.4	1455	-991	456.3	92.1	SVT
70.61	-72.2	13.3	212.4	-231	55.28	517	-498	124.3	444.8	-409	143.7	194.9	-204	78.89	212.6	-245	99.44	90.36	SVT
44.16	-34.5	5.501	157.3	-192	28.08	299.9	-227	48.07	289.7	-207	74.76	254.2	-246	104.9	228.3	-416	138.4	92.68	SVT
46.25	-51.5	6.924	179	-214	33.72	414.1	-386	85.91	383.1	-357	99.24	24.3	-225	105	101.8	-810	150	92.09	SVT
60.07	-93.2	15.03	238.7	-229	50.25	469.7	-546	112	398	-390	124	688.9	-614	131.8	632.7	-474	153.6	90.72	SVT
57.1	-58.2	8.532	183.5	-210	33.86	265.1	-190	53.53	450.6	-266	72.02	481.6	-396	93.19	136.2	-346	84.97	92.07	SVT
57.61	-65.2	10.74	208	-231	42.94	609.3	-495	127.5	733	-494	198.7	480.2	-355	206.4	1455	-991	456.3	92.1	SVT
70.61	-72.2	13.3	212.4	-231	55.28	517	-498	124.3	444.8	-409	143.7	194.9	-204	78.89	212.6	-245	99.44	90.36	SVT
44.16	-34.5	5.501	157.3	-192	28.08	299.9	-227	48.07	289.7	-207	74.76	254.2	-246	104.9	228.3	-416	138.4	92.68	SVT
57.1	-58.2	8.532	183.5	-210	33.86	265.1	-190	53.53	450.6	-266	72.02	481.6	-396	93.19	136.2	-346	84.97	92.07	SVT
72.8	-72.7	11.56	216	-242	45.76	308.2	-262	65.56	180.3	-125	64.01	182.9	-191	96.99	-45.4	-506	101.3	91.33	SVT
43.3	-34.7	5.925	137.5	-163	34.66	270.5	-448	92.41	392.4	-451	143.2	488.8	-727	241.7	235.6	-1706	339.8	91.63	SVT

6.5 Results and Discussion

6.5.1 MLP classifier results

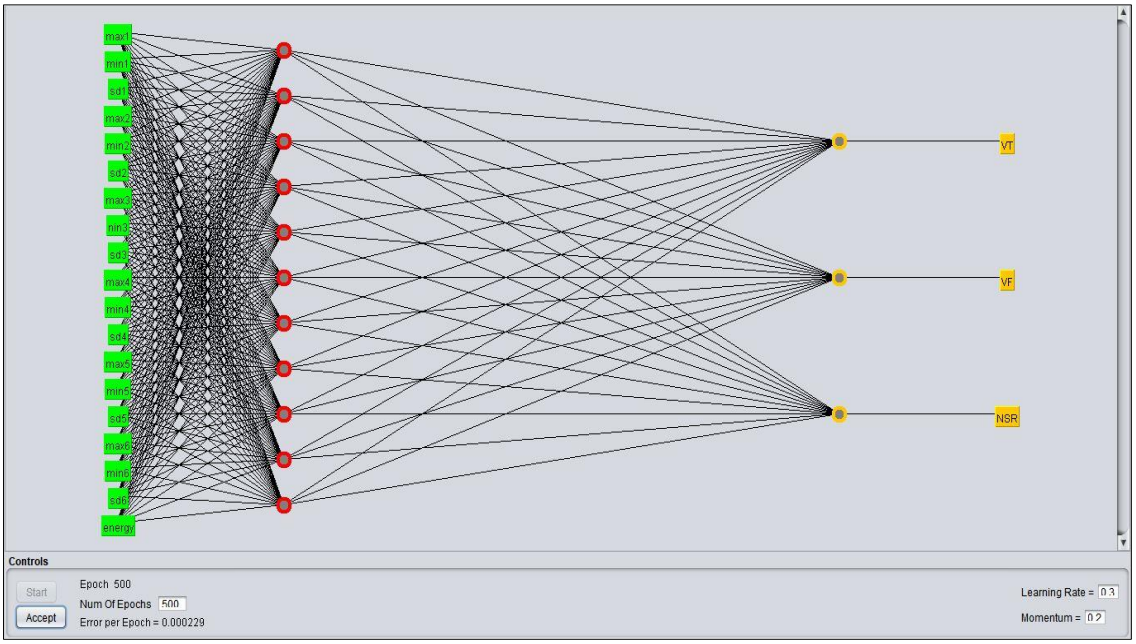

Fig 6.7 ANN structure for NSR, VT and VF (3 types) using wavelet features

The above Fig 6.7 shows neural network architecture of MLP results obtained for NSR, VT and VF. It has one input layer, one output layer and one hidden layer. Input layer has 19 features represented as minimum, maximum and standard deviation values of detailed coefficients in 1 to 5 levels; minimum, maximum and standard deviation values of approximation coefficients in 6^{th} level and the retained energy of each record. The output layer represented as NSR, VT and VF. It has 3 output neurons and 11 hidden neurons. The error per epoch is obtained as 0.000229 and Learning rate obtained as 0.3.

```
Time taken to build model: 0.13 seconds

=== Stratified cross-validation ===
=== Summary ===

Correctly Classified Instances          44               97.7778 %
Incorrectly Classified Instances         1                2.2222 %
Kappa statistic                          0.9667
Mean absolute error                      0.0364
Root mean squared error                  0.1305
Relative absolute error                  8.1533 %
Root relative squared error             27.5277 %
Total Number of Instances               45

=== Detailed Accuracy By Class ===

               TP Rate  FP Rate  Precision  Recall   F-Measure  MCC      ROC Area  PRC Area  Class
               1.000    0.000    1.000      1.000    1.000      1.000    1.000     1.000     VT
               1.000    0.033    0.938      1.000    0.968      0.952    0.998     0.996     VF
               0.933    0.000    1.000      0.933    0.966      0.950    1.000     1.000     NSR
Weighted Avg.  0.978    0.011    0.979      0.978    0.978      0.967    0.999     0.999

=== Confusion Matrix ===

  a  b  c   <-- classified as
 15  0  0 |  a = VT
  0 15  0 |  b = VF
  0  1 14 |  c = NSR
```

Fig 6.8 Simulation results of NSR, VT and VF using MLP Classifier

The above Fig 6.8 shows the simulation results for classification of NSR, VT and VF using MLP classifier. Time taken to build the model is 0.13 Seconds. Correctly classified instances are 44 out of 45 instances. RMSE value is 0.1305.The classification accuracy for classifying NSR, VT and VF is obtained as 97.77% and confusion matrix is shown for VT,VF and NSR.

```
Time taken to build model: 0.25 seconds

=== Stratified cross-validation ===
=== Summary ===

Correctly Classified Instances          56               93.3333 %
Incorrectly Classified Instances         4                6.6667 %
Kappa statistic                          0.9111
Mean absolute error                      0.0452
Root mean squared error                  0.1566
Relative absolute error                 11.9955 %
Root relative squared error             36.0192 %
Total Number of Instances               60

=== Detailed Accuracy By Class ===

               TP Rate   FP Rate   Precision   Recall  F-Measure   ROC Area  Class
                 1         0          1         1         1          1        VT
                 0.8       0.022      0.923     0.8       0.857      0.926    NSR
                 1         0.044      0.882     1         0.938      0.996    VF
                 0.933     0.022      0.933     0.933     0.933      0.981    svt
Weighted Avg.    0.933     0.022      0.935     0.933     0.932      0.976

=== Confusion Matrix ===

  a  b  c  d   <-- classified as
 15  0  0  0 |  a = VT
  0 12  2  1 |  b = NSR
  0  0 15  0 |  c = VF
  0  1  0 14 |  d = svt
```

Fig 6.9 Simulation results of NSR, SVT, VT and VF using MLP Classifier

The above Fig 6.9 shows the simulation results for classification of NSR, SVT, VT and VF using MLP classifier. Time taken to build the model is 0.25 Seconds. Correctly classified instances are 56 out of 60 instances. RMSE value is 0.1566.The classification accuracy for classifying NSR, SVT, VT and VF is obtained as 93.33%.

```
Time taken to build model: 0.45 seconds

=== Stratified cross-validation ===
=== Summary ===

Correctly Classified Instances         100               95.2381 %
Incorrectly Classified Instances         5                4.7619 %
Kappa statistic                          0.9444
Mean absolute error                      0.0336
Root mean squared error                  0.1167
Relative absolute error                 13.6925 %
Root relative squared error             33.2845 %
Total Number of Instances              105

=== Detailed Accuracy By Class ===

               TP Rate   FP Rate   Precision   Recall  F-Measure  MCC      ROC Area  PRC Area  Class
               1.000    0.011     0.938      1.000    0.968      0.963    0.999     0.996     CI
               0.933    0.000     1.000      0.933    0.966      0.961    0.998     0.989     VT
               0.867    0.011     0.929      0.867    0.897      0.881    0.924     0.892     AF
               0.933    0.011     0.933      0.933    0.933      0.922    0.998     0.987     sca
               0.933    0.011     0.933      0.933    0.933      0.922    0.997     0.984     nsr
               1.000    0.011     0.938      1.000    0.968      0.963    0.997     0.981     VF
               1.000    0.000     1.000      1.000    1.000      1.000    1.000     1.000     SVT
Weighted Avg.  0.952    0.008     0.953      0.952    0.952      0.945    0.988     0.976
```

Fig 6.10 Simulation results of 7 types using MLP Classifier

The above Fig 6.10 shows the simulation results for classification of 7 types using MLP classifier. Time taken to build the model is 0.45 Seconds. Correctly classified instances are 100 out of 105 instances. RMSE value is 0.1167. The classification accuracy for classifying 7 types of ECG signals is obtained as 95.231%.

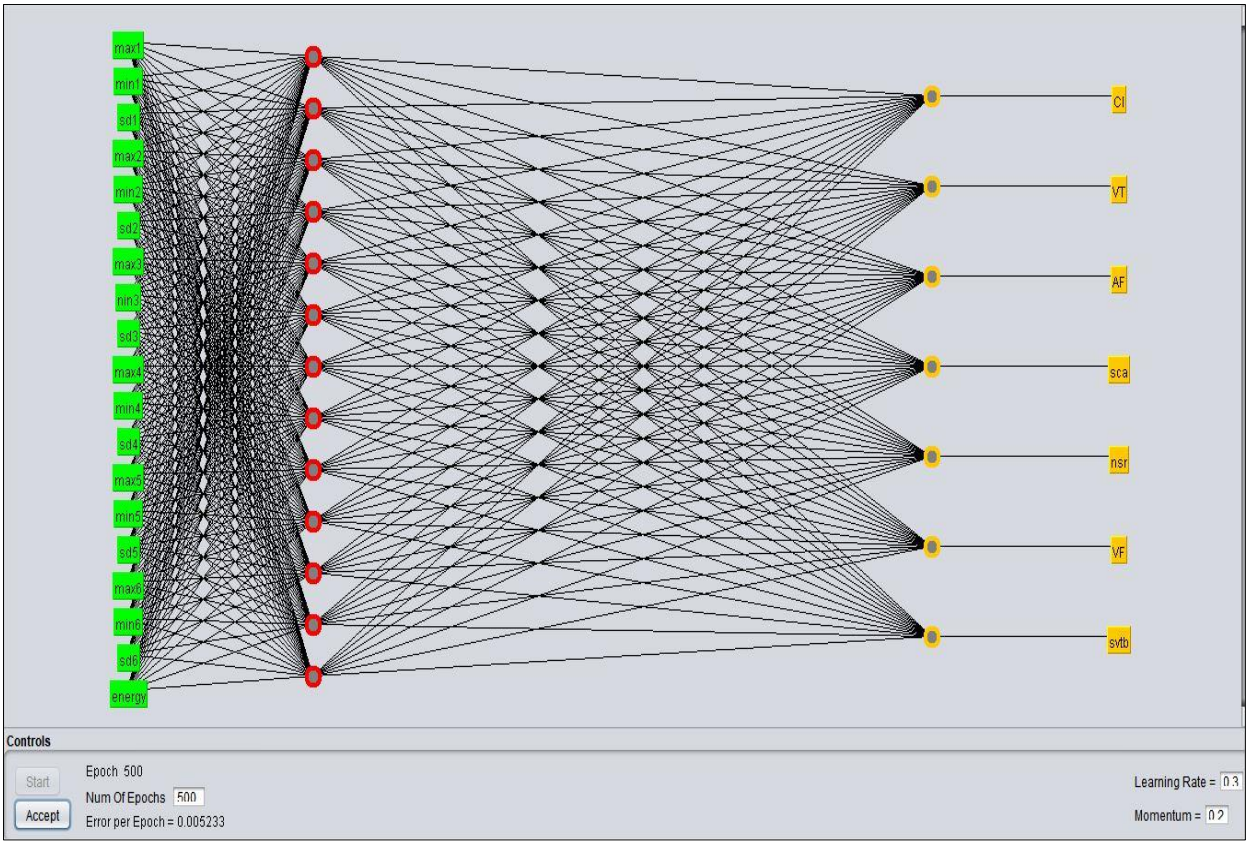

Fig 6.11 ANN structure for 7 types using wavelet features

The above Fig 6.11 shows neural network architecture of MLP results obtained for 7 types of signals. It has one input layer, one output layer and one hidden layer. Input layer 19 features represented as minimum, maximum and standard deviation values of detailed coefficients in 1 to 5 levels; minimum, maximum and standard deviation values of approximation coefficients in 6th level and the retained energy of each record. The output layer represented as NSR, SVT, VT, AF, SCA, CI, AF and VF. It has 7 output neurons and 13 hidden neurons. The error per epoch obtained as 0.005233 and Learning rate obtained as 0.3

6.5.2 RBF classifier results

```
Time taken to build model: 0.02 seconds

=== Stratified cross-validation ===
=== Summary ===

Correctly Classified Instances          43               95.5556 %
Incorrectly Classified Instances         2                4.4444 %
Kappa statistic                          0.9333
Mean absolute error                      0.0296
Root mean squared error                  0.1721
Relative absolute error                  6.6328 %
Root relative squared error             36.3202 %
Total Number of Instances               45

=== Detailed Accuracy By Class ===

               TP Rate   FP Rate   Precision   Recall  F-Measure   ROC Area  Class
                 0.933     0          1         0.933     0.966      0.973    VT
                 1         0.033      0.938     1         0.968      0.968    VF
                 0.933     0.033      0.933     0.933     0.933      0.906    NSR
Weighted Avg.    0.956     0.022      0.957     0.956     0.956      0.949

=== Confusion Matrix ===

  a  b  c   <-- classified as
 14  0  1 |  a = VT
  0 15  0 |  b = VF
  0  1 14 |  c = NSR
```

Fig 6.12 Simulation results of NSR, VT and VF using RBF Classifier

The above Fig 6.12 shows the simulation results for classification of NSR, VT and VF using RBF classifier. Time taken to build the model is 0.02 Seconds. Correctly classified instances are 43 out of 45 instances. RMSE value is 0.1721. The classification accuracy for classifying NSR, VT and VF is obtained as 95.55% and confusion matrix is shown for VT,VF and NSR.

```
Time taken to build model: 0.02 seconds

=== Stratified cross-validation ===
=== Summary ===

Correctly Classified Instances          56               93.3333 %
Incorrectly Classified Instances         4                6.6667 %
Kappa statistic                          0.9111
Mean absolute error                      0.0333
Root mean squared error                  0.1826
Relative absolute error                  8.855  %
Root relative squared error             41.9948 %
Total Number of Instances               60

=== Detailed Accuracy By Class ===

               TP Rate   FP Rate   Precision   Recall  F-Measure   ROC Area  Class
                 1         0          1         1         1          1        VT
                 0.933     0.067      0.824     0.933     0.875      0.98     NSR
                 1         0.022      0.938     1         0.968      1        VF
                 0.8       0          1         0.8       0.889      0.993    svt
Weighted Avg.    0.933     0.022      0.94      0.933     0.933      0.993

=== Confusion Matrix ===

  a  b  c  d   <-- classified as
 15  0  0  0 |  a = VT
  0 14  1  0 |  b = NSR
  0  0 15  0 |  c = VF
  0  3  0 12 |  d = svt
```

Fig 6.13 Simulation results of NSR, SVT, VT and VF using RBF Classifier

The above Fig 6.13 shows the simulation results for classification of NSR, SVT, VT and VF using RBF classifier. Time taken to build the model is 0.02 Seconds. Correctly classified instances are 56 out of 60 instances. RMSE value is 0.1826. The classification accuracy for classifying NSR, SVT, VT and VF is obtained as 93.33%

```
Time taken to build model: 0.06 seconds

=== Stratified cross-validation ===
=== Summary ===

Correctly Classified Instances          97               92.381  %
Incorrectly Classified Instances         8                7.619  %
Kappa statistic                          0.9111
Mean absolute error                      0.0215
Root mean squared error                  0.1351
Relative absolute error                  8.7493 %
Root relative squared error             38.5408 %
Total Number of Instances              105

=== Detailed Accuracy By Class ===

               TP Rate   FP Rate   Precision   Recall  F-Measure   ROC Area  Class
                 1         0.011      0.938     1         0.968      0.994    CI
                 1         0          1         1         1          1        VT
                 0.867     0.022      0.867     0.867     0.867      0.97     AF
                 0.867     0.022      0.867     0.867     0.867      0.886    sca
                 0.867     0.022      0.867     0.867     0.867      0.924    nsr
                 0.933     0.011      0.933     0.933     0.933      0.999    VF
                 0.933     0          1         0.933     0.966      0.973    SVT
Weighted Avg.    0.924     0.013      0.924     0.924     0.924      0.964

=== Confusion Matrix ===

  a  b  c  d  e  f  g   <-- classified as
 15  0  0  0  0  0  0 |  a = CI
  0 15  0  0  0  0  0 |  b = VT
  1  0 13  0  0  1  0 |  c = AF
  0  0  0 13  2  0  0 |  d = sca
  0  0  0  2 13  0  0 |  e = nsr
  0  0  1  0  0 14  0 |  f = VF
  0  0  1  0  0  0 14 |  g = SVT
```

Fig 6.14 Simulation results of 7 types using RBF Classifier

The above Fig 6.14 shows the simulation results for classification of 7 types using RBF classifier. Time taken to build the model is 0.06 Seconds. Correctly classified instances are 97 out of 105 instances. RMSE value is 0.1351.The classification accuracy for classifying 7 types of ECG signals is obtained as 92.381% and confusion matrix is shown for NSR,VT,VF,SVT,CI,AF and SCA.

6.5.3 RF classifier results

```
Time taken to build model: 0.03 seconds

=== Stratified cross-validation ===
=== Summary ===

Correctly Classified Instances          43               95.5556 %
Incorrectly Classified Instances         2                4.4444 %
Kappa statistic                          0.9333
Mean absolute error                      0.0843
Root mean squared error                  0.1582
Relative absolute error                 18.8703 %
Root relative squared error             33.3839 %
Total Number of Instances               45

=== Detailed Accuracy By Class ===

               TP Rate   FP Rate   Precision   Recall  F-Measure  MCC      ROC Area  PRC Area  Class
               0.933     0.033     0.933      0.933    0.933      0.900    0.998     0.996     VT
               0.933     0.033     0.933      0.933    0.933      0.900    0.998     0.996     VF
               1.000     0.000     1.000      1.000    1.000      1.000    1.000     1.000     NSR
Weighted Avg.  0.956     0.022     0.956      0.956    0.956      0.933    0.999     0.997

=== Confusion Matrix ===

  a  b  c   <-- classified as
 14  1  0 |  a = VT
  1 14  0 |  b = VF
  0  0 15 |  c = NSR
```

Fig 6.15 Simulation results of NSR, VT and VF using RF Classifier

The above Fig 6.15 shows the simulation results for classification of NSR,VT and VF using RF classifier. Time taken to build the model is 0.03 Seconds. Correctly classified instances are 43 out of 45 instances. RMSE value is 0.1582.The classification accuracy for classifying NSR,VT and VF is obtained as 95.55% and confusion matrix is shown for VT,VF and NSR.

```
=== Stratified cross-validation ===
=== Summary ===

Correctly Classified Instances          57               95      %
Incorrectly Classified Instances         3                5      %
Kappa statistic                          0.9333
Mean absolute error                      0.0842
Root mean squared error                  0.1713
Relative absolute error                 22.3588 %
Root relative squared error             39.403  %
Total Number of Instances               60

=== Detailed Accuracy By Class ===

               TP Rate   FP Rate   Precision   Recall  F-Measure  MCC      ROC Area  PRC Area  Class
               1.000    0.022    0.938      1.000    0.968      0.957    1.000     1.000     VT
               0.867    0.000    1.000      0.867    0.929      0.911    0.976     0.965     NSR
               0.933    0.000    1.000      0.933    0.966      0.956    0.999     0.996     VF
               1.000    0.044    0.882      1.000    0.938      0.918    0.984     0.930     svt
Weighted Avg.  0.950    0.017    0.955      0.950    0.950      0.936    0.990     0.973

=== Confusion Matrix ===

  a  b  c  d   <-- classified as
 15  0  0  0 |  a = VT
  0 13  0  2 |  b = NSR
  1  0 14  0 |  c = VF
  0  0  0 15 |  d = svt
```

Fig 6.16 Simulation results of NSR, SVT, VT and VF using RF Classifier

The above Fig 6.16 shows the simulation results for classification of NSR, VT, SVT and VF using RF classifier. Time taken to build the model is 0.01 Seconds. Correctly classified instances are 57 out of 60 instances. RMSE value is 0.1713. The classification accuracy for classifying NSR, VT, SVT and VF is obtained as 95% and confusion matrix is shown for NSR,SVT,VT and VF.

```
Time taken to build model: 0.01 seconds

=== Stratified cross-validation ===
=== Summary ===

Correctly Classified Instances          99               94.2857 %
Incorrectly Classified Instances         6                5.7143 %
Kappa statistic                          0.9333
Mean absolute error                      0.0337
Root mean squared error                  0.1104
Relative absolute error                 13.752  %
Root relative squared error             31.4903 %
Total Number of Instances              105

=== Detailed Accuracy By Class ===

               TP Rate   FP Rate   Precision   Recall  F-Measure   ROC Area  Class
                 0.933     0          1         0.933     0.966      1        CI
                 1         0.011      0.938     1         0.968      0.999    VT
                 0.933     0.011      0.933     0.933     0.933      0.959    AF
                 1         0.022      0.882     1         0.938      0.999    sca
                 0.867     0          1         0.867     0.929      0.999    nsr
                 0.867     0          1         0.867     0.929      0.999    VF
                 1         0.022      0.882     1         0.938      1        SVT
Weighted Avg.    0.943     0.01       0.948     0.943     0.943      0.994

=== Confusion Matrix ===

  a  b  c  d  e  f  g   <-- classified as
 14  0  0  0  0  0  1 |  a = CI
  0 15  0  0  0  0  0 |  b = VT
  0  0 14  0  0  0  1 |  c = AF
  0  0  0 15  0  0  0 |  d = sca
  0  0  0  2 13  0  0 |  e = nsr
  0  1  1  0  0 13  0 |  f = VF
  0  0  0  0  0  0 15 |  g = SVT
```

Fig 6.17 Simulation results of 7 types using Random Forest Classifier

The Fig 6.17 shows the simulation results for classification of 7 types using RF classifier. It's built by using random forest of 10 trees, each constructed while considering 5 random features. Out of bag error is 0.181. Time taken to build the model is 0.01 Seconds. RF of 10 trees have been used each constructed while considering 5 random features of 19 wavelet features. Correctly classified instances are 99 out of 105 instances. RMSE value is 0.1104. The classification accuracy for classifying 7 types of ECG signals is obtained as 94.28%

In the proposed work, the above wavelet features (from Table 6.1 to Table 6.4) have been given to MLP, RBF and RF neural network classifiers for automatic classification of 7 types of cardiac signals (normal, 4 types of arrhythmias and 2 cardiac disorders).

Further, compared the performance of all these classifiers is shown in Table 6.5. MLP classifier classification accuracy obtained as 95.23% and the computational time to build the model was 0.45seconds, RBF classifier classification accuracy obtained as 92.381% and the computational time to build the model is 0.06seconds. RF classifier classification accuracy obtained as 94.285% and the computational time to build the model is 0.2seconds.

Table 6.5 Performance comparison of 3-classifiers

	MLP	**RF**	**RBF**
Computational time to build the model (Sec)	0.45	0.2	0.06
Classification Accuracy	95.238%	94.285%	92.381%
Kappa Statistic(K)	0.9444	0.9333	0.9111
Mean Absolute Error	0.0336	0.0414	0.0215
Root Mean Square Error	0.1167	0.1129	0.1351
Correctly classified instances	100	99	97
Total Number of instances	105	105	105

It is observed that wavelet transform technique with MLP classifier produced better accuracy than RBF classifier but computational time to build the model is more in MLP compare to RBF.

6.5.4 Medical statistics

The performance of MLP algorithm of medical statistics are evaluated such as Sensitivity (S)-95.21%, Specificity (Sp) -99.15% and Precision (P) – 95.34% are shown in Table 6.6. The performance of RF algorithm evaluated with the medical statistics are shown in Table 6.7. The performance of RBF algorithms evaluated with the medical statistics are shown in Table 6.8

Table 6.6 Medical Statistics of MLP using confusion matrix

ECG	TP	FP	FN	TN	Sensitivity(S)	Specificity(Sp)	Precision(P)
NSR	14	2	1	88	93.3%	97.7%	95%
AF	13	1	2	89	86.6%	98.8%	92.85%
CI	15	1	0	89	100%	98.8%	93.75%
VT	14	0	1	90	93.3%	98.8%	100%
SVT	15	0	0	90	100%	100%	100%
VF	15	0	0	90	100%	100%	100%
SCA	14	1	1	89	93.3%	98.8%	93.33%
				Average	**95.21**%	**99.15**%	**95.34%**

Table 6.7 Medical Statistics of RF using confusion matrix

ECG	TP	FP	FN	TN	Sensitivity(S)	Specificity(S)	Precision(Pp)
NSR	14	1	1	89	93.33%	98.88%	93.33%
AF	14	1	1	89	93.33%	98.88%	93.33%
CI	14	0	1	90	93.33%	100%	100%
VT	15	1	0	89	100%	98.88%	93.75%
SVT	15	2	0	88	100%	97.77%	88.23%
VF	13	0	2	90	86.66%	100%	100%
SCA	14	1	1	89	93.33%	98.88%	93.33%
				Average	**94.28**%	**99.04**%	**94.56**%

Table 6.8 Medical Statistics of RBF using confusion matrix

ECG	TP	FP	FN	TN	Sensitivity(S)	Specificity(S)	Precision(Pp)
CI	15	1	0	89	100%	98.88%	93.75%
VT	15	0	0	90	100%	100%	100%
AF	13	2	2	87	86.66%	97.75%	86.66%
SCA	13	2	2	87	86.66%	97.75%	86.66%
NSR	13	2	2	87	86.66%	97.75%	86.66%
VF	14	1	1	89	93.33%	98.88%	93.33%
SVT	14	0	1	90	93.33%	100%	100%
				Average	**92.38**%	**98.71**%	**92.44**%

6.6 Performance comparison of cardiac arrhythmias classification

The performance of cardiac signals classification depends on number of cardiac signal records, number of features, type of classifier and number of arrhythmias/disorders/normal signals. Classification reported in the literature have been compared with the proposed classification system is shown in Table 6.9. In the existing work of H. M. Rai et al. [44] used 64 hybrid of features and obtained classification accuracy of two types of signals as 97.8%.

Maedeh Kiani Sarkaleh et al. [45] has classified three types of cardiac signals and produced classification accuracy as 96.5% using MLP classifier. Proposed work classified 2 types of cardiac signals (NSR and VT) and obtained an accuracy as 100% using MLP, RBF and RF classifiers.

Later classified three types of signals-NSR, VT and VF and obtained classification accuracy as 97.77% and specificity is 98.88%. Compare to the existing work of Monalisa Mohanty et al. [47], the proposed work average classification accuracy, sensitivity and specificity are more. Pooja Bhardwaj et al. [49] classified 5 types of cardiac signals with accuracy 95.21% and sensitivity 85.44%. The proposed work classified 7 types of cardiac signals and obtained Precision-95.3%, Accuracy-95.24%, Sensitivity-95.2% and Sensitivity-95.2%

Table 6.9 Summary of performance comparison of cardiac arrhythmias classification

Study by	Records and Features	Classifier	Diseases	Accuracy
H.M.Rai et al. [44]	45 Records (25 arrhythmia and 20 normal) 16 morphological and 48 wavelet features Total : 64 features	BPNN	Normal and Arrhythmia class(2-Types)	97.8%
Maedeh Kiani Sarkaleh et al. [45]	10 Records Features- 24 wavelet features	MLP	Normal and Arrhythmias types (3-Types)	96.5%
Mangesh Singh Tomar et al. [46]	62 Records 14-NSR,48-Arrhythmia Features-20 wavelet features 5 statistical features Total :25 features	BPNN	Normal and Arrhythmia class(2-Types)	98.4%
Proposed	30 Records (NSR-15 and VT-15) Features-19 Wavelet features	MLP, RF and RBF	NSR and VT (2-Types)	MLP-100% RF-100% RBF-100%
Monalisa Mohanty et al. [47]	57 Records Features-13Temporal and Statistical features	SVM and C4.5 classifier	NSR,VT and VF (3-Types)	[SVM] Se-79.43 % Sp-81.44% Acc-92.23% [C4.5] Se-90.97% Sp-97.86% Acc-97.02%
Proposed	45 Records (NSR-15, VT-15 and VF-15) Total: 19 Wavelet features	MLP classifier	NSR,VT and VF (3-Types)	Sensitivity-97.77% Specificity- 98.88% Accuracy-97.77%
Proposed	105 records Only 19 Wavelet based features(db4)	RF	NSR,SVT,VT,VF,AF, SCA, CI (7-Types)	Accuracy-94.21% Sensitivity-94.21% Specificity-99.04%
		RBF	NSR,SVT,VT,VF,AF, SCA, CI (7-Types)	Accuracy-92.38% Sensitivity-92.38% Specificity-98.72%
		MLP	NSR,SVT,VT,VF,AF, SCA, CI (7-Types)	Accuracy-95.24% Sensitivity-95.2% Specificity-99.20% Precision-95.3%

6.7 Conclusion

It has been observed that wavelet based feature scheme played an important role in distinguishing different cardiac arrhythmias and cardiac disorders. It is identified that Neural Network Algorithms are getting better when the complexity of the data set increases. Significant improvement has been observed in terms of classification accuracy of 7 types of cardiac signals compared with the existing works as shown in Table 6.9 which has been the objective of this research work. The proposed work classified 7 types of cardiac signals with 95.21% accuracy, sensitivity 95.2% and specificity 99.20% using MLP algorithm, using RF algorithm obtained accuracy as 94.28% and using RBF algorithm obtained accuracy as 92.38%. From the above results shown in Table 6.9, it is concluded that wavelet transform technique with MLP classifier produced better results than RBF and RF classifier.

In most of the existing works used different number of records and got different values of sensitivity and accuracy. Where as in the proposed work, equal number of records of each category of cardiac signals are used for classification purpose and obtained equal values of sensitivity and accuracy. In the proposed work obtained more specificity than sensitivity. In real time applications it is required to have more specificity than the sensitivity. No patient should be defibrillated except SCA patient, otherwise it causes cardiac arrest to normal persons.

The MLP classifier used for this work has 3 layers (1- input layer, 1- output and 1- hidden layer). The input layer contains 19 nodes, the output layer has 7 nodes. Finally, obtained 13-hidden neurons and 7 output neurons. Further, this efficient wavelet based feature scheme can be extended to classify other types of cardiac arrhythmias and disorders.

The main objective of this research work is to enhance classification accuracy of cardiac signals and improve specificity to enable doctors for early diagnose the type of cardiac disorder to save life of heart patients. The proposed research work has been extended to develop cardiac alert system using wavelet based feature scheme.

Chapter 7

Conclusion and Future Scope

This chapter describes the results and conclusion in a brief and comprehensive manner. Further future scope of the research work has been given.

7.1 Conclusion

Finding efficient feature scheme is an important challenge for automatic classification of cardiac signals. In this research work, four different feature extraction techniques have been proposed for analysis and classification of cardiac signals (cardiac arrhythmias, cardiac disorders and normal).

- Time domain analysis and classification of cardiac signals using artificial intelligence algorithms.
- Spectral analysis and classification of cardiac signals using hybrid (temporal and spectral) features.
- Higher order spectral analysis and classification of cardiac signals using hybrid (temporal, spectral and bispectral) features.
- Wavelet analysis and classification of cardiac signals using wavelet features

In the first approach, Pan Tompkins algorithm is used to extract temporal features such as number of R peaks, amplitude of R peaks, R-R intervals and heart beat rate. It is observed that there is a variation in temporal features of various cardiac signals. Based on this variation, initially proposed to classify two types of cardiac signals. Classification accuracy has been improved from 96.5% existing work to 100% for temporal features. Later proposed to classify 7 types of cardiac signals (1- normal, 4-arrhythmias and 2-cardiac disorders) and obtained an accuracy as 78.09% using Random Forest classifier and also evaluated the results with other neural network classifiers. Performance comparison with the existing work in time domain is shown in Table 7.1

Table 7.1 Performance comparison with the existing work in time domain

Study	Records and Features	Classifier	Cardiac Signals	Classification Accuracy
M. Vijayavanan et al. [5]	300 Records, 12 - Morphological features	PNN	NSR and Cardiac Arrhythmia (2 types)	96.5%
Proposed	30 Records , 4 temporal features	RF, MLP and RBF	[NSR,Ventricular Arrhythmia(VF)](2 types)	100%
	105 records, 4-temporal features	RF	[NSR, SVT,VT,VF,AF,SCA,CI] (7 types)	78.09%

In the second approach, spectral features have been proposed to get more details of the ECG signal in frequency domain. This spectral analysis has given how the ECG signal's energy is distributed over a wide range of frequencies. In the existing work, Usman Rashed et al. [19] used FFT algorithm on 4 minutes ECG data to detect sudden cardiac arrest compared to normal signal. For the proposed work, FFT algorithm is applied on 1 minute ECG data to extract spectral features (mean, median, standard deviation and energy). Spectral features (R1 to R5 regions) are extracted. R1-R4 regions spectral features are used for classifying NSR and SCA and obtained average classification accuracy of 93.3%. Later, using only R3 region spectral features are used to classify NSR & SCA and obtained same classification accuracy as 93.3% and the results are also evaluated with other classifiers. Hence, it is identified that R3 region play a significant role in distinguishing NSR and SCA as R3 frequency range is matching to the QRS complex frequency range. To enhance classification accuracy, hybrid (temporal and spectral features) approach is proposed and obtained classification accuracy as 100% for NSR and SCA signals using MLP and RBF classifiers. Later, the work has been extended to classify 7 types of cardiac signals (1- normal, 4-cardiac arrhythmias and 2- cardiac disorders) and obtained classification accuracy as 78.09% using RF classifier and also evaluated the results with other classifiers. When complexity is less, RF classifier gives better performance compare to MLP and RBF classifiers as shown in Table 7.2.

Table 7.2 Performance comparison with the existing work in spectral domain

Study	Records and Features	Classifier	Cardiac Signals	Classification Accuracy
Usman Rashed et al. [19]	8 Records, 5 Spectral features	Distinguished based on spectral parameters	NSR and SCA (2 types)	-
Proposed	30 Records, 4 Spectral features(R3)	RF, MLP and RBF	NSR and SCA(2 types)	RF-93.33% MLP-93.33% RBF-96.6%
Proposed	Hybrid features (Temporal& Spectral)	RF, MLP and RBF	NSR and SCA	RF-93.33% MLP-100% RBF-100%
			NSR, SVT, VT, VF, AF, CI & SCA (**7** types)	MLP–71.4% RBF-66.6% RF-78.09%

The accuracy did not increase even in hybrid approach also. It is observed that normal spectral analysis of a signal does not give any phase coupled information of the signal. ECG signals are basically non-linear, quasi periodic and non-stationary in nature. There is a need of phase coupled information for identification and classification of cardiac arrhythmias. So, higher order spectral analysis is proposed in the third approach.

In the third approach, hybrid features have been proposed to provide supplementary information about non-gaussianity and non-linearity of the ECG signal for cardiac arrhythmias identification. In the HOSA domain, the bispectrum, bicoherence and QPC plots are used to analyse 7 types of cardiac signals. It is observed that HOSA plots are potential visual aids to distinguish normal, four types of cardiac arrhythmias and two cardiac disorders. In particular the bicoherence indicates that phase coupling decreases as arrhythmia kicks in. In the existing work of L. Khadra et al.[21] classified only 4 types (NSR ,VT, VF and AF) of cardiac signals with sensitivity 89.2%and specificity 93.55%. In the existing work of I. A. Karaye et al. [26] classified 5 types (NSR and 4 diseases) of cardiac signals with sensitivity 88.4% and specificity 96.2%. In the proposed work classified 4 types (NSR, VT, VF and AF) of cardiac signals with improved accuracy of 90% using RF classifier and also evaluated the results with other

classifiers. Later, proposed to classify 7 types of cardiac signals (1- normal, 4- arrhythmias and 2- cardiac disorders) and obtained classification accuracy as 74.2%, sensitivity as 74.2% and specificity as 95.02% using RF, MLP and RBF classifiers. The performance comparison is shown in Table 7.3. There is a need to find time and frequency information at a time using multi resolution analysis. So, wavelet based feature extraction is proposed in the fourth approach to enhance classification accuracy.

Table 7.3 Performance comparison with the existing work in higher order spectral domain

Study by	Number of records and Features	Classifier	Diseases	Accuracy
L. Khadra et al. [21]	43-records (AF-12, VT-11, VF-12 and NSR-08) HOSA features-3	Bispectral contour analysis	NSR ,VT, VF and AF (4 types)	Sensitivity-89.2% Specificity-93.55%
I. A. Karaye et al. [26]	47-records Temporal features-1 HOSA features-3	Feed forward ANN	NSR, LBBB,RBBB, PB and APB (5 types)	Sensitivity-88.4% Specificity-96.2% Accuracy- 94.9%.
Proposed	60 Records (AF-15, VT-15 , VF-15 and NSR-15) Spectral-1, Bispectral-4 and Temporal features-4	RF	NSR ,VT, VF and AF(4 types)	Sensitivity-90 % Accuracy- 90% Specificity-96.62%
	105 Records,(7 types each 15 records) Spectral ,Bispectral and Temporal features(9 features)	MLP	NSR,SVT,VT, VF, AF, CI and SCA	Sensitivity-74.28% Accuracy-74.2% Specificity-95.70% Precision-75.02%

In fourth approach, the wavelet based feature scheme is proposed to classify seven types of cardiac signals. A 6-level wavelet (db4) decomposition technique is used to obtain 19-features and these features provided supplementary information about time and frequency of ECG signals. Existing works classified 2, 3 or 5 types of cardiac signals with less classification accuracy is as shown in Table 7.4. Whereas the proposed technique classified 7 types of cardiac signals (normal, 4 types of cardiac arrhythmias and 2 types of cardiac disorders). The proposed work enhance classification accuracy to 95.21% using 19 wavelet features. Medical statistics

obtained as Sensitivity 95.21%, Specificity 99.15% and Positive Predictivity 95.34% using MLP classifier. The specificity is more important than the sensitivity. Since, no patient should be defibrillated except SCA patient .Otherwise, this error may cause to sudden cardiac arrest [16] for normal persons.

Table 7.4 Performance comparison of cardiac arrhythmias classification in wavelet domain

Study by	**Records and Features**	**Classifier**	**Diseases**	**Accuracy**
Monalisa Mohanty et al. [47]	57 Records VT-35, VF-11, NSR-11 Features-13 Temporal &Statistical features(hybrid)	SVM C4.5	NSR,VT and VF (3-Types)	[SVM] Se-79.43 % Sp-81.44% Acc-92.23% [C4.5] Se-90.97% Sp-97.86% Acc-97.02%
Proposed	45 Records (NSR-15, VT-15 and VF-15) 19 Wavelet features	MLP	NSR,VT and VF (3-Types)	Sensitivity-97.77% Specificity- 98.88% Accuracy-97.77%
	105 records 19 Wavelet based features	MLP	NSR,SVT,VT, VF, AF, CI and SCA	Accuracy-95.24% Sensitivity-95.2% Specificity-99.20% Precision-95.3%

Table 7.5 Comparison of cardiac arrhythmias classification in different domains

Features Scheme	Features used	Cardiac Signals	Classifier	Accuracy
Temporal	No. of R peaks, R peak amplitude, R-R interval and Heart beat rate [4 features]	7 types of cardiac signals (105 records)	MLP	70.47%
			RBF	70.05%
			RF	**78.09%**
Temporal & spectral	4-Temporal features (No. of R peaks, R peak amplitude, R-R interval and Heart beat rate) and 4-Spectral features (Mean, Median , SD and Energy in R3)- [8-features]	7 types of cardiac signals (105 records)	MLP	71.4%
			RBF	66.6%
			RF	78.09%
Temporal, Spectral and Bispectral	Total Features-10; Bispectral features (Kurtosis, skewness, variance and bicoherence); Spectral features (energy) and Temporal features (No. of R peaks, R peak amplitude, R-R interval and Heart beat rate) [10-features]	7 types of cardiac signals (105 records)	**MLP**	**74.28%**
			RBF	74.2%
			RF	74.2%
Wavelet based features (db4)	Detailed coefficients of maximum, minimum and standard deviation of 1-5 levels; Approximation coefficients of maximum, minimum and standard deviation of 6th level and the energy retained of each record.[19- features]	7 types of cardiac signals (105 records)	**MLP**	**95.24%**
			RBF	92.38%
			RF	94.21%

All the four methods developed in this thesis are novel, however third and fourth methods are efficient feature schemes and are superior in terms of classification accuracy when compared to the existing work. Comparison of 7 types of cardiac signals classification in different domains is shown Table 7.5. For temporal and spectral features (less than 10 features) RF classifier is giving better accuracy. In HOSA using hybrid features all three classifiers produced same performance, though their learning mechanism is different. In wavelet domain, MLP produced better performance compare to MLP and RF classifiers.

7.2 Future scope

In this research work, 7 types of cardiac signals (NSR, 4 types of cardiac arrhythmias-VT,VF,SVT,AF and 2 types of cardiac disorders-SCA,CI) have been analyzed in time domain, spectral domain, higher order spectral domain and wavelet domain and classified using three supervised classifiers(RF, MLP and RBF). An experimental setup of cardiac alert system has been developed using efficient wavelet based feature scheme for remote monitoring of cardiac patients. This application has been included in Appendix.

This research work may be further extended to identify and classify few more cardiac disorders such as Right Bundle Branch Block (RBBB), Paced Beat (PB), Left Bundle Block Branch (LBBB), Atrial Premature Beats (APB) and Premature Ventricular Contraction (PVC). Deep neural networks such as Convolutional neural networks (CNN) and Recurrent Neural Networks (RNN) do not require any other signal processing techniques for feature extraction purpose. Directly CNN or RNN can be used to classify different types of cardiac arrhythmias and disorders. Further a proto type cardiac alert system can be developed by using wavelet based feature scheme for tele cardiology application.

7.3 Limitations

Number of records can be increased in order to make the results statistically more sound and improve the research into a biomedical application. There are several issues with application of Artificial Intelligence. Reading the data at real time and classifying is a requirement to use this technology in clinical setting. In order to extend this application to into a version where a person can wear a smart watch at all times, the use of highly sensitive sensors are needed which produce signals that can match the level of a standard ECG.

Application of this classification to be used in clinical settings is not possible at this stage as the consequences are various such as bioethical issue of liability in case of misdiagnosis; should the onus be on researcher who is the owner of the patent or the company which bought it and capitalized it or the doctor that depended on this algorithm.

Appendix

Cardiac Alert System

A.1 Introduction

Significant improvement has been observed in terms of classification accuracy with the present work shown in Chapter 6. Further, this efficient wavelet feature scheme is used to develop a Cardiac Alert System with the help of Arduino Uno and GSM SIM 900A. For wireless real time transmission of signal, GSM module is being used. With this remote monitoring of heart patients is possible which is important to save the life of heart patients. An Arduino Uno board takes the signal directly from a computer and is connected to a GSM board. This GSM board sends an SMS text message with the results of the classification. For example when cardiologist receives the message alert of sudden cardiac arrest with patient details from intensive care unit of hospital, he can alert the clinical staff members to take care of cardiac patients according to cardiac pulmonary resuscitation (CPR) guidelines, till he reaches the hospital. High-quality CPR at a rate of 100-120 chest compressions per minute must be started immediately to keep oxygenated blood flowing to their brain. CPR must be used in tandem with an Automated External Defibrillators (AED) to improve chances of survival exponentially.

Objective of this research work application is to alert cardiologist for remote monitoring of heart patients and to diagnose the type of cardiac disorder/arrhythmia for immediate treatment to save life of heart patients. This research will be suitable for tele cardiology application of telemedicine as it has unique capacity to improve the health care service to millions of rural people.

A.2 Cardiac Alert System

The Block diagram of Cardiac Alert System is shown below in Fig A.1. ECG data will be given to computer for feature extraction using wavelet analysis. These wavelet features are used to develop matlab code to identify the type of cardiac problem.

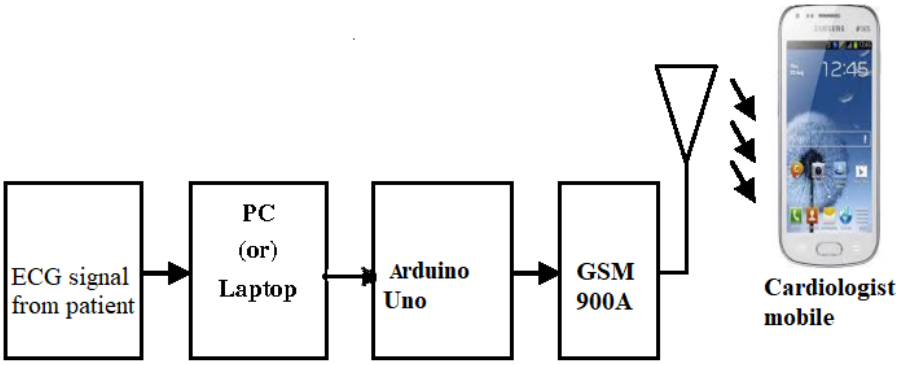

Fig A.1 Block Diagram of Cardiac Alert System

Fig A.2 Experimental set-up of Cardiac Alert System

The Arduino UNO board (ATmega328P) has been connected to the computer using a USB cable to establish a serial communication at a baud rate of 9600. Arduino board is usually powered using USB cable connecting the computer. The experimental set-up of Cardiac Alert System has been shown in Fig A.2. The voltage provided to Arduino is controlled by the voltage regulator and stabilizes the DC voltage which is used by processor. Arduino UNO board has 14 digital I/O pins (of which 6 can be used as Pulse Width Modulation outputs), 6 analog inputs, a 16 MHz ceramic resonator, a USB connection, a power jack, an ICSP header and a reset button. On top of crystal, printed number is 16.000H9H, which indicates that the frequency used is 16 MHz. Arduino board can be reset when program is initiated. Many ground pins are present on board which can be used to ground the circuitry. Voltage input provides supply to the board. When Arduino is plugged to power, LED glows indicating that the board is powered up correctly. If LED doesn't glow, it states that connection is wrong. TX and RX LEDs are used for representing the pins which are accountable for communicating serially. While

transmitting data serially, TX LED does flashing with various speeds which is based on baud rate and while receiving the data, RX LED flashes. GSM/GPRS-compatible Quad-band mobile phone functions on a frequency related to 850/900 and also be used for communication not only for accessing the net. Module got managed through AMR926EJ-S processor that controls data and mobile communication through the integrated TCP/IP stack.

The following steps are required to operate GSM module:

1. Insert SIM card to GSM module and lock it.
2. GSM module should be operated by providing 12V supply.
3. Initially blinking rate of network LED will be high. Once the connection is established successfully, the LED will blink continuously for every 3 seconds.

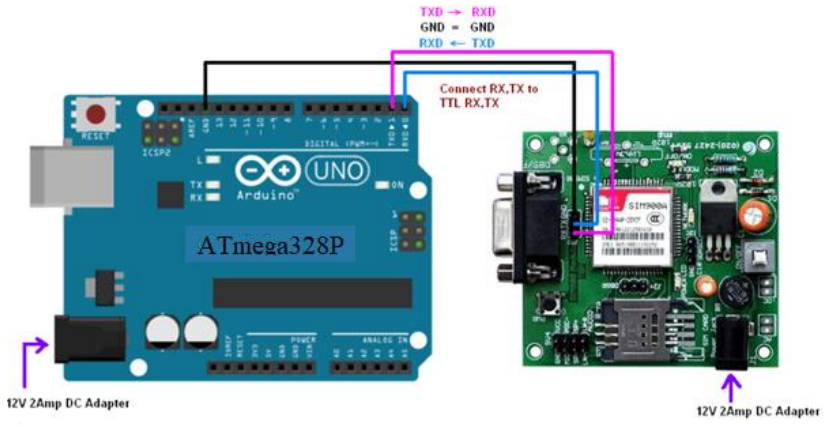

Fig A.3 Interfacing of Arduino with GSM

GSM module has been connected to Arduino UNO using the digital pins as shown in Fig A.3 TX pin of GSM Module is connected to Arduino Uno RX pin. RX pin-9 of GSM module is connected to Arduino Uno TX pin. GND pin of GSM module is connected to Arduino Uno GND pin. The Arduino UNO was interfaced with GSM module at a baud rate of 9600. Interfaced the Computer, Arduino and GSM. An Arduino UNO board was used for the processing. GSM SIM900A was used to transmit the SMS and make phone calls to the respective doctor when a cardiac abnormality was detected. The phone calls lasts for 10 seconds and hang up automatically. MATLAB code is written based on the wavelet feature scheme to identify the type of cardiac arrhythmias and disorders. The control program is supplemented in Arduino code with patient details and doctor mobile number is given in Section A.3.

A.3 Arduino Code for Cardiac Alert System

```
#include <SoftwareSerial.h>

Software Serial my Serial(9, 10);

int a;

void setup()

 {mySerial.begin (9600);   // Setting the baud rate of GSM Module

Serial.begin(9600);}

void loop()

{  //Serial.println("check");

while (!Serial.available()) {}

int a = Serial.parseInt();

Serial.println(a);

if (a == 10)

{  sca();   }

else if( a == 20)

  {    ci();}

  else if(a == 30)

  {    nsr(); }

    else if(a == 40)

  {    vf(); }

    else if(a == 50)

  {    vt(); }

    else if(a == 60)

  {    svt(); }

    else if(a == 70)

  {    af(); }}

void sca()
```

```
{   MakeCall();
  mySerial.println("AT+CMGF=1");    //Sets the GSM Module in Text Mode
  delay(1000);  // Delay of 1000 milli seconds or 1 second
  mySerial.println("AT+CMGS=\"+919440762744\"\r"); // Replace x with mobile number
  delay(1000);
  mySerial.println("WARNING: CODE BLUE");
  mySerial.println("PATIENT ID= ######");
  mySerial.println("BED NUMBER= #####");
  mySerial.println("PATIENT NAME= #####");
  mySerial.println("CASE OF SUDDEN CARDIAC ARREST");
  //mySerial.print("");
  //mySerial.println(BPM);
  //mySerial.println("CASE OF BRADYCARDIA");
  delay(100);
  mySerial.println((char)26);// ASCII code of CTRL+Z
  delay(1000);
  MakeCall();}
void ci()
{   MakeCall();
  mySerial.println("AT+CMGF=1");    //Sets the GSM Module in Text Mode
  delay(1000);  // Delay of 1000 milli seconds or 1 second
  mySerial.println("AT+CMGS=\"+919440762744\"\r"); // Replace x with mobile number
  delay(1000);
  mySerial.println("WARNING: CODE BLUE");
  mySerial.println ("PATIENT ID= ######");
  mySerial.println("BED NUMBER= #####");
  mySerial.println("PATIENT NAME= #####");
```

```
  mySerial.println("CASE OF CARDIAC ISCHEMIA");
  //mySerial.print("");
  //mySerial.println(BPM);
  //mySerial.println("CASE OF BRADYCARDIA");
  delay(100);
  mySerial.println ((char) 26);// ASCII code of CTRL+Z
  delay(1000);
  MakeCall();
}
void snr()
{ MakeCall();
  mySerial.println("AT+CMGF=1");    //Sets the GSM Module in Text Mode
  delay(1000);  // Delay of 1000 milli seconds or 1 second
  mySerial.println("AT+CMGS=\"+919440762744\"\r"); // Replace x with mobile number
  delay(1000);
  mySerial.println("WARNING: CODE BLUE");
  mySerial.println("PATIENT ID= ######");
  mySerial.println("BED NUMBER= #####");
  mySerial.println("PATIENT NAME= #####");
  mySerial.println("CASE OF NORMAL SINUS RYTHM");
  delay(100);
  mySerial.println((char)26);// ASCII code of CTRL+Z
  delay(1000);
  MakeCall();
}
void vf()
{  MakeCall();
```

```
  mySerial.println("AT+CMGF=1");    //Sets the GSM Module in Text Mode
  delay(1000);  // Delay of 1000 milli seconds or 1 second
  mySerial.println("AT+CMGS=\"+919440762744\"\r"); // Replace x with mobile number
  delay(1000);
  mySerial.println("WARNING: CODE BLUE");
  mySerial.println("PATIENT ID= ######");
  mySerial.println("BED NUMBER= #####");
  mySerial.println("PATIENT NAME= #####");
  mySerial.println("CASE OF Ventricular Fibrillation");
  delay(100);
  mySerial.println((char)26);// ASCII code of CTRL+Z
  delay(1000);
  MakeCall();
}
void vt()
{   MakeCall();
  mySerial.println("AT+CMGF=1");    //Sets the GSM Module in Text Mode
  delay(1000);  // Delay of 1000 milli seconds or 1 second
  mySerial.println("AT+CMGS=\"+919440762744\"\r"); // Replace x with mobile number
  delay(1000);
  mySerial.println("WARNING: CODE BLUE");
  mySerial.println("PATIENT ID= ######");
  mySerial.println("BED NUMBER= #####");
  mySerial.println("PATIENT NAME= #####");
  mySerial.println("CASE OF Ventricular tachycardia");
  delay(100);
  mySerial.println((char)26);// ASCII code of CTRL+Z
```

```
  delay(1000);
  MakeCall();
}
void svt()
{   MakeCall();
  mySerial.println("AT+CMGF=1");    //Sets the GSM Module in Text Mode
  delay(1000);  // Delay of 1000 milli seconds or 1 second
  mySerial.println("AT+CMGS=\"+919440762744\"\r"); // Replace x with mobile number
  delay(1000);
  mySerial.println("WARNING: CODE BLUE");
  mySerial.println("PATIENT ID= ######");
  mySerial.println ("BED NUMBER= #####");
  mySerial.println("PATIENT NAME= #####");
  mySerial.println("CASE OF  Supra Ventricular tachycardia");
  delay(100);
  mySerial.println((char)26);// ASCII code of CTRL+Z
  delay(1000);
  MakeCall();
}
void af()
{   MakeCall();
  mySerial.println("AT+CMGF=1");    //Sets the GSM Module in Text Mode
  delay(1000);  // Delay of 1000 milli seconds or 1 second
  mySerial.println("AT+CMGS=\"+919440762744\"\r"); // Replace x with mobile number
  delay(1000);
  mySerial.println("WARNING: CODE BLUE");
  mySerial.println("PATIENT ID= ######");
```

```
  mySerial.println("BED NUMBER= #####");

  mySerial.println("PATIENT NAME= #####");

  mySerial.println("CASE OF Atrial fibrillation");

  delay(100);

  mySerial.println((char)26);// ASCII code of CTRL+Z

  delay(1000);

  MakeCall();

}

void MakeCall()

{  mySerial.println("ATD+919440762744;"); // ATDxxxxxxxxxx; -- watch out here for
semicolon at the end!!

  Serial.println("Calling  "); // print response over serial port

  delay(1000);

  delay(20000);

  HangupCall();

}

void HangupCall()

{  mySerial.println("ATH");

  Serial.println("Hangup Call");

  delay(1000);}
```

A.4 Matlab Code for Cardiac Alert System

```
A = xlsread ('pro.xlsx')
%sudden cardiac arrest (1 to 15 rows)
%cardiac ischemia (17 to 39 rows)
%normal sinus rythm (41 to 50 rows)
data = A(60 ,:)
if(data(3) < 5 && data(19) < 97 && data(18) < 752 && data(2) < -10  && 2 < data(3) &&
data(17) < -61 && data(16) < 880 && data(5) < -28 &&  92 < data(19) &&  39 < data(18)
&&  -38 < data(2) &&  -1578 < data(17) &&  50 < data(16) &&  -200 < data(5))
    disp('atrial fibrillation')
   a=70
elseif(data(3) < 16 && data(19) < 94 && data(18) < 457 && data(2) < -34 && data(1) < 71
&& 5 < data(3) &&  90 < data(19) &&  84 < data(18) &&  -94 < data(2) &&  44 < data(1))
    disp('super ventricular tachycardia')
   a=60
elseif(data(3) < 3 && data(19) < 101 && data(18) < 439 && data(2) < -3  && 1 < data(3)
&&  99 < data(19) &&  19 < data(18) &&  -9 < data(2))
    disp('Ventricular tachycardia')
   a=50
elseif(data(3) < 6 && data(19) < 99.8 && data(18) < 2802 && data(2) < -6 && data(17) < -
300 && data(16) < 5131 && data(5) < -10 && 1 < data(3) &&  93 < data(19) &&  131 <
data(18) &&  -39 < data(2) &&  -5002 < data(17) &&  345 < data(16) && -164 < data(5))
    disp('Ventricular fibrillation')
   a=40
elseif( data(3) < 5  &&  data(19) < 90 && 0 < data(3) && 74 < data(19))
   disp('sudden cardiac arrest')
   a=10
elseif( data(3) < 200 && data(19) < 98 && 30 < data(3) &&  92 < data(19))
  disp('cardiac ischemia')
   a=20
elseif(data(3) < 25 && data(19) < 92 && data(5) < -259 && 10 < data(3) &&  86 < data(19)
&& -565 < data(5))
  disp('normal sinus rythm')
   a=30
end
arduino=serial('COM3','BaudRate',9600);
% create serial communication object on port COM4
disp('stage1')
fopen(arduino); % initiate arduino communication
disp('serial communication initiated')
pause(2);
 fprintf(arduino,'%d',a);
 val =  fscanf(arduino);
disp(val);
pause(0.1);
disp('serial communication successful')
fclose(arduino);
```

A.5 Results and Conclusion

The simulation results have been verified by using Arduino and matlab codes. An alert system alerts the cardiologist /clinical doctors by making a call and sending an SMS alert to indicate the type of cardiac disorder. The text SMS which has been sent to doctor consisted of various fields like Patient ID, Patient Name, Patient Bed Number and type of cardiac disease is displayed as shown in Fig A.4.

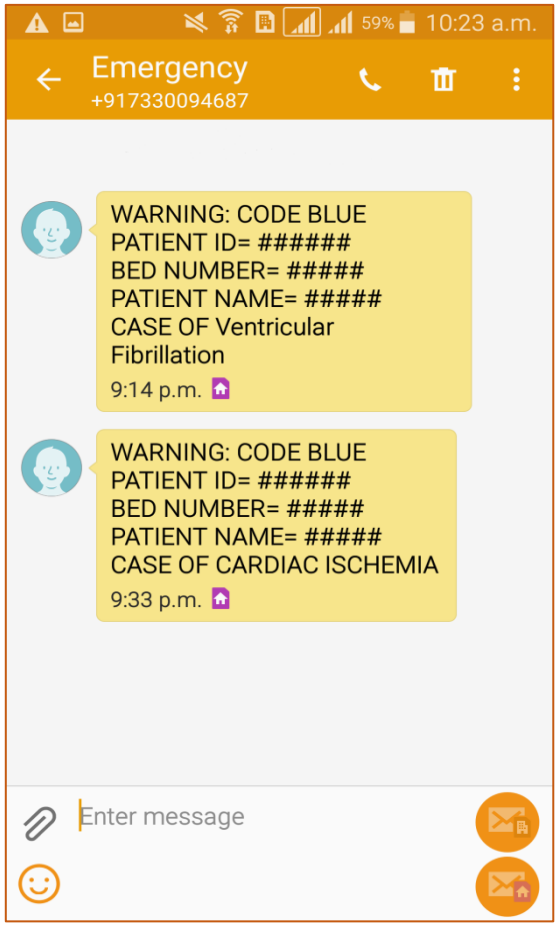

Fig A.4 SMS alert to cardiologist

The main objective of the cardiac alert system is to monitor the patients remotely with the help of GSM technology to alert the clinical staff/cardiologist to take care of the heart patient. This type of Cardiac Alert System is very much useful in early detection of cardiac disorder in Tele-Cardiology application.

Fig A.5 Tele Cardiology for remote monitoring of heart patient [13]

Tele cardiology enhances the telemedicine application to deliver cardiac care to the remote patient as shown in Fig A.5. This Tele cardiology application has tremendous potential to improve basic health care facility in both rural and urban populated areas.

References

1. G. B. Moody and R. G. Mark, "The impact of the MIT-BIH Arrhythmia Database," in IEEE Engineering in Medicine and Biology Magazine, vol. 20, no. 3, pp. 45-50, May-June 2001.
2. Pan, J. and Tompkins, W.T "A Real-Time QRS Detection Algorithm" IEEE Trans. Biomed.Eng. Vol 32, pp.230-236, 1985.
3. V.X. Alfonso, W.J. Tompkins, T.Q. Nguyen, and S. Luo, "ECG beat detection using Filter Banks", IEEE Trans. Biomed. Eng., vol. 46, pp.192–202, 1999.
4. V. Vijaya, K. Kishan. Rao and P. Sahrudai, "Identification of Sudden Cardiac Arrest Using the Pan-Tompkins Algorithm," 2012 UKSim 14th International Conference on Computer Modelling and Simulation, Cambridge, 2012, pp. 97-100.
5. M.Vijayavanan, "Automatic Classification of ECG Signal for Heart Disease Diagnosis using morphological features", International Journal of Computer Science & Engineering Technology, ISSN: 2229-3345, Vol. 5, pp 449, Apr 2014
6. K. K. Mujeeb Rahman and M. Monica Subashini, "ECG Signal Processing and Analysis for Accurate Features Extraction," 2019 IEEE International Symposium on Signal Processing and Information Technology (ISSPIT), Ajman, United Arab Emirates, 2019, pp. 1-5.
7. Philip de Chazal, M. O'Dwyer and R. B. Reilly, "Automatic classification of heartbeats using ECG morphology and heartbeat interval features," in IEEE Transactions on Biomedical Engineering, vol. 51, no. 7, pp. 1196-1206, July 2004
8. Sachin Singh NetajiGandhi.N ,"Pattern analysis of different ECG signal using Pan-Tompkin's algorithm" International Journal on Computer Science and Engineering ,Vol. 02, No. 07, 2010, 2502-2505
9. M. Akay, K. F. Tan, K. L. Chan and K. Choi, "Detection of the QRS complex, P wave and T wave in Electrocardiogram", IEEE transactions on biomedical engineering, vol. 47, no.12, Dec, 2000.
10. V.Vijaya, K.Kishan.Rao, V.Rama, "Arrhythmia Detection through ECG Feature Extraction using Wavelet Analysis" European Journal of Scientific Research, ISSN 1450-216X Vol.66 No.3 (2011), pp. 441-448.
11. Figure sourced Parekh, Asha. "Calcification of Bovine Pericardial Aortic Heart Valves." (2015).

12. S. B. Kotsiantis, I. D. Zaharakis, and P. E. Pintelas, “Machine learning: a review of classification and combining techniques”, Artificial Intelligence, vol. 26, no. 3, pp. 159–190, Nov. 2007.
13. Figure sourced from Flickr, Tele Cardiology, July 17, 2013.
14. Zhen Zhang, Weimin Shao and Hong Zhang, "A learning algorithm for multilayer perceptron as classifier," IJCNN'99. International Joint Conference on Neural Networks. Proceedings, Washington, DC, USA, 1999, pp. 1681-1684 .vol.3
15. K. Minami, H. Nakajima and T. Toyoshima, "Real-time discrimination of ventricular tachyarrhythmia with Fourier-transform neural network," in IEEE Transactions on Biomedical Engineering, vol. 46, no. 2, pp. 179-185, Feb. 1999
16. A. Amann, R. Tratnig and K. Unterkofler, "Detecting Ventricular Fibrillation by Time-Delay Methods," in IEEE Transactions on Biomedical Engineering, vol. 54, no. 1, pp. 174-177, Jan. 2007
17. Nguyen, Minh Tuan et al. “Deep Feature Learning for Sudden Cardiac Arrest Detection in Automated External Defibrillators.” Scientific reports vol. 8,1 17196. 21 Nov. 2018
18. Myers, Glenn A., Gary J. Martin, Norman M. Magid, Phillip S. Barnett, John W. Schaad, Jerry S. Weiss, Michael Lesch, and Donald H. Singer. “Power Spectral Analysis of Heart Rate Variability in Sudden Cardiac Death: Comparison to Other Methods.” IEEE Transactions on Biomedical Engineering BME-33, no. 12, pp 1149–56, 1986.
19. Rashed, U. Mirza, M.J. “Identification of sudden cardiac death using spectral domain analysis of Electrocardiogram (ECG),” 4th International Conference on Emerging Technologies, 2008., vol., no., pp.309-314, 18-19 Oct. 2008
20. S. Bose, V. Rama, N. Warangal and C. B. Rama Rao, "EEG signal analysis for Seizure detection using Discrete Wavelet Transform and Random Forest," 2017 International Conference on Computer and Applications (ICCA), Doha, 2017, pp. 369-378,
21. L. Khadra, A. S. Al-Fahoum and S. Binajjaj, "A quantitative analysis approach for cardiac arrhythmia classification using higher order spectral techniques," in IEEE Transactions on Biomedical Engineering, vol. 52, no. 11, pp. 1840-1845, Nov. 2005.
22. S.Karimifard, A.Ahmadian, “Morphological Heart Arrhythmia Classification using Hermitian model of Higher Order Statistics”, France, Aug 23-26, 2007
23. K. C. Chua, V. Chandran, U. R. Acharya& C. M. Lim (2008) Cardiac state diagnosis using higher order spectra of heart rate variability, Journal of Medical Engineering & Technology, 32:2, 145-155.

24. Safdarian, N., Maghooli, K., & Dabanloo, N.J. (2012). Classification of Cardiac Arrhythmias with TSK Fuzzy System using Genetic Algorithm.
25. K. Sharmila, E. H. Krishna, N. R. Komalla and K.A. Reddy, “Use of higher order spectral analysis for the identification of sudden cardiac death,” 2012IEEE International Symposium on Medical Measurements and Applications Proceedings, Budapest, 2012, pp.1-4.
26. A. Karaye, S. Saminu and N. Özkurt, “Analysis of cardiac beats using higher order spectra,” 2014 IEEE 6th International Conference on Adaptive Science & Technology (ICAST), Ota, 2014, pp. 1-8.
27. S. Dubnov, N. Tishby, “Spectral Estimation using Higher Order Statistics”, Proceedings of the 12th International Conference on Pattern Recognition, Jerusalem, Israel, 1994.
28. S. Arakaran and P. Vaidyanathan, “Bifrequency and bispectrum maps: A new look at multirate systems with stochastic inputs,” IEEE Trans. Signal Processing, vol. 48, no. 3, pp. 723–36, Mar. 2000.
29. R. Sahab , Y. MehrzadGilmalek, “An Automatic Diagnostic Machine for ECG Arrhythmias classification Based on Wavelet Transformation and Neural Networks”, International Journal of Circuits, Systems And Signal Processing, Issue 3, Volume 5, 2011
30. Y. C. Kim and E. J. Powers, “Digital bispectral analysis and its applications to nonlinear wave interactions,” IEEE Trans. Plasma Sci., vol. PS-7, pp. 120–131, Jun. 1979.
31. Choudhury, M.A.S.S., Shah, S.L., Thornhill, N.F., “Detection and diagnosis of System Nonlinearities using higher order statistics”, 15th Triennial world congress, Barcelona, Spain, PP 1-6, 2002.
32. Nidhyananthan, Selva. (2016). Myocardial Infarction Detection and Heart Patient Identity Verification.
33. F. S. SAYIN and Ö. AKGÜN, “Higher Order Spectral Analysis of Ventricular Arrhythmic ECG Signals with MATLAB HOSA Toolbox,” 2018 6th International Conference on Control Engineering & Information Technology (CEIT), Istanbul, Turkey, 2018, pp. 1-4
34. M. Nichols, C. C. Olson, J. V. Michalowicz and F. Bucholtz, “The Bispectrum and Bicoherence for Quadratically Nonlinear Systems Subject to Non-Gaussian Inputs,” in IEEE Transactions on Signal Processing, vol. 57, no. 10, pp. 3879-3890, Oct. 2009
35. A. Brian, N. Sabna and G. G. Paulson, "ECG based algorithm for detecting ventricular arrhythmia and atrial fibrillation," 2017 International Conference on Intelligent Computing and Control Systems (ICICCS), Madurai, 2017, pp. 506-511

36. G. Azarnia, M. A. Tinati and R. G. Afkhami, "Heart blocks detection in ECG signals using time frequency distribution techniques," 2016 24th Iranian Conference on Electrical Engineering (ICEE), Shiraz, 2016, pp. 1568-1573,
37. Rathnakara. S., Srinidhi. H. and Janardhan. M., "An effective algorithm to differentiate NSR and Arrhythmia," 2018 International Conference on Applied Electromagnetics, Signal Processing and Communication (AESPC), Bhubaneswar, India, 2018, pp. 1-4,
38. Yakup Kutlu , DamlaKuntalp, "A Multi-Stage Automatic Arrhythmia Recognition and Classification System", ELSEVIER, Computers in Biology and Medicine 41 (2011) 37–45
39. A. Taddei, G. Distante, M. Emdin, P.G.B. Moody, C. Zeelenberg, C. Marchesi ,The European ST-T database: standard for evaluating systems for the analysis of ST-T changes in ambulatory electrocardiography Eur. Heart J., 13 (1992), pp. 1164-1172
40. M. Nolle, F.K. Badura, J.M. Catlett, R.W. Bowser, M.H. Sketch CREI-GARD, a new concept in computerized arrhythmia monitoring systems Comput. Cardiol., 13 (1986), pp. 515-518
41. A. Khazaee, "Heart Beat Classification Using Particle Swarm Optimization", Int. J. of Intelligent Syst. and Applicat. (IJISA), vol. 5, no. 6, pp. 25-33, 2013.
42. A. Mousa and A. Yimaz, "Neural network detection of ventricular late potentials in ECG signals using wavelet transform extracted parameters," 2001 Conference Proceedings of the 23rd Annual International Conference of the IEEE Engineering in Medicine and Biology Society, Istanbul, Turkey, 2001, pp. 1668-1671 vol.2.
43. A. S. Al-Fahoum and I. Howitt, "Combined wavelet transformation and radial basis neural networks for classifying life-threatening cardiac arrhythmias," Inst. Elect. Eng. Med. Biol. Eng. Comput., vol. 37, pp. 566–73, 1999.
44. H. M. Rai and A. Trivedi, "ECG signal classification using wavelet transform and Back Propagation Neural Network," 2012 ,5th International Conference on Computers and Devices for Communication (CODEC), Kolkata, 2012, pp. 1-4
45. Maedeh Kiani Sarkaleh and Asadollah Shahbahrami "Classification of ECG Arrhythmias using Discrete Wavelet Transform and Neural Networks", International Journal of Computer Science, Engineering and Applications (IJCSEA) vol.2, No.1, February 2012.
46. Mangesh Singh Tomar ,Manoj Kumar Bandil , D B V Singh "ECG feature extraction and classification for Arrhythmia using wavelet & Scaled Conjugate-Back Propagation Neural Network" , International Journal of Advanced Research in Computer Science, Volume 4, No. 11, Nov-Dec 2013.

47. S. Sukanta & M. Mohanty, Monalisa & Sahoo, Santanu & Biswal, Pradyut. (2018). Efficient classification of ventricular arrhythmias using feature selection and C4.5 classifier. Biomedical Signal Processing and Control 44, pp. 200-208.1.
48. Roshan.J.Martis, U.RajendraAcharya, Ajoy.K.Ray, ChandanChakraborthy: "Application of Higher order Cumulants to ECG signals for the cardiac health diagnosis", 33rd Annual International Conference of the IEEE-EMBS Boston, Massachusetts', August 30-september 3, 2011, 1697-1700.
49. Pooja Bharadwaj, Rahul R Choudhary, RavindraDayama, "Analysis and Classification of Cardiac Arrhythmia using ECG Signals", International Journal of Computer Applications (0975 – 8887) Volume 38– No.1, January 2012
50. Ubeyli E.D. "Combining recurrent neural networks with eigenvector methods for classification of ECG beats", Digit. Signal Process.Vol.19, pp 320–329, 2009.
51. Ali Sadr, NajmehMohsenifar, Raziyeh Sadat Okhovat, "Comparison of MLP and RBF neural networks for Prediction of ECG Signals" International Journal of Computer Science and Network Security, Vol.11 No.11, November 2011
52. HyontaiSug "Performance Comparison of RBF networks and MLPs for Classification" proceedings of 9th WSEAS International Conference on Applied Informatics And Communications (AIC '09)
53. S. H. Jambukia, V. K. Dabhi and H. B. Prajapati, "Classification of ECG signals using machine learning techniques: A survey," 2015 International Conference on Advances in Computer Engineering and Applications, Ghaziabad, 2015, pp. 714-721.
54. I. Daubechies, "Where Do Wavelets Come From? – A Personal Point of View," Proceedings of the IEEE, Vol. 84, No.4, April 1996, pp. 510- 513.
55. Physiobank Archive Index, MIT-BIH Arrhythmia Database. *http://www.nhlbi.nih.gov/health/health-topics/topics/ekg/*
http://www.physionet.org/physiobank/databaseElectrocardiogram information
56. Mark, R. G., "Biological Measurement: Electrical Characteristics of the Heart," in Systems & Control Encyclopedia, Singh, M. G., (ed.), Oxford, U.K.: Permagon Press, 1990, pp. 450–456.
57. R.M.Rangayyan, "Biomedical Signal analysis: A Case study Approach", IEEE press / Wiley, New York, NY, 2002.
58. Candan, C., Kutay, M. A., Ozaktas, H. M., " The discrete fractional Fourier transform," IEEE Trans. on Signal Processing, 48(5), pp. 1329–37, 2000.

59. Witten, Ian H.; Frank, Eibe; Hall, Mark A.; Pal, Christopher J. (2011). "Data Mining: Practical machine learning tools and techniques, 3rd Edition". Morgan Kaufmann, San Francisco (CA). Retrieved 2011-01-19.
60. Mateo J., Sanchez-Morla E.M., Santos J.L. A new method for removal of power line interference in ECG and EEG recordings.Comput.Electr.Eng. 2015; 45:235–248.
61. S.Karpagachelvi, Dr.M.Arthanari, M.Sivakumar,"ECG Feature Extraction Techniques", International Journal of Computer Science and Information Security, Vol. 8, No. 1, April 2010
62. Jerry M Mendel, "Tutorial on Higher Order Spectra in signal processing and system theory: Theoretical results and some applications", Proceeding of IEEE, vol. 79, no. 3, March 1991.
63. Ananthrama Swami, Jerry M. Mendel, Chrysostomes L. (Max) Nikias "Higher Order Spectral Analysis Toolbox: User's Guide ver 2.0"
64. Math Works, (2012). Bioinformatics Toolbox: User's Guide (R2012a). Retrieved July 14, 2012 from www.mathworks.com/help/pdf_doc/bioinfo/bioinfo_ug.pdf
65. C. L. Nikias, M.R. Raghu veer, "Bispectrum Estimation: A digital signal processing framework", Proc. IEEE, vol. 75, no.7 pp.867-891, 1987.
66. Haykin, Simon. Neural Networks and Learning Machines, New Jersey: Pearson Prentice Hall, 2008.
67. J. Proakis and D. Manolakis, "Digital Signal Processing Principles, Algorithms and Applications", Second ed. Macmillan Publishing Company, New York, 1992.
68. Nithya and S. Ravindra kumar, "Detection of cardiovascular abnormalities using peak detection and adaptive thresholding: A synthetic and real time approach," 2012 International Conference on Computing, Communication and Applications, Dindigul, Tamilnadu, 2012, pp.1-5.63.
69. S. Cerutti and C. Marchesi (Editors), "Advanced Methods of Biomedical Signal Processing", IEEE and Wiley, New York, NY, 2011
70. M. Akay , Time Frequency and Wavelets in Biomedical Signal Processing, IEEE, New York, NY,1998
71. M. Akay, Nonlinear Biomedical Signal Processing, Volume II: Dynamic analysis and modeling, IEEE, New York, NY, 2010.
72. A. R. Sahab , Y. Mehrzad Gilmalek, "An Automatic Diagnostic Machine for ECG Arrhythmias classification Based on Wavelet Transformation and Neural Networks", International Journal of Circuits, Systems And Signal Processing, Issue 3, Volume 5, 2011

73. Elias Ebrahimzadeh, Mohammad Pooyan “Early detection of sudden cardiac death by using classical linear techniques and time-frequency methods on electrocardiogram signals” J. Biomedical Science and Engineering, 2011, 4, 699-706.
74. Chrysostomas L.Nikias, AthinaP.Petropulu, “Higher order spectral Analysis: A Non Linear Signal Processing Frame Work”, Prentice Hall, 1993
75. T. Shen, H. Shen, C. Lin and Y. Ou, "Detection and Prediction of Sudden Cardiac Death (SCD) For Personal Healthcare," 2007 29th Annual International Conference of the IEEE Engineering in Medicine and Biology Society, Lyon, 2007, pp. 2575-2578
76. Zadeh A.E., Khazaee A. High efficient system for automatic classification of the electrocardiogram beats. Ann. Biomed.Eng. 2011; 39:996–1011.
77. Plonsey R., Barr R.C. Bioelectricity: A Quantitative Approach. Springer; New York, NY, USA: 2000. pp. 522–526.
78. E. N. Bruce, Biomedical Signal Processing and Signal Modelling, Wiley, New York, NY, 2001
79. G. D. Baura, System Theory and Practical Applications of Biomedical Signals, IEEE, Piscataway, NJ,2002
80. S. R. Devasahayam, Signals and Systems in Biomedical Engineering: Signal Processing and Physiological Systems Modeling, Kluwer Academic/ Plenum, New York, NY, 2000
81. J. L. Semmlow, Biosignal and Biomedical Image Processing, Marcel Dekker, New York, NY, 2004
82. S.Mallat, “A Wavelet Tour of Signal Processing”, Academic Press, Burlington, MA, 1999
83. Daubechies, “The wavelet transform, time-frequency localization and signal analysis,” IEEE Trans. on Information Theory, vol. 36, no.5, pp. 961-1005, 1990.
84. I. H. Witten and E. Frank, Data Mining: Practical Machine Learning Tools and Techniques, 2nd ed. San Francisco, CA: Morgan Kaufmann, 2005.
85. Amjed Al-Fahoum, Ausilah Al-Fraihat & Aseel Al-Araida (2014) Detection of cardiac ischemia using bispectral analysis approach, Journal of Medical Engineering & Technology, 38:6, 311-316.
86. Miller-Keane Encyclopedia and Dictionary of Medicine, Nursing, and Allied Health, Seventh Edition. (2003).
87. L. Yu and H. Liu, “Efficient feature selection via analysis of relevance and redundancy”, J. Mach. Learn.Res., vol. 5, pp. 1205–1224, 2004.
88. C. Yeh, W. J. Wang, and C. W. Chiou, “Cardiac arrhythmia diagnosis method using linear discriminant analysis on ECG signals,” Meas., vol. 42, no. 5, pp. 778–789, 2009.

89. S. Dubnov, N. Tishby, “Spectral Estimation using Higher Order Statistics”, Proceedings of the 12th International Conference on Pattern Recognition, Jerusalem, Israel, 1994.
90. Math Works, (2012). Bioinformatics Toolbox: User's Guide (R2012a). Retrieved July 14, 2012 from *www.mathworks.com/help/pdf_doc/bioinfo/bioinfo_ug.pdf*
91. Eibe Frank, Mark A. Hall, and Ian H. Witten (2016). The WEKA Workbench. Online Appendix for "Data Mining: Practical Machine Learning Tools and Techniques", Morgan Kaufmann, Fourth Edition, 2016.
92. Athina P. Petropulu. “Higher-Order Spectral Analysis.” 2000 CRC Press LLC.
93. US Food and Drug Administration, Automated External Defibrillators (AEDs)
94. Bhalke D. G., Ram Rao C.B., Bormane D.S. ”Musical Instrument Classification using Higher Order Spectra.”, International Conference on Signal Processing and Integrated Networks (SPIN-2014), 20-21 Feb, 2014. (IEEE)
95. Bhalke D. G., Rama Rao C. B., Bormane D.S. “Automatic Musical Instrument classification using Fractional Fourier Transform based-MFCC Features and Counter Propagation Neural Network”, Journal of Intelligent Information Systems, Springer International Publishing, DOI: 10.1007/s10844-015-0360-9al
96. M. R. Azimi-Sadjadi and S. A. Stricker, "Detection and classification of buried dielectric anomalies using neural networks-further results," in IEEE Transactions on Instrumentation and Measurement, vol. 43, no. 1, pp. 34-39, Feb. 1994
97. L. J. Tick, “The estimation of transfer functions of quadratic systems,” Technometrics, vol.3, pp. 563–567.
98. National Center for Biotechnology Information, https://www.ncbi.nlm.nih.gov/pubmed/12766530
99. Classification of heart rate variability signals using higher order spectra and neural networks, Obayy, M.I.Abou-Chadi, ICNM 2009 Networking & Media Convergence
100. MathWorks, https://in.mathworks.com/help/wavelet/gs/introduction-to-the-wavelet-families.html
101. Liang, B. & Iwnicki, Simon & Zhao, Yunshi. (2013). Application of power spectrum, higher order spectrum and neural network analyses for induction motor fault diagnosis. Mechanical Systems and Signal Processing. 39. 342-360. 10.1016/j.ymssp.2013.02.016.
102. H. H. So and K. L. Chan, “Development of QRS detection method for Real-time ambulatory cardiac monitor”, Proceedings,19th International Conference - IEEE/EMBS Oct.30 -Nov. 2, 1997

103. E. R. Adams and A. Choi, "Using neural networks to predict cardiac arrhythmias," 2012 IEEE International Conference on Systems, Man, and Cybernetics (SMC), Seoul, 2012, pp. 402-407.
104. https://upload.wikimedia.org/wikipedia/commons/a/ae/ConductionsystemoftheheartwithouttheHeart-en.svg
105. https://upload.wikimedia.org/wikipedia/commons/a/ae/ConductionsystemoftheheartwithoutheHeart-en.svg
106. N. K. Dewangan and S. P. Shukla, "ECG arrhythmia classification using discrete wavelet transform and artificial neural network," 2016 IEEE International Conference on Recent Trends in Electronics, Information & Communication Technology (RTEICT), Bangalore, 2016, pp. 1892-1896.
107. Castillo, E., Morales, D.P. Palma, A.J., "Noise suppression in ECG signals through efficient one-step wavelet processing techniques. Journal of Applied Mathematics" Journal of Applied Mathematics 2013.
108. Gore S.N., Ingole D.T. "A novel approach to ECG signal analysis using higher-order spectrum", PiseS.J.Thinkquest2010.Springer, New Delhi.
109. J.A. Gutierrez-Gnecchi, R. Morfin-Magaña, A. del, C. Tellez-Anguiano, D. Lorias-Espinoza, E. Reyes-Archundia, O. Hernandez-Diaz "Cardiac arrhythmia classification using a combination of quadratic spline wavelet transform and artificial neural classification network" Proceedings of the 2nd International Work-Conference on Bioinformatics and Biomedical Engineering, Granada, Spain, April 7th–9th (2014), pp. 1743-1754
110. Sumathi, H. L. Beaulah, and R. Vanithamani, ''A wavelet transform based feature extraction and classification of cardiac disorders,'' Journal of Medical Systems, vol. 38, pp. 98-1–98-11, Sep. 2014.
111. Goshvarpour.A, Rahati.S & Saadatian.V, "Bispectrum Estimation of Electroencephalogram Signal during Meditation", Iran J Psychiatry BehavSci, vol. 6, no 2, 2012.
112. Matsuyama, A., Jonkman, M. The application of wavelet and feature vectors to ECG signals. Australas. Phys. Eng. Sci. Med. 29, 13 (2006).
113. Ghorbani Afkhami, Rashid & Azarnia, Ghanbar & Tinati, Mohammad Ali. (2016). Cardiac Arrhythmia Classification Using Statistical and Mixture Modeling Features of ECG Signals. Pattern Recognition Letters. 70. 45-51. 10.1016/j.patrec.2015.11.018.
114. K. Giri, S. Saraswat, A. K. Yadav and S. Singh, "Classification of Supraventricular Arrhythmias using Wavelet Decomposition," 2019 9th International Conference on Cloud Computing, Data Science & Engineering (Confluence), Noida, India, 2019, pp. 387-391,

115. Hopkins, Angioplasty and stent placement for the heart
116. https://centralgaheart.com/implanting-a-difibrillator/
117. Stock photo-Surgeons perform open heart surgery

Publications

International Journals:

1. V.Rama, C.B. Rama Rao, "Automatic classification of Cardiac arrhythmias using MLP and RBF neural network classifiers," Advanced Research in Electrical and Electronic Engineering p-ISSN: 2349-5804; e-ISSN: 2349-5812 Volume 3, Issue 4, July-September, 2016, pp. 302-306.
2. V.Rama, C.B. Rama Rao, "Higher Order Spectral Analysis To Identify Cardiac Arrhythmias," International Journal of Humanities, Arts, Medicine and. Sciences ISSN (P): 2348-0521, ISSN (E): 2454-4728 Vol. 4, Issue 12, Dec 2016, pp.41-46
3. V.Rama, C.B.Rama Rao, "Early detection of Cardiac disorder using Artificial Intelligence," Primary Healthcare Open Access Journal, Volume 7, Issue 4 | ISSN: 2167-1079.
4. V.Rama, C.B.Rama Rao "Automatic classification of cardiac disorders for cardiac alert system", Journal of Geriatric Research, Volume 2, Issue 2, Nov 2018.

Conference Publications:

1. R. Valupadasu , B. R. R. Chunduri, "Identification of Cardiac Ischemia Using Spectral Domain Analysis of Electrocardiogram," 2012 UKSim 14th International Conference on Computer Modelling and Simulation, Cambridge, 2012, pp. 92-96
2. R. Valupadasu, B. R. Chunduri and V. Chanagoni, "Identification of Cardiac Ischemia using bispectral analysis of ECG," 2012 IEEE-EMBS Conference on Biomedical Engineering and Sciences, Langkawi, 2012, pp. 999-1003
3. R. Valupadasu , B. R. R. Chunduri, "Automatic Classification of Cardiac Disorders Using MLP Algorithm," 2019 IEEE Prognostics and System Health Management Conference (PHM-Paris), Paris, France, 2019, pp. 253-257